Nuclear Science ISBN 978-92-64-99073-9

Inter-code Comparison Exercise for Criticality Excursion Analysis

Benchmark Phase I: Pulse Mode Experiments with Uranyl Nitrate Solution in the TRACY and SILENE Facilities

Yoshinori Miyoshi, Yuichi Yamane, Kiyoshi Okubo
Japan Atomic Energy Agency, Japan

Ludovic Reverdy, Pascal Grivot
Commisariat à l'Énergie Atomique, France

Hideo Konishi, Susumu Mitake
Japan Nuclear Energy Safety Organization, Japan

Peng Hong Liem
NAIS Co. Inc., Japan

NEA No. 6285

NUCLEAR ENERGY AGENCY
Organisation for Economic Co-operation and Development

ORGANISATION FOR ECONOMIC CO-OPERATION AND DEVELOPMENT

The OECD is a unique forum where the governments of 30 democracies work together to address the economic, social and environmental challenges of globalisation. The OECD is also at the forefront of efforts to understand and to help governments respond to new developments and concerns, such as corporate governance, the information economy and the challenges of an ageing population. The Organisation provides a setting where governments can compare policy experiences, seek answers to common problems, identify good practice and work to co-ordinate domestic and international policies.

The OECD member countries are: Australia, Austria, Belgium, Canada, the Czech Republic, Denmark, Finland, France, Germany, Greece, Hungary, Iceland, Ireland, Italy, Japan, Korea, Luxembourg, Mexico, the Netherlands, New Zealand, Norway, Poland, Portugal, the Slovak Republic, Spain, Sweden, Switzerland, Turkey, the United Kingdom and the United States. The Commission of the European Communities takes part in the work of the OECD.

OECD Publishing disseminates widely the results of the Organisation's statistics gathering and research on economic, social and environmental issues, as well as the conventions, guidelines and standards agreed by its members.

NUCLEAR ENERGY AGENCY

The OECD Nuclear Energy Agency (NEA) was established on 1st February 1958 under the name of the OEEC European Nuclear Energy Agency. It received its present designation on 20th April 1972, when Japan became its first non-European full member. NEA membership today consists of 28 OECD member countries: Australia, Austria, Belgium, Canada, the Czech Republic, Denmark, Finland, France, Germany, Greece, Hungary, Iceland, Ireland, Italy, Japan, Luxembourg, Mexico, the Netherlands, Norway, Portugal, Republic of Korea, the Slovak Republic, Spain, Sweden, Switzerland, Turkey, the United Kingdom and the United States. The Commission of the European Communities also takes part in the work of the Agency.

The mission of the NEA is:

- to assist its member countries in maintaining and further developing, through international co-operation, the scientific, technological and legal bases required for a safe, environmentally friendly and economical use of nuclear energy for peaceful purposes, as well as
- to provide authoritative assessments and to forge common understandings on key issues, as input to government decisions on nuclear energy policy and to broader OECD policy analyses in areas such as energy and sustainable development.

Specific areas of competence of the NEA include safety and regulation of nuclear activities, radioactive waste management, radiological protection, nuclear science, economic and technical analyses of the nuclear fuel cycle, nuclear law and liability, and public information.

The NEA Data Bank provides nuclear data and computer program services for participating countries. In these and related tasks, the NEA works in close collaboration with the International Atomic Energy Agency in Vienna, with which it has a Co-operation Agreement, as well as with other international organisations in the nuclear field.

Corrigenda to OECD publications may be found on line at: *www.oecd.org/publishing/corrigenda*.

Cover photo credit: Courtesy of the French Atomic Energy Commission (CEA).

Foreword

Criticality excursion evaluation methods have been developed by a small group of researchers and access to transient codes and experimental data is restricted. The NEA Working Party on Nuclear Criticality Safety established an Expert Group on Criticality Excursion Analysis in 2001 to explore the current situation and to organise benchmarks and exercises on transient codes to evaluate a criticality accident in a fissile solution.

In order to compare calculation results for criticality accident phenomena in uranyl nitrate solution, benchmark analyses were organised using a set of transient experiments with low- and high-enriched uranyl nitrate solution conducted at the TRACY and SILENE reactors respectively.

For the first benchmark, representative data were selected from pulse mode experiments of both sets. The reactivity rod was inserted very rapidly assisted by a pressurised mechanism. In these transient experiments, the pattern of reactivity insertion was almost the same for both facilities. However, different features describe both sets of experiments (neutron leakage, lifetime, feedback reactivity coefficients) that help validate the transient codes in a larger area of application.

A follow-up exercise using experimental data from a ramp feed operational mode has been proposed. In the ramp feed mode, the reactivity increases when the fuel solution increases. The use of this type of experimental data will provide information about the performance of transient codes in estimating power and core pressure.

Acknowledgements

The authors express their sincere gratitude to Paul Smith (SERCO, UK) for the time he has devoted to the review and editing of this benchmark exercise.

Table of contents

List of tables

List of figures

Executive summary

In order to provide important validation and benchmarking of criticality accident analysis codes, the Expert Group on Criticality Excursion Analysis within the Working Party on Nuclear Criticality Safety in the OECD/NEA Nuclear Science Committee organised an inter-code comparison exercise involving four transient criticality codes, (AGNES, CRITEX, INCTAC and TRACE), based on typical transient criticality experiments in the TRACY and SILENE facilities. The first benchmark analyses were performed using a set of transient experiments with low- and high-enriched uranyl nitrate solutions conducted at the TRACY and SILENE facilities, respectively. Typical transient experiments encompassing a range of reactivity insertions were selected from the available database of the two transient criticality facilities. TRACY and SILENE have the same core geometry, consisting of a cylinder with central guide tube for a control rod.

For the first benchmark problems, data were selected from the pulsed mode experiments, in which the reactivity is inserted by the rapid withdrawal of the control rod. In these experiments, the reactivity insertion is close to an instantaneous, or "step" insertion of reactivity. For this mode of operation, the most important parameter is the magnitude of the inserted reactivity. The experiments chosen for Phase I of the benchmark exercise cover a range of reactivity insertions from 0.3$ to3$, thus including both delayed-critical and prompt-critical transients.

The most significant difference between the TRACY and SILENE experiments is the enrichment of the uranium fuel. The TRACY experiments use low-enriched uranium (LEU, 10% enriched in ^{235}U), whereas the SILENE experiments use high-enriched uranium (HEU, 93% enriched in ^{235}U). The two facilities consequently have different critical volumes and reactor physics parameters; neutron leakage, neutron lifetime and reactivity feedback coefficients differ between the facilities. Thus, benchmarking against experiments from these two facilities provides validation over a broad range of conditions.

In this report, the calculated power profiles, energy releases, core temperatures and pressures are compared with the measured experimental values. The codes generally simulate the major features of the criticality transients well, *i.e.* the power rise to an initial peak after which it falls towards a long-term lower value; the rise in temperature associated with the power generation; the time of gas release or the maximum pressure associated with the gas release. The calculated values mostly agree with the measured parameters to within about 20%. Significantly larger discrepancies occur in some cases; many of these are understood and result from a poor choice of value for one or more input parameters. In particular, for tests that were initialised in a subcritical condition (*i.e.* with no specified initial power) and had no external neutron source, some of the calculations significantly underestimate the time of the first power peak. This is due to the difficulty in specifying appropriate initial conditions (power and delayed neutron precursor concentrations) for the calculations for initially subcritical experiments without an external neutron source. The resulting inaccuracies in the estimated time to the first peak are not thought to have a significant impact on the other calculated parameters associated with the first peak (maximum inverse period, peak power or energy to the first peak). In addition, one set of code calculations exhibits significant discrepancies with many of the measurements for the SILENE experiments. This is believed to be due to an error in the value of the heat capacity of the fissile solution used in these calculations. It has been shown that small adjustments to the reactivity insertion can produce overall improvements in the predicted behaviour to the first power peak (*i.e.* to the inverse period, peak power and energy released to the first peak), while having little effect on the total energy.

A feature that is inconsistently reproduced by the calculations is the oscillatory behaviour that was observed in six of the eight experiments analysed. However, each of the participating codes predicts oscillatory behaviour in at least one of the experiments; though the predicted magnitude,

period and number of the oscillations often differ significantly from the observed values. When the calculations fail to predict the observed oscillations they still tend to reproduce the underlying average behaviour quite well.

The experiments analysed in this study provide important validation and benchmarking of the participating codes for short duration criticality transients in fissile LEU and HEU solutions with step reactivity insertions. However, criticality accidents can be initiated by the addition of fissile material to the system, for example the JCO accident at Tokai Mura; therefore it is important to validate the transient criticality codes for this mode of reactivity insertion. For longer duration transients, heat loss to the surroundings becomes a controlling process, which requires additional validation. Therefore, for future exercises, consideration should be given to benchmarking codes against TRACY and SILENE experiments using the ramp-feed mode of reactivity insertion (*i.e.* by feeding additional fissile solution into the reactor) and tests of longer duration.

Chapter 1: Background

A number of transient codes have been developed in several countries for the evaluation of criticality accidents in fissile solutions. These transient codes are generally used to calculate the power history, release energy, temperature and pressure of the fissile media during criticality excursions. In order to determine the accuracy of the predictions of such codes it is necessary to validate them against measured experimental data and compare them with other such codes.

Numerous transient criticality experiments have been performed in various facilities, including the TRACY facility since the 1990s and in the SILENE facility since the 1970s (Dunenfeld, 1963; Lécorché, 1973; Barbry, 1989; Nakajima, 2002b, 2002c, 2002d; Yamane, 2003; CEA, 2002). Experimental data have been accumulated for a range of excess reactivities and reactivity addition rates. However, the data obtained have not been readily available in a useful form.

In the Expert Group on Criticality Excursion Analysis within the Working Party on Nuclear Criticality Safety in the OECD/NEA Nuclear Science Committee, an inter-code comparison exercise has been performed involving four transient criticality codes, [AGNES (Nakajima, 2002a), CRITEX (Mather, 1984), INCTAC (Mitake, 2003) and TRACE (Basoglu, 1998)], based on typical transient criticality experiments in the TRACY and SILENE facilities.

Two sets of benchmarks have been performed. These benchmarks are based on experimental programmes performed in the TRACY reactor (JAERI, NUCEF, Japan) and the SILENE reactor (CEA, Valduc, France). The TRACY experiments use a solution of low-enriched (10 wt.%) uranyl nitrate solution in the reactor core, while the SILENE reactor core consists of high-enriched (93 wt.%) uranyl nitrate solution. Thus the chosen experiments provide benchmarks for both low-enriched and high-enriched uranium systems. Examples of delayed-critical and prompt-critical transients are chosen from both series of experiments.

The data from five experiments in the TRACY facility and three experiments in the SILENE facility are used to provide the initial and boundary conditions for a set of code comparison (*i.e.* benchmark) calculations. The benchmark is expected to benefit participating criticality transient codes by providing useful validation and identifying any areas requiring further development; it will also improve the general understanding of criticality accidents.

Chapter 2: Overview of experimental facilities

Both the TRACY and SILENE reactors have an annular cylindrical geometry. The core is contained within a cylindrical steel container, which has an inner cylindrical guide tube along the central axis into which an absorber rod can be inserted to control the reactivity. The annular region between the guide tube and the outer cylinder contains a solution of uranyl nitrate and nitric acid. There are a number of ways of initiating a transient in these reactors. For the experiments reported here the transients are all initiated by the rapid withdrawal of the absorber rod (in less than 0.2 s). The height of the uranyl nitrate solution for each experiment is chosen to give the desired reactivity when the absorber rod is removed. One of the tests uses an external neutron source to initiate the chain reaction. Once the transient is initiated it is allowed to run for the chosen duration before being terminated by the insertion of the absorber rod.

During the transient the temperature of the uranyl nitrate solution is measured at a number of locations and the pressure within the solution is measured at one or two points. Neutron detectors are used to determine the fission rate as a function of time. The fission rate is then used to infer the power history during the transient.

Chapter 3: Description of transient progression

3.1 The initial state

The reactor begins with the absorber rod fully inserted and therefore in a subcritical condition. In some cases the reactor is taken critical and run at a specified power to define the initial conditions for the transient.

If the reactor is left to stand for sufficient time with the absorber rod inserted, the delayed neutron precursors will reach their equilibrium concentrations. Typical decay constants and the equivalent half-lives for a six-delayed-neutron-group scheme are displayed in Table 3.1. The half-life of the longest-lived group is almost a minute. Therefore, if the system is left at constant power for an order of ten minutes the delayed neutron precursors will have time to reach their equilibrium concentrations.

Table 3.1. Decay constants and half-lives of delayed neutrons

Group	Decay constant (s^{-1})	Half-life (s)
1	0.0127	54.6
2	0.0317	21.9
3	0.115	6.03
4	0.312	2.22
5	1.40	0.495
6	3.87	0.179

The point kinetics equations relate the neutron concentration, n, (m^{-3}) reactivity, ρ, and the concentrations of the delayed neutron precursor groups, C_i (m^{-3}):

$$\frac{dn}{dt} = \frac{\rho - B}{\Lambda} n + \sum_{i=1}^{6} \lambda_i C_i + S$$
$$\frac{dC_i}{dt} = \frac{\beta_i}{\Lambda} n - \lambda_i C_i \qquad (3.1)$$

where: β = delayed neutron fraction = $\sum_i \beta_i$

β_i = delayed neutron fraction of the i^{th} group

λ_i = decay constant of the i^{th} group (s^{-1})

Λ = neutron generation time (s)

When the system is left to reach a steady state, the time derivatives in the equations approach zero and thus the initial equilibrium concentrations of the delayed neutron precursors are determined by the initial neutron concentration, which is, in turn, determined by the source and the reactivity before the absorber rod is withdrawn (see Appendix A). If an external neutron source is used in the experiment, it will determine the initial neutron density and hence the concentrations of the delayed neutron precursors. If the reactor is run at power prior to the transient, then the specified power will determine the initial neutron concentration (by dividing the power by the thermal velocity of the neutrons and the macroscopic cross-section). If the reactor is initially subcritical and no external neutron source is provided, the initial source is provided by spontaneous fission of uranium isotopes.

Note that the time scale for the reactivity insertion is the time taken to withdraw the absorber rod, which is approximately 0.15 s. This is comparable with the half-life of precursor group six and fast compared to the half-lives for the other groups. Therefore the delayed neutron precursors will not be at their equilibrium concentrations at the end of the reactivity insertion.

If the system is initially subcritical, the concentrations of the delayed neutron precursors will be small compared to the values that will apply when the reactor is critical.

3.2 The transient

The insertion of reactivity into the system results in an increase in the neutron population, as represented approximately by Eq. (3.1). The solution grows exponentially if the reactivity remains constant (see Appendix A). As the neutron flux is equal to the neutron density multiplied by the neutron speed, this implies that the flux and therefore the power would grow without limit.

However, the increase in power increases the temperature of the fissile solution. The change in temperature of the uranyl nitrate solution, in turn, changes the reactivity of the system. The effect of temperature on reactivity has been estimated by the code participants, using sophisticated neutronics codes – see Chapter 4. The analysis shows that increasing the temperature reduces the reactivity of the system. It is important to determine if the reactivity feedback limits the power transient.

The extreme case of a prompt-critical transient with negative temperature feedback on the reactivity was studied by Nordheim & Fuchs and by Fuchs & Hansen. This case is of particular relevance to the current exercise, as half of the experiments studied are prompt-critical excursions. The analysis shows that the power reaches a peak and then declines (see Appendix A). They showed that the maximum power in the pulse is simply related to the kinetics parameters, the total heat capacity of the fuel (solution), MC_p, and the temperature feedback coefficient on reactivity, α_T:

$$P_{max} = -\frac{MC_p(\rho_0 - \beta)^2}{2\Lambda\alpha_T} \tag{3.2}$$

Note the minus sign, as α_T is negative.

Once the power has peaked it starts to decline and ultimately tends to the value required to offset the heat loss from the reactor vessel when the temperature of the fissile solution is at the value required to reduce the reactivity to zero. This value is determined by the initial reactivity and the temperature feedback on the reactivity.

Temperature is not the only parameter to have an effect on the reactivity. If the radiation field becomes sufficiently intense, radiolytic gas is produced and if the fissile solution becomes hot enough boiling occurs. Both of these phenomena reduce the density and consequently increase the volume of the fissile solution. In the first approximation it is assumed that the void is introduced homogeneously throughout the solution. In this case the effective density of the fissile solution decreases and the height of the solution increases correspondingly. This causes a reduction in the reactivity of the system (see Appendix A).

Therefore the onset of radiolytic gas production and/or boiling reduces the reactivity and consequently results in lower temperatures being attained. It also provides a mechanism for producing oscillations in the experiments. The onset of gas production decreases the reactivity of the system, possibly causing it to go subcritical and terminating gas production. When the gas bubbles rise to the surface due to buoyancy, the void fraction falls thereby increasing the reactivity and causing the system to go critical again.

Other phenomena may also induce oscillatory behaviour in such a system. For instance, if gas production is inhomogeneous it can result in a non-uniform height for the fissile solution. This increases the surface area for leakage, thus reducing the reactivity and possibly making the system go subcritical. Such sloshing of the liquid therefore has the potential to induce oscillatory behaviour.

The estimates of the total number of fissions that occurred indicate that burn-up was not a significant process in these experiments.

3.3 Summary

The reactors are given time before the rod is withdrawn to ensure that the delayed neutron precursors reach their equilibrium concentrations. The rod withdrawal is too rapid to allow the equilibrium condition to be maintained during the reactivity insertion. The reactivity insertion induces an initial power pulse before the system tends to an average temperature determined by the magnitude of the reactivity insertion and the negative feedback effects on reactivity. The magnitude of the reactivity insertion and temperature feedback coefficient determine the quasi-steady-state temperature in some cases. In other cases radiolytic gas production and/or boiling further reduce the reactivity and consequently reduce the temperature rise necessary to offset the reactivity insertion. Gas production and inhomogeneous phenomena, such as sloshing of the fissile solution, may also lead to oscillatory behaviour. The duration of the transients is too short for burn-up of the fissile material to have a significant effect.

Chapter 4: Description of computer codes

Four kinetics codes, AGNES (Nakajima, 2002a), CRITEX (Mather, 1984), INCTAC (Mitake, 2003) and TRACE (Basoglu, 1998) were used for sample calculations of the benchmark problems. AGNES, CRITEX and TRACE are based on one-point kinetics approximation and INCTAC solves the neutron transport equation by the finite difference method. Brief summaries of the codes are provided in Sections 4.1 to 4.4.

4.1 AGNES

AGNES (Nakajima, 2002a) models the transient criticality of a fissile solution contained in a cylindrical vessel with vertical walls. Temperature, radiolytic gas void and boiling void feedbacks on reactivity are taken into account. Cooling by natural convection to the air outside of the reactor or forced cooling by water can be calculated. The total number of fissions is calculated based on the power profile.

4.1.1 Neutronics

The point kinetics equation with six delayed neutron precursor groups [Eq. (3.4)] is solved in AGNES2. The calculation geometry consists of three regions such as fuel, container and coolant, though neutronic behaviour is calculated in the fuel region only. The fissile solution fuel region is assumed to be homogeneous and cylindrical and is modelled using r-z co-ordinates. The effect of parameters such as temperature and volumetric expansion on reactivity can be taken into account by the use of reactivity feedback coefficients that must be calculated beforehand and supplied as user input.

4.1.2 Thermal-hydraulics

Average values are used to represent the temperature in each of the regions (fuel, container and coolant). Fission energy is generated in the fuel region and is transferred to the container. Heat is then transferred from the container to the surrounding coolant.

The temperatures, denoted by T_i, are calculated from the energy equation:

$$V_i\left(\rho C_p\right)_i \frac{\partial T_i}{\partial t} = \gamma_i P V_i + \left(hA\right)_{i-1}\left(T_{i-1} - T_i\right) - \left(hA\right)_i\left(T_i - T_{i+1}\right) \tag{4.1}$$

where i denotes region number (1 for fuel, 2 for container and 3 for coolant).

The first term of the right-hand side is the energy released in region i, and the second and third terms represent the energy transferred from or to the adjacent regions (note that the second term is absent for region 1 and the third term is absent for region 3). The heat transfer from the container region via conduction to the structural materials connected directly to the container and via natural convection to the surrounding air is calculated.

4.1.3 Radiolytic gas

The energy model is modified to incorporate radiolytic gas production. The following assumptions are made in the model:

- Radiolytic gas is created in proportion to the power.
- Once the concentration of radiolytic gas exceeds a threshold it gives rise to void within the fissile solution that affects the reactivity via user supplied reactivity feedback coefficients.

- The growth rate of void is proportional to the power and the excess radiolytic gas concentration above the threshold.
- The void rises to the surface due to buoyancy and disappears.

The main parameters of the radiolytic gas model are:

- $C_{i,j}$, the molar density of radiolytic gas in mesh (i,j) (mol m^{-3}).
- F_{ij}, the void fraction in a mesh (i,j).
- ν_t, the void-energy transfer coefficient ($m^6\ J^{-1}\ mol^{-1}$).
- C_0, the saturation molar density of dissociation gas (mol m^{-3}).
- G, the gas production rate constant (mol J^{-1}).

4.1.4 Calculation of user input parameters

The atomic number densities for the fuel solution are calculated using the SST (Sakurai, 1996) formula developed by JAERI. Using those values, kinetic parameters such as delayed neutron fraction, etc., are estimated using the SRAC (Okamura, 1996) and TWODANT (Alcouffe, 1995) codes with JENDL-3.2 (Nakagawa, 1995) nuclear data library, as were the temperature and void reactivity feedback coefficients. In each simulation, the temperature and void reactivity feedback coefficients are used with a weight, to allow for the effect of inhomogeneous temperature and void distributions. The weight is initially set to 1.6 and was then changed to be unity exponentially with time to represent convective mixing due to thermal expansion and/or void production.

4.2 CRITEX

CRITEX (Mather, 1984) models the transient criticality of a fissile solution contained in an open cylindrical vessel with vertical walls, so that the solution is able to expand vertically (*e.g.* due to thermal expansion or the production of radiolytic gas bubbles). Vertically the solution is divided with axial meshes into a number of volumes that allow the axial movement of the solution to be calculated along with the resulting effect on the reactivity.

4.2.1 Neutronics

The point kinetics equation [Eq. (3.1)] is solved to calculate the total power. The energy deposited in the axial volumes is calculated based on the power profile corresponding to the fundamental eigen-mode, i.*e.* a cosine axial distribution.

4.2.2 Thermal-hydraulics

Within the fissile solution mixing is included via a mixing time constant, M (s^{-1}) such that the temperature, T, is driven towards the mean temperature, T_{av}, via the relationship:

$$\delta T = -M(T - T_{av})\delta t \tag{4.2}$$

where δT is calculated temperature change due to fission energy, and δt is a time step.

If boiling occurs the temperature change is calculated taking into account the two-phase nature of the fluid, using values from inbuilt steam tables. Heat loss to the surrounding air is calculated using an estimated heat transfer coefficient.

4.2.3 Radiolytic gas

Radiolytic gas bubble migration is modelled by means of a conservation equation, in terms of B, the volume of radiolytic gas per unit mass of liquid, V, the bubble rise velocity, and C/C_0 the concentrations of gas away from/at the bubble surface, respectively:

$$\frac{\partial B}{\partial t} + V\frac{\partial B}{\partial z} = X(C - C_0) \tag{4.3}$$

The source rate constant for gas release, X, is obtained from an empirical correlation with the maximum inverse time period, ω_{max}:

$$X = 0.0275\omega_{max} \tag{4.4}$$

The concentration, C, of dissolved gas in solution, is determined by the energy deposition due to fission fragments and is directly related to the local power. The value of C_0 is determined by the partial pressure, p_{rg}, of radiolytic gas in the bubble, via the Henry's law constant, $K(T)$:

$$p_{rg} = K(T)C_0 \tag{4.5}$$

For nucleation of radiolytic gas bubbles to commence, a threshold of 10^{15} fissions/l has to be attained.

4.2.4 Calculation of user input parameters

Kinetics parameters such as neutron lifetime, delayed neutron constants, Doppler coefficients, etc., are tabulated as internal data (calculated using the WIMS or APOLLO deterministic neutronics codes). For tests initiated in a subcritical state and without an external neutron source, the SOURCE 4C code (Wilson, 2002) is used to estimate the neutron source intrinsic to the fissile solution, *i.e.* the number of neutrons originating from (α,n) reactions and spontaneous fission.

4.3 INCTAC

INCTAC (Mitake, 2003) is applicable to the analysis of criticality accidents in aqueous homogeneous fuel solution systems.

4.3.1 Neutronics

A number of neutronics modelling options are available, including point kinetics, diffusion theory or transport perturbation theory. The transient neutronics model is composed of equations for the kinetics and for the spatial distribution, which are deduced from the time-dependent multi-group transport equations with a quasi-steady-state assumption.

4.3.2 Thermal-hydraulics

Heat transfer is solved in a pseudo three-dimensional (r,θ,z) calculation. The fluid flow model is a two-phase flow model with liquid and gas phases. The thermal-hydraulic transient model is composed of a set of six differential equations for the mass, momentum and energy. This includes terms to represent the momentum and energy transfer between the phases and the friction loss and heat transfer at wall surfaces.

4.3.3 Radiolytic gas

The radiolytic gas concentration is calculated as follows:

$$\frac{\partial C}{\partial t} + \nabla \cdot (Cv_l) = \Gamma_{mol} = GN : \text{before saturation } (C < C_0) \tag{4.6}$$

where: v_l = liquid flow velocity [m/s]

$\Gamma_{mol} = GN$ = radiolysis gas generation rate [(mol/m^3)/s]

$C = C_0$ = after the saturation ($C \geq C_0$)

The gas (void) generation rate is:

$$\Gamma = M_a GN \tag{4.7}$$

where: Γ = radiolysis gas (void) generation rate [(kg/m^3)/s]

M_a = molecular weight of radiolysis gas [kg/mol]

G = energy to generate radiolysis gas [mol/J]

N = power density [watt/m^3]

C = radiolysis gas concentration [mol/m^3]

C_0 = radiolysis gas saturation (threshold) concentration [mol/m^3]

Mass conservation of non-condensable gas (void) is determined as follows:

$$\frac{\partial \alpha \rho_a}{\partial t} + \nabla \cdot \left(\alpha \rho_a v_g\right) = 0 \tag{4.8}$$

where: α = void fraction [-]

ρ_a = density of void [kg/m^3]

v_g = void flow velocity [m/s]

4.3.4 Calculation of user input parameters

The atomic number densities are calculated using the SST (Sakurai, 1996) formula. The neutron cross-sections used are based on the SCALE-4.4 44-group library. Delayed neutrons are evaluated using SRAC95 (Okamura, 1996) with the JENDL-3.2 (Nakagawa, 1995) nuclear data library.

Based on the atomic compositions and the neutron cross-sections from the JENDL-3.2 nuclear data library, the macroscopic effective cross-sections, collapsed to as low as nine groups, are evaluated with SRAC, a general purpose nuclear calculation code developed in JAERI. The cross-sections are then converted to formulae of the following forms using the least-squares fitting technique:

$$\Sigma_X^g = \Sigma_{X,0}^g + A_1(\rho - \rho_0) + A_2(\rho - \rho_0)^2 + (1 + A_3\rho)\left(\sqrt{T} - \sqrt{T_0}\right)\left\{A_4 + A_5\left(\sqrt{T} - \sqrt{T_0}\right)\right\} \tag{4.9}$$

where: Σ_X^g = macroscopic effective cross-section of nuclear reaction X of energy group g, for fuel solution of temperature T and density ρ (cm^{-1})

$\Sigma_{X,0}^g$ = macroscopic effective cross-section of nuclear reaction X at base state, for energy group g (cm^{-1})

A_1-A_5 = fitting constants

ρ = fuel solution density (g cm^{-3})

T = fuel solution temperature (K)

ρ_0 = fuel solution density at base state (g cm^{-3})

T_0 = fuel solution temperature at base state (K)

Nuclear kinetics parameters for the fuel solution of the SILENE experiments are also evaluated with SRAC: delayed neutron fractions (β_i and β_{eff}), decay constants (λ_i) and spectra (allocated to the first three groups of the nine-group energy structure) of the delayed neutrons (in six groups).

4.4 TRACE

4.4.1 Neutronics

The TRACE (Basoglu, 1998) code adopts the point kinetics approximation with six-group neutron precursors. The code assumes that calculations begin when the system attains delayed criticality ($k_{eff} = 1$) at time zero. The spatial power distribution is assumed constant during transients. The effect of the fissile solution temperature and void fraction on reactivity are taken into account using reactivity feedback coefficients. The fuel solution region is divided into coarse meshes in a 2-D cylindrical geometry. The effect on reactivity of fissile solution temperature changes and void generation are calculated by using a spatial weighting function. For the present benchmark calculations the power weighting function is adopted, *i.e.* cosine dependence axially and J_0 Bessel functions dependence radially.

4.4.2 Thermal-hydraulics

The heat transfer model in the fissile solution is represented by a transient heat conduction model in 2-D cylindrical co-ordinates. The spatial distribution of heat generation from fission reactions is assumed constant during the simulation (represented by cosine and J_0 Bessel functions in the axial and radial dimensions, respectively). The effect of complex fluid motion on the distribution of solution temperature is modelled by a temperature mixing parameter. The vessel is divided into two regions, the side wall and the bottom. The heat transfer from the vessel walls to the surrounding air is approximated by natural convection. The natural convection heat transfer coefficients (at the inner and outer sides of the vessel walls) are calculated inside the code. Different coefficients are used for horizontal and vertical surfaces.

The TRACE code does not solve the fluid flow equations within the fissile solution region. However, a strong acceleration of the fuel solution may take place during criticality transients due to sudden nucleation and growth of gas bubbles. In order to estimate the system pressure the TRACE code adopts an equation of motion in which the fissile solution is treated as one region and the pressure is a linear function of height. It is also assumed that the fuel solution is contained in an open vessel with vertical cylindrical walls so that the liquid can expand and move only in the vertical direction and friction effects are ignored. The above assumptions should be borne in mind when interpreting the calculated pressures. In particular, the sharp pressure peak in the vicinity of the first power peak cannot be accurately estimated with the open vessel condition.

4.4.3 Radiolytic gas

The radiolytic gas modelling of the TRACE code mainly consists of two models, one for radiolytic gas bubble nucleation and another for the gas bubble velocity. The main parameters for this model are the G value (proportional to the number of radiolytic gas molecules formed for each 100 eV of energy absorbed by the system (mol/J) and the critical number of moles of radiolytic gas per unit void volume (mol/m^3). It should be noted here that, although the fissile solution region is divided into coarse meshes in a 2-D cylindrical geometry, the bubble movement is treated in the axial direction only (no bubble movement in the radial direction). For the gas bubble velocity a model which is originally based on the CRITEX code empirical model is adopted, where a continuous function of bubble velocity is developed based on the absolute value and the sign of the inverse period. The absolute value of the inverse period is a measure of how fast the power is changing and the sign of the inverse period is set to -1, 0 and 1 for negative (decreasing power), zero (local minima or maxima) and positive inverse period (increasing power), respectively.

4.4.4 Calculation of user input parameters

The kinetic parameters (delayed neutron fractions, prompt neutron lifetime, neutron generation time, temperature coefficients and void coefficients) are determined by using the SRAC code system with

the JENDL-3.2 nuclear data library. First, using SRAC's PIJ module (1-D collision probability method) transport group constants are prepared in 107 neutron energy groups for each region, *i.e.* the fuel, vessel and surrounding air. Then, using SRAC's ANISN module (1-D neutron transport approximation, S8 P1, cylindrical geometry) 16 group diffusion constants are prepared. SRAC's CITATION module (neutron diffusion approximation, cylindrical geometry) is then used for estimating the delayed neutron fractions, prompt neutron lifetime and neutron generation time. The temperature coefficients are calculated using SRAC's TWOTRAN module to evaluate the reactivity for five different fissile solution temperatures (up to a maximum of 100°C and allowing for thermal expansion) and then applying second-order polynomial fitting to obtain the coefficients. Similarly, the void coefficients are calculated by evaluating the reactivity at four different fissile solution densities (up to a maximum of 60%), keeping the fuel solution temperature constant (at room temperature) and then fitting a second-order polynomial to obtain the coefficients.

Chapter 5: TRACY benchmark description

5.1 Overview

The TRACY benchmark problems consist of a low-enriched uranyl nitrate solution in an annular cylindrical steel tank. The central channel in the tank is a guide tube containing a control rod. Three methods of reactivity insertion are available in the TRACY facility. In this benchmark, experiments with pulsed reactivity insertion are investigated; that is the simplest method of reactivity insertion for the TRACY facility. In this method the tank is filled with the fissile solution to the desired height, with the control rod inserted. The transient is started by rapidly withdrawing the control rod to achieve the desired reactivity insertion. The selected experiments, their ID numbers and their associated excess reactivity insertions are displayed in Table 5.1.

Table 5.1: Benchmark experiments and reactivity insertion

ID number	Run number	Excess reactivity ($)
001	100	0.30
002	143	0.70
003	72	1.10
004	196	2.00
005	203	2.97

The annular core tank is made of SUS304L stainless steel and is shown in Figure 5.1.1. There is a guide tube in the centre containing a boron carbide (B_4C) control rod, referred to as the transient rod or Tr-rod, for short. After pumping fuel solution into the core tank, the Tr-rod is withdrawn from the core in order to insert reactivity. The desired reactivity is achieved by tuning the height (and consequently the volume) of the fuel solution. During the criticality excursion the power, temperature and core pressure are measured. At the end the Tr-rod is inserted to shut down the system.

5.2 Geometry specification

Detailed geometrical information is provided in Figures 5.2.1, 5.2.2 and 5.2.3. The core tank has an annular shape with a 52 cm outer diameter and 7.6 cm inner diameter. The effective cross-sectional area for the fuel solution is 1 918 cm^2. The position of the Tr-rod in Figure 5.2.3 means that the bottom of the boron carbide inside the Tr-rod is 90 mm below the bottom of the fuel solution. The solution height is measured using a needle-type level gauge with an accuracy of ±0.25 mm.

Figure 5.1.1: Photograph of the TRACY reactor tank

Figure 5.2.1: Schematic view of the TRACY reactor tank

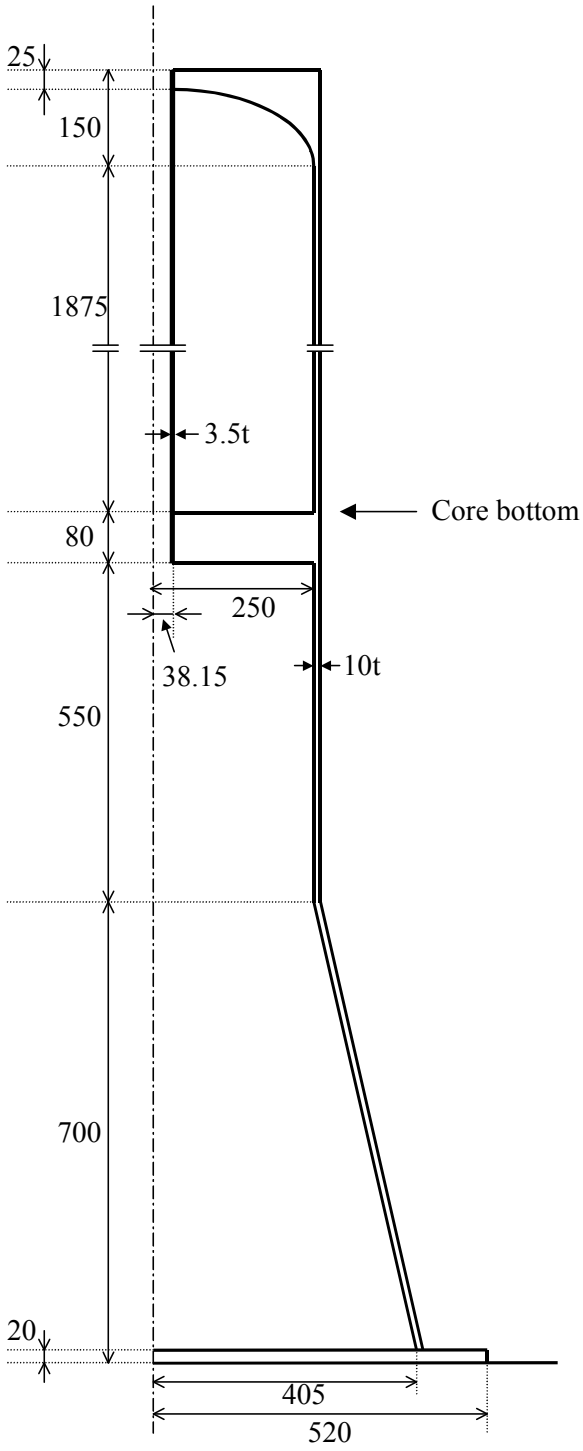

Figure 5.2.2: Detailed views of the TRACY reactor tank

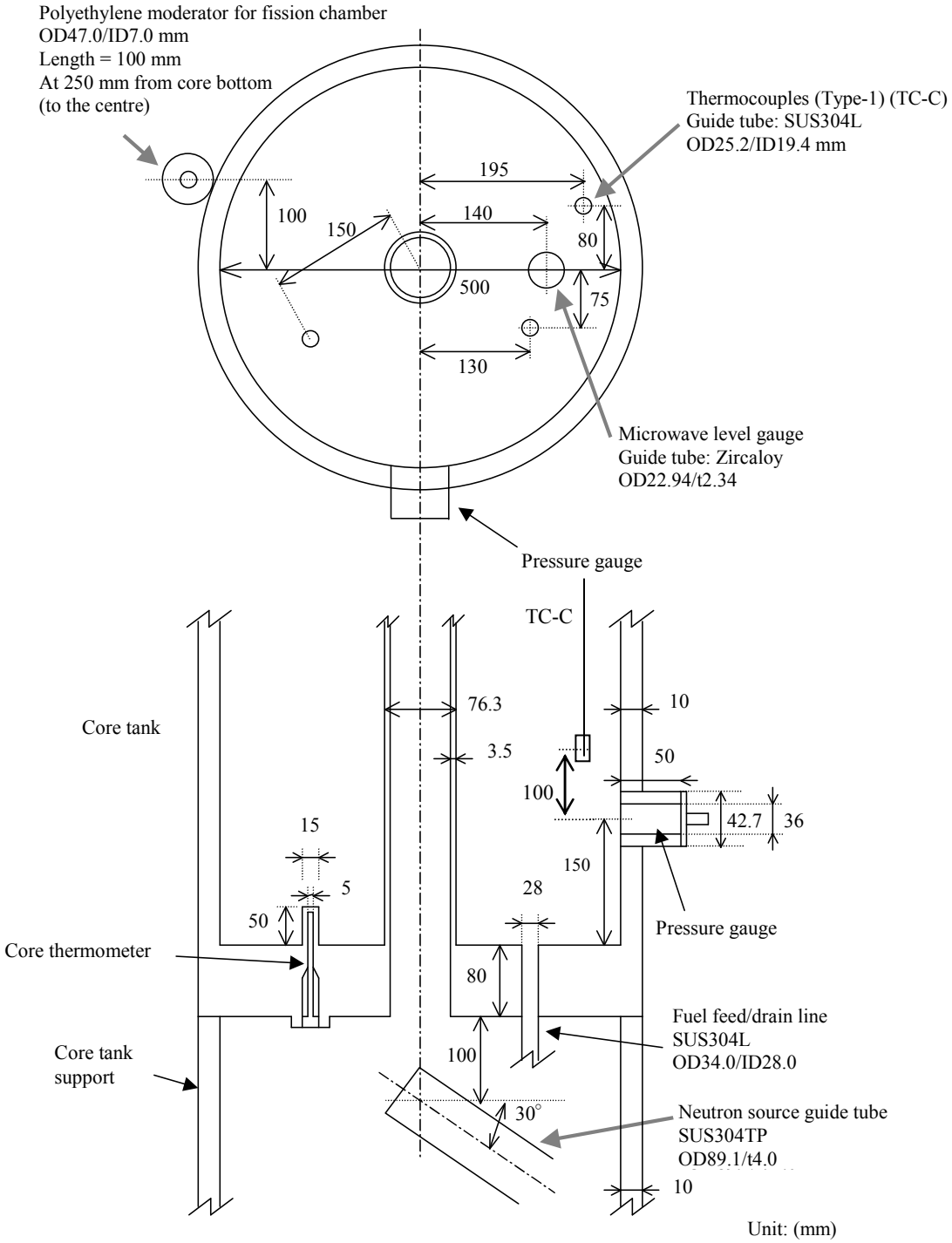

Figure 5.2.3: Details of the transient rod

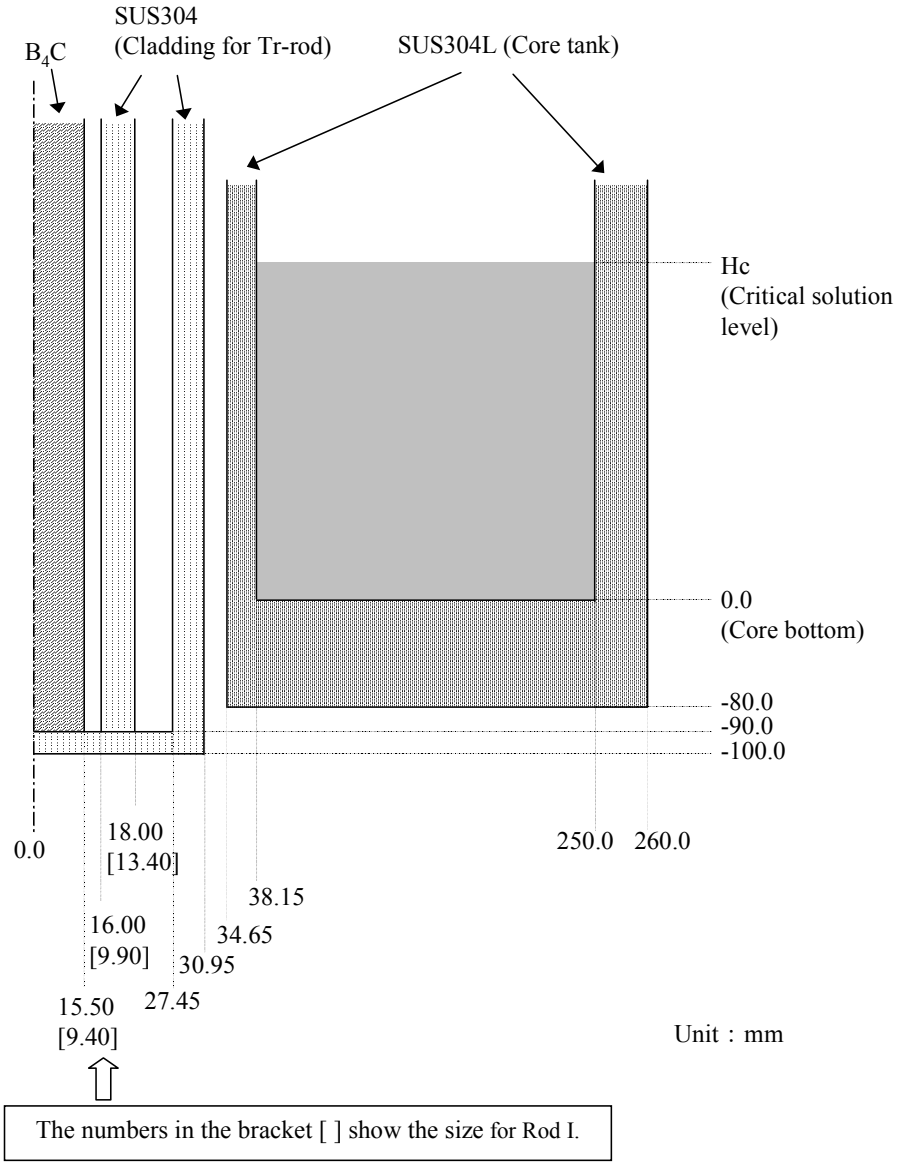

5.3 Material data

The fuel solution is uranyl nitrate solution, which consists of uranyl nitrate [$UO_2(NO_3)_2$], free nitric acid [HNO_3] and water [H_2O]. The enrichment of the ^{235}U fuel is 9.98 wt.%. The uranium concentration and acidity in each of the tests is given in Table 5.3.1.

Table 5.3.1: Fissile solution specification and inserted reactivity at 25°C

ID	Run no.	IR ($)	U conc. (gU/L)	Acidity (N)
001	100	0.30	392.9	0.66
002	143	0.70	375.9	0.64
003	72	1.10	393.5	0.74
004	196	2.00	385.5	0.58
005	203	2.97	388.2	0.58

N = normal = mol/litre for nitric acid

A typical atomic composition for the fissile solution is given in Appendix B, along with the derived kinetics parameters (multiplication factor, delayed neutron fraction, prompt neutron generation time). These data can be used to perform approximate transient calculations.

The composition of the steel is shown in Table 5.3.2, and the approximate atomic composition of air is shown in Table 5.3.3.

Table 5.3.2: Atomic number densities of SUS304L at 25.5°C

Nucleus	Number density (atoms/barn.cm)
C	1.1939×10^{-4}
Si	1.7004×10^{-3}
Cr	1.7450×10^{-2}
Mn	1.7385×10^{-3}
Fe	5.7180×10^{-2}
Ni	8.9482×10^{-3}
S	4.4682×10^{-5}

Table 5.3.3: Atom number densities of air at 25.5°C

Nucleus	Number density (atoms/barn.cm)
O16	1.0295×10^{-5}
N14	3.8376×10^{-5}

5.4 External neutron source

No external neutron source is used for these experiments.

5.5 Initial states

In each experiment, the reactivity is inserted by rapid withdrawal of the transient rod, and there is no external neutron source. The initial conditions are displayed in Table 5.5.1.

Table 5.5.1: Selected experiments and their initial states

ID	Run no.	Inserted reactivity ($)	Initial state			
			Criticality (power)	Sol. level (mm)	Fuel temp. (°C)	Tr-rod position (mm)
001	100	0.30	Cri. (1 W)	508.52	26.2	471.7
002	143	0.70	Sub	551.83	24.8	0.0
003	72	1.10	Sub	537.05	26.2	0.0
004	196	2.00	Sub	582.50	25.9	0.0
005	203	2.97	Cri. (1 W)	623.76	26.1	0.0

5.6 Reactivity insertion

In each experiment, the Tr-rod is initially fully inserted and is fully withdrawn within 0.2 seconds. The desired reactivity was achieved as follows:

1) The critical solution height with the Tr-rod fully withdrawn, H_c, is measured. From Eq. (A.14), this corresponds to a critical buckling, B_c of:

$$B_c^2 = \left(\frac{2.405}{R+\lambda_R}\right)^2 + \left(\frac{\pi}{H_c+2\lambda_H}\right) \tag{5.1}$$

From Eq. (A.13), with reactivity equal to zero the critical buckling must also satisfy:

$$0 = \frac{k_\infty - 1 - M^2 B_c^2}{k_\infty} \tag{5.2}$$

2) The solution level, H, corresponding to the desired reactivity, ρ_I, for the experiment is determined by subtracting Eq. (5.2) from Eq. (A.13) and using Eq. (A.14) to yield:

$$\rho_I = \frac{M^2}{k_\infty}\left(B_c^2 - B^2\right) = \frac{C}{2}\left\{\frac{1}{(H+2\lambda_H)^2} - \frac{1}{(H_c+2\lambda_H)^2}\right\} \tag{5.3}$$

where $C = \dfrac{2\pi^2 M^2}{k_\infty}$.

The values of C and λ_H are determined by noting from Eqs. (A.13) and (A.14) that the derivative of the reactivity with respect to the solution height is given by:

$$\frac{\partial \rho}{\partial h} = \frac{2\pi^2 M^2}{k_\infty (H+2\lambda_H)^3} = \frac{C}{(H+2\lambda_H)^3} \tag{5.4}$$

This equation has been fitted to experimental data, yielding the values $C = 7.67 \times 108$ (cent mm^{-2}) and $2\lambda_H = 0.102$ m.

3) The solution level is raised to the desired level H with the Tr-rod fully inserted.

4) The Tr-rod is withdrawn pneumatically at time 0.

5.7 Detector/measurement systems

The reactor power, fuel solution temperature and core pressure are all measured, as described below.

5.7.1 Measurement of power levels

There are three neutron detectors. Two are linear channels and one is a log channel. They are positioned on the ceiling of the core room right above the core tank as shown in Figure 5.7.1. The log detector is a

cadmium-covered ^{235}U fission chamber which is covered with 10-mm thick polyethylene and 1-mm thick cadmium in order to detect epithermal neutrons. It is placed in lead shielding 10-cm thick to reduce the noise due to gamma rays and is positioned about 2.5 m above the core. The power profile measured with the log channel is adjusted so that the total released energy estimated from the integral of the power profile fits to the total released fissions estimated from the analysis of the fission products, and is used as the benchmark data. The calibration of neutron instrumentation for power measurement is based on the chemical analysis of the fission products. Analysis of the fission products by gamma rays has error of about 5% including that of the detection efficiency and the total count. The uncertainty on the power measurement is between 5% and 10%.

There is a difference in measured values between the log channel and the linear channels. The difference is less than 5% for reactivity insertions less than 1.5$. However, it increases as the inserted reactivity increases. The peak difference is about 17% for R196 (2.0$) and about 48% for R203 (2.97$). Most of the log channel measurements are higher than the linear channel data.

5.7.2 Temperature measurement

Almel-chromel thermocouples are used to measure the temperature distribution of the fissile solution. Type-1 group thermocouples are used for all experiments, which have a response time of 0.1 to 1 s and an accuracy of ±1.5°C. Ten thermocouples are placed in the reactor tank, situated vertically in line at 10-cm intervals. Details of the instrument placement are shown in Figure 5.7.1.

5.7.3 Measurement of pressure levels

The fissile solution pressure is measured with a pressure gauge installed in the side wall of the reactor tank. The pressure is measured for tests with reactivity insertions exceeding 1.5$ (*i.e.* tests R196 and R203 in this case). The base line of the pressure measurements decreased after the first power peak. The reason for this is not understood, but it may be due to the change of the fissile solution temperature and/or noise due to radiation.

Figure 5.7.1: Layout of instruments

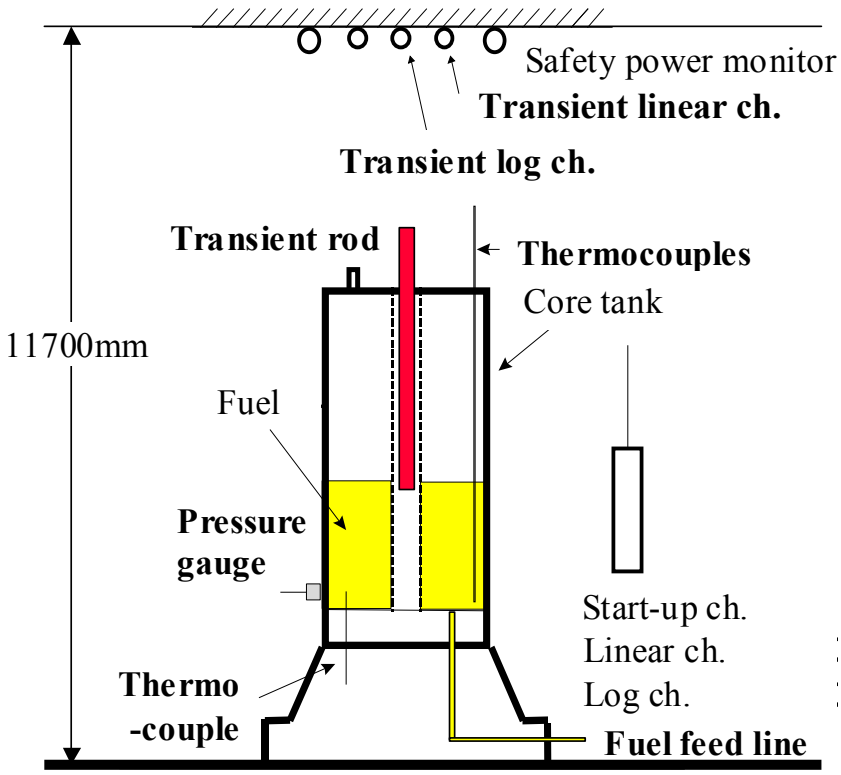

Figure 5.7.2: Position of Type-1 thermocouples

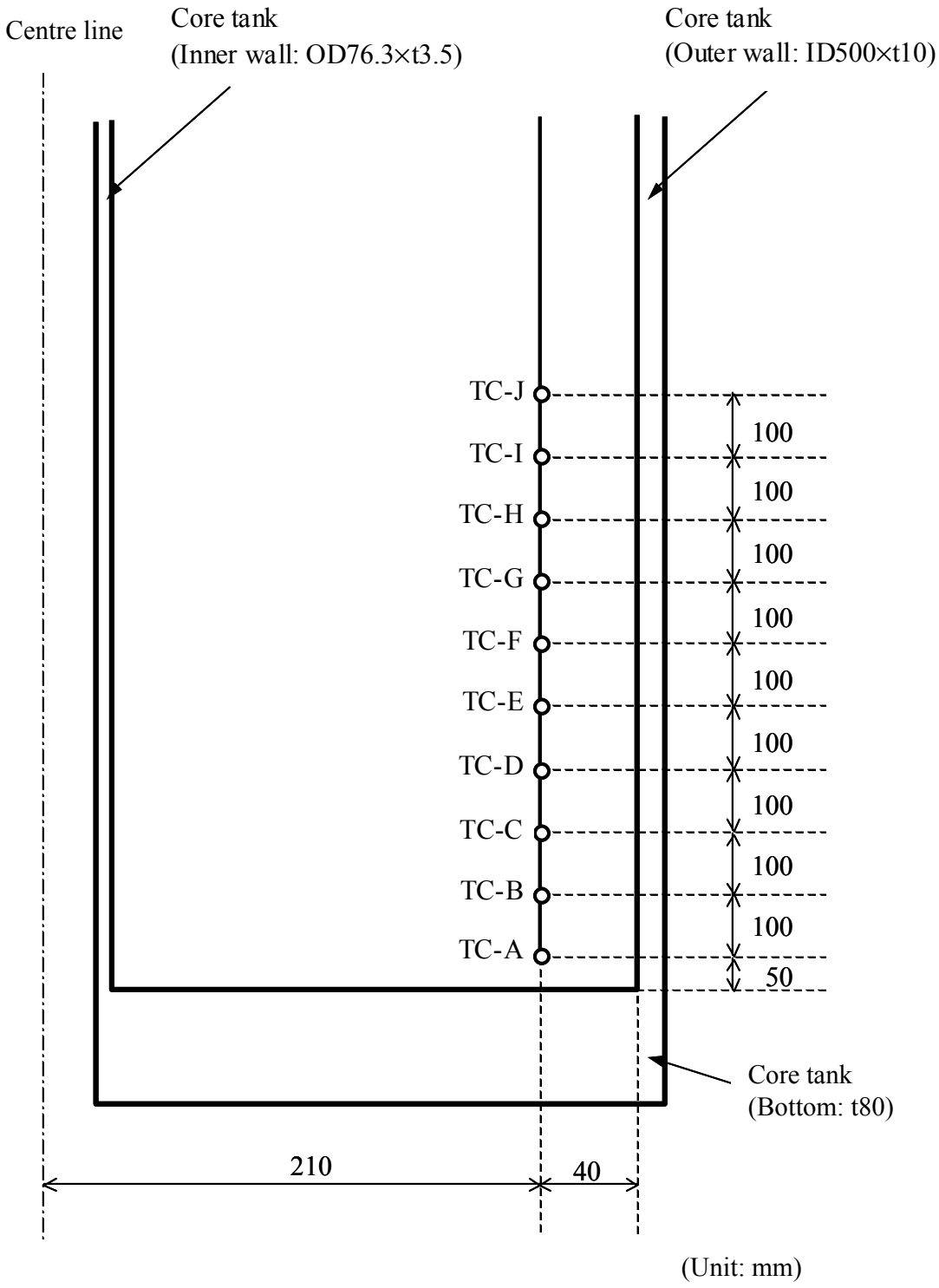

Chapter 6: TRACY experimental results

The main results from each of the five tests are presented in Table 6.1 and are further discussed in Sections 6.1 to 6.5.

Table 6.1: Summary of measured results for STEP-001 to STEP-005

Items	001	002	003	004	005
Max. inverse period (s^{-1})	0.0651	0.629	25.5	169	334
Time to first peak (s)	189.39	39.313	1.5756	0.344	0.1854
No. of min. periods to first peak	12.3	24.7	40.2	58.1	61.9
Power at first peak (MW)	0.0316	0.372	14.4	566	2080
Energy to first peak (MJ)	1.47	1.78	1.10	6.09	10.3
Fissions to first peak $\times 10^{-17}$	0.458	0.555	0.343	1.90	3.20
Time to first minimum (s)	–	–	14.23	–	–
Power at first min. (kW)	–	–	37.7	–	–
Energy to first min. (MJ)	–	–	8.75	–	–
Fissions to first min. $\times 10^{-17}$	–	–	2.74	–	–
Total energy (MJ)	4.20	4.80	10.3	11.1	20.3
Total fissions $\times 10^{-17}$	1.31	1.50	3.22	3.48	6.32
Initial temperature (°C)	26.2	24.8	26.2	25.9	26.1
Final temperature (°C)	36.2	35.8	50.8	51.5	66.7
Max. pressure (bar)	–	–	–	3.04	8.95

6.1 Results for STEP-001 (R100)

The power history is plotted in Figure 6.1.1. The power rises to a peak value of 31.6 kW after 189.39 s. The measured fission energy up to this time is 1.47 MJ, corresponding to a total of 4.48×10^{16} fissions. The measured maximum inverse period is 0.0652 s^{-1} and it takes 12.3 minimum periods (the inverse of the maximum inverse period) to reach the first peak. After the power has peaked it falls off monotonically to a value of just under 1 kW by the time the test is terminated, after about 555 s. The total energy released by this time is 4.20 MJ, corresponding to 1.31×10^{17} fissions. There is no evidence of any oscillatory behaviour in this test.

The temperature history from thermocouple TC-C is plotted in Figure 6.1.2. The temperature rises smoothly to approach an asymptotic value towards the end.

6.2 Results for STEP-002 (R143)

The power history is plotted in Figure 6.2.1. The power rises to a peak value of 372 kW after 39.313 s. The measured fission energy to this time is 1.78 MJ, corresponding to a total of 5.55×10^{16} fissions, which is a 21% increase over STEP-001. Thus, although the time to reach the first peak is roughly five times less than STEP-001, the power is much higher and results in a larger energy release by the time the first peak is reached. The measured maximum inverse period is 0.629 s^{-1} and it takes 24.7 minimum periods to reach the first peak. After the power has peaked it falls off until around 60 s when it starts to increase again before the test is terminated, after about 73 s. The total energy released by the end is 4.80 MJ, corresponding to 1.50×10^{17} fissions. There is clear evidence of oscillatory behaviour in this test.

The temperature history from thermocouple TC-C is plotted in Figure 6.2.2. The temperature rise is very spiky in this case. As TC-C provides a point measurement the variations probably reflect

temperature differences in the solution being convected past the measurement point. If this is the case the large rise just before 50 s indicates that temperature differences of a few degrees exist at that time. The temperature is still rising at the end of the test, indicating that the asymptotic temperature has not yet been reached.

6.3 Results for STEP-003 (R72)

The power history is plotted in Figure 6.3.1. This shows the power rising to an initial peak value of 14.4 MW after 1.5756 s. The measured fission energy to this time is 1.10 MJ, corresponding to a total of 3.43×10^{16} fissions, which is 38% less than STEP-002 and 25% less than STEP-001. This is the first prompt-critical transient in the series reported here. This results in a much faster transient, with the time to reach the first peak being 25 times shorter than for STEP-002. The increase in the peak power is insufficient to compensate for such a large reduction in the time scale and so the number of fissions and the energy released up to the time of the first peak is less than for STEP-002 or STEP-001. The measured maximum inverse period is 25.5 s^{-1} and it takes 40.2 minimum periods to reach the first peak. After the power has peaked it falls to a minimum of 37.7 kW at 14.23 s. The power then increases again before the test was terminated, after about 138 s. The total energy released by the end is 10.3 MJ, corresponding to 3.22×10^{17} fissions. There is clear evidence of oscillatory behaviour in this test.

The temperature history from thermocouple TC-C is plotted in Figure 6.3.2. The temperature rise is reasonably smooth, but there are indications of temperature differences of the order of a few degrees in the fluid at around 10 s. The impact of the second power peak at around 30 s is also evident. The temperature is still rising at the end of the test, but appears to be getting close to the asymptotic value.

6.4 Results for STEP-004 (R196)

The power history is plotted in Figure 6.4.1. The figure shows the power rise to the peak value of 566 MW after 0.344 s. The measured fission energy to this time is 6.09 MJ, corresponding to a total of 1.90×10^{17} fissions, which is a factor of 39.3 times greater than STEP-003. The measured maximum inverse period is 169 s^{-1} and it takes 58.1 minimum periods to reach the first peak. After the power has peaked it falls to a minimum of around 100 kW at roughly 0.8 s. There is then evidence of further oscillatory behaviour, superimposed upon a decreasing trend, until the test was terminated, after a little under 19 s. The total energy released by the end is 11.1 MJ, corresponding to 3.48×10^{17} fissions.

The temperature history from thermocouple TC-C is plotted in Figure 6.4.2. There is significant structure in the observed temperature rise over the first 7 s, though it is difficult to determine to what extent this reflects structure in the power history and how much is due to temperature variations in the solution. After 10 s the temperature levels off at the asymptotic value.

The pressure rises to a peak of 3.04 bar in this test, indicating the release of a significant amount or radiolytic gas.

6.5 Results for STEP-005 (R203)

The power history is plotted in Figure 6.5.1. This shows the power rise to the peak value of 2 080 MW after 0.1854 s. The measured fission energy to this time is 10.3 MJ, corresponding to a total of 3.20×10^{17} fissions, which is 69.1% greater than STEP-004. The measured maximum inverse period is 334 s^{-1} and it takes 61.9 minimum periods to reach the first peak. After the power has peaked it falls to a minimum of just over 100 kW after 0.5 s. There is then further oscillatory behaviour, superimposed upon an increasing trend until around 4 s, followed by a decreasing trend, until the test was terminated, after a little under 8 s. The total energy released is 20.3 MJ, corresponding to 6.32×10^{17} fissions.

The temperature history from thermocouple TC-C is plotted in Figure 6.5.2. The temperature rises rapidly and reasonably smoothly, though there are suggestions of temperature variations in the solution of the order of a few degrees at around 2 s. After that the temperature starts to level off at the asymptotic value.

This shows that the pressure rises to a peak of 8.95 bar, indicating the release of a significant amount or radiolytic gas.

Figure 6.1.1: Measured power data for STEP-001

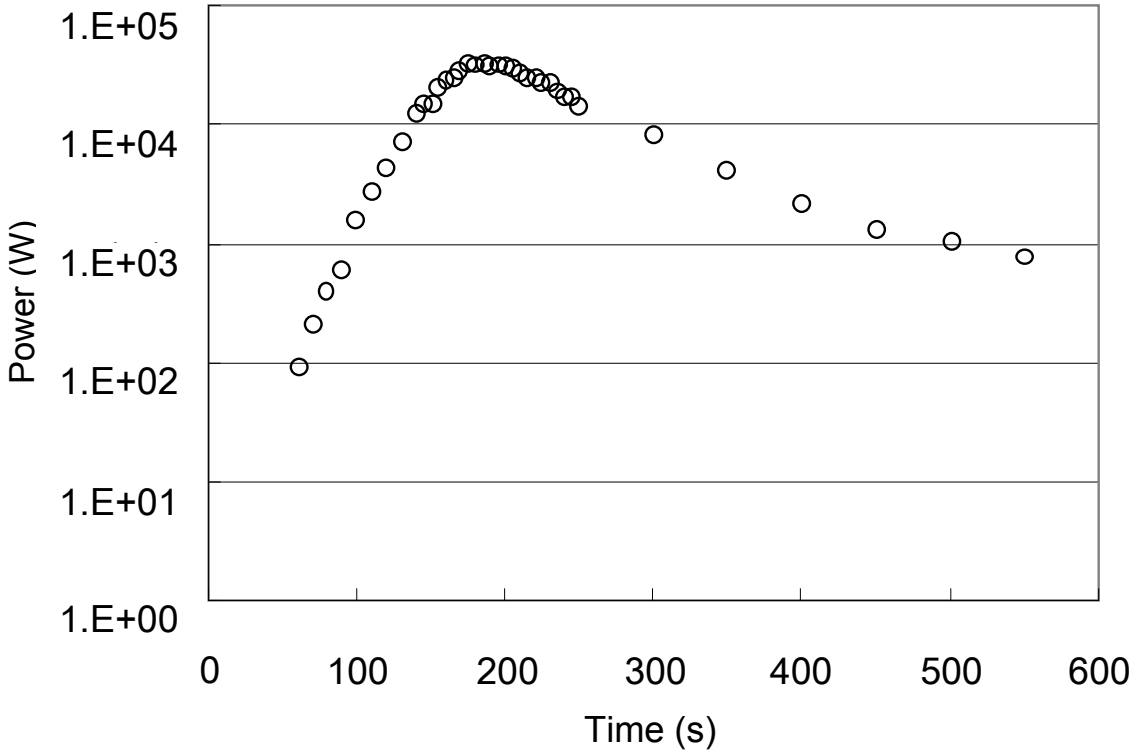

Figure 6.1.2: Measured temperature data for STEP-001

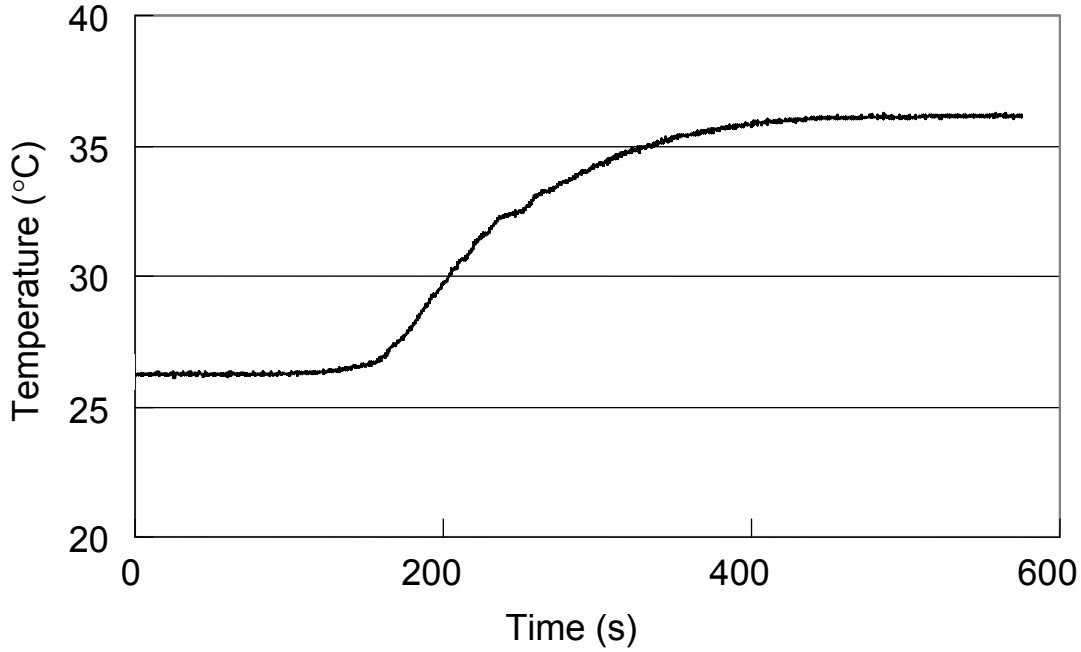

Figure 6.2.1: Measured power data for STEP-002

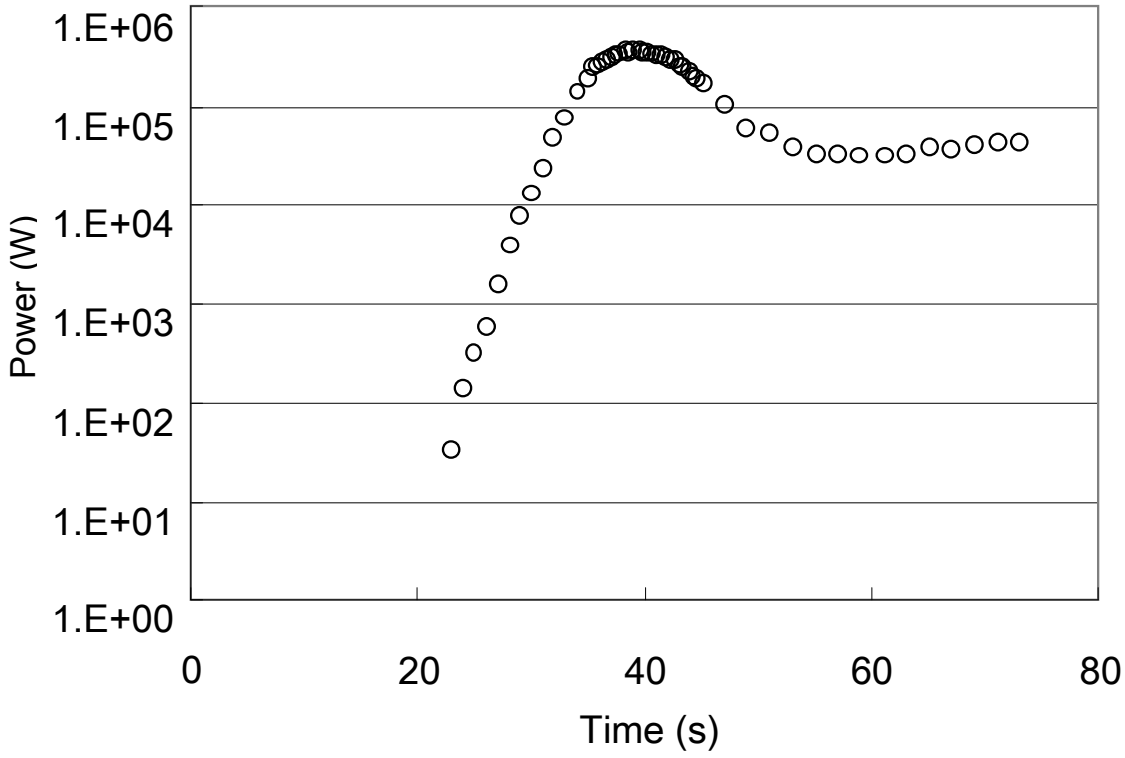

Figure 6.2.2: Measured temperature data for STEP-002

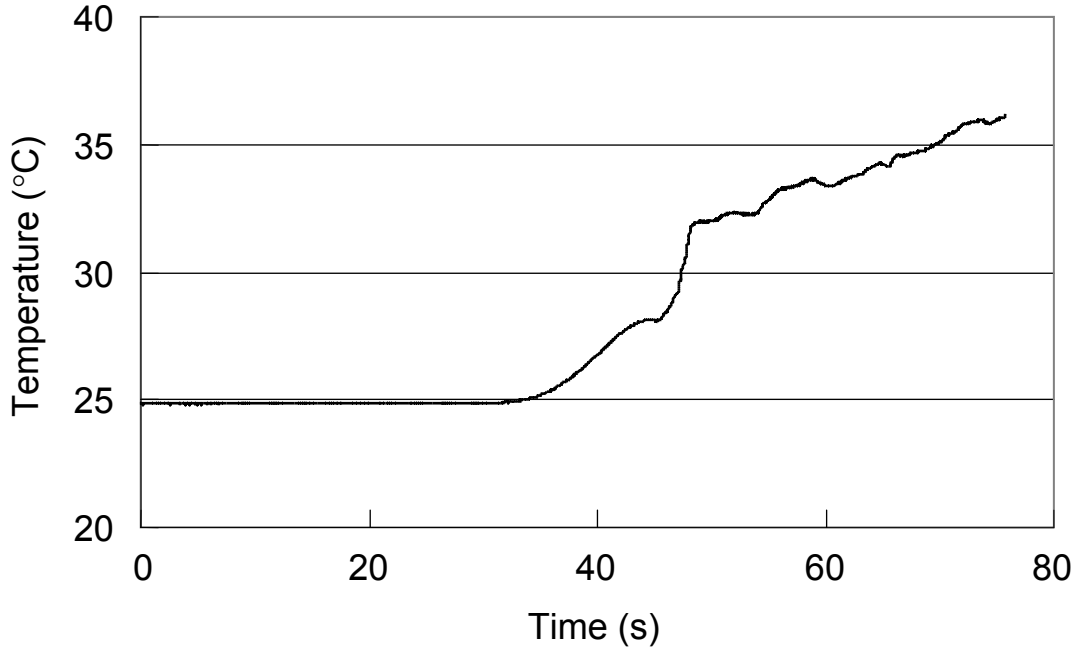

Figure 6.3.1: Measured power data for STEP-003

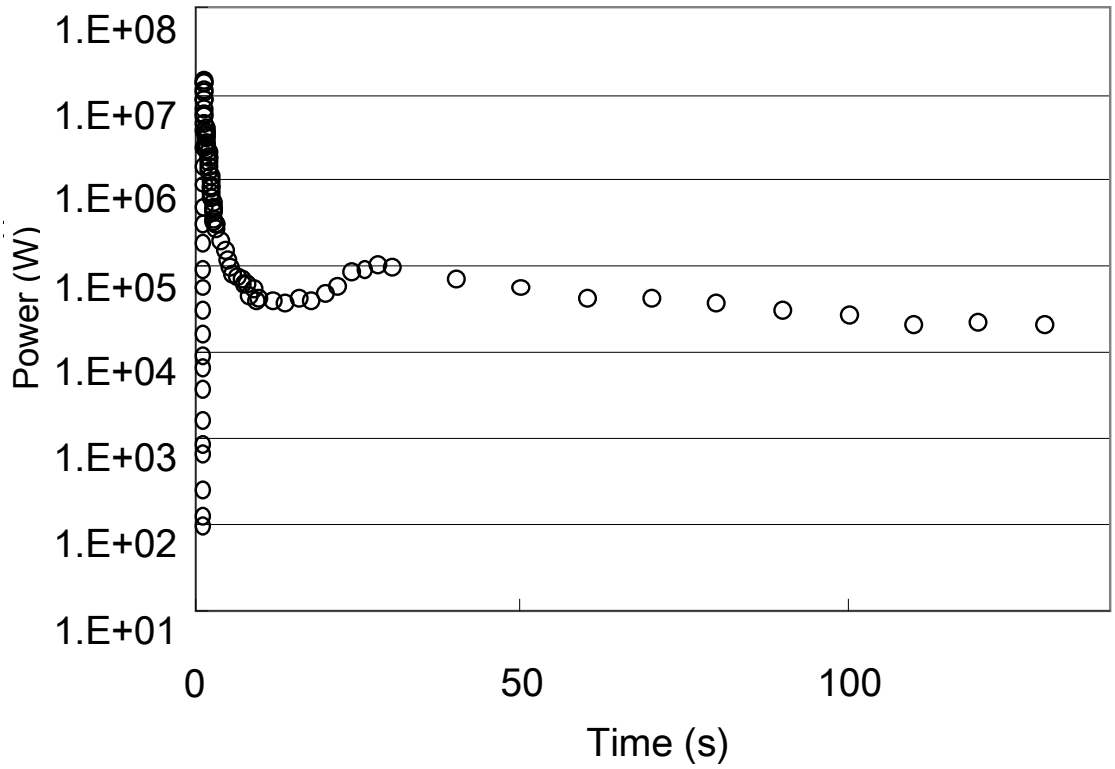

Figure 6.3.2: Measured temperature data for STEP-003

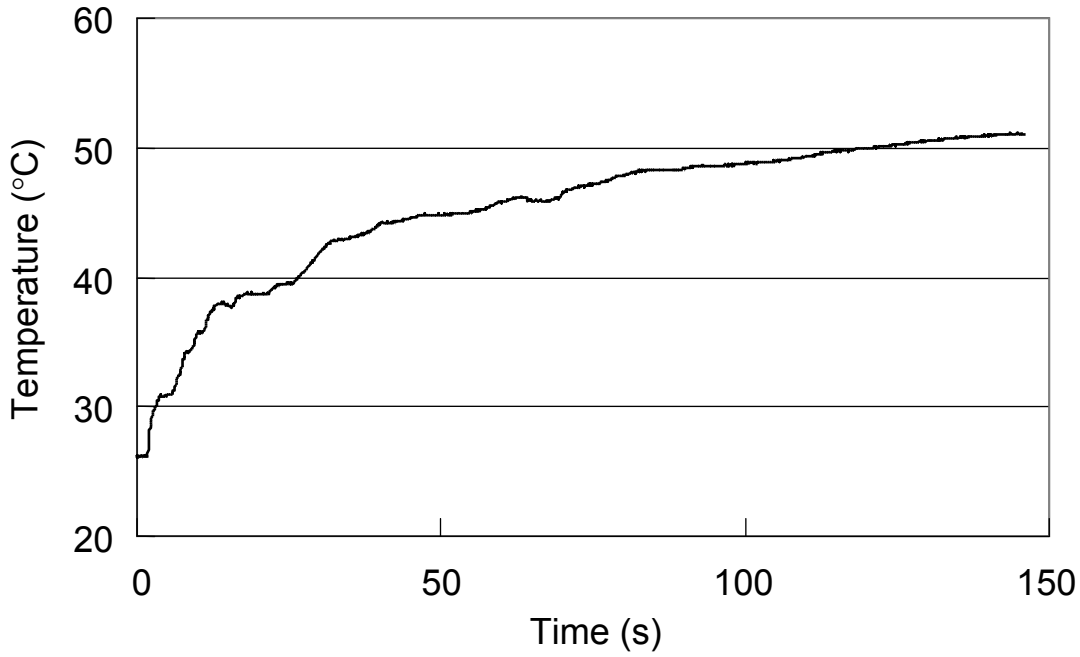

Figure 6.4.1: Measured power data for STEP-004

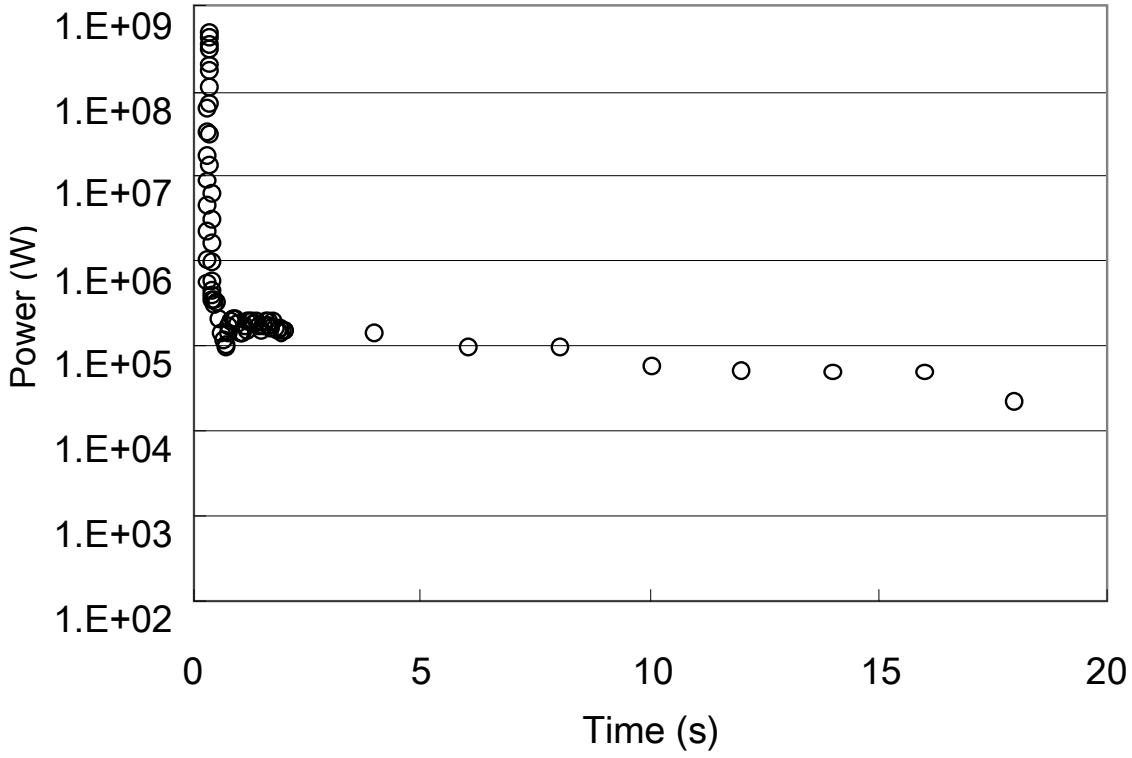

Figure 6.4.2: Measured temperature data for STEP-004

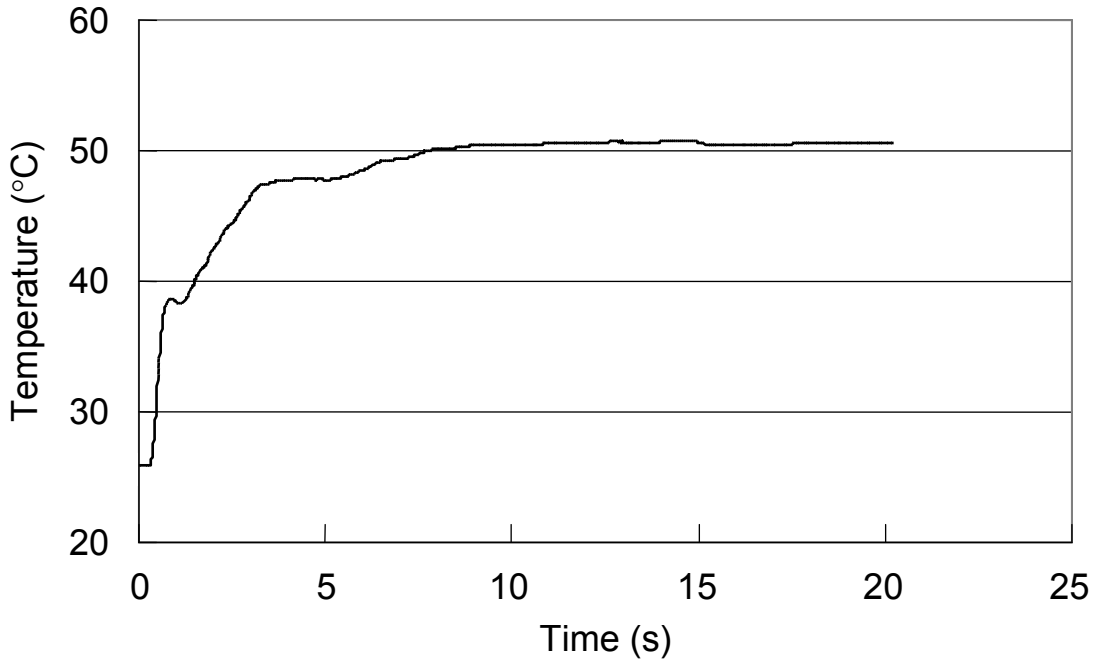

Figure 6.5.1: Measured power data for STEP-005

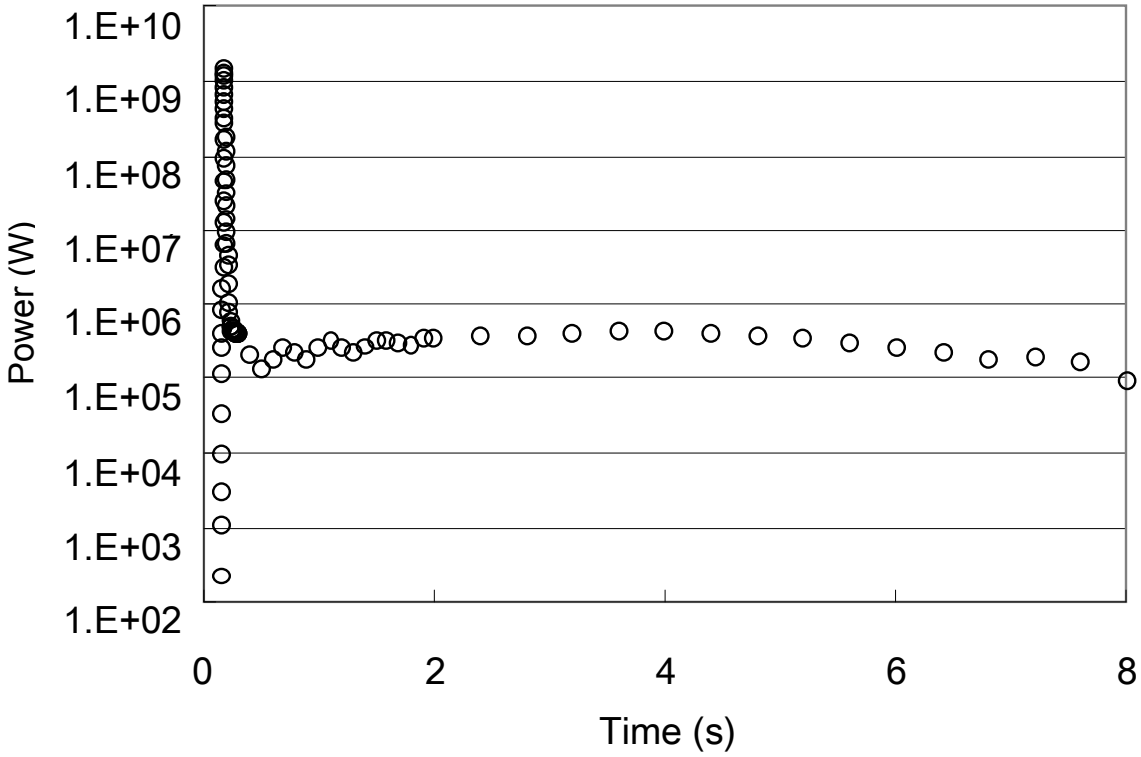

Figure 6.5.2: Measured temperature data for STEP-005

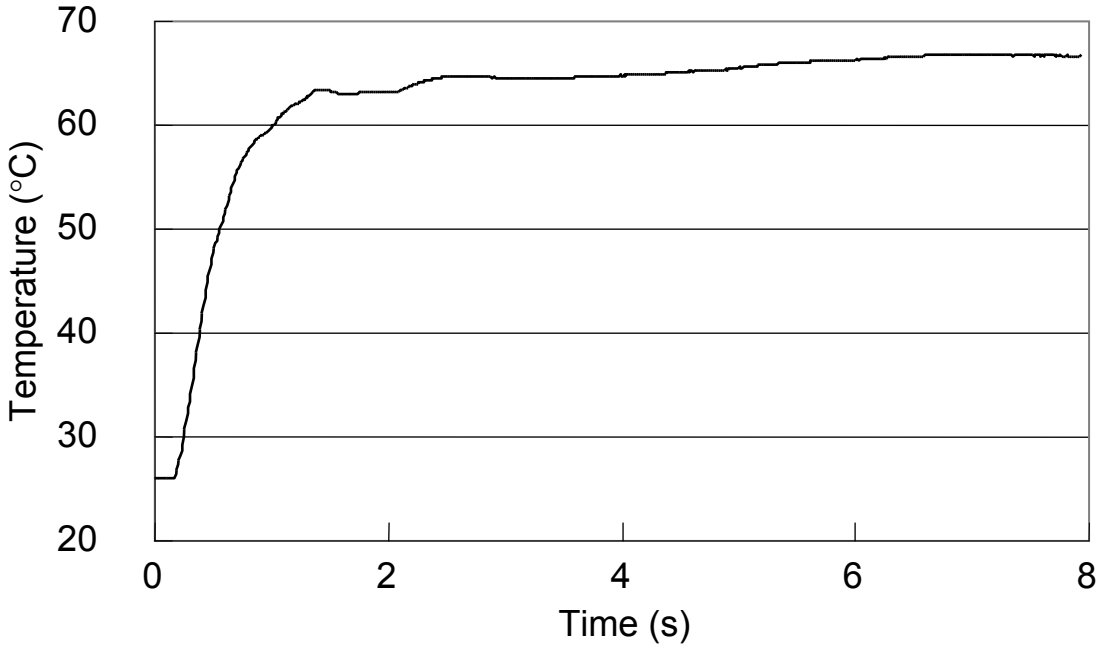

6.6 General observations

Using the quadratic temperature feedback derived for the AGNES calculations the asymptotic temperatures for the TRACY experiments are estimated to be as indicated in Table 6.6.1.

Table 6.6.1: Comparison of final and asymptotic temperatures

Test	STEP-001	STEP-002	STEP-003	STEP-004	STEP-005
Asymptotic temperature (°C)	33.4	40.2	48.1	61.4	73.2
Final temperature (°C)	36.2	35.8	50.8	51.5	66.7

It is seen that the final temperatures are reasonably close to the estimated asymptotic values, though it is noted above that STEP-002 had not reached the asymptotic value when the test was terminated, though the others were all close to the asymptote. The estimated asymptotic values neglect the effect of radiolytic gas release on the reactivity, which is probably the reason for the larger differences for STEP-004 and STEP-005.

Dividing the measured energy release by the heat capacity of the fissile solution provides an estimate of the temperature rise of the solution, in the absence of heat loss from the solution. These estimates are compared with the measured temperature rises in Table 6.6.2.

Table 6.6.2: Estimating heat loss from the fissile solution

Test	STEP-001	STEP-002	STEP-003	STEP-004	STEP-005
Adiabatic temperature rise (°C)	11.5	12.1	26.6	26.5	45.3
Measured temperature rise (°C)	10.0	11.0	24.6	25.6	40.6
Percentage heat loss	13	9	8	3	10

The results indicate that roughly 10% of the heat generated in the experiments is transferred to the vessel and it surroundings, *i.e.* heat loss from the fissile solution is not very important in these tests.

For the prompt-critical tests, STEP-003 to STEP-005, the Norheim-Fuchs-Hansen Eq. (3.2) can be used to give an approximate estimate of the peak power. This is compared with the measured peak powers in Table 6.6.3.

Table 6.6.3: Comparison of measured peak powers with Nordheim-Fuchs-Hansen

Test	STEP-003	STEP-004	STEP-005
Measured peak power	14.4 MW	566 MW	2.08 GW
Norheim-Fuchs-Hansen peak power	12.7 MW	848 MW	3.65 GW

The results are in good agreement for STEP-003, the smallest of the prompt-critical reactivity insertions. As the reactivity insertions get larger the agreement becomes worse. This is an indication that it is not solely the negative temperature feedback on the reactivity that terminates the power rise. In STEP-004 and STEP-005 the Norheim-Fuchs-Hansen equation overestimates the peak power because the power spike is terminated by a combination of negative reactivity feedback due to temperature rise and negative reactivity feedback due to radiolytic gas release. From Eq. (3.2) this suggests that, to get good agreement with the measured peak power, accurate input values are required for the heat capacity of the fissile solution, the neutron lifetime, the temperature feedback coefficient on reactivity, and especially for the delayed neutron fraction. For experiments with significant radiolytic gas generation (*i.e.* STEP-004 and STEP-005) it is also important to have accurate input values for the parameters pertaining to radiolytic gas release.

The maximum inverse period, ω, is given in terms of the power, P, and its time derivative, or, equivalently the neutron density, n, and its time derivative by:

$$\omega = \frac{1}{P}\frac{dP}{dt} = \frac{1}{n}\frac{dn}{dt} \tag{6.1}$$

From the point kinetics Eq. (3.1), for prompt-critical systems it is clear that the first term on the right-hand side of the first equation will grow exponentially and will soon dominate the right-hand side. Hence, to a good approximation the first equation becomes:

$$\omega = \frac{1}{n}\frac{dn}{dt} = \frac{(\rho_{\$} - 1)\beta}{\Lambda} \tag{6.2}$$

where $\rho_{\$}$ is the inserted reactivity in dollars.

This provides a useful estimate with the maximum inverse period for the prompt-critical tests and is compared with the measured values for STEP-003 to STEP-005, as displayed in Table 6.6.4.

Table 6.6.4: Simple estimates of maximum inverse period

Test	STEP-003	STEP-004	STEP-005
Measured max. inverse period (s^{-1})	25.5	169	334
Max. inverse period from Eq. 6.2 (s^{-1})	15.5	155	306

The estimated values are seen to be in reasonable agreement with the measured values, especially for the higher reactivity insertions, as expected. In Eq. (6.2) the contribution of the delayed neutrons is neglected. This approximation is expected to become better as the reactivity insertion is increased. This suggests that the codes should be in reasonable agreement with the measured maximum inverse periods in STEP-004 and STEP-005, if accurate values are input for the delayed neutron fraction and the neutron lifetime.

Chapter 7: Code predictions and comparison with TRACY results

A summary of calculations using the four transient criticality codes described in Chapter 4 is presented in Sections 7.1 to 7.4, where they are compared with the measured values from the experiments. The parameters compared with experiment are the power history, the maximum inverse period, the time to the first peak and the energy released and number of fissions to the first peak, and the energy and number of fissions at the time of termination of the transient. In STEP-003 the time to the first minimum of the power history and the energy and number of fissions to this time are also compared.

7.1 AGNES

7.1.1 Input parameters

The atomic number densities for the fuel solution are calculated using the SST (Basoglu, 1998) formula and are displayed in Table 7.1.1. Using these values, kinetic parameters such as delayed neutron fraction, etc., are estimated as described in Section 4.1.4 and are shown in Tables 7.1.2 to 7.1.6. The reactivity temperature coefficients are also estimated and are shown in Table 7.1.7. For the void feedback on the reactivity, the same function is used for all cases: ρ_v(cent) = -43.7 %V – 0.946 %V^2. The reactivity insertion time is set to be 0.15 s, which is almost the same as the time taken for the transient rod to pass through the full height of the fuel solution. For STEP-002, STEP-003 and STEP-004, the initial power density is set to 1×10^{-5}W/m^3, which is based on a measurement by neutron detectors for start-up with no external neutron source. For STEP-001 and STEP-005 a value of 1 kW/m^3 is used as the initial power density.

The following parameters are used to characterise radiolytic gas production:

- The saturation concentration of radiolytic gas, CD, was 15 mol/m^3.
- The generation rate of dissociation gas, *G*, was: 6×10^{-7} mol/J for reactivity insertions < 1\$ and 3×10^{-7} mol/J for reactivity insertions > 1\$.
- These values are chosen so that the power profile is reproduced the best.
- The energy-void transfer coefficient, ν, was 1×10^{-7} m^6/J/mol for all cases. This value is chosen to give the best fit to the experimental data.

Table 7.1.1: Atomic number densities for the fissile solution

Run no.	R100	R143	R72	R196	R203
Nucleus	Atomic number density (atoms/barn.cm)				
^{235}U	1.0051E-04	9.6029E-05	1.0046E-04	9.8433E-05	9.9113E-05
^{238}U	8.9617E-04	8.5620E-04	8.9571E-04	8.7763E-04	8.8369E-04
H	5.7705E-02	5.8185E-02	5.7583E-02	5.8028E-02	5.7960E-02
N	2.3906E-03	2.2899E-03	2.4377E-03	2.3013E-03	2.3147E-03
O	3.7819E-02	3.7674E-02	3.7874E-02	3.7695E-02	3.7715E-02

Table 7.1.2: Kinetics parameters for R100

Delayed neutron fraction		Decay constant [1/s]
β_1	2.5490E-04	1.2703E-02
β_2	1.6521E-03	3.1704E-02
β_3	1.4940E-03	1.1525E-01
β_4	3.0053E-03	3.1161E-01
β_5	8.9084E-04	1.4003E+00
β_6	3.2420E-04	3.8740E+00
β_{eff} (total)	7.6213E-03	–
Prompt neutron lifetime (s)		4.8640E-05

Table 7.1.3: Kinetics parameters for R143

Delayed neutron fraction		Decay constant [1/s]
β_1	2.5384E-04	1.2703E-02
β_2	1.6464E-03	3.1704E-02
β_3	1.4883E-03	1.1524E-01
β_4	2.9939E-03	3.1158E-01
β_5	8.8685E-04	1.4003E+00
β_6	3.2279E-04	3.8738E+00
β_{eff} (total)	7.5921E-03	–
Prompt neutron lifetime (s)		5.0315E-05

Table 7.1.4: Kinetics parameters for R72

Delayed neutron fraction		Decay constant [1/s]
β_1	2.5490E-04	1.2703E-02
β_2	1.6521E-03	3.1704E-02
β_3	1.4940E-03	1.1525E-01
β_4	3.0053E-03	3.1161E-01
β_5	8.9088E-04	1.4003E+00
β_6	3.2422E-04	3.8740E+00
β_{eff} (total)	7.6214E-03	–
Prompt neutron lifetime (s)		4.8593E-05

Table 7.1.5: Kinetics parameters for R196

Delayed neutron fraction		Decay constant [1/s]
β_1	2.5439E-04	1.2703E-02
β_2	1.6493E-03	3.1704E-02
β_3	1.4912E-03	1.1524E-01
β_4	2.9997E-03	3.1160E-01
β_5	8.8888E-04	1.4003E+00
β_6	3.2351E-04	3.8739E+00
β_{eff} (total)	7.6071E-03	–
Prompt neutron lifetime (s)		4.9342E-05

Table 7.1.6: Kinetics parameters for R203

Delayed neutron fraction		Decay constant [1/s]
β_1	2.5448E-04	1.2703E-02
β_2	1.6498E-03	3.1704E-02
β_3	1.4918E-03	1.1524E-01
β_4	3.0008E-03	3.1160E-01
β_5	8.8928E-04	1.4003E+00
β_6	3.2365E-04	3.8739E+00
β_{eff} (total)	7.6098E-03	–
Prompt neutron lifetime (s)		4.9056E-05

Table 7.1.7: Reactivity temperature coefficients

	α_{T1} (cent/°C)	α_{T2} (cent/°C^2)
R100	-3.76E+00	-5.44E-02
R143	-3.75E+00	-5.21E-02
R072	-3.90E+00	-5.18E-02
R196	-3.83E+00	-5.11E-02
R203	-3.70E+00	-5.52E-02

7.1.2 Comparison with experiment

STEP-001

This is the case with the lowest excess reactivity and no radiolytic gas production was observed. As shown in Figure 7.1.1, the AGNES calculation faithfully reproduces the gradual power increase to the peak value at 189 s along with the initial cooling of the solution. All of the calculated parameters (maximum inverse period, peak power, time to reach the peak and the energy and fissions to the peak) are within 13% of the measured values. The calculated total energy and fissions are only 5% less than the experimental values and the temperature rise is 6% less than observed. The slight over-prediction of the cooling rate towards the end of the experiment is thought to be due to the neglect of heat transfer from the fissile solution to the steel vessel.

STEP-002

This case also has a reactivity insertion less than 1$ (*i.e.* is delayed-critical). As shown in Figure 7.1.2, the AGNES calculation faithfully represents the gradual power increase to the peak at value at 39 s. All of the calculated parameters (maximum inverse period, peak power, time to reach the peak and the energy and fissions to the peak) are within 10% of the measured values. It also produces a reasonable estimate of the magnitude of the power reduction after the peak, but does not reproduce the oscillatory behaviour observed in the experiment. It is suspected that the failure to reproduce the observed oscillatory nature may be due to inadequate representation of radiolytic gas bubble behaviour. The calculated total energy and fissions are 3% higher than the experimental values and the temperature rise is 5% higher than observed.

STEP-003

In this case the reactivity insertion is slightly in excess of 1$ (*i.e.* a prompt-critical excursion). As shown in Figure 7.1.3, the AGNES calculation is in good agreement with the observed rapid power rise to the first peak and the initial reduction from the peak power. All of the calculated parameters (maximum inverse period, peak power, time to reach the peak and the energy and fissions to the peak) are within 9% of the measured values.

Figure 7.1.4 shows that the AGNES calculation also produces a reasonable estimate of the power towards the end of the experiment, which is three orders of magnitude lower than the peak value. However, the calculation fails to reproduce the observed minimum in the power history after 14 s or

the occurrence of a second maximum after 28 s. It is thought that this may be due to radiolytic gas bubbles being created and removed more quickly in the experiment than predicted by the code. The calculated total energy and fissions are about 16% higher than the experimental values and the temperature rise is 16% higher than observed.

STEP-004

In this case the excess reactivity is sufficiently high that a significant pressure rise due to radiolytic gas bubble production is observed. The calculated peak pressure due to gas bubble production is 9% higher than the measured value. As shown in Figure 7.1.5 the AGNES calculation accurately predicts the rapid power rise to the first peak. All of the calculated parameters (maximum inverse period, peak power, time to reach the peak and the energy and fissions to the peak) are within 1% of the measured values.

However, the calculation over-predicts the initial rate of power decrease (for the first two and one-half orders of magnitude) and then subsequently under-predicts the rate at which the power falls. Figure 7.1.6 shows that the calculation over-predicts the long-term power and does not reproduce the observed minimum in the power history after three-quarters of a second or the subsequent oscillatory behaviour; this may be due to underestimating radiolytic gas bubble production. The calculated total energy and fissions are about 13% higher than the experimental values and the temperature rise is 3% higher than observed.

STEP-005

This is the case with the highest excess reactivity and a significant pressure rise due to radiolytic gas bubble production is observed. The calculated peak pressure due to gas bubble production is 13% higher than the measured value. Figures 7.1.7 and 7.1.8 show that the comparison between the AGNES calculation and the measured power history is very similar to that for STEP-004. The rise to the initial peak is well reproduced; all of the calculated parameters (maximum inverse period, peak power, time to reach the peak and the energy and fissions to the peak) are within 12% of the measured values. The long term is also well predicted; the calculated total energy and fissions are 11% lower than the experimental values and the temperature rise is 8% lower than observed. The observed oscillatory behaviour is not predicted by the code. The longer-term discrepancies may be due to underestimating radiolytic gas bubble production.

7.1.3 Conclusions

The agreement between the AGNES calculations and experiment is very good. The calculated values of all of the parameters generally agree with the measured values to within about 10%. However, the calculations do not reproduce any of the oscillatory behaviour observed in tests STEP-002 to STEP-005.

Figure 7.1.1: AGNES power calculation – R100 (0.3$)

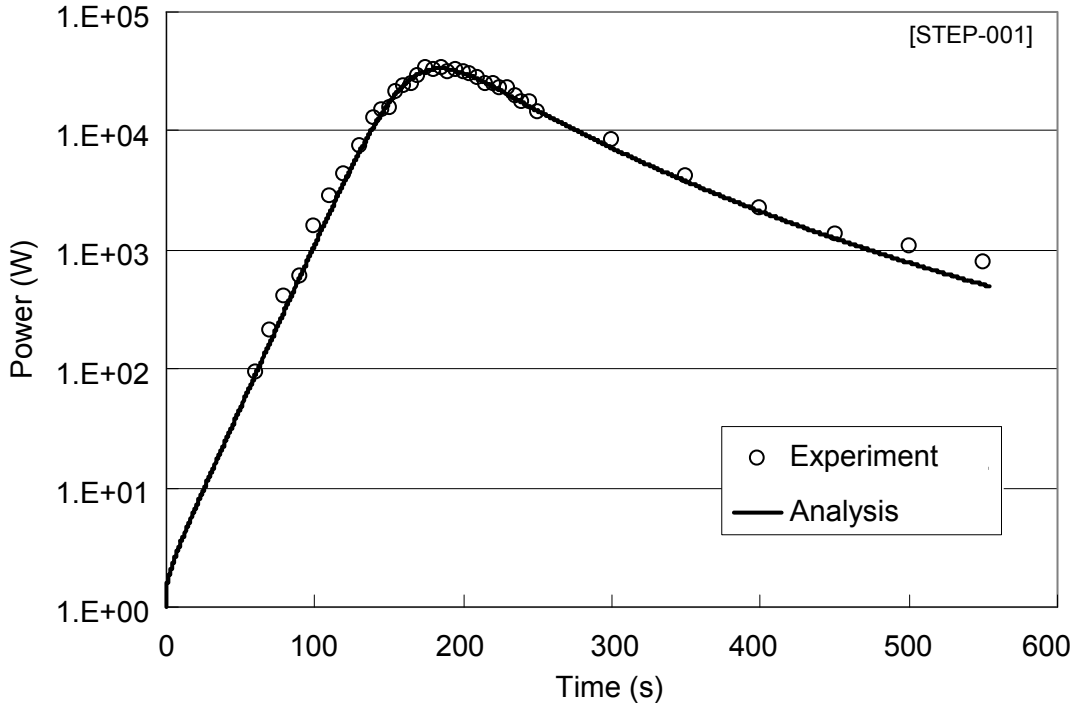

Figure 7.1.2: AGNES power calculation – R143 (0.7$)

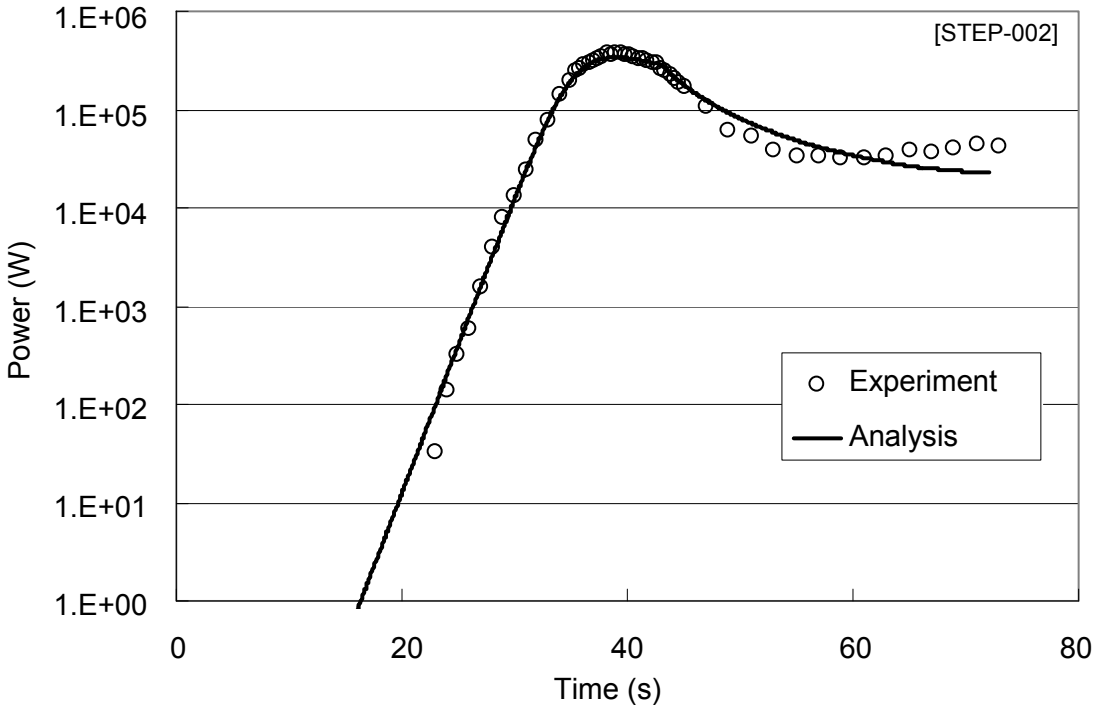

Figure 7.1.3: AGNES power calculation – R72 (1.1$) (1-2 s)

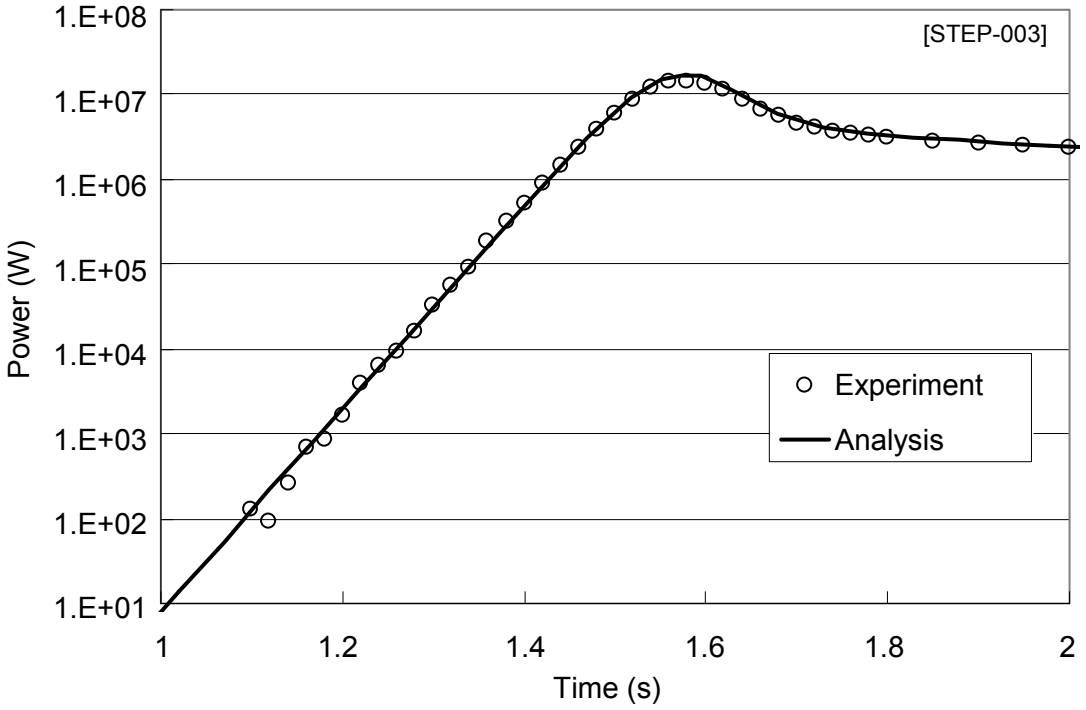

Figure 7.1.4: AGNES power calculation – R72 (1.1$)

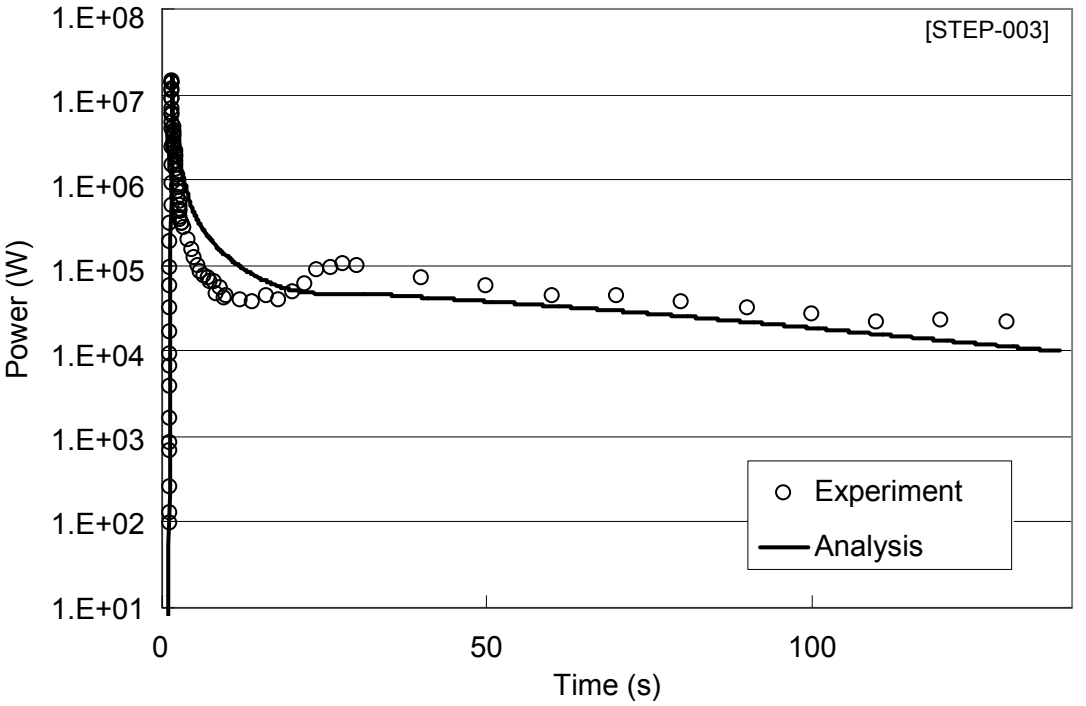

Figure 7.1.5: AGNES power calculation – R196 (2.0$) (0.2-0.4 s)

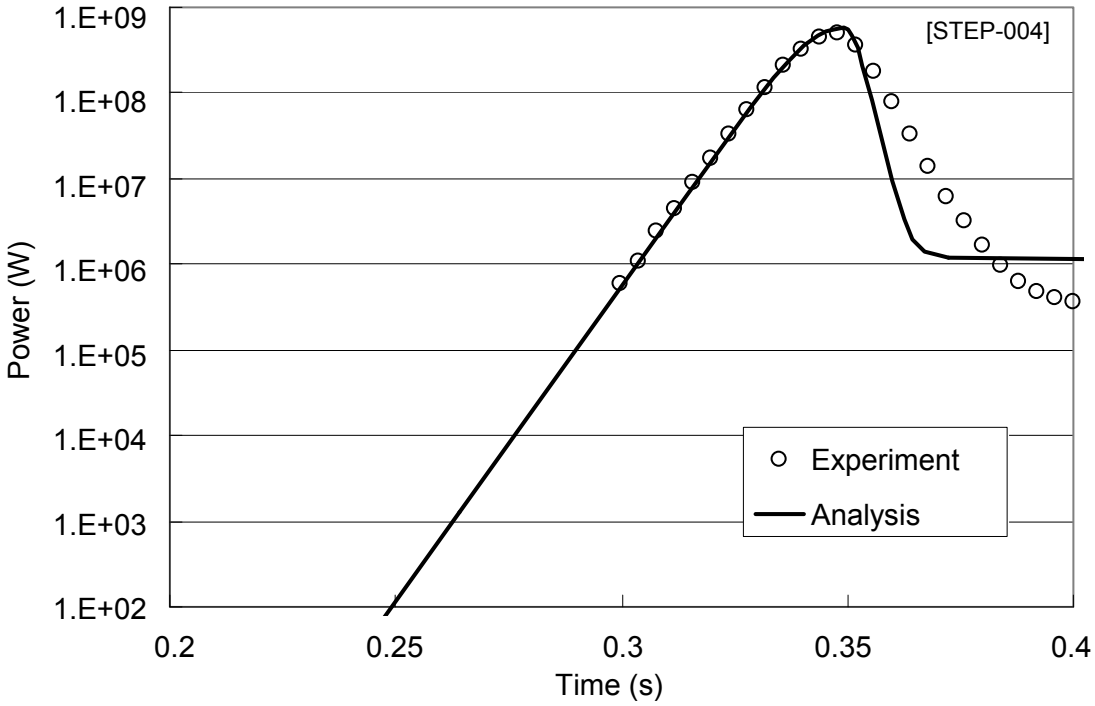

Figure 7.1.6: AGNES power calculation – R196 (2.0$)

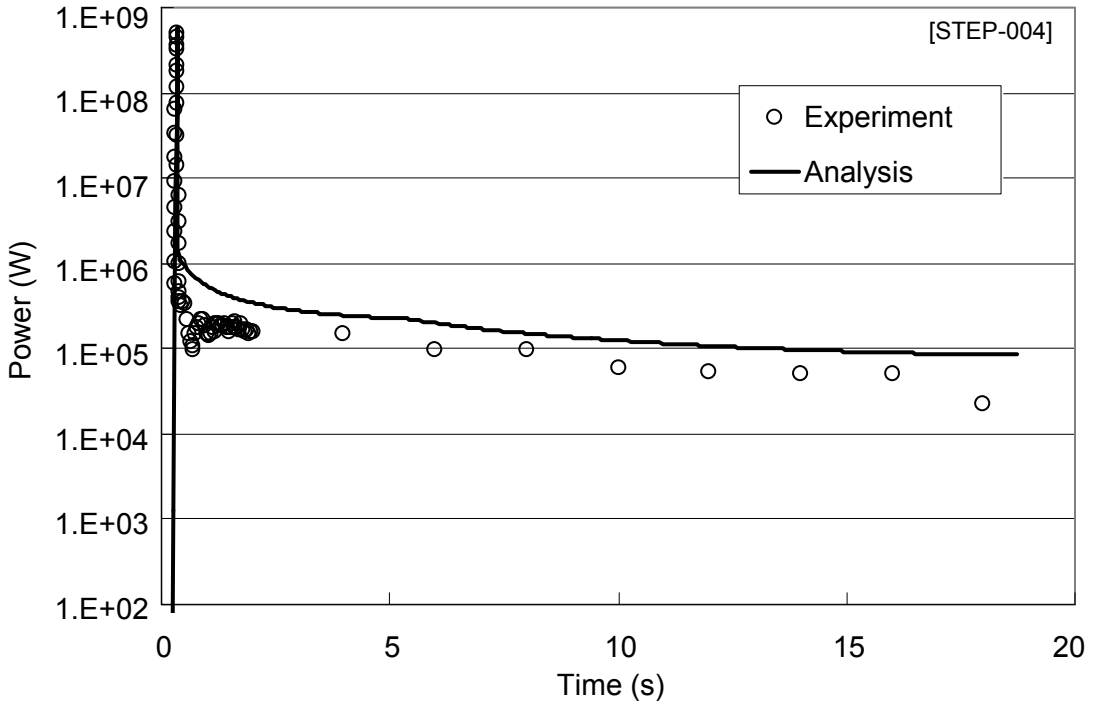

Figure 7.1.7: AGNES power calculation – R203 (2.97$) (0.1-0.3 s)

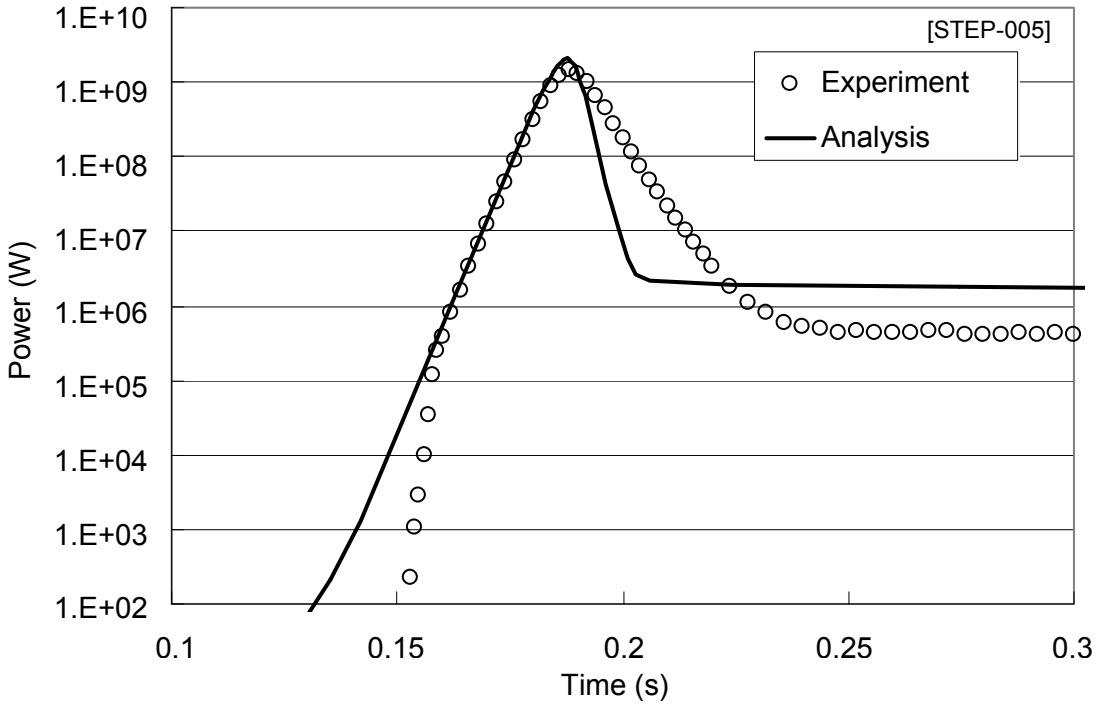

Figure 7.1.8: AGNES power calculation – R203 (2.97$)

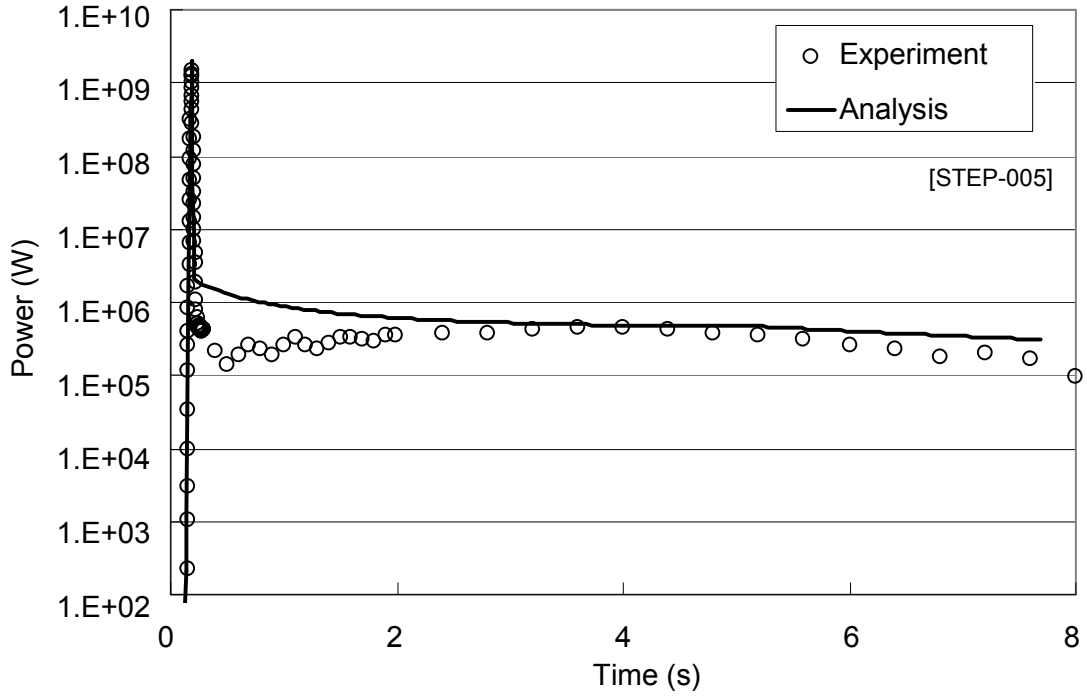

7.2 CRITEX

7.2.1 Input parameters

The fissile solution modelled with the CRITEX (Grivot, 2004) code is uranyl nitrate, with a ^{235}U enrichment of 10%. Table 7.2.1 shows the main physicochemical characteristics of this solution for the various experiments studied.

Table 7.2.1: Physicochemical characteristics

Experiment	STEP-001	STEP-002	STEP-003	STEP-004	STEP-005
$C(U_{total})$ (g/l)	392.9	375.9	393.5	385.5	388.2
Free acidity, H+ ($mol.l^{-1}$)	0.66	0.64	0.74	0.58	0.58
Density (g/cm^3)	1.54934	1.52371	1.55001	1.53481	1.53693

The isotopic composition of the fissile solution is as displayed in Table 7.2.2 for a concentration of 390 $g.l^{-1}$ (at 21°C):

Table 7.2.2: Isotopic composition of fuel solution

Isotope	Number of atoms per 10^{-24} cm^{-3}
Hydrogen	5.7902×10^{-2}
Nitrogen	2.43943×10^{-3}
Oxygen	3.80132×10^{-2}
Uranium 235	9.99226×10^{-5}
Uranium 238	8.87944×10^{-4}

The value calculated for β_{eff} is 737 pcm.

The central cavity that receives the transient rod is not included in the geometric model of the experiments. The SOURCE 4C code (Wilson, 2002) was used to estimate the neutron source intrinsic to the fissile solution for STEP-003 and STEP-004. The resulting initial specific powers for these tests are displayed in Table 7.2.4 and correspond to total powers of 0.476 μW and 0.907 μW, respectively.

STEP-001 and STEP-005 involved no external neutron source, but were initiated on the basis of a measured initial power of 1 W. Under such conditions, the number of neutrons produced in the fissile solution by (α,n) reactions and spontaneous fissions is negligible with respect to the number resulting from fissions associated with initial reactor power level. Note that although experiment STEP-002 (R143) is carried out with no external neutron source or measured initial power, for calculation reasons the CRITEX calculation for this experiment is started with an initial power of 1 W.

The initial power densities used in the CRITEX calculations are delayed in Table 7.2.3, along with the input extrapolation lengths.

Table 7.2.3: Input power densities and extrapolation lengths for CRITEX calculations

	STEP-001	STEP-002	STEP-003	STEP-004	STEP-005
Extrapolation length,λ_Z (cm)	2.198	2.420	2.175	2.439	2.078
Extrapolation length, λ_R (cm)	0.886	0.862	0.901	0.746	0.820
Initial specific power (fissions s^{-1} g^{-1})	2.065×10^5	1.935×10^5	9.3×10^{-2}	1.65×10^{-1}	1.697×10^5

For STEP-004 and STEP-005 the withdrawal of the Tr-rod is modelled as a constant rate of reactivity insertion with a duration of 0.15 s (this is close to the measured time to withdraw the transient rod pneumatically of less than 0.2 s). For STEP-004 the reactivity insertion rate is 13.334 $/s for 0.15 s, producing a total reactivity insertion of $2. For STEP-006 the reactivity insertion rate is 19.8 $/s for 0.15 s, producing a total reactivity insertion of $2.97.

Other experimental conditions are displayed in Table 7.2.4.

Table 7.2.4: Experimental characteristics

	STEP-001	STEP-002	STEP-003	STEP-004	STEP-005
Level worth ($/mm)	0.0371	0.0314	0.0367	0.0339	0.0356
Inserted reactivity ($)	0.3	0.7	1.1	2	2.97
Critical height (cm)	49.976	52.76	50.253	51.166	50.962
Final height (cm)	50.852	55.182	53.705	58.25	62.376
Initial temperature (°C)	25.7	25	26	25.6	25.7
Duration of experiment (s)	554.75	73.37	137.67	18.55	7.59

The radiolytic gas release time is not explicitly stated for these experiments. However, experience with SILENE has shown that the pressure wave measured during the experiments is due to gas release. The gas release time in TRACY can thus be considered the same as that of the pressure peak measured by the gauge immersed in the fissile solution. Therefore, for STEP-004 and STEP-005 the gas release times are taken to be 0.344 s and 0.185 s, respectively. There is no measured pressure for STEP-001 to STEP-003.

7.2.2 Comparison with experiment

STEP-001

Figure 7.2.1 shows the calculated and measured pressure histories. The calculated key parameters all agree with the measured values to better than 20%. The overall shape of the power curve is similar to the measured power history though calculated rise to the power peak is a little slower than observed and the reduction in the rate of power decrease at the end of the test is not reproduced by the calculation.

STEP-002

Figure 7.2.2 shows the calculated and measured pressure histories. In this case the calculation rises to the first peak earlier than the experiment and releases 40% more energy in doing so, though the power at the first peak is within 15% of the experimental value. Despite the calculated power rise being quicker than observed, the CRITEX estimate of the maximum inverse period is 19% lower than the measured value. This indicates that the underestimate of the time to the first peak arises from the assumption of an initial power of 1 W for this test, which is at odds with Table 5.5.1, indicating that this test was initially subcritical, like STEP-003 and STEP-004.

The early power rise results in the calculated transient being at power roughly 30% longer than the experiment and leads to the total energy released during the test being overestimated by 45%. This, in turn leads to the calculated temperature rise being 55% greated than measured.

After the first peak the calculated power decreases at roughly the right rate. However, the calculation fails to reproduce the observed oscillatory behaviour, resulting in a minimum in the power, which then rises to a second peak just before termination.

STEP-003

Figure 7.2.3 indicates that the CRITEX calculation seems to have started at a higher power than measured, but underestimated the maximum inverse period by over 30% and the first peak power by 37%. The estimated maximum inverse power is similar to the value obtained from Eq. (3.2) and displayed in Table 6.6.4. This suggests that the role of the delayed neutrons is underestimated in the CRITEX calculation. However, all the other calculated parameters (energy and fissions to first peak, total energy and fissions and temperature rise) were within 10% of the measured values. Figure 7.2.4 displays the longer-term behaviour and shows that the calculation exhibits an oscillatory power history with a similar magnitude as the measured one, but with roughly half the observed period. Thus the CRITEX calculation reaches the first minimum earlier than the experiment and the estimated power at the first minimum is in good agreement with measurement. The CRITEX-calculated power history is seen to agree well with the experiment in the long term.

STEP-004

Figure 7.2.5 displays the short-term power histories and shows that the key CRITEX parameter values (maximum inverse period, time to first peak and energy and fissions to first peak) all agree with the measured values to better than 10%. Figure 7.2.6 displays the long-term power histories. The experimental curve displays oscillatory behaviour in the first few seconds, in contrast to the CRITEX calculation which oscillates with a period approaching 20 s. This difference in the long-term behaviour results in the total energy being overestimated by 27% and the final temperature rise is 17% higher than measured.

STEP-005

Figure 7.2.7 displays the measured and calculated power histories in the short term. The calculated time to the first peak is underestimated by 14%; however, the calculated maximum inverse period, power at first peak and energy and fissions to the first peak all agree with the measured values to better than 10%. Figure 7.2.8 displays the long-term power histories and shows that the CRITEX simulation fails to reproduce the observed oscillatory behaviour of experiment or the observed rise to a peak at around 4 s. However, the total energy and fissions are in excellent agreement with the experimental values and the estimated temperature rise is 12% higher than the measured value.

7.2.3 Conclusions

The CRITEX calculations reproduce the dynamics and the key parameters associated with the rise to the first peak power well, with the exception of the time taken to reach the peak. This is probably due to difficulty in establishing adequate initial conditions for the calculation, in particular in determining the time at which a chain reaction is established once the system becomes critical. Inaccuracies in the predicted time to the first peak appear to have little impact on the predicted values of the other parameters associated with the first peak (*i.e.* maximum inverse period, peak power and energy to the peak).

In the longer term reasonable agreement with experiment is obtained, in particular for STEP-003 where the observed oscillatory behaviour is reasonably well reproduced and the long-term behaviour agrees well with experiment.

Figure 7.2.1: CRITEX power calculation – R100 (0.3$)

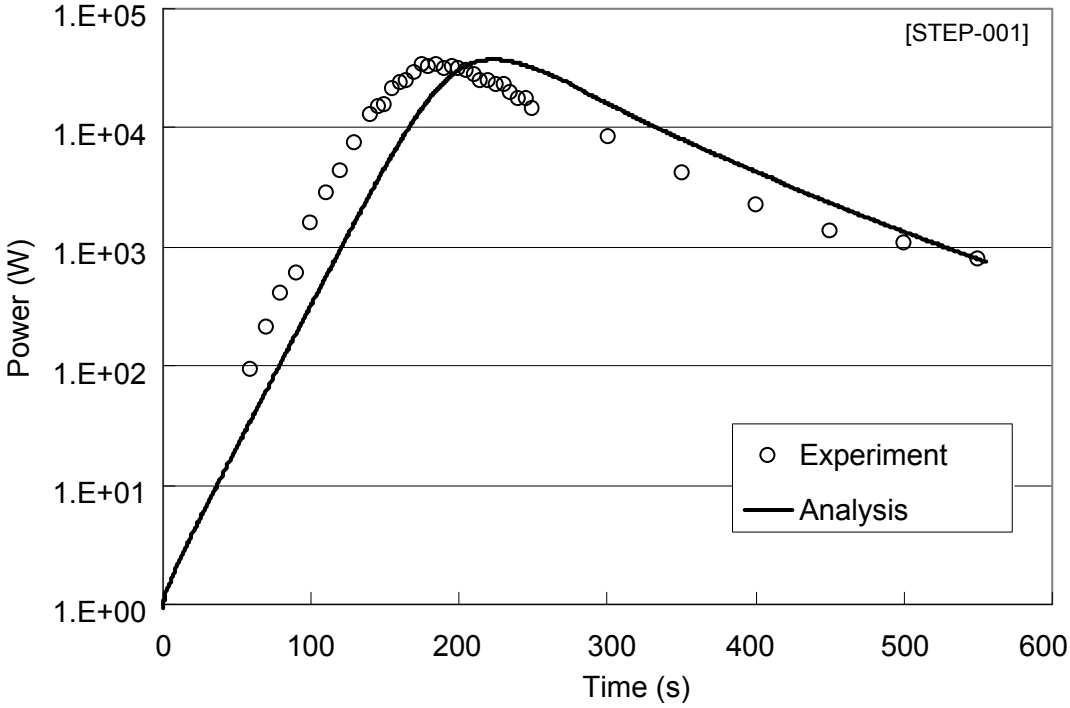

Figure 7.2.2: CRITEX power calculation – R143 (0.7$)

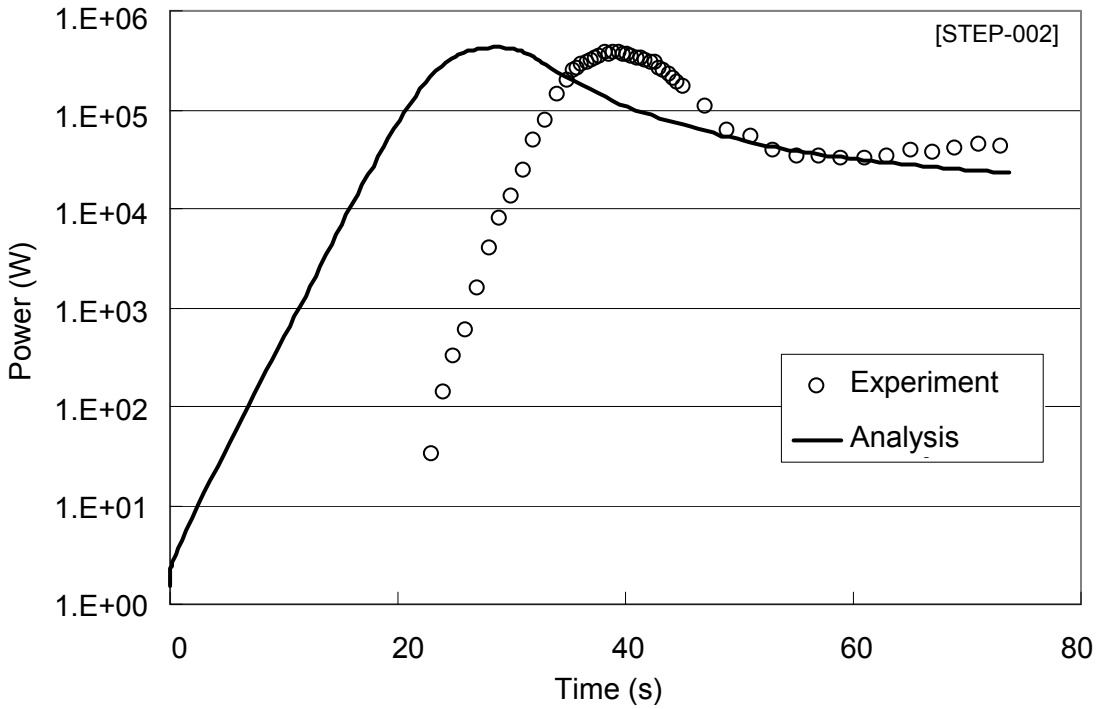

Figure 7.2.3: CRITEX power calculation – R72 (1.1$) (1-2 s)

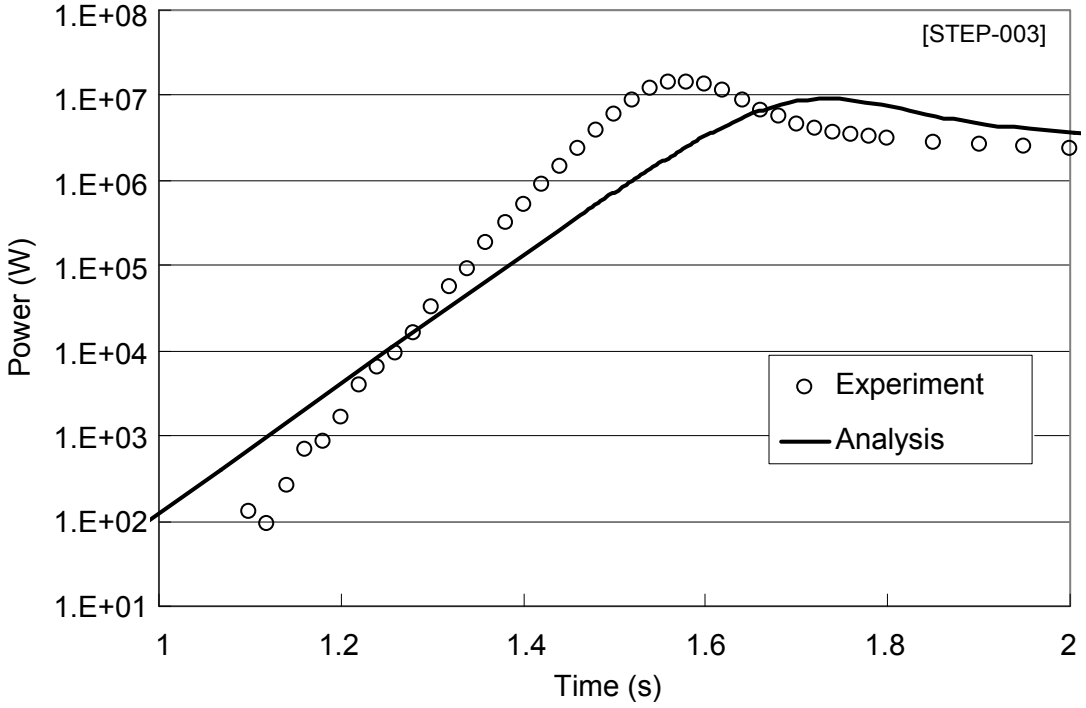

Figure 7.2.4: CRITEX power calculation – R72 (1.1$)

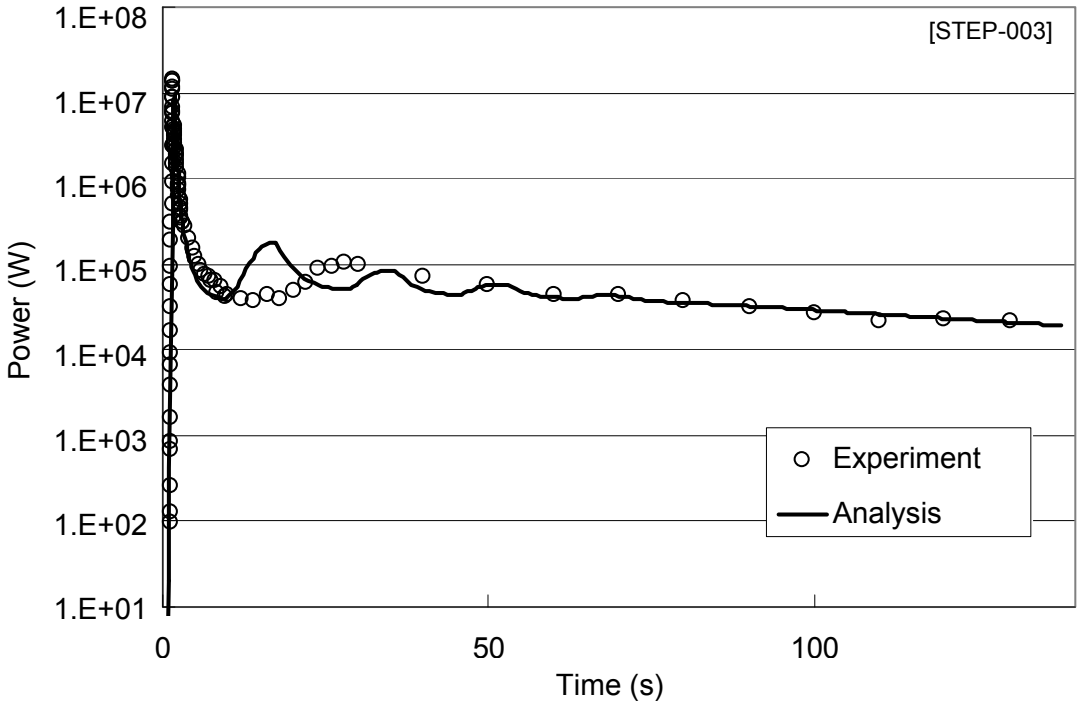

Figure 7.2.5: CRITEX power calculation – R196 (2.0$) (0.1-0.5 s)

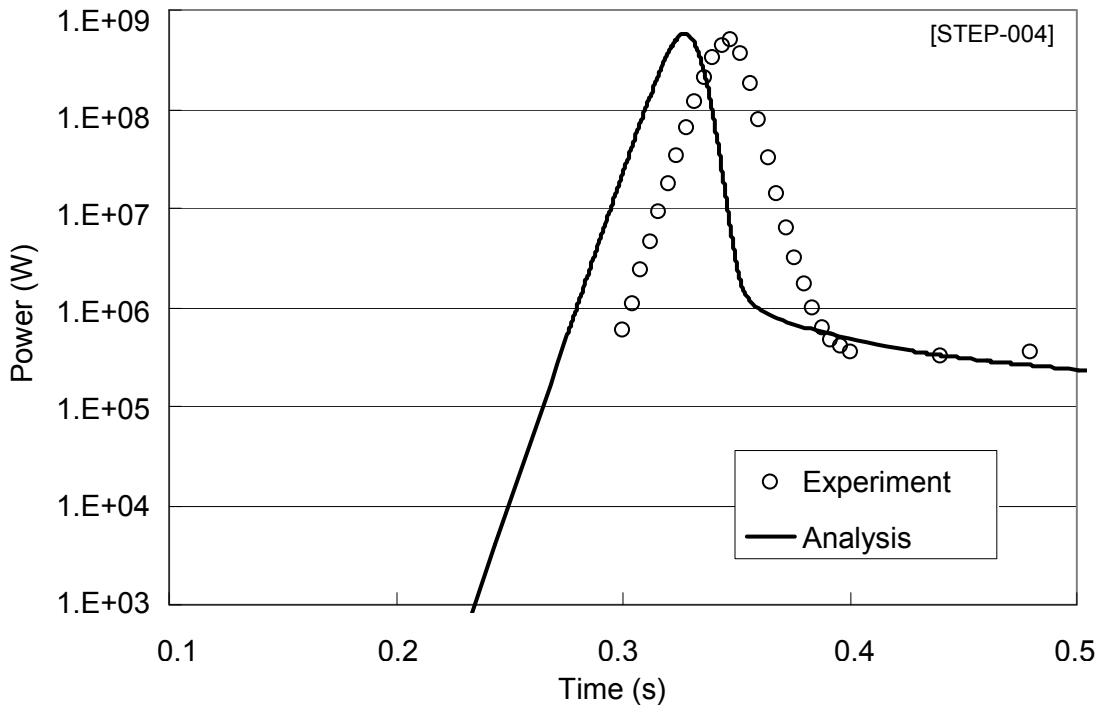

Figure 7.2.6: CRITEX power calculation – R196 (2.0$)

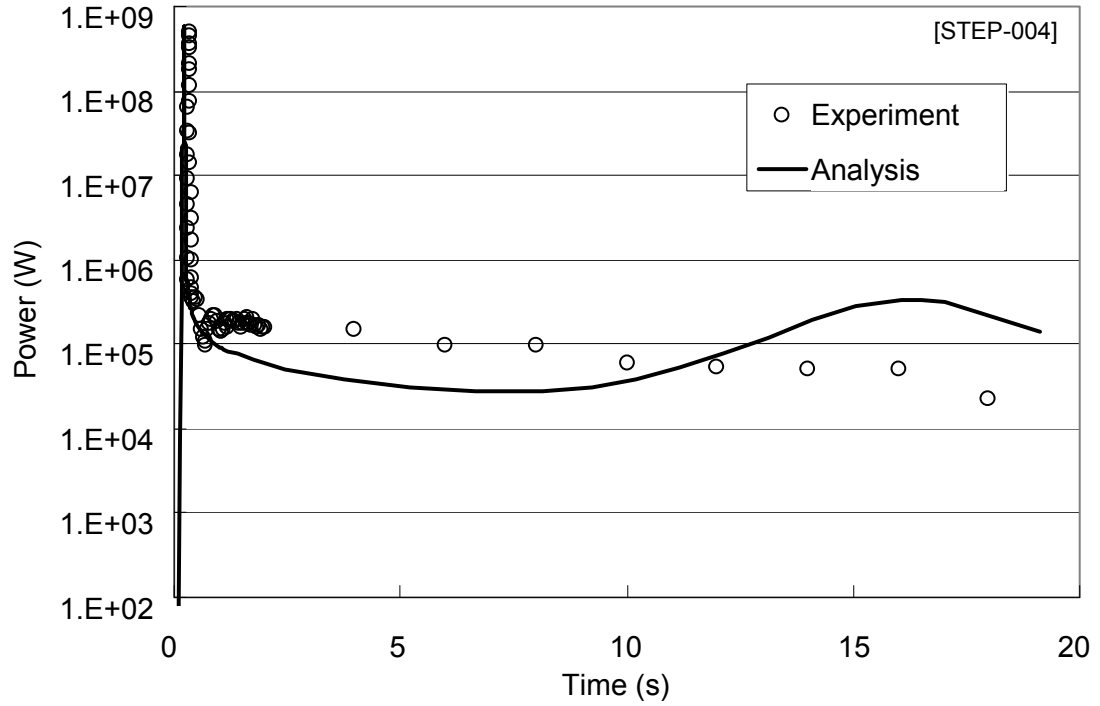

Figure 7.2.7: CRITEX power calculation – R203 (2.97$) (0.1-0.3 s)

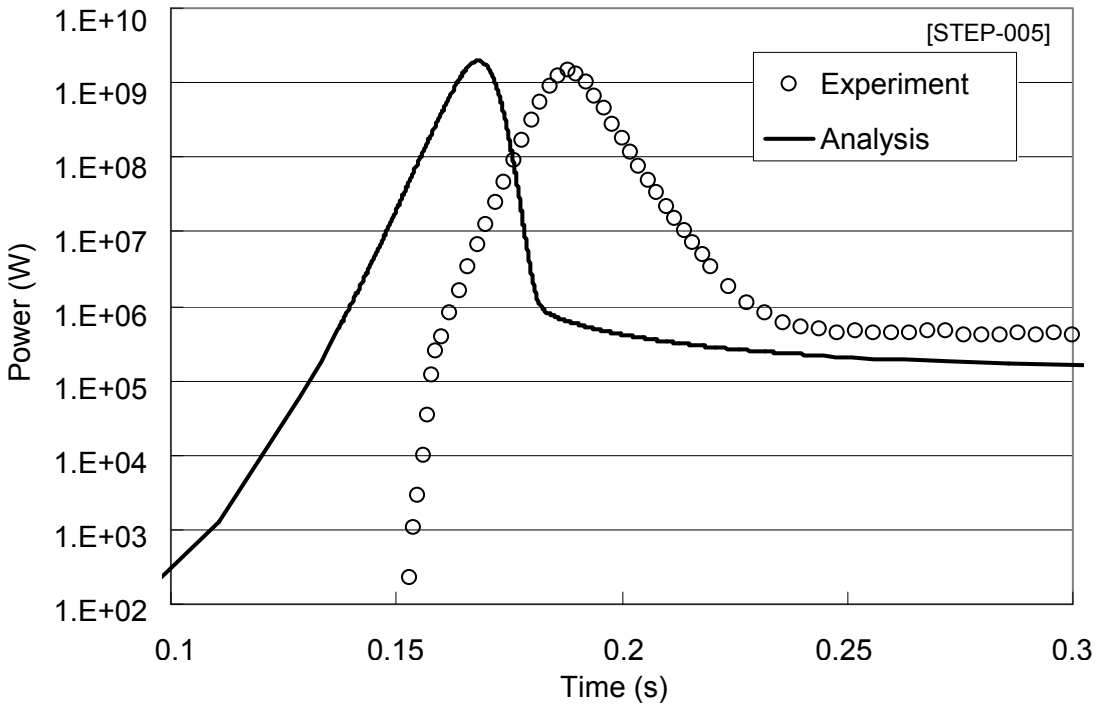

Figure 7.2.8: CRITEX power calculation – R203 (2.97$)

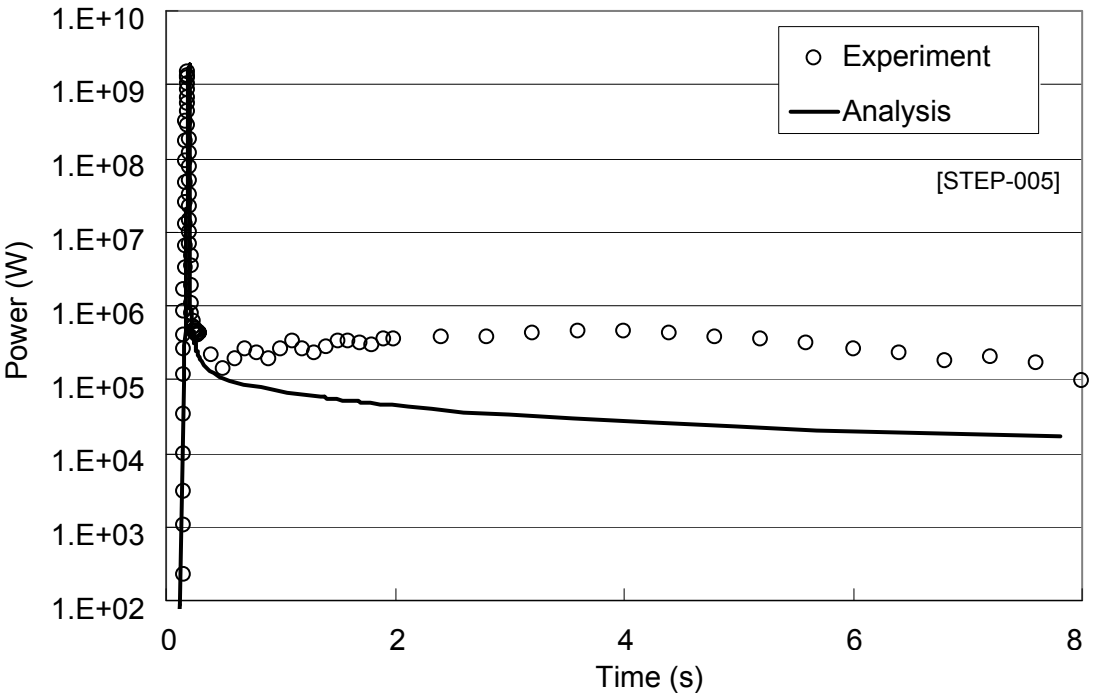

7.3 INCTAC

7.3.1 Input parameters

The atomic number densities calculated with INCTAC (Mitake, 2005) are shown in Table 7.3.1. Based on those values, the evaluated kinetics parameters are displayed in Table 7.3.2.

Table 7.3.1: Atomic number densities of fissile solution with 390 gU/L at 20°C

H	5.7917E-02
N	2.3371E-03
O	3.7765E-02
^{235}U	9.9723E-05
^{238}U	8.8814E-04
At base state: 20°C and no void.	

Table 7.3.2: Delayed neutron fractions and decay constants

Delayed neutron fraction		Decay constant [1/s]
β_1	2.5084E-04	1.2710E-02
β_2	1.6285E-03	3.1704E-02
β_3	1.4697E-03	1.1525E-01
β_4	2.9606E-03	3.1162E-01
β_5	8.7734E-04	1.4003E+00
β_6	3.1936E-04	3.8740E+00
β_{eff} (total)	7.5064E-03	–

The parameter values used to model radiolytic gas formation are:

G:	energy to generate radiolysis gas [mol/J]	8.82E-08
C_0:	radiolysis gas saturation concentration [mol/m^3]	5.0

The nodalisation of the reactor vessel for the thermal-hydraulics calculations is displayed in Figure 7.3.1.

7.3.2 Comparison with experiment

STEP-001

The measured and calculated power histories for R100 are plotted in Figure 7.3.2. For this test, the reactor was taken critical and its power level was adjusted to 1 W before the excursion. This critical power level was taken as the initial power condition for the transient analysis. These results are in good agreement, to within 12%, with the measured parameters: maximum inverse period, time to first peak and energy and fissions to first peak. Longer-term agreement is also good, with calculation agreeing with experiment to within 8% for the total power and fissions and 7% for the temperature rise. However, the calculation fails to simulate the observed reduction in the rate of decline of the power towards the end of the test.

STEP-002

The measured and calculated power histories for R143 are plotted in Figure 7.3.3. The reactor was subcritical before the criticality excursion for this experiment. An arbitrary initial critical power level of 1 W was chosen to start the calculation. This resulted in the discrepancy in the calculated and measured times (50%) to the peak power, with the calculation rising to the peak significantly earlier. On the other hand, good agreement is obtained for the other parameters (maximum inverse period,

peak power and energy and fissions to first peak) to the first peak which are within 21% of the measured values. However, the longer time at power in the calculation results in the total energy and fissions being overestimated by 49% and the final temperature by 47%. The calculation fails to simulate the observed oscillatory behaviour towards the end of the test.

STEP-003

The measured and calculated power histories are compared in Figures 7.3.4 and 7.3.5. As the reactor was subcritical at the start of this experiment, an arbitrary initial critical power level of 1 W was chosen to start the calculation. This resulted in the discrepancy in the calculated and measured times (46%) to the peak power, with the calculation rising to the peak significantly earlier. The peak power was underestimated by 31% in this case and the maximum inverse period was underestimated by 22%; the latter effect partially compensates for the former, with the result that the calculated energy and fissions to the first peak agree with the measured values to within 3%.

In the long term, the calculated power decreases faster than observed in the experiment. The calculation does not reproduce the observed oscillatory behaviour after the first peak and, in particular, does not exhibit the observed fall to a minimum power of under 38 kW at 14 s. As a result the calculated total energy and fissions are about 12% higher than measured and the temperature rise is overestimated by 8%.

STEP-004

The measured and calculated power histories are compared in Figures 7.3.6 and 7.3.7. Good agreement is obtained (better than 8%) between most of the calculated and the measured parameters to the first peak power. The only significant discrepancy is in the underestimation of the time to the first peak by 39%, which is due to an inappropriate choice of 1 W for the initial critical power level.

In the long term the calculated rate of power reduction is lower than observed and consequently the total energy and fissions are overestimated by over 80% and the calculated temperature rise is 56% higher than observed. The calculation fails to reproduce the observed oscillatory behaviour after the first power peak.

STEP-005

The measured and calculated power histories are compared in Figures 7.3.8 and 7.3.9. Figure 7.3.8 shows good agreement between the calculated and measured parameters to the first peak power; the maximum inverse period, time to first peak and the peak power all agree to within 7% and the energy and fissions to the first peak agree to within 23%. Good agreement in the time of the first peak (to within 2%) is obtained in this case as the initial power 1 W used in the calculation is in agreement with the measured power at the start of the transient.

Figure 7.3.9 shows that the calculated power declines more slowly than observed and consequently the total energy and fissions are overestimated by 33% and the calculated temperature rise is 53% higher than observed. The calculation does not reproduce the observed oscillatory behaviour after the first peak.

7.3.3 Conclusions

The predicted behaviour to the first peak in fission power is generally good, agreeing with measured parameters to within about 20%. The exception is the much larger discrepancies in the estimated time to the first peak for STEP-002 to STEP-004, which resulted from the use of a poor estimate for the initial power in the corresponding calculations. In the longer term the agreement with experiment remains reasonable, being within roughly 50% of the measured values. However, the calculations fail to reproduce any oscillatory behaviour, though such behaviour was observed in all of the tests except STEP-001.

Figure 7.3.1: INCTAC code thermal-hydraulic modelling for TRACY

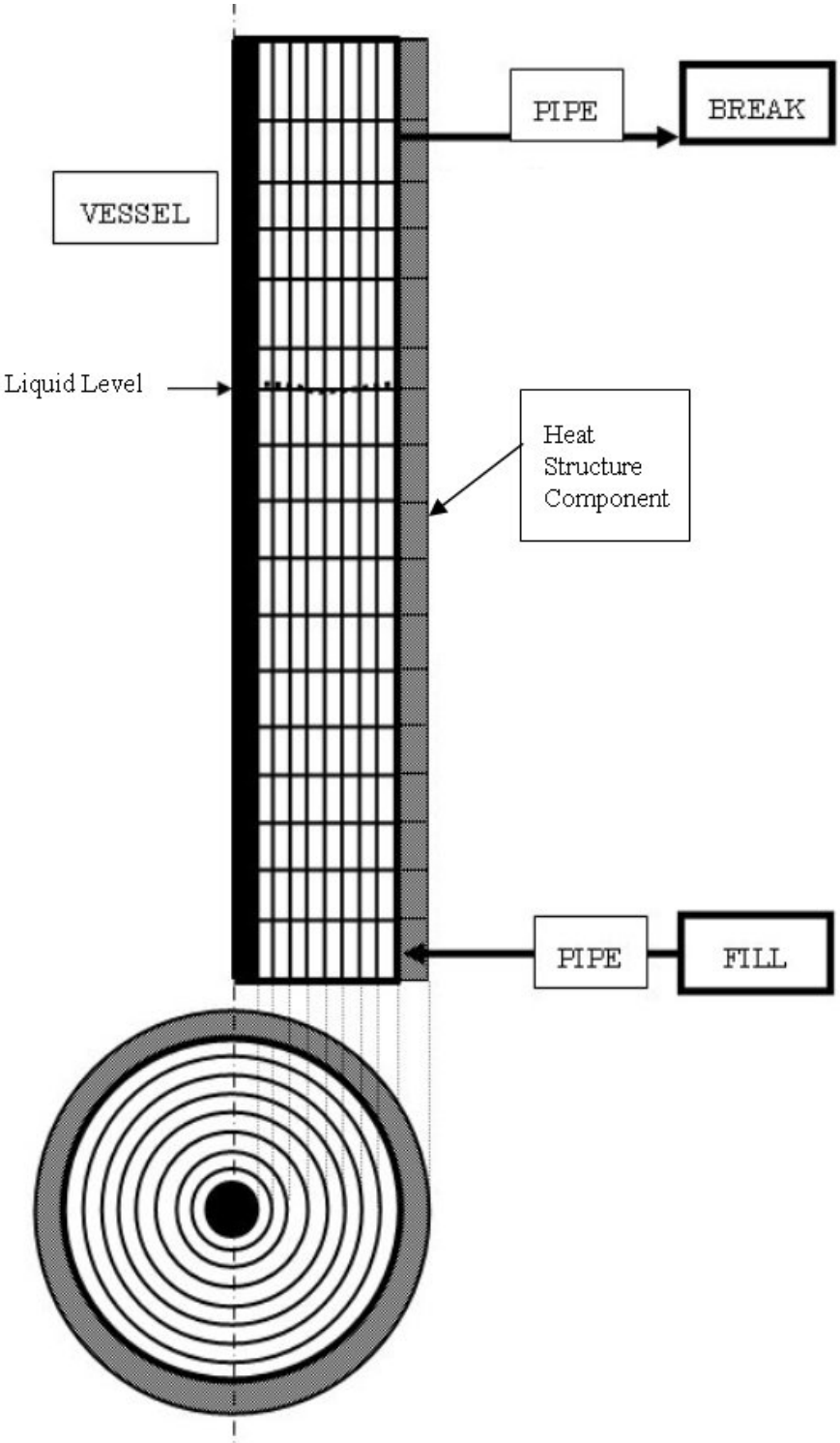

Figure 7.3.2: INCTAC power calculation – R100 (0.3$)

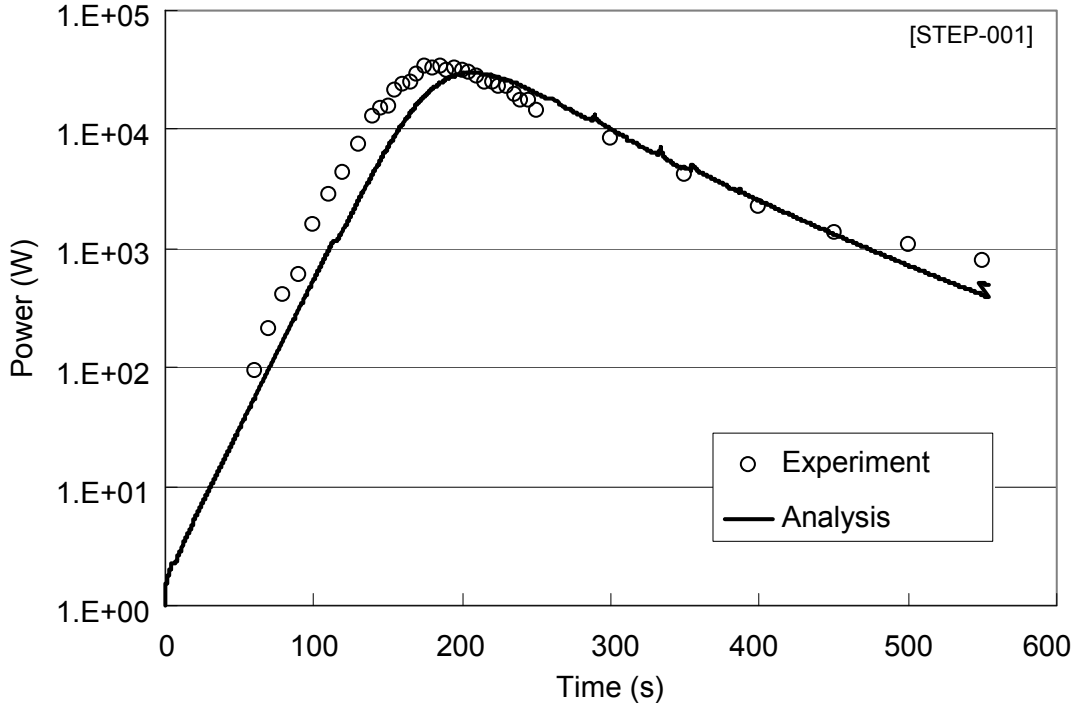

Figure 7.3.3: INCTAC power calculation – R143 (0.7$)

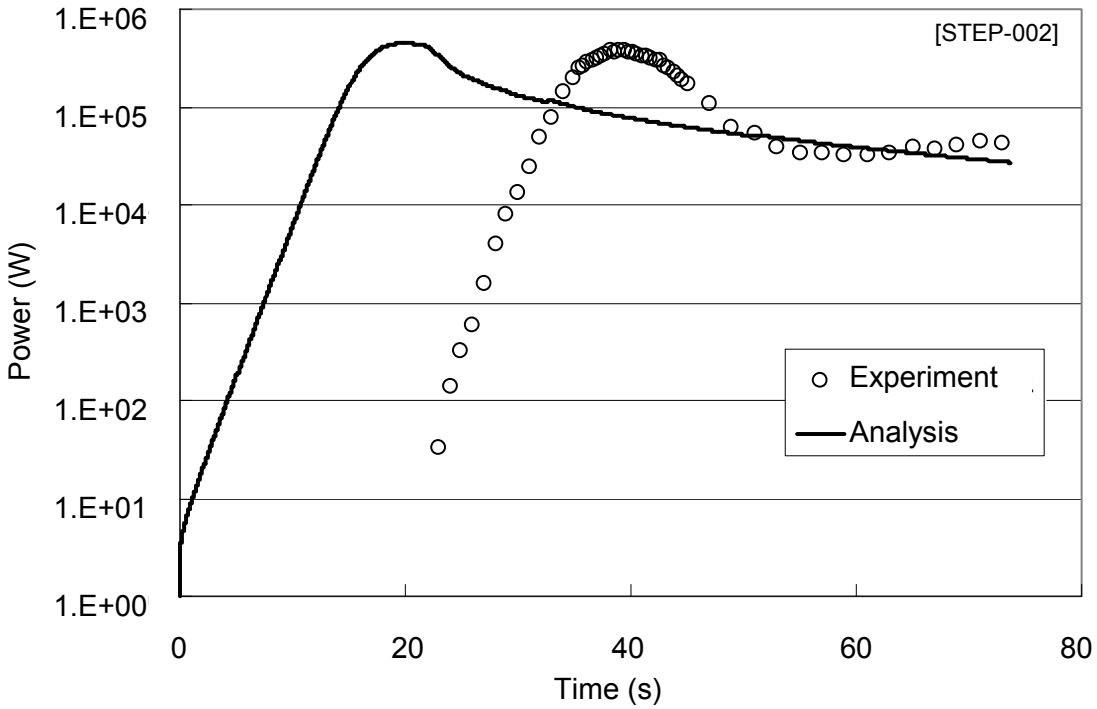

Figure 7.3.4: INCTAC power calculation – R72 (1.1$) (0-3 s)

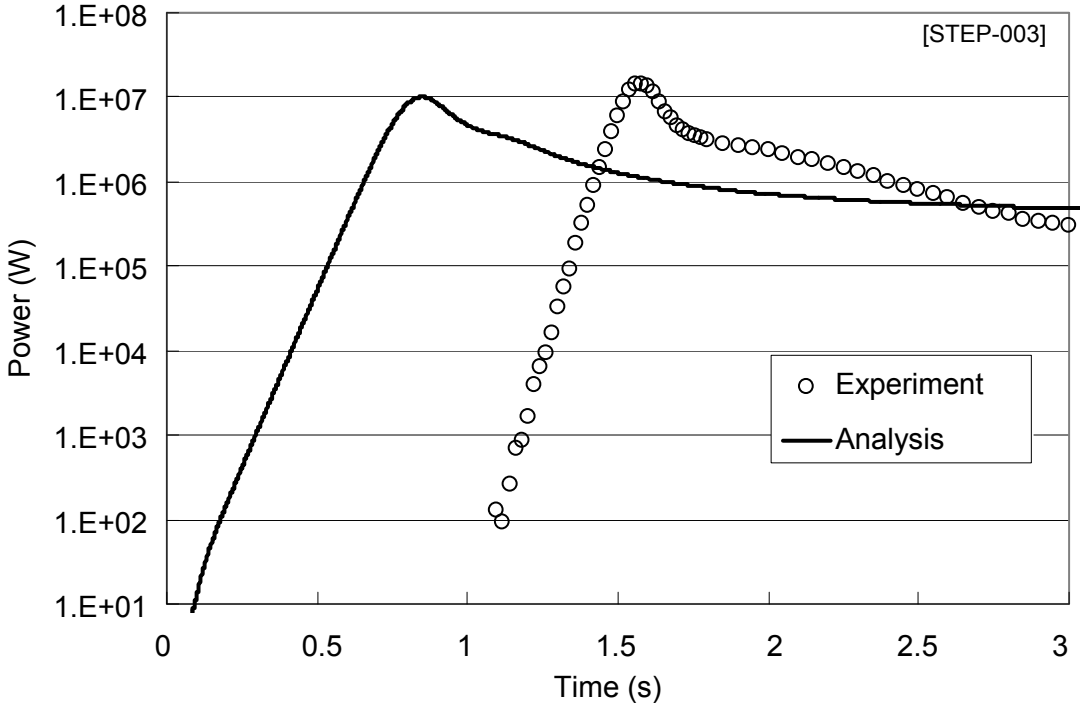

Figure 7.3.5: INCTAC power calculation – R72 (1.1$)

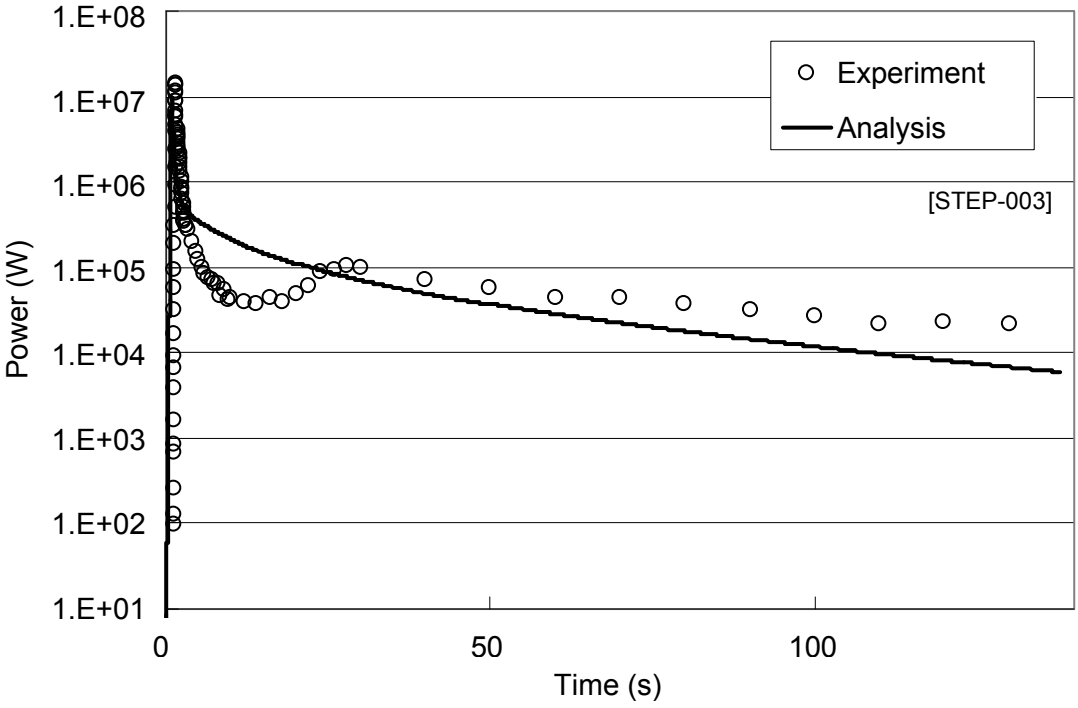

Figure 7.3.6: INCTAC power calculation – R196 (2.0$) (0-0.5 s)

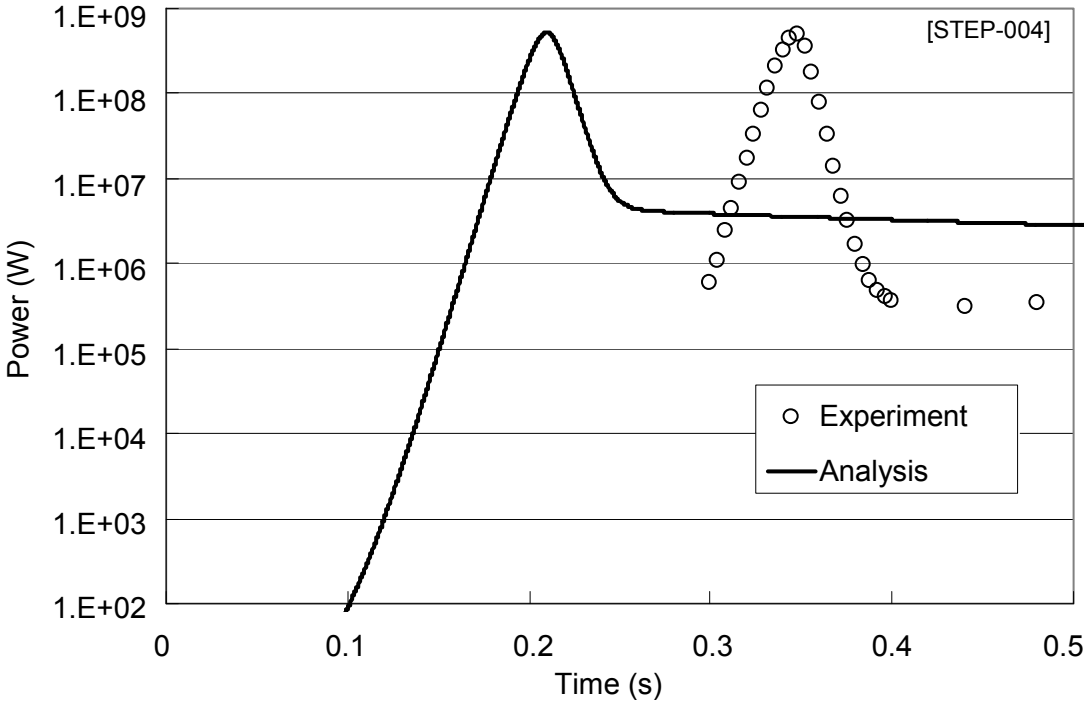

Figure 7.3.7: INCTAC power calculation – R196 (2.0$)

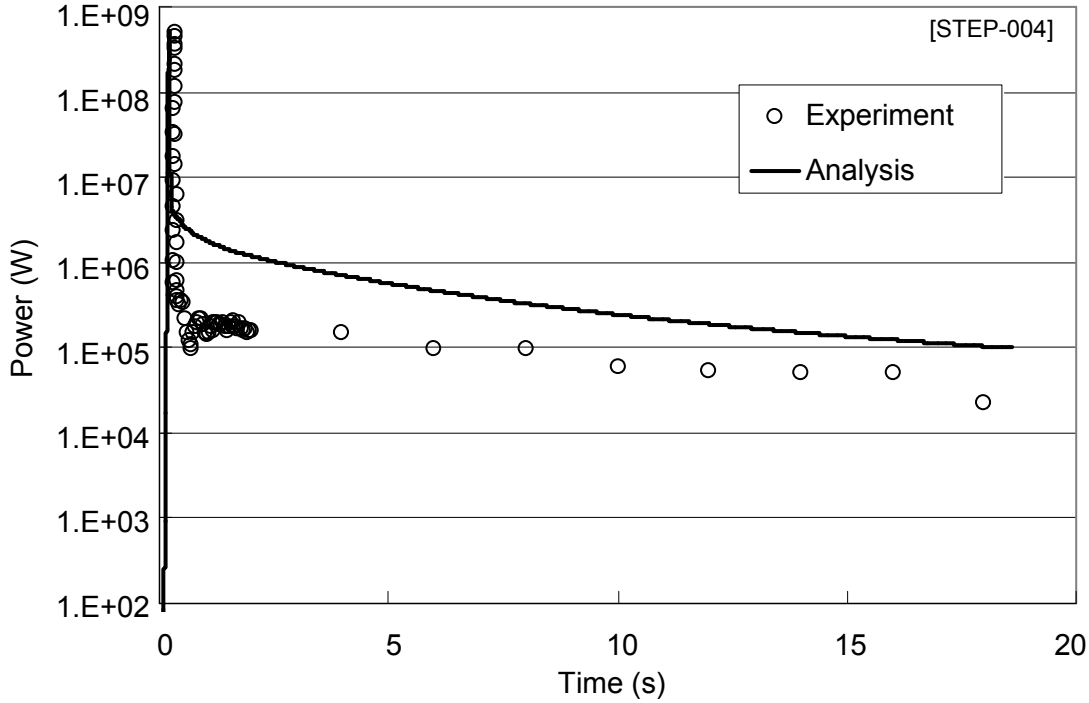

Figure 7.3.8: INCTAC power calculation – R203 (2.97$) (0.1-0.3 s)

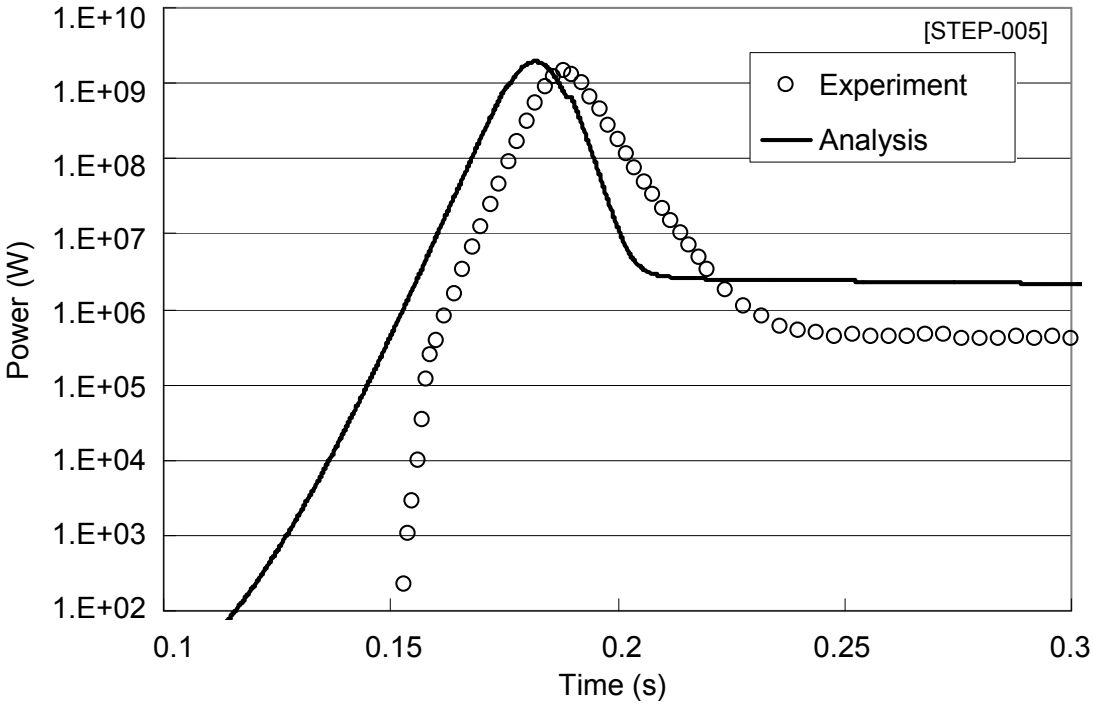

Figure 7.3.9: INCTAC power calculation – R203 (2.97$)

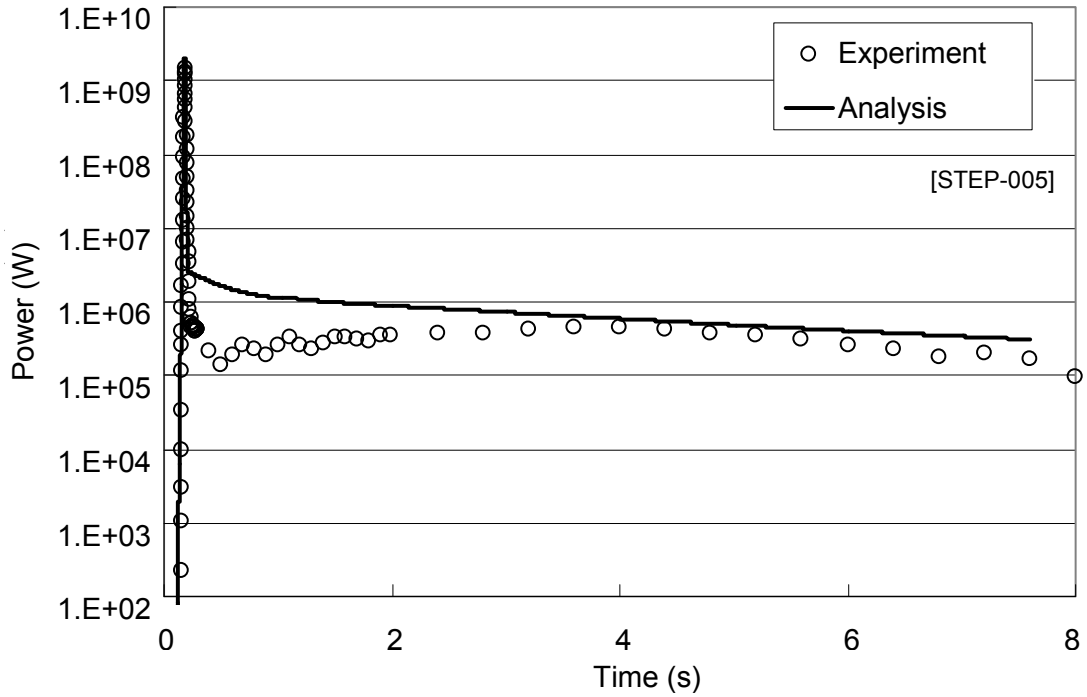

7.4 TRACE

7.4.1 Input parameters

The basic modelling parameters chosen to simulate the TRACY experiments with the TRACE (Mitake, 2005) code are displayed in Table 7.4.1 and the kinetic parameter values are given in Table 7.4.2. The variation of reactivity with temperature and void fraction is specified in Table 7.4.3.

Table 7.4.1: TRACE modelling and parameters for TRACY benchmark calculations

	Model/parameter	Adopted value
Geometry	2-D cylindrical geometry	Axial: 8 meshes Radial: 5 meshes
Neutronics	Delayed neutron precursors group	6
	Constant power distribution	Axial: cosine Radial: Bessel J_0
Reactivity feedback	Weighting function for temperature and void reactivity feedback calculation	Power
Radiolytic gas formation	G value	1×10^{-7} mol/J
	Volume of void produced per energy added per number of moles of radiolytic gas	0.5×10^{-7} m^3/J.mol
	Critical value for radiolytic gas concentration	20 mol/m^3
Gas bubble velocity	New model (continuous velocity) $\nu = \nu_o + sign(\omega)\nu_g \ln(1 + \lvert\omega\rvert)$ ω: reactor period (s)	ν_o = 0.01 m/s ν_g = 0.07 m/s
Thermal-hydraulic	Fuel solution region: 2-D cylindrical conduction Mixing parameter	1.0 s^{-1}
	Vessel/tank region: Natural circulation at the inner side and bottom walls (lumped parameters)	Heat transfer coefficients are internally calculated in the code
	Surrounding air region: Air natural circulation at the outer side and bottom walls (lumped parameters)	Heat transfer coefficients are internally calculated in the code
Motion	Axial direction motion equation (lumped parameter)	Momentum dissipation coefficient 2 600 m/s^2

Table 7.4.2: Kinetic parameters for TRACY benchmark calculations by TRACE code

Parameter	Value
Delayed neutron fractions	2.5140E-04
	1.6199E-03
	1.4689E-03
	2.9505E-03
	8.7515E-04
	3.1892E-04
Precursor decay constant (1/s)	1.2703E-02
	3.1704E-02
	1.1524E-01
	3.1160E-01
	1.4003E+00
	3.8739E+00
Generation time (s)	4.8585E-05
Prompt neutron lifetime (s)	4.7624E-05

Table 7.4.3: Temperature and void fraction reactivity feedback coefficients

Parameter	Symbol	Units	Reactivity feedback ($)
Temperature	ΔT	K	$6.0 \times 10^{-5}\ \Delta T^2 - 0.0335 \Delta T$
Void fraction	V	% volume	$-0.0015V^2 - 0.4715V$

7.4.2 Comparison with experiment

STEP-001

This is a very slow transient experiment. The calculated power history is compared with experiment in Figure 7.4.1. The trends are similar and the calculated maximum inverse period and time to the first peak only differ from the experiment by roughly 10%. The peak power is overestimated by 43% and the energy and fissions to the peak by 32%. The overestimation of the power continues to the end of the test where the total energy and fissions are overestimated by 54% and the calculated temperature rise is 65% higher than observed. The observed reduction in the rate of power decrease at the end of the test is not reproduced by the calculation.

STEP-002

The calculated power history is compared with the experimental values in Figure 7.4.2. There is agreement to within 12% on all parameters (maximum inverse period, time to peak, peak power and energy and fissions to first peak) up to the first peak. However, the rate of power increase to the first peak suggests that input the reactivity insertion rate may have been an underestimate. Beyond the first peak the calculation overestimates the power, yielding a total energy release and fissions that exceed the experimental value by 36% and a temperature rise that is 51% higher than observed. The calculation does not reproduce the observed oscillatory behaviour.

STEP-003

The TRACE power history is compared with experiment in Figures 7.4.3 and 7.4.4. Figure 7.4.3 indicates that the input reactivity insertion rate to the calculation may have been an underestimate. The calculation overestimates the maximum inverse period by 55% and underestimates the peak power by 34%. However, the predicted time to the first peak and the energy and fissions to the peak agree with the measured values to within 7%.

Figure 7.4.4 shows that the calculation captures the qualitative long-term behaviour well, including the minimum in the power at around 14 s and the occurrence of a second peak. However, the power is consistently overestimated in the long term leading to total energy and fissions that are double the measured values and a temperature rise that is 90% higher than observed.

STEP-004

The calculated power history is compared with experiment in Figures 7.4.5 and 7.4.6. Figure 7.4.5 shows that there is good qualitative agreement in the early stages, though the peak power and energy and fissions to the first peak are underestimated by about 55%. Figure 7.4.6 shows reasonable agreement in the long term, though the underestimation of the first peak leads to total energy and fissions that are 13% lower than measured and the calculated temperature rise is 20% lower than observed. The calculation fails to predict the observed oscillatory behaviour. The predicted maximum pressure rise is much lower than observed.

STEP-005

The calculated power history is compared with experiment in Figures 7.4.7 and 7.4.8. The results are very similar to STEP-004. Qualitative behaviour in the early stages is good, but the calculated time to the first peak is 30% less than measured, the peak power is 43% lower and the energy and fissions to the peak are 35% low. This results in the total energy and fissions being 25% less than measured and the temperature rise is underestimated by 22%. The calculation does not reproduce the observed oscillatory behaviour.

7.4.3 Conclusions

In general, for the slow transient benchmark problems STEP-001 and STEP-002, the TRACE calculations overestimate the first power peaks and the total energy and fissions. For the fast (prompt-critical) transient benchmark problems STEP-003 to STEP-005, the TRACE calculations underestimate the first power peaks. These discrepancies probably result from the use of inaccurate temperature reactivity feedbacks. More accurate estimates of the temperature feedback coefficients on reactivity are suggested for future investigations. The calculated results are also sensitive to the temperature mixing parameter used in the thermal-hydraulic model. This parameter should be more carefully adjusted in the future. Finally, further consideration should be given to the weighting function used on the temperature feedback coefficients of reactivity.

It is noted that the TRACE calculation reproduces the observed oscillatory behaviour in STEP-003 very well, but failed to reproduce the oscillatory behaviour observed in STEP-002, STEP-004 or STEP-005.

Figure 7.4.1: TRACE power calculation – R100 (0.3$)

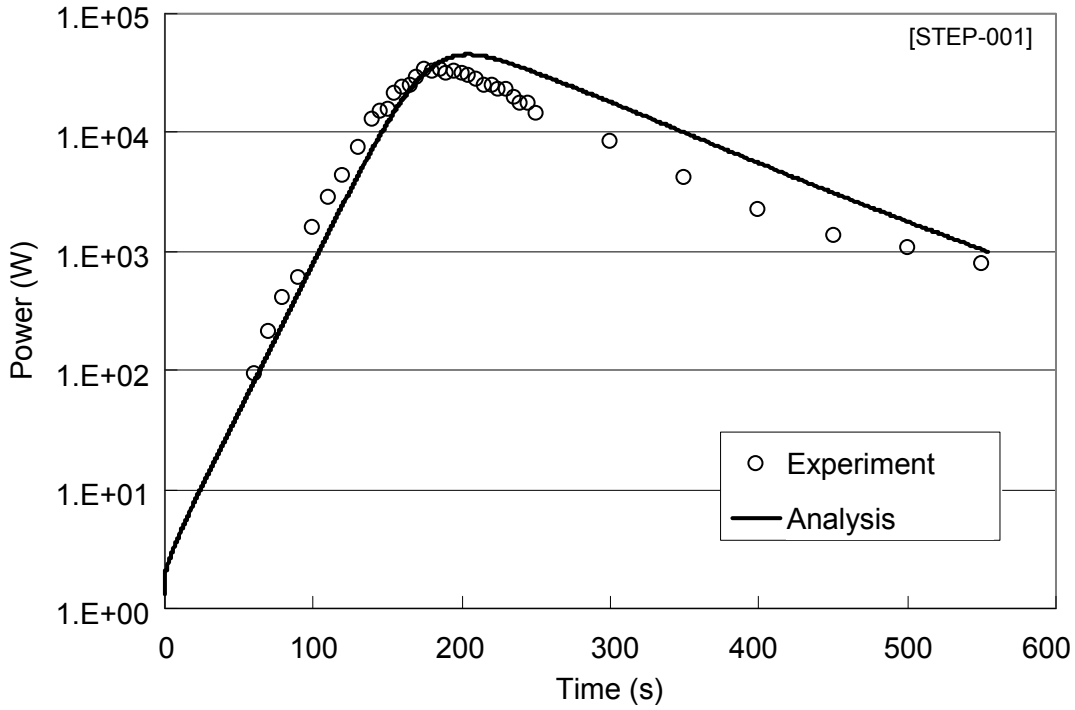

Figure 7.4.2: TRACE power calculation – R143 (0.7$)

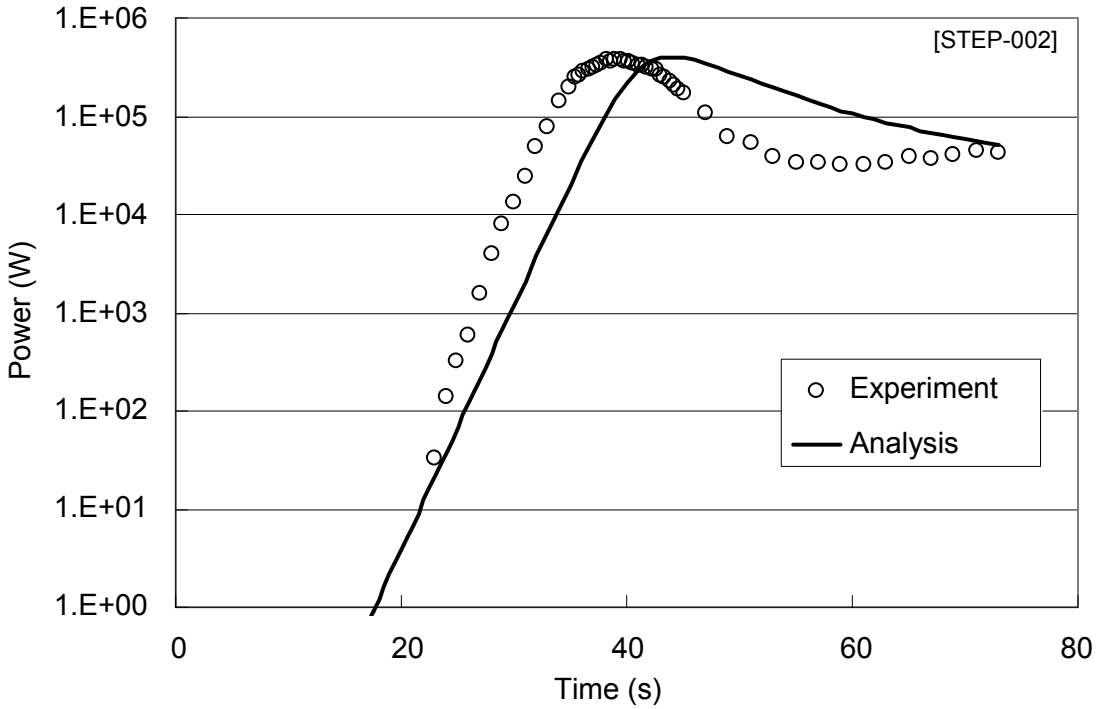

Figure 7.4.3: TRACE power calculation – R72 (1.1$) (0-4 s)

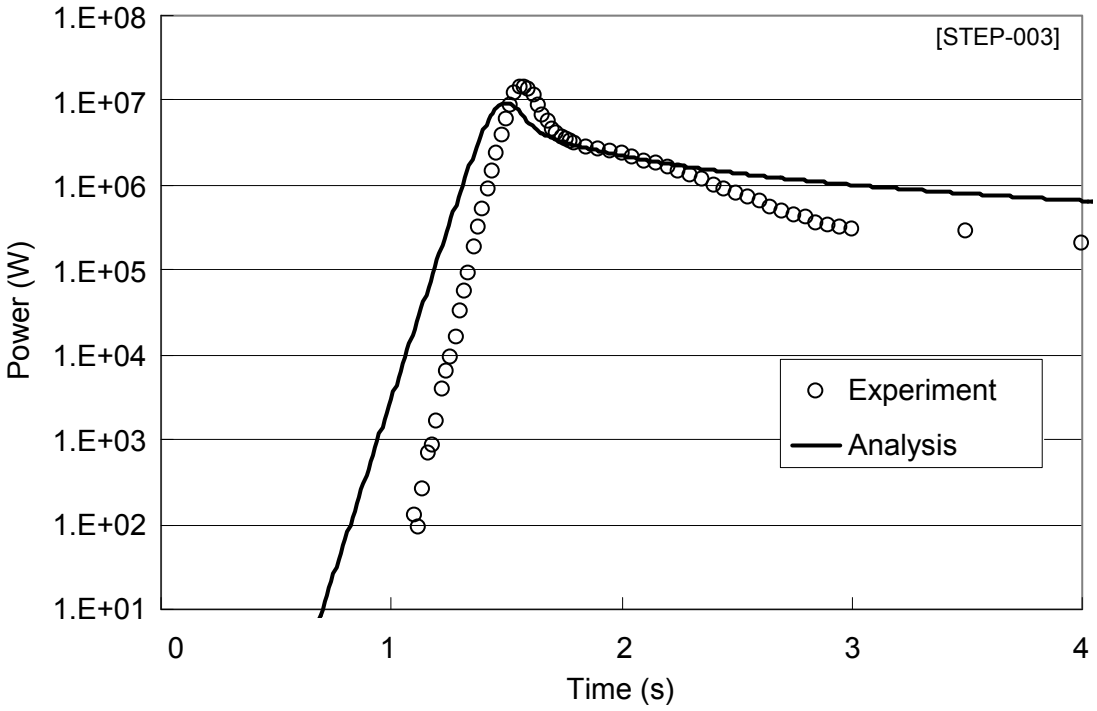

Figure 7.4.4: TRACE power calculation – R72 (1.1$)

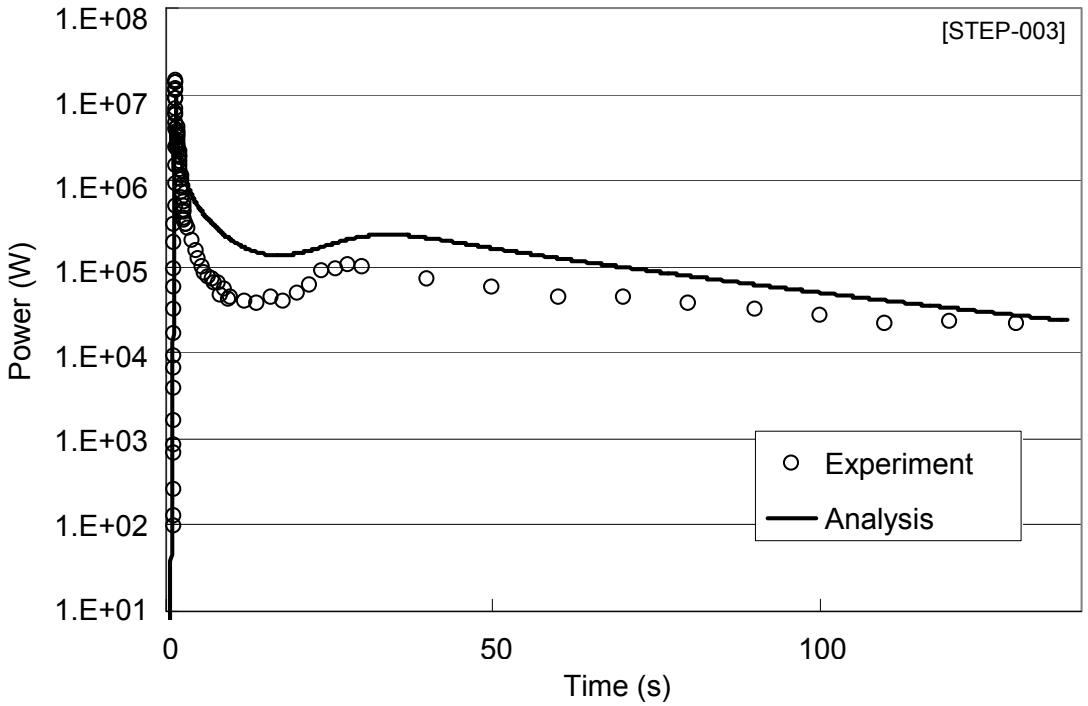

Figure 7.4.5: TRACE power calculation – R196 (2.0$) (0-0.5 s)

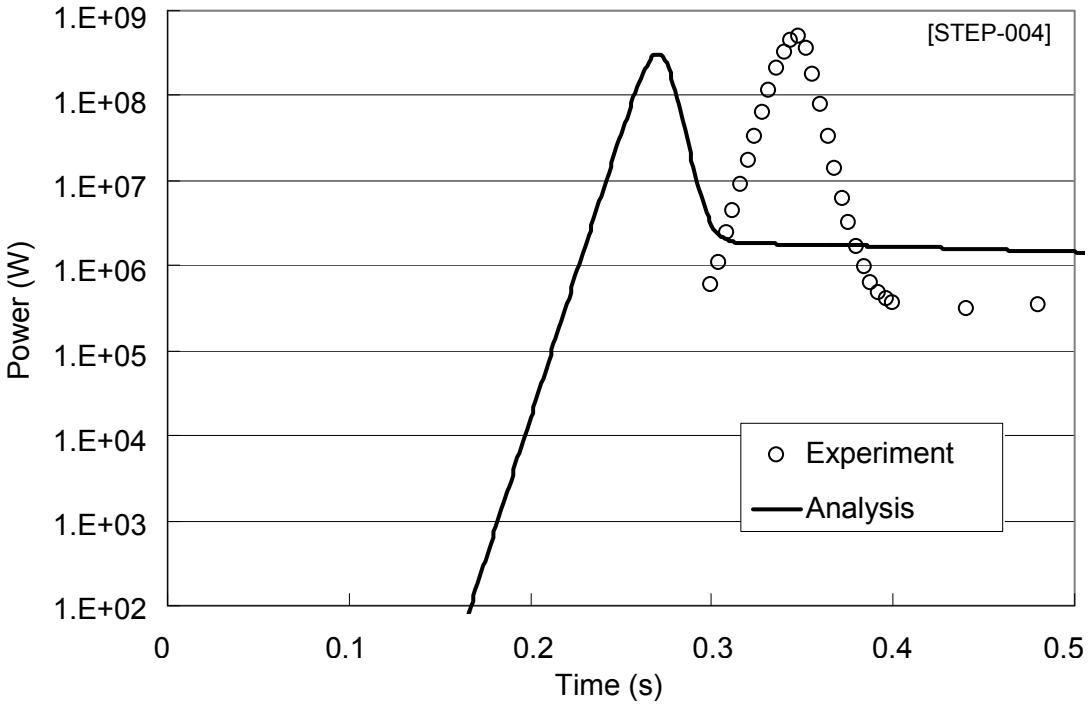

Figure 7.4.6: TRACE power calculation – R196 (2.0$)

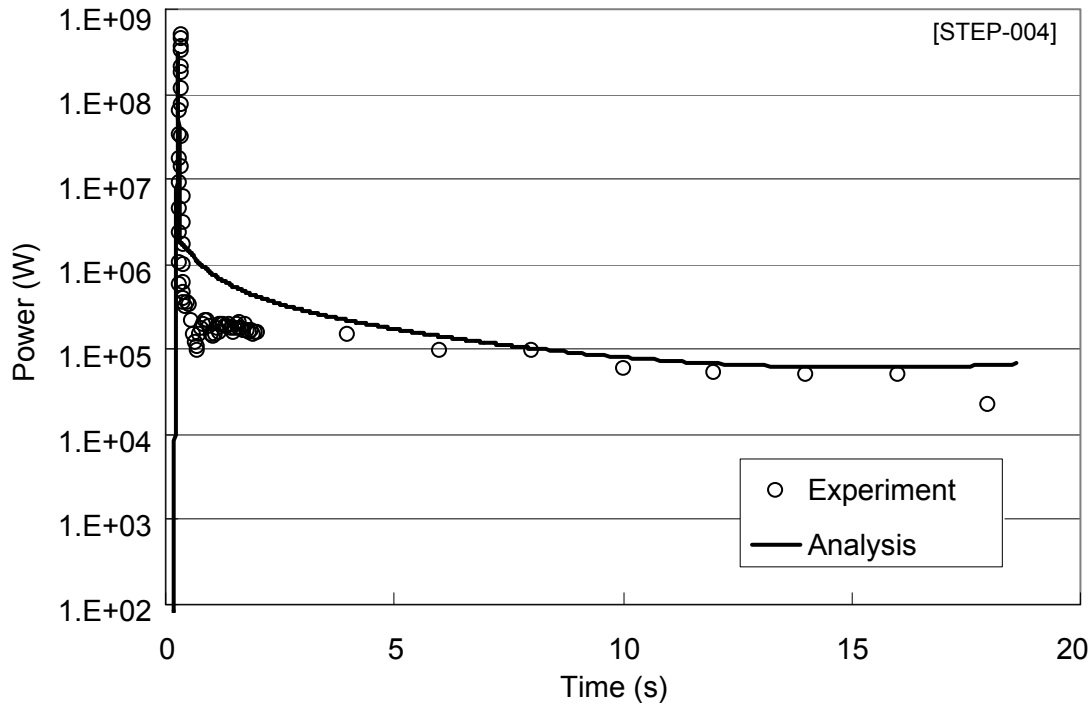

Figure 7.4.7: TRACE power calculation – R203 (2.97$) (0-0.3 s)

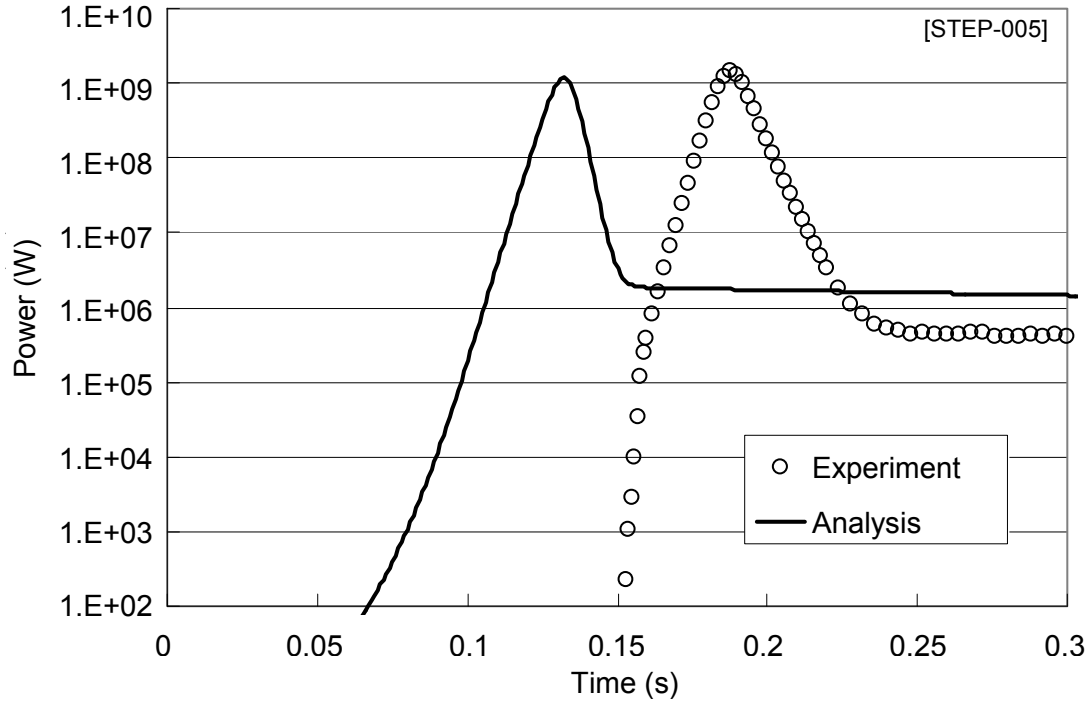

Figure 7.4.8: TRACE power calculation – R203 (2.97$)

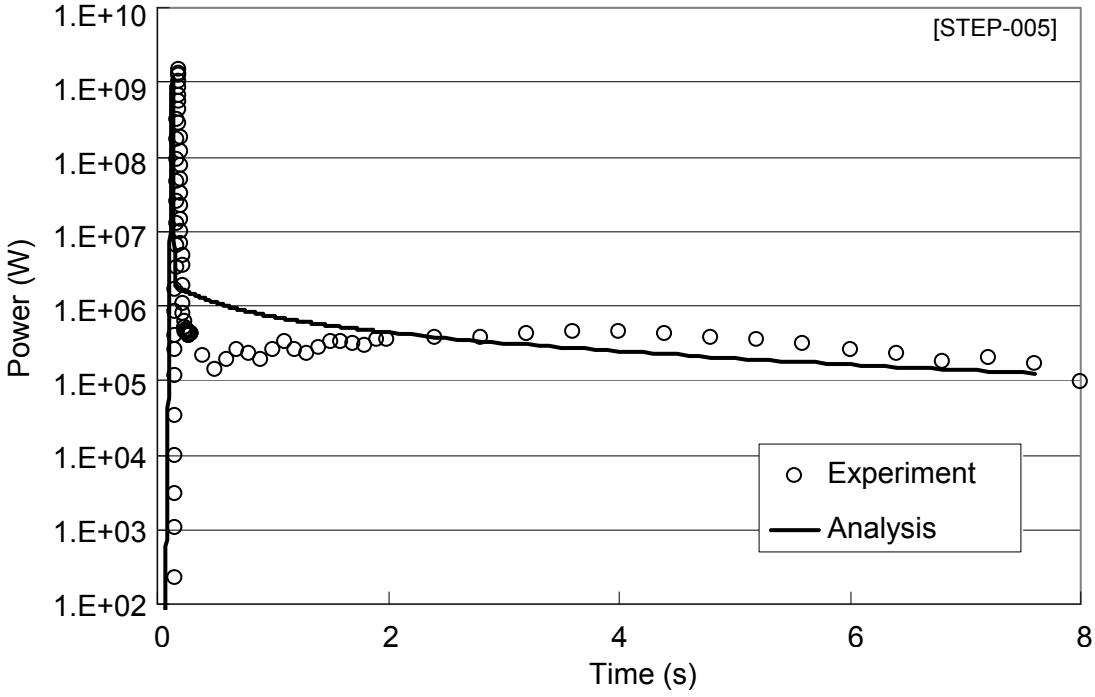

7.5 Summary

The comparison of the code benchmark calculations with the experimental measurements is summarised in Tables 7.5.1 to 7.5.5 and Figures 7.5.1 to 7.5.7.

STEP-001

Table 7.5.1 summarises the results for R100 [STEP-001]. Each code reproduces the whole power profile well and the calculated maximum inverse periods agree with the experimental value to within 3-16%. The estimated time to the power peak is accurate to within 19% in all cases. The calculated peak power, energy to the peak, total energy and the temperature rise agree with the measured values to within 19% for all codes except TRACE. The TRACE calculation overestimates these parameters by between 32% and 65%.

Table 7.5.1: Summary of calculation results for R100 [STEP-001]

Items	B. MARK	AGNES	C/E	CRITEX	C/E	INCTAC	C/E	TRACE	C/E
Max. inverse period (s^{-1})	6.51E-02	6.34E-02	0.97	5.5E-02	0.84	5.7E-02	0.88	5.70E-02	0.88
Time to first peak (s)	189.39	184.29	0.97	223	1.18	206.55	1.09	204.1	1.08
Power at first peak (w)	3.16E+04	3.34E+04	1.06	3.75E+04	1.19	2.99E+04	0.95	4.53E+04	1.43
Energy to first peak (J)	1.47E+06	1.28E+06	0.87	1.69E+06	1.15	1.29E+06	0.88	1.94E+06	1.32
Fissions to first peak	4.58E+16	4.00E+16	0.87	5.26E+16	1.15	4.03E+16	0.88	6.06E+16	1.32
Total energy (J)	4.20E+06	3.99E+06	0.95	5.00E+06	1.19	3.85E+06	0.92	6.45E+06	1.54
Total fissions	1.31E+17	1.25E+17	0.95	1.56E+17	1.19	1.20E+17	0.92	2.02E+17	1.54
Temperature									
Initial temperature (°C)	26.2	26.2	1.00	26.2	1.00	26.2	1.00	26.2	1.00
Final temperature (°C)	36.2	35.6	0.98	37.3	1.03	35.5	0.98	42.7	1.18
Pressure									
Maximum pressure (MPa)	–	–	–	–	–	–	–	3.53E-03	–

STEP-002

Table 7.5.2 summarises the results for R143 [STEP-002]. All of the calculations agree with the measured maximum inverse period and maximum power to within approximately 20%. However, the CRITEX and INCTAC calculations rise to the first peak 28% and 50% too early, respectively, due to the use of an inappropriate initial power of 1 W. The early power rise results in these codes overestimating the total energy and the temperature rise by roughly 50%. All the calculations estimate the energy to the first power peak to within 9% except CRITEX which has an error of 40%. AGNES estimates the total energy and temperature rise to within 3% while TRACE overestimates the total energy by 36% and the temperature rise by 51% due to the power decreasing too slowly after the first peak.

None of the calculations reproduce the observed oscillatory behaviour in this test.

Table 7.5.2: Summary of calculation results for R143 [STEP-002]

Items	B. MARK	AGNES	C/E	CRITEX	C/E	INCTAC	C/E	TRACE	C/E
Max. inverse period (s^{-1})	6.29E-01	6.93E-01	1.10	5.10E-01	0.81	6.90E-01	1.10	5.80E-01	0.92
Time to first peak (s)	39.313	39.021	0.99	28.4	0.72	19.841	0.50	44.1	1.12
Power at first peak (w)	3.72E+05	3.41E+05	0.92	4.23E+05	1.14	4.49E+05	1.21	4.01E+05	1.08
Energy to first peak (J)	1.78E+06	1.79E+06	1.01	2.50E+06	1.40	1.94E+06	1.09	1.84E+06	1.03
Fissions to first peak	5.55E+16	5.58E+16	1.01	7.80E+16	1.41	6.06E+16	1.09	5.75E+16	1.04
Total energy (J)	4.80E+06	4.95E+06	1.03	6.96E+06	1.45	7.15E+06	1.49	6.53E+06	1.36
Total fissions	1.50E+17	1.55E+17	1.03	2.17E+17	1.45	2.23E+17	1.49	2.04E+17	1.36
Temperature									
Initial temperature (°C)	24.8	24.8	1.00	24.8	1.00	24.8	1.00	24.8	1.00
Final temperature (°C)	35.8	36.4	1.02	41.8	1.17	41	1.15	41.4	1.16
Pressure									
Maximum pressure (MPa)	–	–	–	–	–	–	–	1.57E-02	–

STEP-003

Table 7.5.3 summarises the results for R72 [STEP-003]. There is considerable spread in the error in the calculated maximum inverse periods for this experiment, varying from -29% to +55%. The calculated time to the first peak is within 10% of the observed value, except for the INCTAC calculation which underestimates the time by 46%, due to the use of an inappropriate value of 1 W for the initial power. All of the codes calculate the energy to the first peak to within 4%. However, although AGNES accurately estimates the peak power, the other codes all underestimate the measured value by over 30%. All the calculations estimate the total energy and temperature rise to better than 20%, except TRACE which overestimates both parameters by a factor of roughly two.

In this experiment both the CRITEX and TRACE calculations reproduce the observed oscillatory behaviour quite well.

Table 7.5.3: Summary of calculation results for R72 [STEP-003]

Items	B. MARK	AGNES	C/E	CRITEX	C/E	INCTAC	C/E	TRACE	C/E
Max. inverse period (s^{-1})	2.55E+01	2.77E+01	1.09	1.76E+01	0.69	2.00E+01	0.78	3.94E+01	1.55
Time to first peak (s)	1.5756	1.5727	1.00	1.73	1.10	0.848	0.54	1.5	0.95
Power at first peak (w)	1.44E+07	1.47E+07	1.02	9.10E+06	0.63	1.00E+07	0.69	9.45E+06	0.66
Energy to first peak (J)	1.10E+06	1.14E+06	1.04	1.06E+06	0.96	1.07E+06	0.97	1.02E+06	0.93
Fissions to first peak	3.43E+16	3.58E+16	1.04	3.31E+16	0.97	3.35E+16	0.98	3.19E+16	0.93
Time to first minimum (s)	14.23	–	–	–	–	–	–	–	–
Power at first minimum (w)	3.77E+04	–	–	–	–	–	–	–	–
Energy to first minimum (J)	8.75E+06	–	–	–	–	–	–	–	–
Fissions to first minimum	2.74E+17	–	–	–	–	–	–	–	–
Total energy (J)	1.03E+07	1.19E+07	1.16	1.03E+07	1.00	1.15E+07	1.12	2.09E+07	2.03
Total fissions	3.22E+17	3.71E+17	1.15	3.20E+17	0.99	3.58E+17	1.11	6.53E+17	2.03
Temperature									
Initial temperature (°C)	26.2	26.2	1.00	26.2	1.00	26.2	1.00	26.2	1.00
Final temperature (°C)	50.8	54.74	1.08	48.3	0.95	52.8	1.04	76.1	1.50
Pressure									
Maximum pressure (MPa)	–	–	–	–	–	–	–	2.21E-02	–

STEP-004

Table 7.5.4 summarises the results for R196 [STEP-004]. All of the codes estimate the maximum inverse period to within 8% and all except INCTAC also estimate the time to the first peak to within 8%. INCTAC underestimates the time to the first peak by almost 40% due to the use of an inappropriate value of 1 W for the initial power. The calculations estimate the peak power and energy to the peak to

Table 7.5.4: Summary of calculation results for R196 [STEP-004]

Items	B. MARK	AGNES	C/E	CRITEX	C/E	INCTAC	C/E	TRACE	C/E
Max. inverse period (s^{-1})	1.69E+02	1.70E+02	1.01	1.55E+02	0.92	1.62E+02	0.96	1.55E+02	0.92
Time to first peak (s)	0.344	0.3451	1.00	0.33	0.96	0.21	0.61	0.27	0.78
Power at first peak (w)	5.66E+08	5.69E+08	1.01	5.77E+08	1.02	5.21E+08	0.92	3.10E+08	0.55
Energy to first peak (J)	6.09E+06	6.14E+06	1.01	6.60E+06	1.08	5.68E+06	0.93	3.40E+06	0.56
Fissions to first peak	1.90E+17	1.92E+17	1.01	2.06E+17	1.08	1.77E+17	0.93	1.06E+17	0.56
Total energy (J)	1.11E+07	1.25E+07	1.13	1.41E+07	1.27	2.02E+07	1.82	9.62E+06	0.87
Total fissions	3.48E+17	3.91E+17	1.12	4.39E+17	1.26	6.31E+17	1.81	3.01E+17	0.86
Temperature									
Initial temperature (°C)	25.9	25.9	1.00	25.9	1.00	25.9	1.00	25.9	1.00
Final temperature (°C)	51.5	52.39	1.02	55.9	1.09	65.9	1.28	46.4	0.90
Pressure									
Maximum pressure (MPa)	3.04E-01	3.30E-01	1.09	–	–	–	–	2.08E-02	0.07

within roughly 20%, except TRACE which underestimates these parameters by about 45%. All of the calculations estimate the total power to within 27% and the temperature rise to within 20%, except INCTAC which overestimates the temperature rise by 56%.

In this case CRITEX was the only code to simulate oscillatory behaviour, though with a significantly longer period than observed.

The measured pressure rise indicates significant radiolytic gas release from the fissile solution, which contributes to the four decades of power decrease after the peak due to the large negative feedback effect on reactivity. The maximum pressure due to radiolytic gas bubble production is reproduced well by AGNES, but is significantly underestimated by TRACE.

STEP-005

Table 7.5.5 summarises the results for R203 [STEP-005]. The AGNES and CRITEX calculations agree with the measured values of all parameters to better than 14%. The INCTAC calculation estimates the maximum inverse period, peak power and time to the first peak to within 6%, but overestimates the energy to the first peak by 23%, the total energy by 33% and the temperature rise by 53%. The TRACE calculation underestimates the peak power, time to the peak and energy to the peak by between 30% and 43%. It also underestimates the total energy and temperature rise by roughly 25%.

None of the calculations reproduce the observed oscillatory behaviour.

Table 7.5.5: Summary of calculation results for R203 [STEP-005]

Items	B. MARK	AGNES	C/E	CRITEX	C/E	INCTAC	C/E	TRACE	C/E
Max. inverse period (s^{-1})	3.34E+02	3.34E+02	1.00	3.05E+02	0.91	3.10E+02	0.93	3.04E+02	0.91
Time to first peak (s)	0.1854	0.1874	1.01	0.16	0.86	0.182	0.98	0.13	0.70
Power at first peak (w)	2.08E+09	2.00E+09	0.96	1.98E+09	0.95	1.95E+09	0.94	1.18E+09	0.57
Energy to first peak (J)	1.03E+07	9.08E+06	0.88	1.04E+07	1.01	1.27E+07	1.23	6.71E+06	0.65
Fissions to first peak	3.20E+17	2.84E+17	0.89	3.23E+17	1.01	3.96E+17	1.23	2.10E+17	0.66
Total energy (J)	2.03E+07	1.80E+07	0.89	2.03E+07	1.00	2.69E+07	1.33	1.51E+07	0.74
Total fissions	6.32E+17	5.63E+17	0.89	6.32E+17	1.00	8.41E+17	1.33	4.72E+17	0.75
Temperature									
Initial temperature (°C)	26.1	26.1	1.00	26.1	1.00	26.1	1.00	26.1	1.00
Final temperature (°C)	66.7	61.43	0.92	71.6	1.07	88.4	1.33	57.6	0.86
Pressure									
Maximum pressure (MPa)	8.95E-01	1.01E+00	1.13	–	–	8.40E-01	0.94	2.66E-02	0.03

The measured maximum pressure indicates significant radiolytic gas release from the fissile solution, which contributes to the four decades of power decrease after the peak due to large negative feedback reactivity. The maximum pressure due to radiolytic gas bubble production is reproduced well by AGNES and INCTAC, but is significantly underestimated by TRACE.

7.5.1 General observations

Graphical comparison of the ratio between calculation and experimental results, C/E, for the maximum inverse period, time to the first power peak, first peak power, fissions to the first power peak, total fissions, final temperature and maximum pressure are shown in Figures 7.5.1 to 7.5.7, respectively.

The maximum inverse time periods are compared in Figure 7.5.1. The calculated values for this parameter are generally in good agreement with experiment, *i.e.* accurate to within 20%. The exception is STEP-003, for which this parameter is underestimated by roughly 30% by CRITEX and overestimated by more than 50% by TRACE.

The times to the first power peak are compared in Figure 7.5.2. Again the calculated values generally agree with experiment to within roughly 20%. The exceptions include the INCTAC values for STEP-002 to STEP-004, which are underestimated by 40-50%, due to the use of the inappropriate value of 1 W for the initial power. The CRITEX value for STEP-002 is 30% too low, for the same reason. The TRACE calculation is 30% too low for STEP-005, though this is believed to be due to the use of inaccurate

values for the temperature feedback coefficients on reactivity and possibly also to the use of unoptimised values for the thermal mixing parameter and weighting function.

The powers at the first peak are compared in Figure 7.5.3. The calculated values generally agree with experiment to within 20%. The main exception is the TRACE calculations which overestimate the power by more than 40% for STEP-001 and underestimate it by roughly 40% for STEP-003 to STEP-005. This is believed to be due to the use of inaccurate values for the temperature feedback coefficients on reactivity and possibly also to the use of unoptimised values for the thermal mixing parameter and weighting function. The CRITEX and INCTAC calculations also underestimate the power by more than 30% for STEP-003; the reason for this is not evident, though it may be related to the underestimation of the maximum inverse period by 31%/22%, respectively, for this test.

The fissions to the first peak are compared in Figure 7.5.4. The calculated values generally agree with experiment to within 20%. Exceptions include the TRACE calculations which overestimate the fissions by about 30% for STEP-001 and underestimate them by roughly 40% for STEP-004 and STEP-005, for the same reasons as above. The CRITEX calculation overestimates the fissions for STEP-002 by 40%, though the reason for this is not evident.

The total fissions are compared in Figure 7.5.5. The calculated values generally agree with experiment to within 25%. Exceptions include the TRACE calculations for STEP-001 to STEP-003, which overestimate the total fissions by 54%, 36% and 103%, respectively, for reasons mentioned above. The CRITEX and INCTAC calculations overestimate the total fissions for STEP-003 by almost 50% as a result of the early rise to the peak power, due to the use of an inappropriate value of 1 W for the initial power. The INCTAC calculations for STEP-004 and STEP-005 also overestimate the total fissions, by 81% and 33%, respectively. This is due to overestimating the long-term power.

The final temperatures are compared in Figure 7.5.6. The calculated values generally agree with experiment to within 20%. Exceptions include the TRACE calculation for STEP-003 which overestimates the final temperature by about 50% for reasons mentioned above. The INCTAC calculations overestimate the final temperature for STEP-004 and STEP-005 by roughly 30%, as a result of overestimating the long-term power.

The maximum pressures for STEP-004 and STEP-005 are compared in Figure 7.5.7. Only AGNES and TRACE pressure calculations are available for STEP-004 and AGNES, INCTAC and TRACE calculations for STEP-005. The AGNES and INCTAC estimates agree with experiment to within roughly 10%. The TRACE calculations significantly underestimate the maximum pressure.

Figure 7.5.1: C/E for maximum inverse period

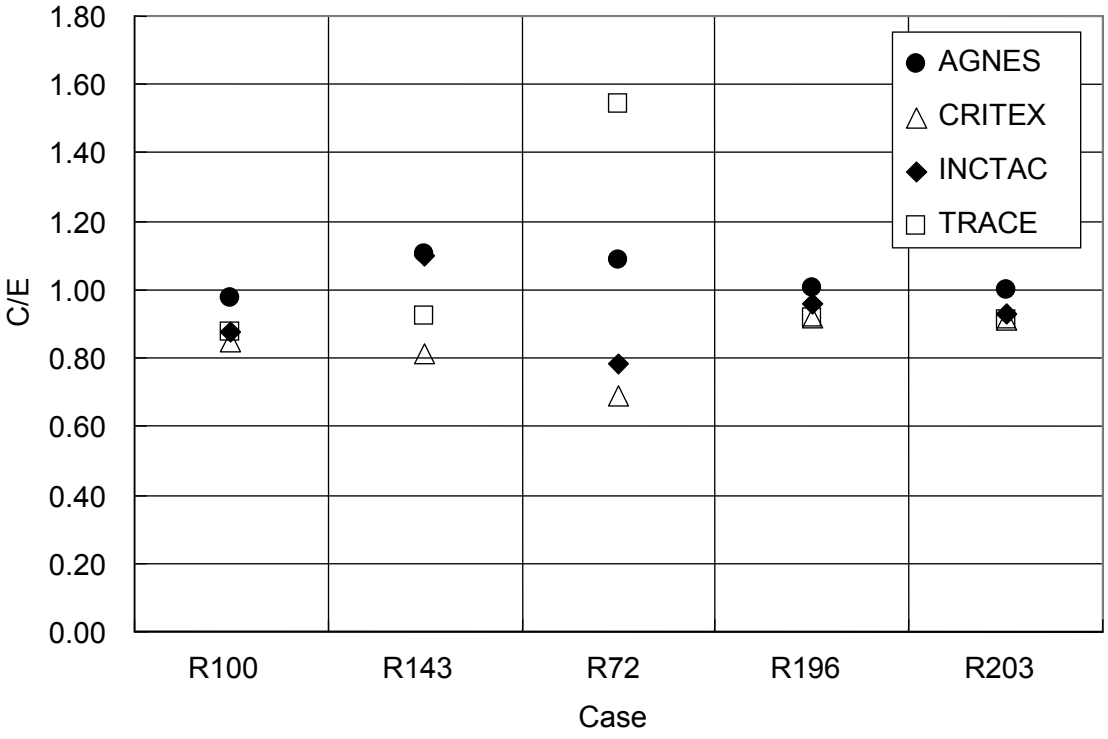

Figure 7.5.2: C/E for time to the first power peak

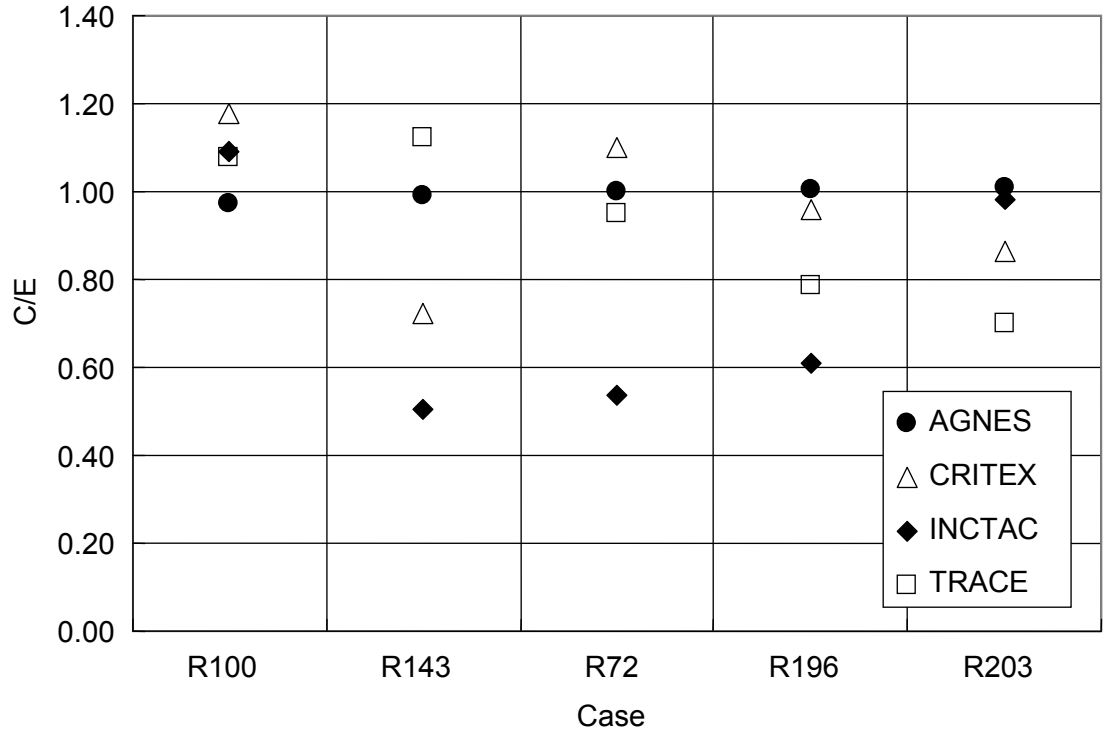

Figure 7.5.3: C/E for power at first peak

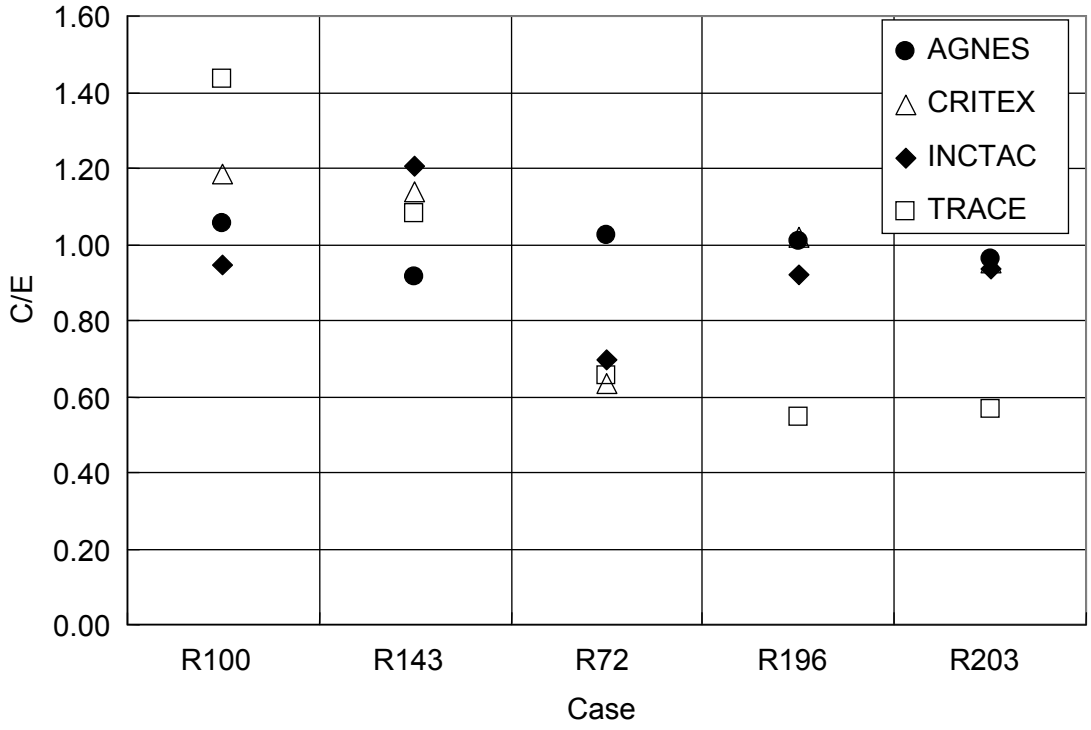

Figure 7.5.4: C/E for fission to the first power peak

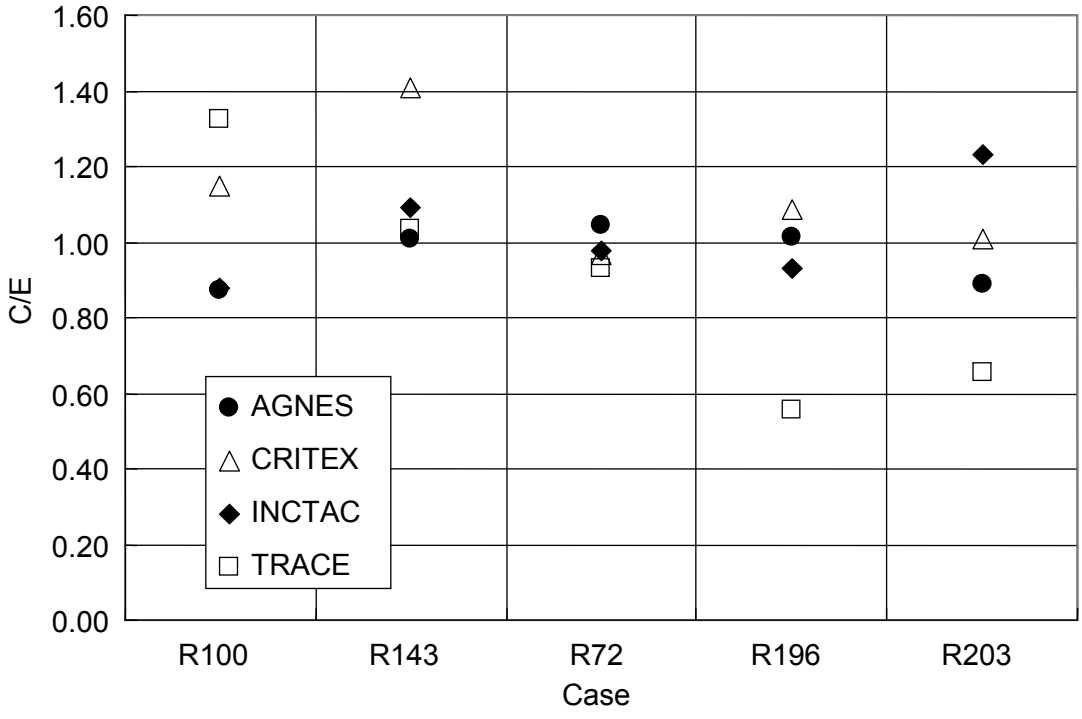

Figure 7.5.5: C/E for total fission

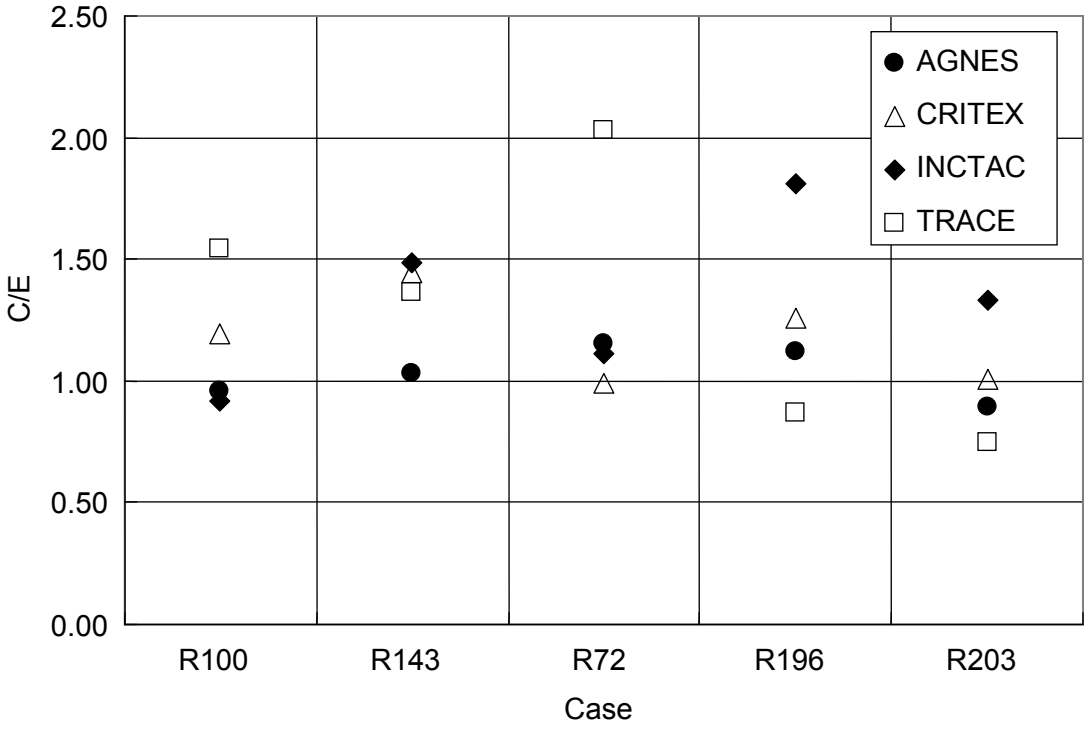

Figure 7.5.6: C/E for final temperature

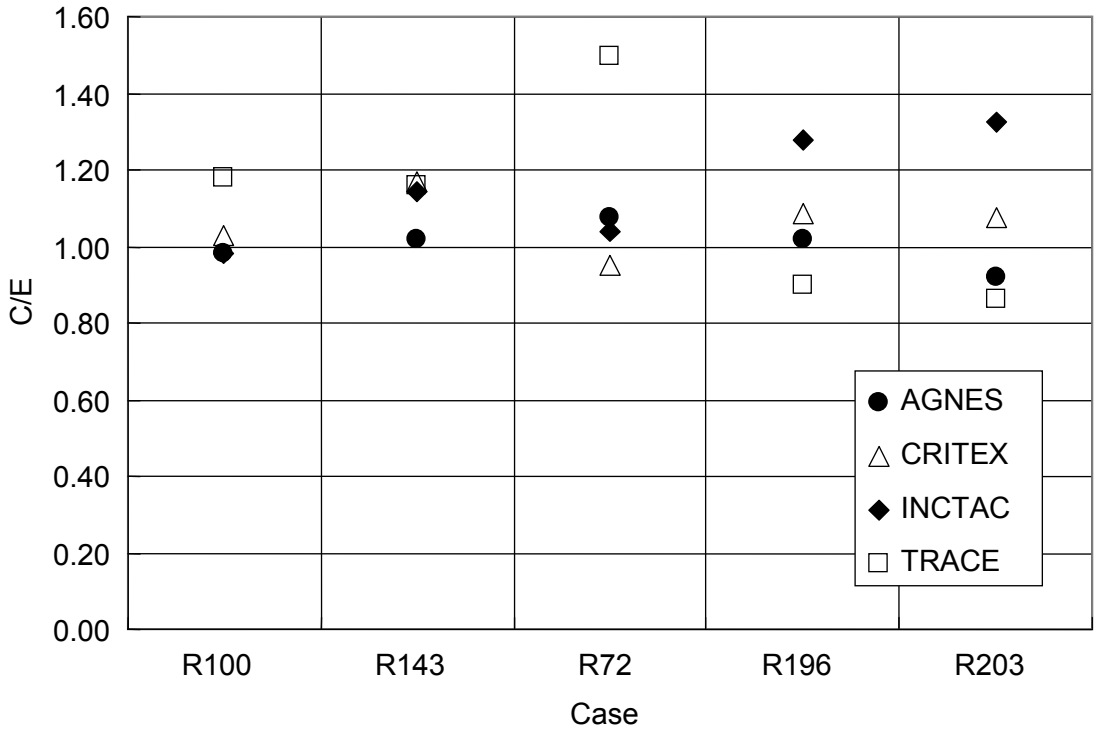

Figure 7.5.7: C/E for maximum pressure

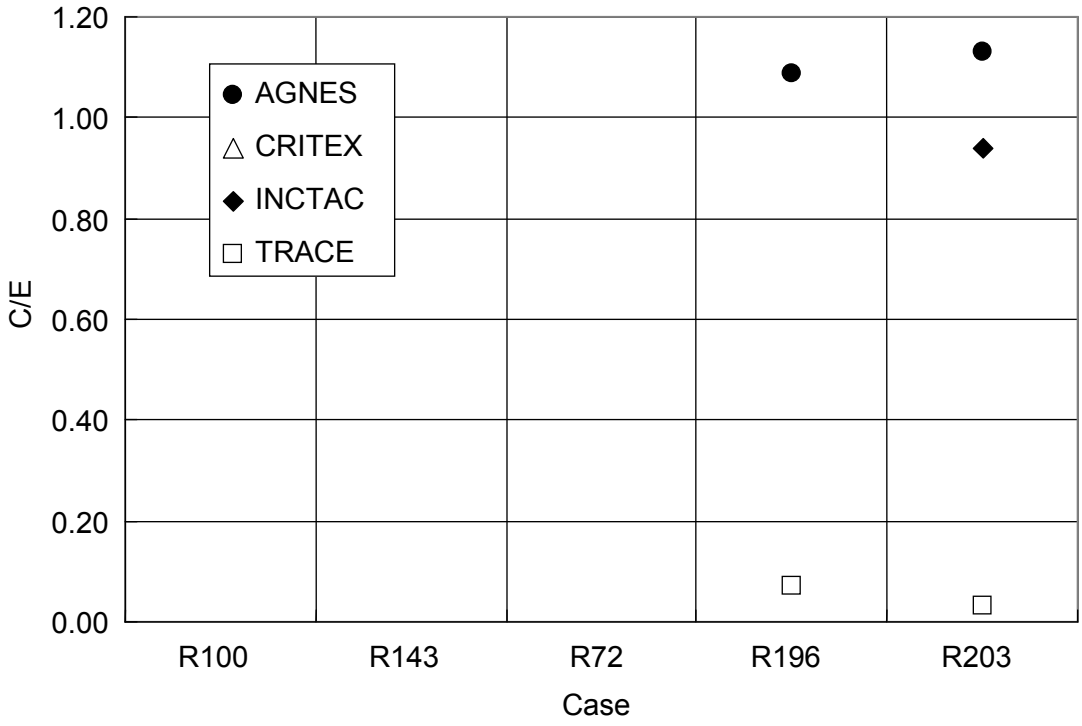

Chapter 8: SILENE benchmark

8.1 Overview

The SILENE benchmark is described in detail in a CEA internal document (CEA, 2006). The SILENE reactor comprises an annular cylindrical tank containing a fissile solution, as shown in Figure 8.1.1. The central channel in the tank is a guide tube containing a control rod. In this benchmark, three experiments with pulsed reactivity insertion are investigated. In this method the tank is filled with the fissile solution to the desired height, with the control rod inserted. The transient is started by rapidly withdrawing the control rod to achieve the desired reactivity insertion. The selected experiments and their associated excess reactivity insertions are displayed in Table 8.1.1. The three pulsed experiments are designated benchmark SILENE-HEU-SOL-STEP-001.

Figure 8.1.1: Photograph and schematic view of SILENE core

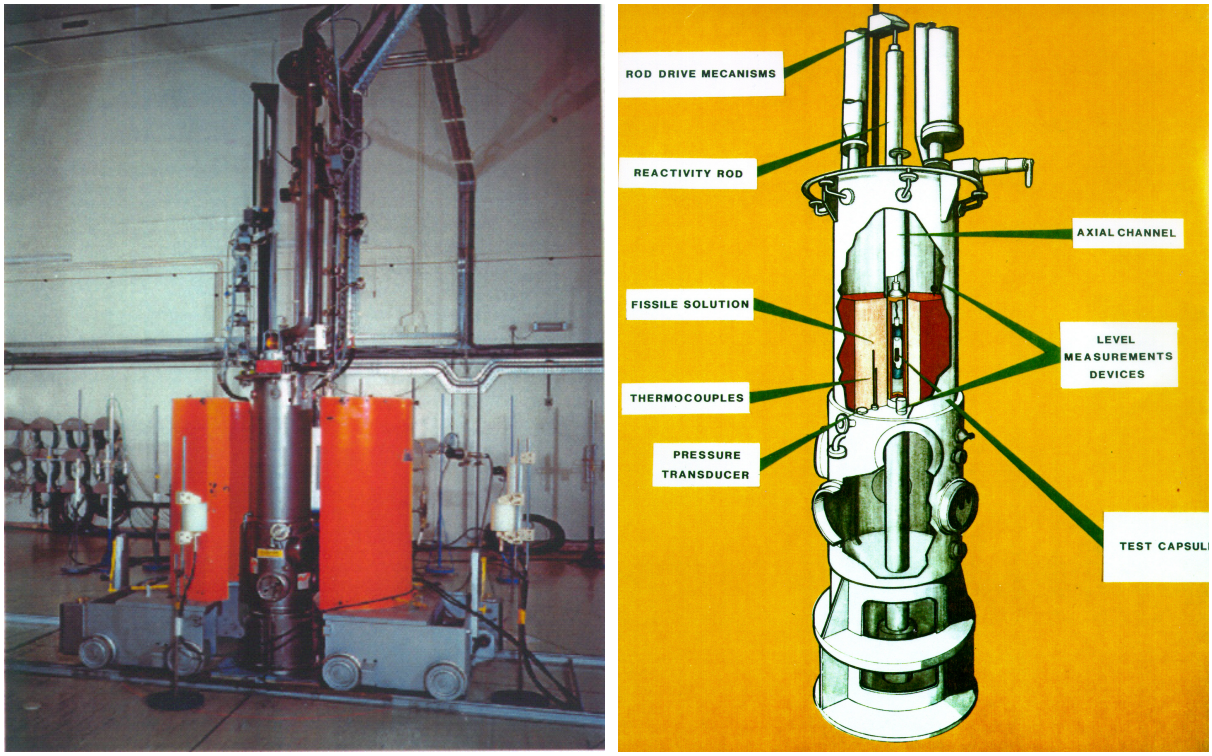

Table 8.1.1: Benchmark experiments and reactivity insertion

Run number	Excess reactivity ($)
S1-300	0.51
S2-300	0.97
S3-300	2.31

The annular core tank is made of stainless steel and the guide tube in the centre contains a cadmium control rod. After pumping fuel solution into the core tank, the control rod is withdrawn from the core in order to insert reactivity. The desired reactivity is achieved by adjusting the height (and consequently the volume) of the fuel solution. During the criticality excursion the fission rate (power), temperature and core pressure are measured. At the end the control rod is inserted to shut down the system. The control rod used during these experiments has a reactivity worth of 3 230 pcm (4.1$).

8.2 Geometry

The reactor core is an annular cylinder, the details of which are presented in Figure 8.2.1. The main dimensions are:

- External diameter: 360/368 mm.
- Internal diameter: 70/76 mm.
- Bottom thickness: 36 mm.
- Cover thickness: 30 mm.
- Vessel height: 1 036 mm.

Figure 8.2.1: SILENE core geometry

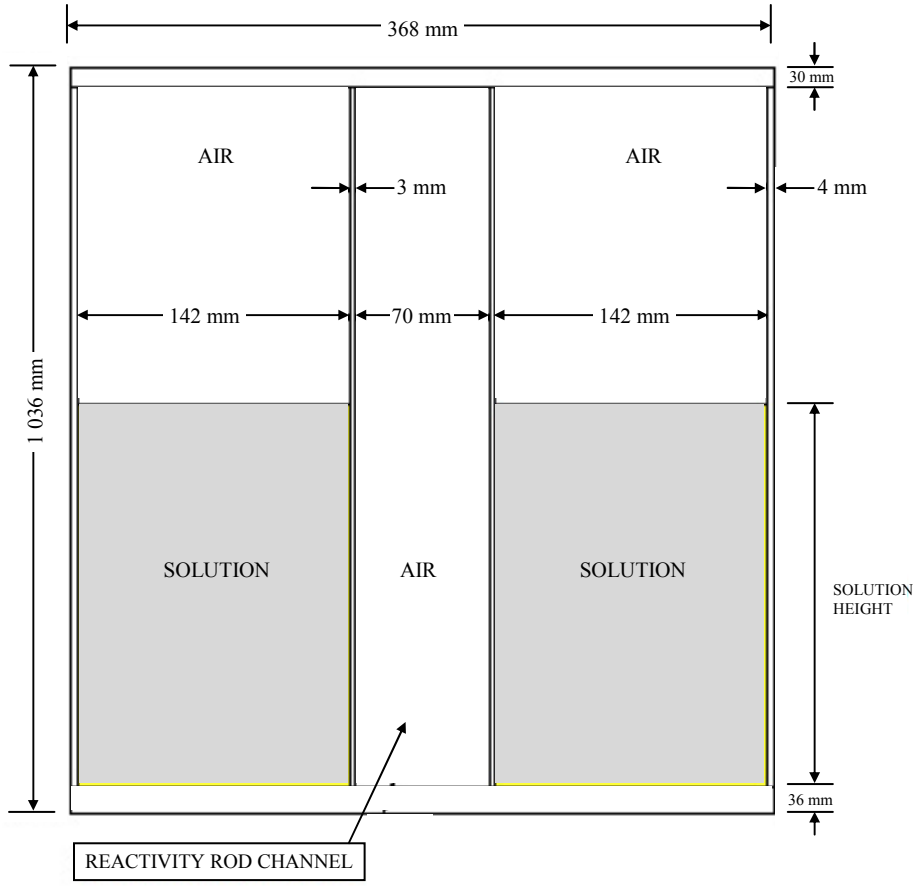

All dimensions in mm.

Description of concrete cell:

- The reactor core is in a large concrete cell 1 910 cm long, 1 210 cm wide and 1 000 cm high.
- The thickness of the concrete side walls is 145 cm.
- The thickness of the concrete floor is 40 cm.
- The thickness of the ceiling varies from 70 cm (side) to 110 cm (middle).
- The distance between the zero level of the solution and the concrete floor is 103.6 cm.
- The distances between the reactor core axis and the 1 910 cm long side walls are 585 cm and 625 cm.
- The distances between the reactor core axis and the 1 210 cm long side walls are 771 cm and 1 139 cm.

8.3 Material data

The fissile solution is a uranyl nitrate solution, with composition during the S1-300, S2-300 and S3-300 experiments, evaluated as:

- Density: 1.1588 $g.cm^{-3}$.
- Total uranium concentration: 70.78 $g.l^{-1}$.
- Free acidity H^+: 2 $moles.l^{-1}$.
- ^{235}U enrichment: 93%.
- Weight fraction of U^{234}: 0.57 ± 0.01%.
- Weight fraction of U^{235}: 92.74 ± 0.1%.
- Weight fraction of U^{236}: 0.25 ± 0.01%.
- Weight fraction of U^{238}: 6.44 ± 0.1%.

The atomic composition of this solution is displayed in Table 8.3.1.

Table 8.3.1: Atomic composition of fissile solution

	Atoms/barn.cm
Hydrogen	$6.2381\ 10^{-2}$
Nitrogen	$1.56682\ 10^{-3}$
Oxygen	$3.56511\ 10^{-2}$
Uranium 234	$1.03811\ 10^{-6}$
Uranium 235	$1.68181\ 10^{-4}$
Uranium 236	$4.51443\ 10^{-7}$
Uranium 238	$1.15312\ 10^{-5}$

For uranyl nitrate solution, the specific heat has been determined from experiments carried out in the Valduc laboratory:

- $Cp = 4\ 187(1 - 0.0008154 \times C_{Ut} - 0.06\ H^+)\ J\ kg^{-1}\ K^{-1}$.
- C_{Ut}: uranium total concentration ($g.l^{-1}$).
- H^+: acidity (N).

For a uranium concentration of C_{Ut} = 70.78 g.l^{-1} and acidity H^+ = 2N, this yields a heat capacity of Cp = 3443 J kg^{-1} K^{-1}.

This is 4% higher than the value obtained from UKAEA Technical Data Sheet Part 2 number 22, of 3 310 J kg^{-1} K^{-1}, which has an estimated accuracy of ±4%.

The core vessel is made from grade Z2 CN 18-10 stainless steel with density 7 900 kg m^{-3} and main constituents:

- Weight fraction of chromium: 18 ± 1%.
- Weight fraction of nickel: 10 ± 1%.
- Weight fraction of manganese: ≤ 2%.
- Weight fraction of silicon: ≤ 1%.
- Weight fraction of phosphorus: ≤ 0.04%.
- Weight fraction of sulphur: ≤ 0.03%.
- Weight fraction of carbon: ≤ 0.03%.
- Weight fraction of iron: 68.9% (balance).

The atomic composition of the Z2 CN 18-10 stainless steel is displayed in Table 8.3.2. The atomic composition of the concrete is displayed in Table 8.3.3. The density corresponding to the reported atomic composition of the concrete is 2 401.3 kg m^{-3}.

Table 8.3.2: Atomic composition of Z2 CN18-10

Isotopes	Atom/barn-cm
Iron	$5.8694\ 10^{-2}$
Chromium	$1.6469\ 10^{-2}$
Nickel	$8.1061\ 10^{-3}$
Manganese	$1.7319\ 10^{-3}$
Silicon	$1.6939\ 10^{-3}$
Phosphorus	$6.1438\ 10^{-5}$
Sulphur	$4.4640\ 10^{-5}$
Carbon	$1.1883\ 10^{-5}$

Table 8.3.3: Composition of concrete

Isotopes	Atom /barn-cm
Hydrogen	$1.035\ 10^{-2}$
Boron 10	$1.602\ 10^{-6}$
Oxgen	$4.347\ 10^{-2}$
Alminum	$1.563\ 10^{-3}$
Silicon	$1.417\ 10^{-2}$
Calcium	$6.424\ 10^{-3}$
Iron	$7.621\ 10^{-4}$

8.4 External neutron source

For the S1-300 experiment, an external neutron source was present during the test. The source consists of a cylinder of americium beryllium alloy which is covered by a cylinder of stainless steel (grade Z2 CN 18-10). The diameter of americium beryllium cylinder is 10 mm and the height is 10 mm. The diameter of the stainless steel cylinder is 18 mm and the height is 18 mm. The thickness of stainless steel is 4 mm. The source emission is isotropic with a strength of 270 000 neutrons per second.

The source is positioned under the reactor core bottom, as shown in Figure 8.4.1. The distance between the source centre and the core bottom is 1.4 cm, the distance between the source centre and the zero level of the solution is 5 cm and the distance between the source centre and the axis of the reactor core is 5 cm.

Figure 8.4.1: Positions of neutron source and detectors in SILENE

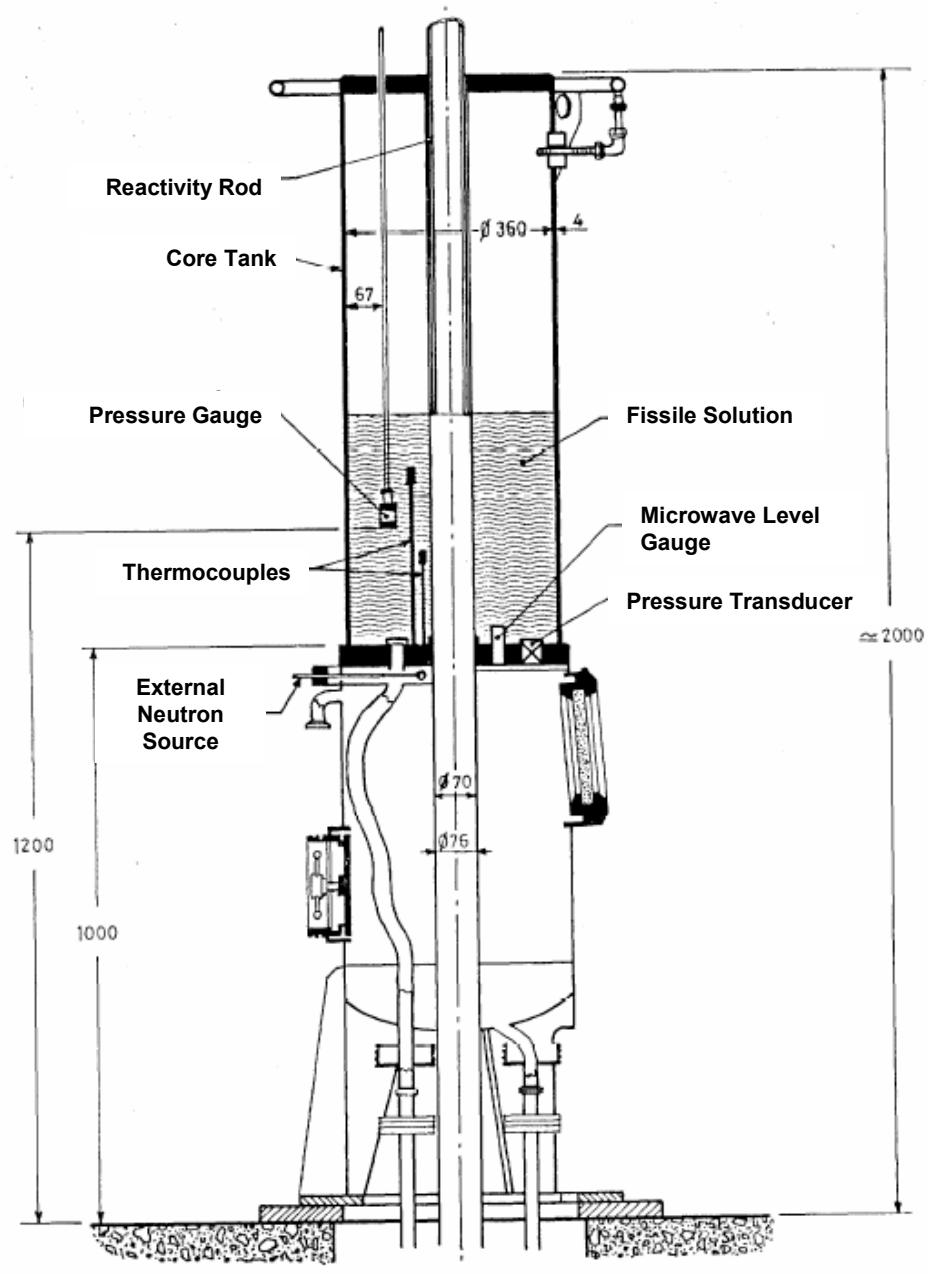

8.5 Initial data

Table 8.5.1 shows the initial conditions for the experiments. The temperature given in the table is the mean temperature measured by two thermocouples located at 20 cm and 30 cm from the zero level of the solution.

Table 8.5.1: Experimental characteristics

	S1-300	S2-300	S3-300
β_{eff} (pcm)	794	794	794
Inserted reactivity ($) Inserted reactivity (pcm)	0.51 405	0.97 769	2.31 1832
Critical height (cm)	37.36	37.36	37.36
Experimental height (cm)	38.16	38.91	40.96
Initial temperature (°C)	22.2	22.1	22.3
Duration (s)	1 100	265	120
External source	Yes	No	No

8.6 Reactivity insertion

The fissile solution is pumped into the reactor core with the reactivity rod inserted until the required solution height is attained. With this solution height, the reactor is super-critical when the control rod is removed from the core. The pulsed experiments are started by the rapid removal of the control rod effectively creating a step reactivity insertion. The relationship between the inserted reactivity and the solution height is determined by the reactivity worth of the solution near criticality which is 510 pcm per cm of solution.

The control rod is an annular cylinder whose main dimensions and composition are as follows:

- Rod length: 580 mm.
- 0 < radius < 30 mm: air.
- 30 mm < radius < 31 mm: stainless steel grade Z2 CN 18-10.
- 31 mm < radius < 32 mm: natural cadmium (density 8.65 g/cm^3).
- 32 mm < radius < 33 mm: stainless steel grade Z2 CN 18-10.

The axis of the control rod is the axis of the reactor core. When the control rod is completely inserted in the reactor core, the distance between the zero level of the control rod and the zero level of the solution is 10 cm.

When the control rod is completely inserted in the reactor core, the reactivity worth of the rod has been determined experimentally to be 3 230 pcm (±60 pcm).

8.7 Detector/measurement systems

The positions of the thermocouples, pressure transducers and the level gauge are all displayed in Figure 8.4.1.

8.7.1 Temperature

The temperature is measured by two thermocouples placed at heights of 20 cm and 30 cm from the bottom of the vessel. The reported temperature is the means of the two measurements.

8.7.2 Pressure

The pressure is measured by a transducer located in the base of the reactor vessel. A second determination of the pressure is made using a pressure gauge that is suspended in the solution, as shown in Figure 8.4.1.

8.7.3 Fissile solution height

The height of the fissile solution is determined by a microwave level gauge located in the base of the reactor vessel, as indicated in Figure 8.4.1.

Chapter 9: SILENE experimental results

The main results from each of the five tests are presented in Table 9.1 and are discussed in Sections 9.1 to 9.3.

Table 9.1: Summary of SILENE experimental data

	S1-300	S2-300	S3-300
Maximum inverse period (s^{-1})	0.182	5.3	285
Fission rate at first peak (fissions/s)	1.3×10^{15}	1.7×10^{16}	1.1×10^{19}
Fissions to first peak	2.2×10^{16}	1.3×10^{16}	6.6×10^{16}
Time of first peak (s)	110	9.5	1.31
Final temperature (°C)	35.9	43.8	62.2
Total fissions	6.5×10^{16}	1.1×10^{17}	2.1×10^{17}
Gas release time (s)	132.5	10.5	1.31

9.1 Results for S1-300

The fission rate is displayed in Figure 9.1.1 and shows an initial peak just in excess of 10^{15} fissions s^{-1}. The first peak occurs after 110 s and then the fission rate falls off, rapidly at first and then more slowly until a small peak occurs just before the transient is terminated after 1 100 s. The number of fissions to the first peak is 2.2×10^{16} and the total number of fissions is treble this value, as shown in Figure 9.1.2. This causes a temperature rise of 13.7°C by the end of the test. A rise in the measured pressure indicates that radiolytic gas was produced at 132.5 s, *i.e.* a little after the first peak in fission rate.

9.2 Results for S2-300

The fission rate is displayed in Figure 9.2.1 and shows an initial peak of over 10^{16} fissions s^{-1}, an order of magnitude greater than in the first test. The first peak occurs after 9.5 s and then the fission rate falls off, before climbing to a second distinct peak, followed by a slight third peak before declining monotonically until the transient is terminated after 265 s. The number of fissions to the first peak is 1.3×10^{16}, which is 40% less than in the first test and the total number of fissions is over 10^{17}, which is 70% more than in the first test. Figure 9.2.2 shows that the number of fissions increases rapidly over the first 15 s or so, but rises little beyond 100 s. This causes a temperature rise of 21.7°C by the end of the test, which is 60% higher than in the first test. Figure 9.2.3 shows that the temperature rise at the location of the thermocouple is slower than the energy rise depicted in Figure 9.2.2. This must be due to non-uniform heating of the solution, which requires convective mixing on a longer time scale to equilibrate the temperature. The jumps in temperature at around 100 s indicate the presence of temperature differences in the fluid of order a degree at this time. The temperature is still rising at the end of the test, but looks as if it is getting close to its asymptotic value. A rise in the measured pressure indicates that radiolytic gas was produced at 10.5 s, *i.e.* a little after the first peak in fission rate.

9.3 Results for S3-300

This is the only prompt-critical transient chosen for the SILENE benchmark. The fission rate is displayed in Figure 9.3.1 and shows an initial peak of over 10^{19} fissions s^{-1}, three orders of magnitude

greater than in the second test. The first peak occurs after 1.31 s and then the fission rate falls off, before climbing to a second distinct peak after about 12 s, followed by a higher third peak after about 50 s. The power then declines slowly until the transient is terminated after 120 s. However, there are oscillations of much smaller magnitude and period superimposed upon the general fission rate curve, throughout the duration of the transient. The number of fissions to the first peak is 6.6×10^{16}, which is five times the number in the second test and the total number of fissions is over 2×10^{17}, which is double that in the second test. Figure 9.3.2 shows that the number of fissions rise sharply over the first 1.31 s and then rises slowly, but steadily, to roughly double this number by the end of the test. This causes a temperature rise of 39.9°C by the end of the test, which is almost double that in the second test. Figure 9.3.3 shows that there is a temperature spike reaching over 60°C at the location of the thermocouple after 1.31 s, followed by a cooling of about 20°C over the next two seconds. As the power is always positive, the cooling must be a local effect and indicates temperature differences of order 20°C in the fluid at this time. Figure 9.3.4 shows that the temperature then recovers to over 60°C by the end of the test, at which point it is still rising. The sudden rise in temperature at around 50 s is probably a consequence of the observed power peak at this time. A rise in the measured pressure indicates that radiolytic gas was produced at 1.31 s, *i.e.* coincident with the first peak in fission rate.

9.4 General observations

Using the quadratic temperature feedback derived for the AGNES calculations the asymptotic temperatures for the SILENE experiments are estimated to be as listed in Table 9.4.1.

Table 9.4.1: Comparison of final and asymptotic temperatures

Test	S1-300	S2-300	S3-300
Asymptotic temperature (°C)	33.6	42.4	64.0
Final temperature (°C)	35.9	43.8	62.2

It is seen that the final temperatures are reasonably close to the estimated asymptotic values. In the discussion above it is noted that the temperature in S2-300 was observed to be close to its asymptotic value at the end of the test, whereas in S3-300 the temperature was still rising at the end of the test.

Dividing the measured energy release by the heat capacity of the fissile solution provides an estimate of the temperature rise of the solution, in the absence of heat loss from the fluid. These estimates are compared with the measured temperature rises in the table below. The adiabatic temperature rise is estimated using both the Valduc and the UKAEA values for the specific heat capacity of the fissile solution.

Table 9.4.2: Estimating heat loss from the fissile solution

Test	S1-300	S2-300	S3-300
Adiabatic temperature rise (°C) – Valduc heat capacity	14.1	23.3	42.3
Adiabatic temperature rise (°C) – UKAEA heat capacity	14.6	24.3	44.0
Measured temperature rise (°C)	13.7	21.7	39.9
Percentage heat loss – Valduc heat capacity	2.6	7.0	5.7
Percentage heat loss – UKAEA heat capacity	6.3	10.6	9.3

The results indicate that roughly 5% of the heat generated in the experiments is transferred to the vessel and it surroundings, if the Valduc estimate of specific heat capacity is used, or 9% if the UKAEA estimate of specific heat capacity is used. In either case the heat lost from the solution is small and the heat lost up to the first peak in fission rate will be much smaller. Hence neglecting heat loss from the fissile solution during the rise to the first peak should produce little error.

For the prompt-critical test, S3-300, the Norheim-Fuchs-Hansen equation [Eq. (3.2)] can be used to give an approximate estimate of the peak power. This yields a value of 2.4×10^{19} fissions per second (assuming an energy deposition of 200 MeV in the fissile solution per fission). This is just over double

the measured value of 1.1×10^{19}. This is an indication that the negative feedback of the temperature rise on the reactivity is not the only phenomenon responsible for terminating the power rise. This is consistent with the measured time of radiolytic gas bubble release, which suggests that the negative effect of void production on reactivity also played a role in terminating the power rise.

Recall that an approximate estimate of the maximum inverse period, ω, is given in terms of the excess reactivity, the delayed neutron fraction and the prompt neutron generation time by Eq. (6.2). Using the delayed neutron fraction and prompt neutron generation time estimated for the AGNES calculations leads to an estimate of 312 s^{-1} for the maximum inverse period, which is nearly 10% greater than the measured value of 285 s^{-1}. Using the delayed neutron fraction and prompt neutron generation time estimated for the TRACE calculations leads to an estimate of 305 s^{-1} for the maximum inverse period, which is 7% greater than the measured value of 285 s^{-1}. This simple approximate value is expected to give an underestimate of the maximum inverse period, as it neglects the positive contribution from the delayed neutron precursors [see Eq. (3.1)]. The fact that it overestimates the measured value indicates errors in either the estimated values of the delayed neutron fraction and/or neutron lifetime, or in the point kinetics equation (which is only approximate) or in the measured value of the maximum inverse period.

Figure 9.1.1: Measured fission rate for S1-300

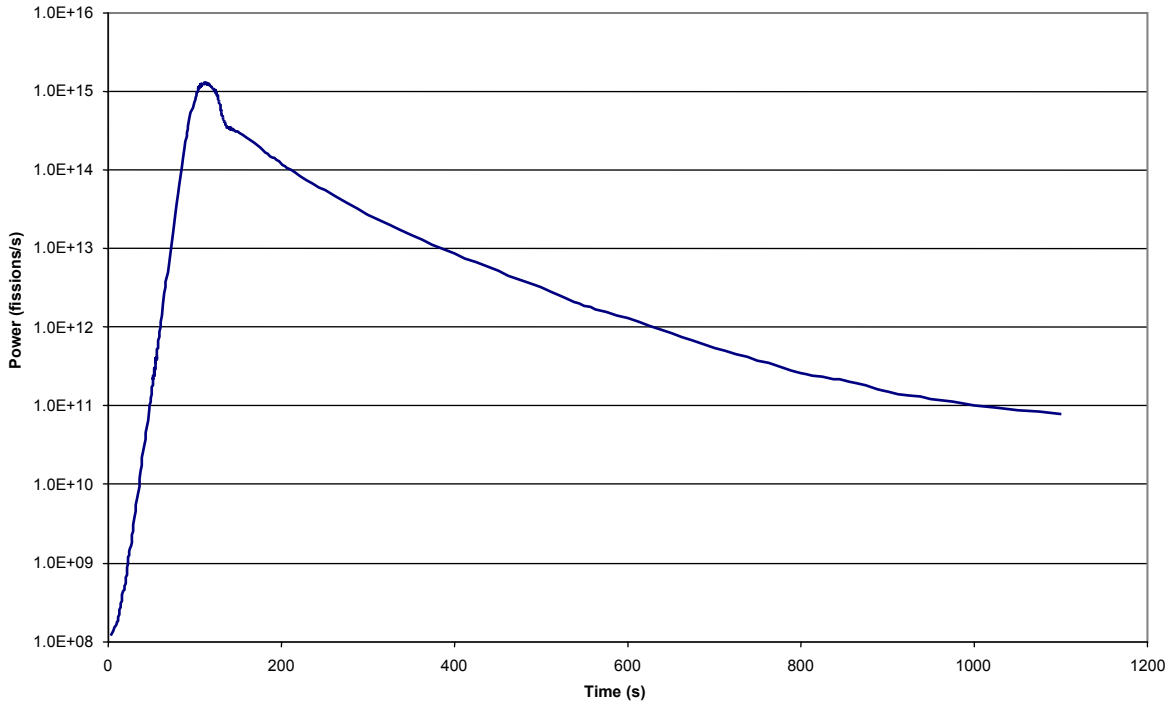

Figure 9.1.2: Measured fissions for S1-300

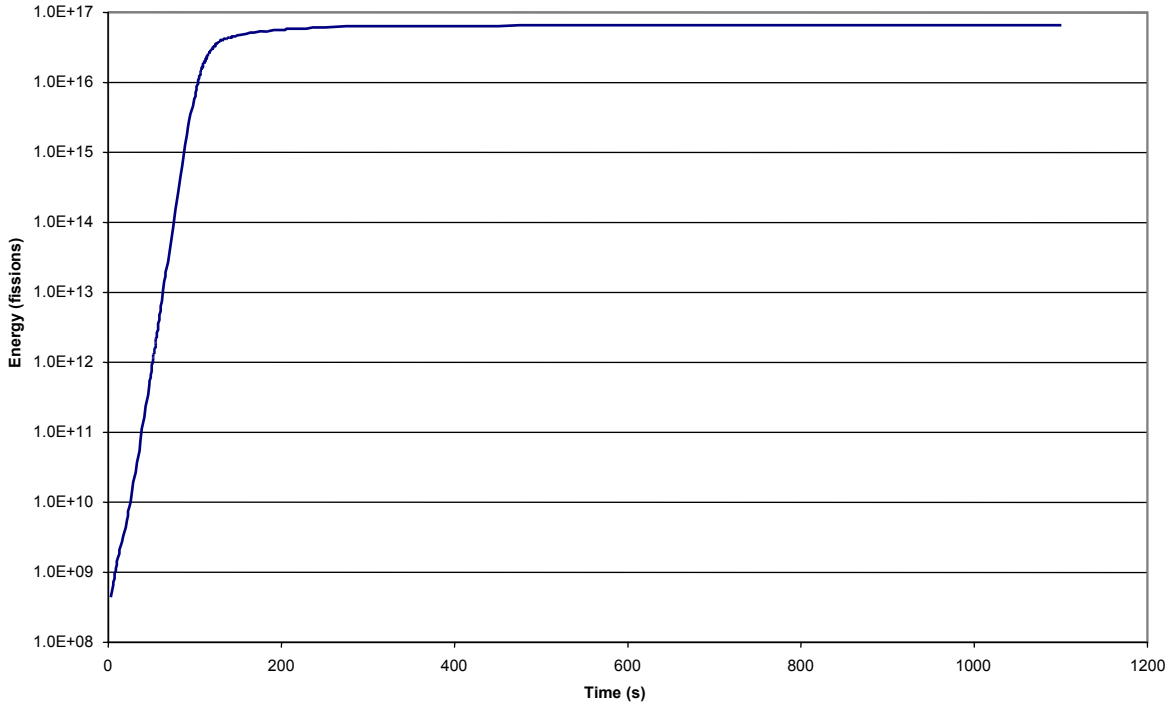

Figure 9.2.1: Measured fission rate for S2-300

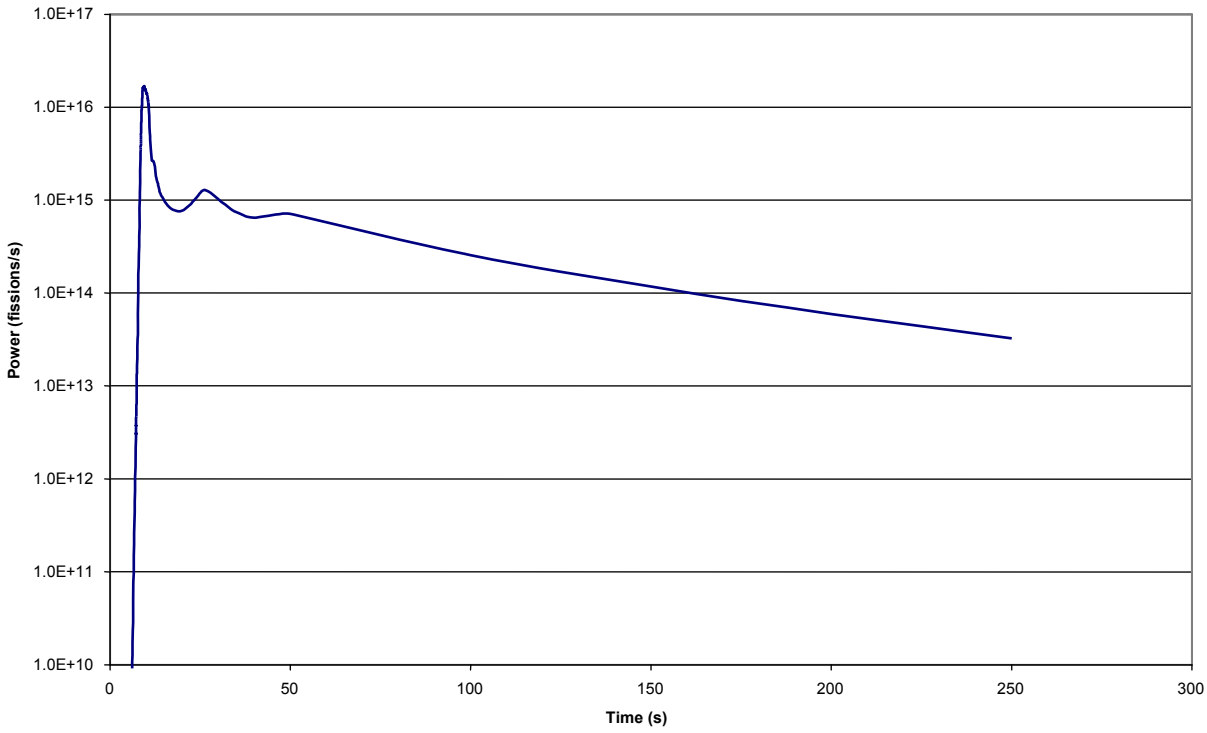

Figure 9.2.2: Measured fissions for S2-300

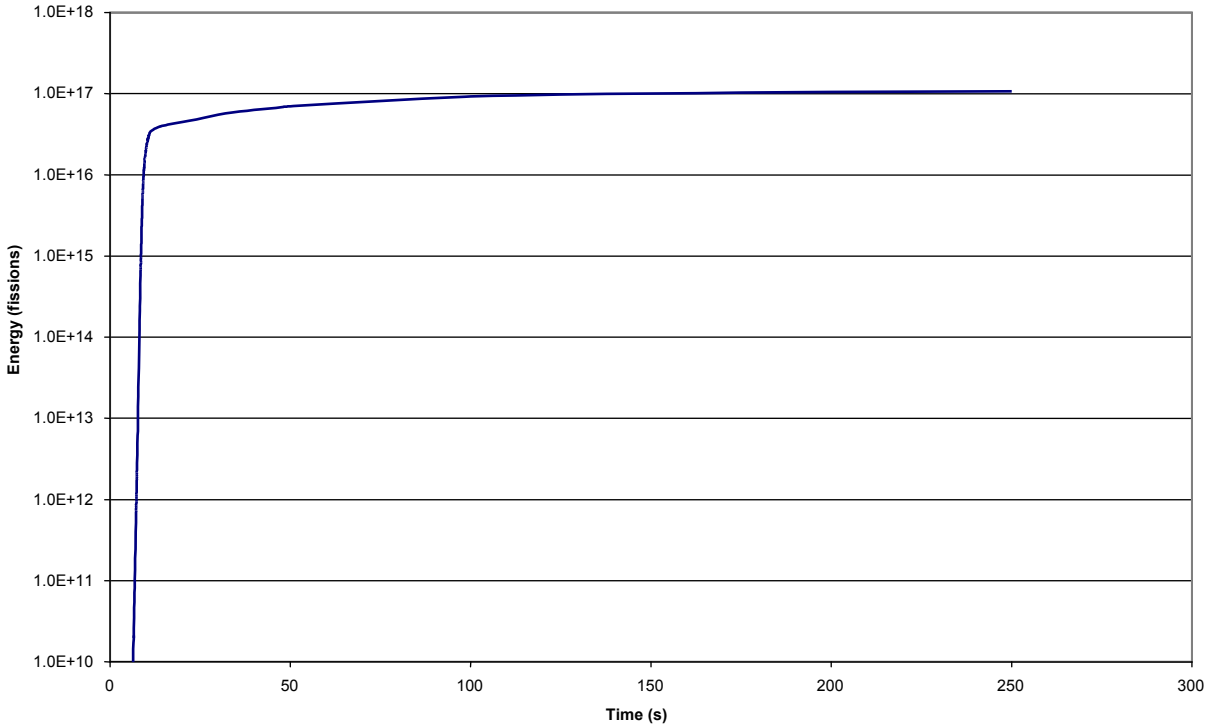

Figure 9.2.3: Measured temperature history for S2-300

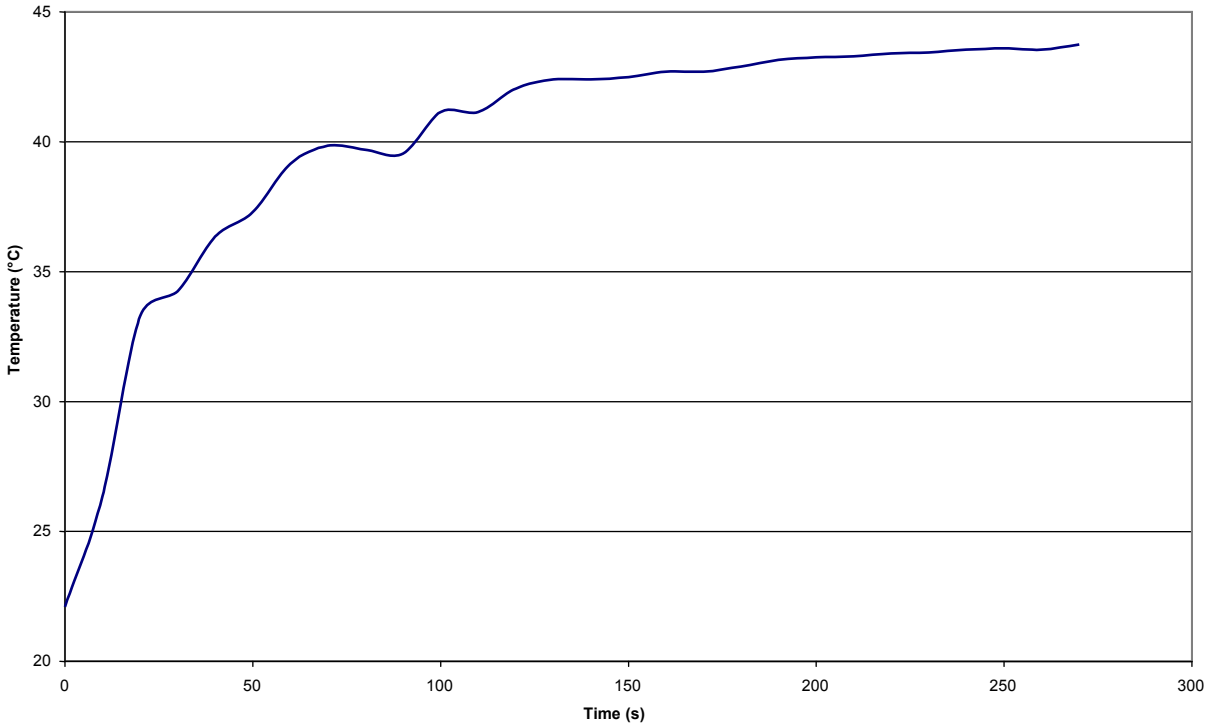

Figure 9.3.1: Measured fission rate for S3-300

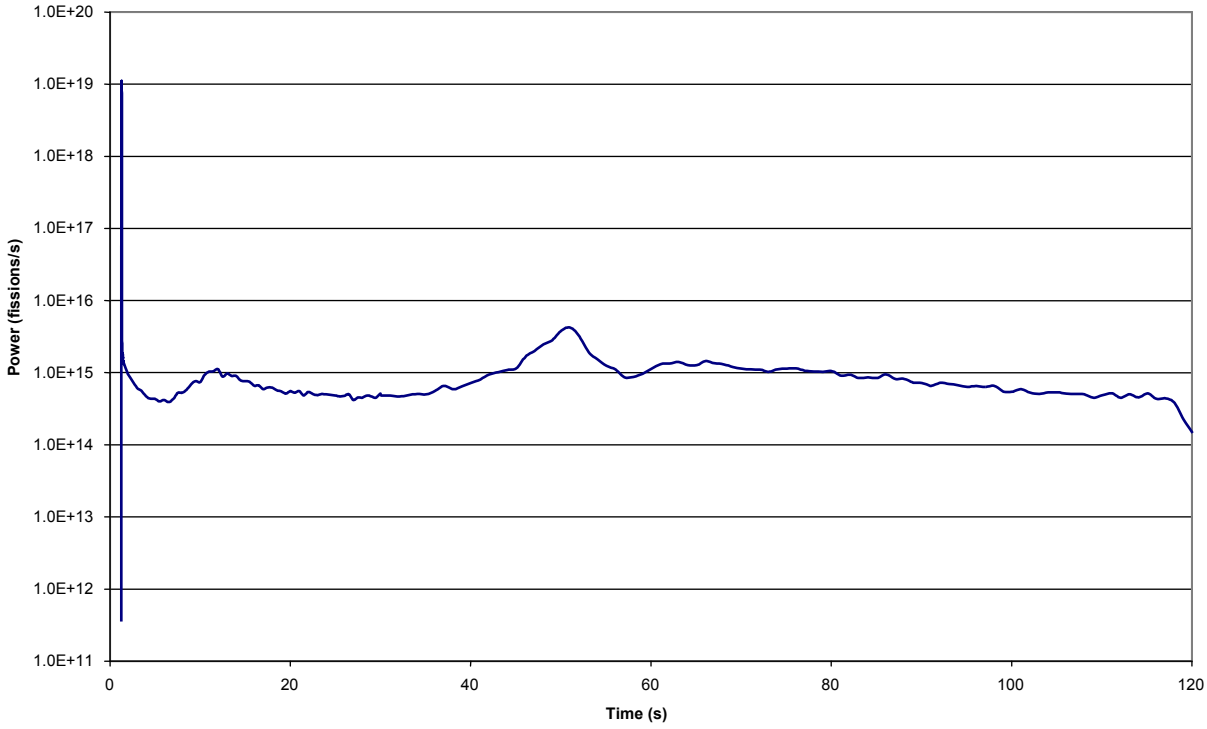

Figure 9.3.2: Measured fissions for S3-300

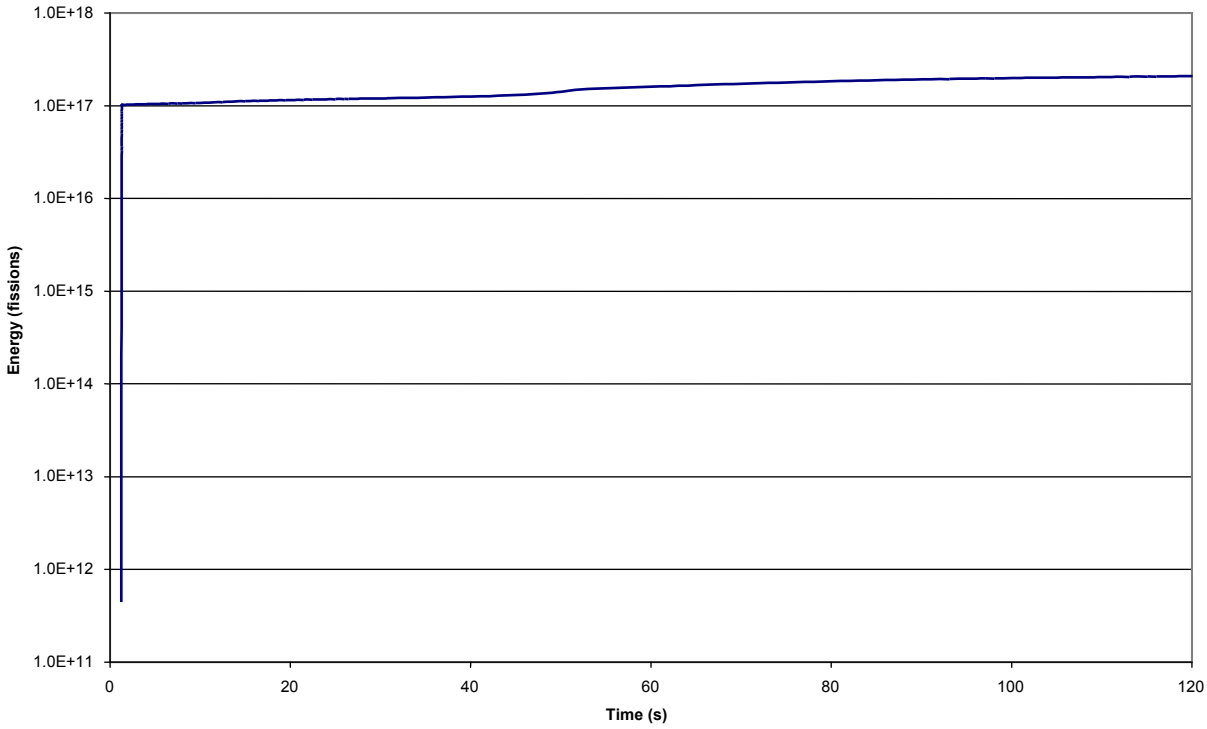

Figure 9.3.3: Measured temperature history for S3-300 (first 20 s)

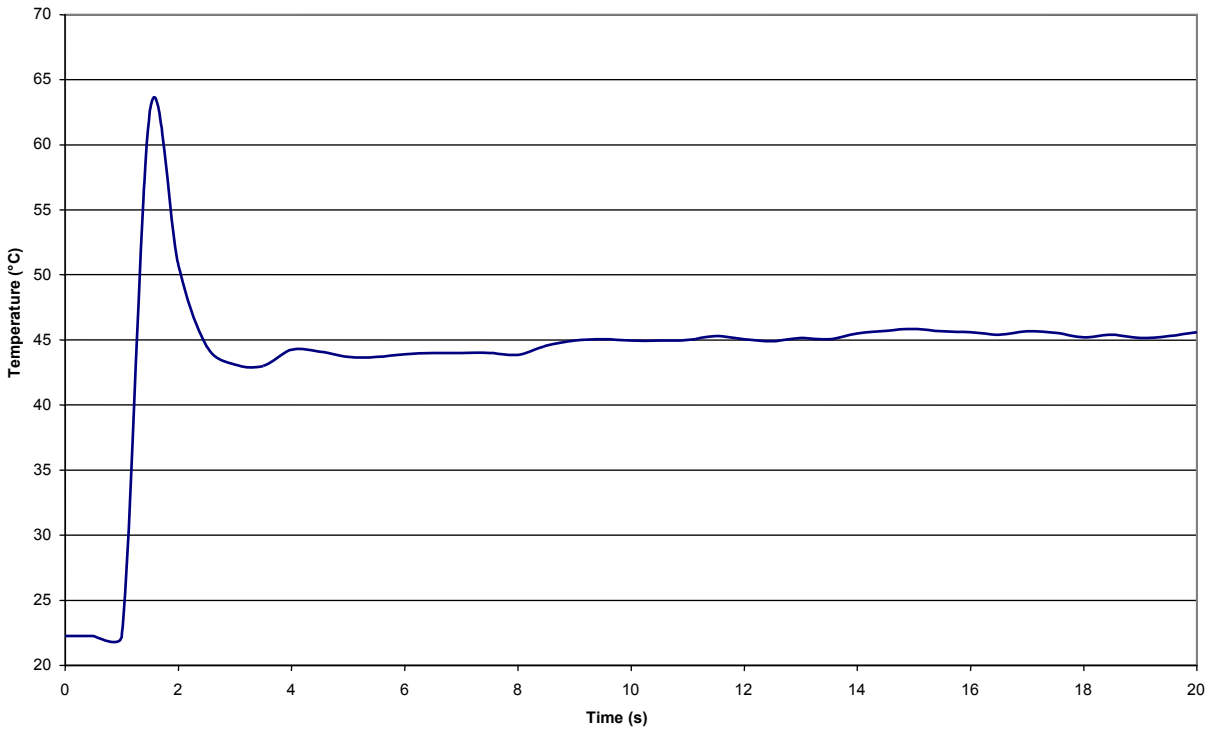

Figure 9.3.4: Measured temperature history for S3-300 (complete)

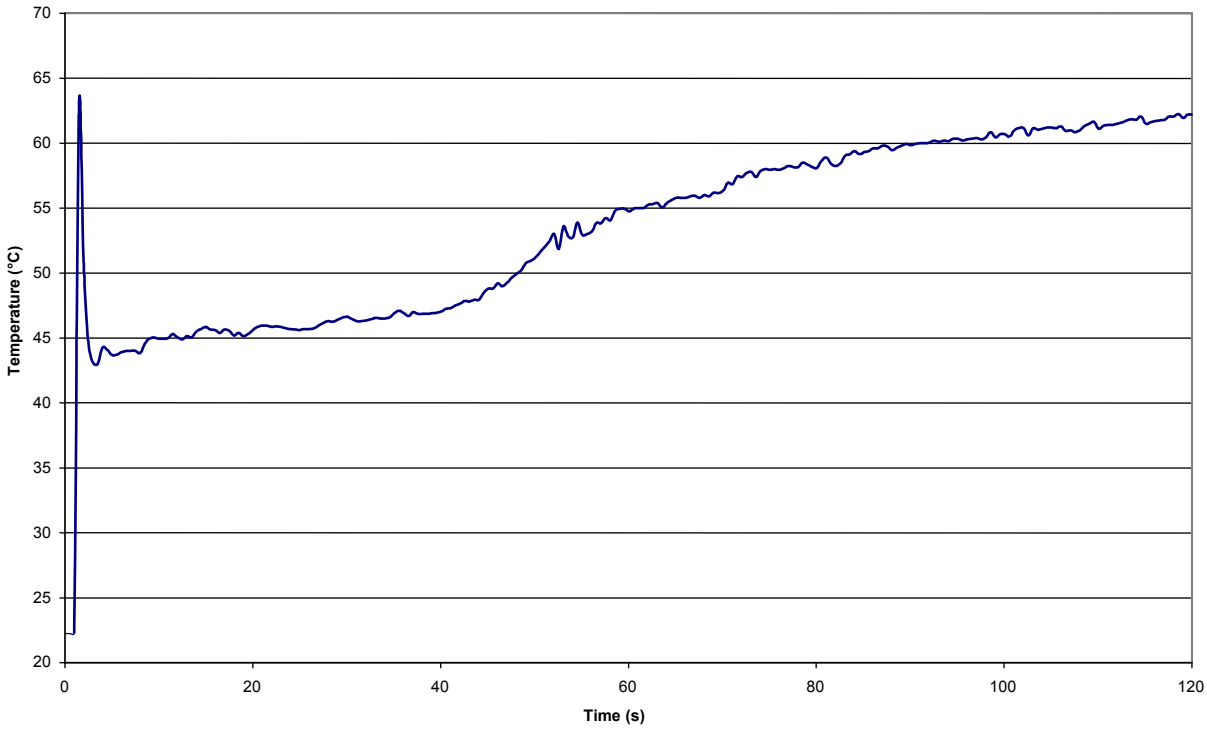

Chapter 10: Code predictions and comparison with SILENE results

10.1 AGNES

10.1.1 Input parameters

The atomic compositions used in the AGNES (Yamane, 2005) code for the specified fuel are as listed in Table 10.1.1.

Table 10.1.1: Atomic number density (atoms/barn-cm)

Temperature (°C)	22.2	30	40	50
Density (g/cm^3)	1.1651	1.1610	1.1548	1.1475
^{235}U	1.68381E-4	1.67789E-4	1.66890E-4	1.65835E-4
^{238}U	1.30149E-5	1.29692E-5	1.28997E-5	1.28181E-5
H	6.27833E-2	6.25626E-2	6.22276E-2	6.18339E-2
N	1.56864E-3	1.56313E-3	1.55476E-3	1.54492E-3
O	3.58574E-2	3.57314E-2	3.55401E-2	3.53152E-2

Based on the atomic compositions above, the estimated kinetic parameters are displayed in Table 10.1.2 and the reactivity feedback coefficients are displayed in Table 10.1.3.

Table 10.1.2: Kinetic parameter

Neutron generation time (s)	3.28E-5	Total delayed neutron fraction	7.82E-3

Group	1	2	3	4	5	6
Delayed neutron fraction	2.63E-04	1.72E-03	1.56E-03	3.06E-03	9.00E-04	3.28E-04
Decay constant (s)	1.24E-02	3.05E-02	1.11E-01	3.01E-01	1.14E+00	3.01E+00

Table 10.1.3: Reactivity coefficient

Reactivity temperature coefficient	
First order (cent/°C)	-4.069
Second order (cent/°C^2)	-0.03510

Reactivity void coefficient	
First order (cent/%)	-68.09
Second order (cent/%^{2})	-1.614

The reactivity insertion time is assumed to be 0.15 s, which is almost the same as the time for the transient rod to pass through the full height of the fuel solution. The initial power density is assumed to be 1×10^{-5}W/m^3 which is the value used for the TRACY tests with no external neutron source. In each simulation, the temperature and void reactivity feedback coefficients are used with a weighting factor to allow for the effect of non-uniform distribution of the temperature and gas bubble void. The weighting factor is initially set to 1.6 and then reduces exponentially to unity with time constant, TCT, to simulate the effect of buoyancy driven convection. TCT is set to 20 s for S1-300 and S2-300, and to 10 s for S3-300.

The parameters used to characterise radiolytic gas production are the same as those used for the TRACY simulations:

- The saturation concentration of radiolytic gas, CD, was 15 mol/m^3.
- The generation rate of dissociation gas, G, was 6×10^{-7} mol/J for reactivity insertions < 1\$ and 3×10^{-7} mol/J for reactivity insertions > 1\$. These values were chosen so that the power profile is reproduced the best.
- The energy-void transfer coefficient, ν, was 1×10^{-7} m^6/J/mol for all cases. This value was chosen to give the best fit to the experimental data.

10.1.2 Results

S1-300

Figures 10.1.1 to 10.1.3 show the results for S1-300 and indicate good overall agreement. Figure 10.1.1 shows that the calculated inverse period is very close to the measured value. An external neutron source is used in this test and Figure 10.1.2 shows that the experiment started from a higher initial power and consequently the simulation takes over 30% longer to reach the peak power. Figures 10.1.1 and 10.1.2 also show that the calculation climbs to a second power peak after about 200 s, which is not observed in the experiment. Figure 10.1.3 shows that this results in the simulation overestimating the total energy by 26% and the temperature rise by 30%. The calculation overestimates the radiolytic gas release time by 18%, but this is a result of the longer time for the calculation to reach the peak. Indeed, radiolytic gas release occurs much sooner after the power peak in the simulation.

S2-300

Figures 10.1.4 to 10.1.6 show the results for S2-300 and show very good agreement between calculation and measurement. There is no external neutron source in this test and Figure 10.1.4 shows that the simulation rises to the peak power in half the time taken in the experiment; this could result from inaccuracies in the initial conditions for the calculation. The agreement at peak power is very good, but the calculation overestimates the inverse period by 14%, rising to the peak faster and generating 30% less energy on the way. Figure 10.1.5 shows very good qualitative agreement in the longer term, though the second power peak is larger in the simulation and leads to an overestimate of the total energy by 20% and the temperature rise by 29%. Radiolytic gas is released 1.6 s after the power peak in the calculation, compared to 1 s after the peak in the experiment.

S3-300

Figures 10.1.7 to 10.1.9 show the results for S3-300 and demonstrate generally good agreement between calculation and observation. This experiment has no external neutron source and rises much later to the peak power than the calculation; this could result from inaccuracies in the initial conditions for the calculation. The calculation overestimates the inverse period, peak power, energy to first peak, total energy and temperature rise by between 9% and 26%. After the first power peak the calculation predicts a second quite large peak, compared to several smaller peaks observed in the experiment. The calculation does not reproduce the very small scale, short period variations observed in the experiment. The calculation predicts radiolytic gas release coincident with the first power peak, as observed in the experiment.

Figure 10.1.1: AGNES – S1-300 power history – first 250 s

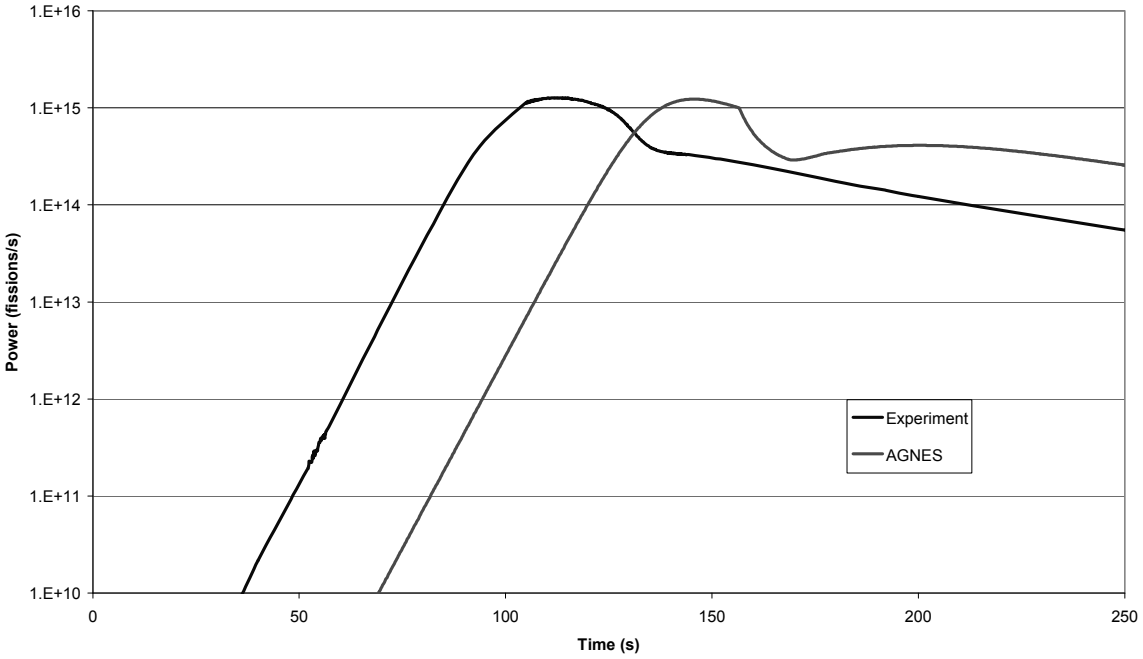

Figure 10.1.2: AGNES – S1-300 power history – whole profile

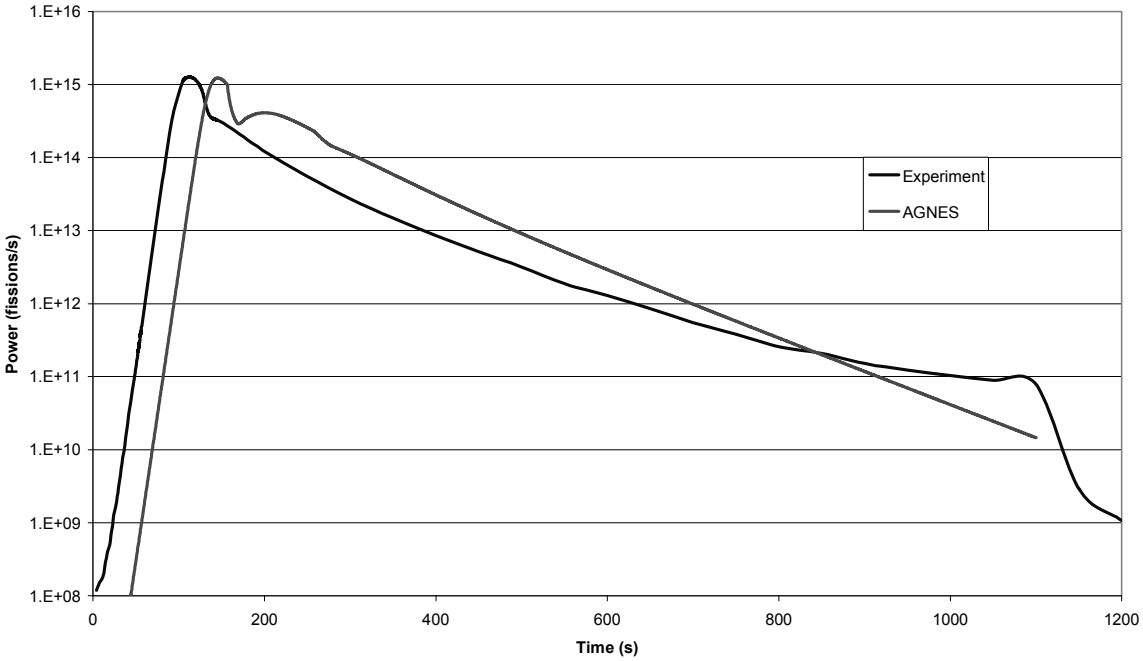

Figure 10.1.3: AGNES – S1-300 energy history – whole profile

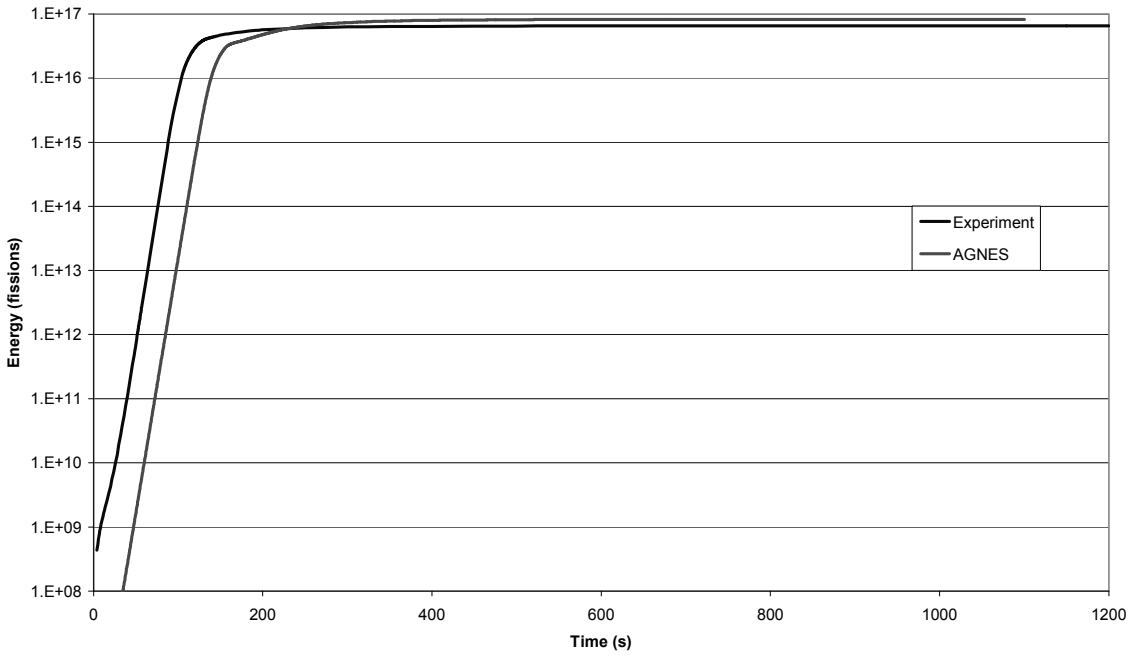

Figure 10.1.4: AGNES – S2-300 power history – first 30 s

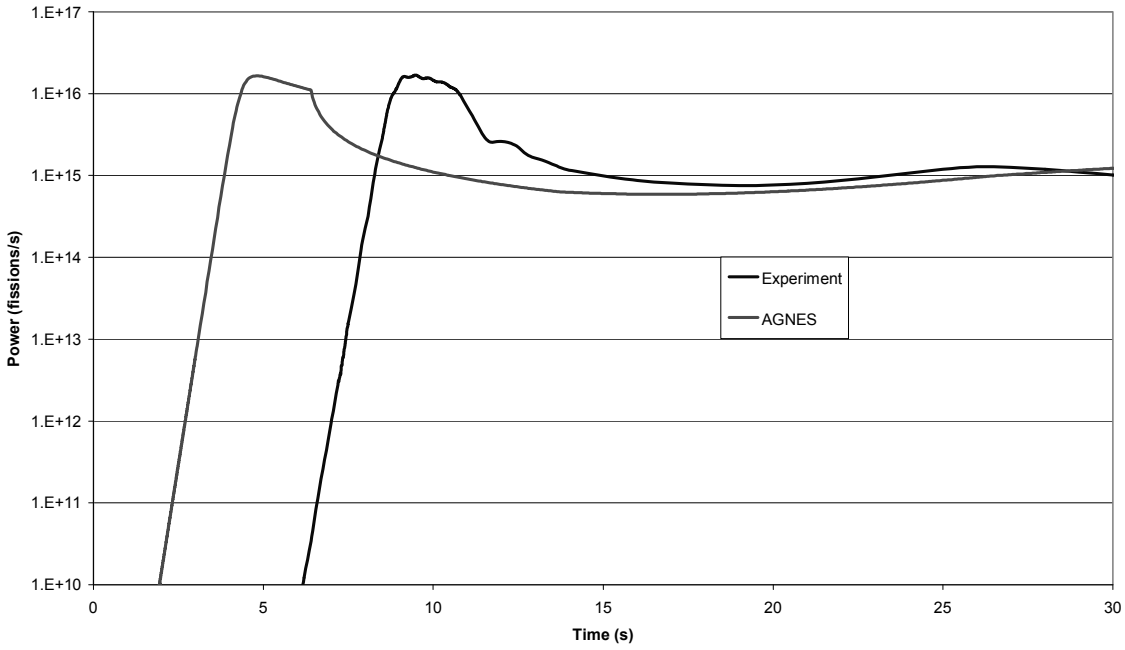

Figure 10.1.5: AGNES – S2-300 power history – whole profile

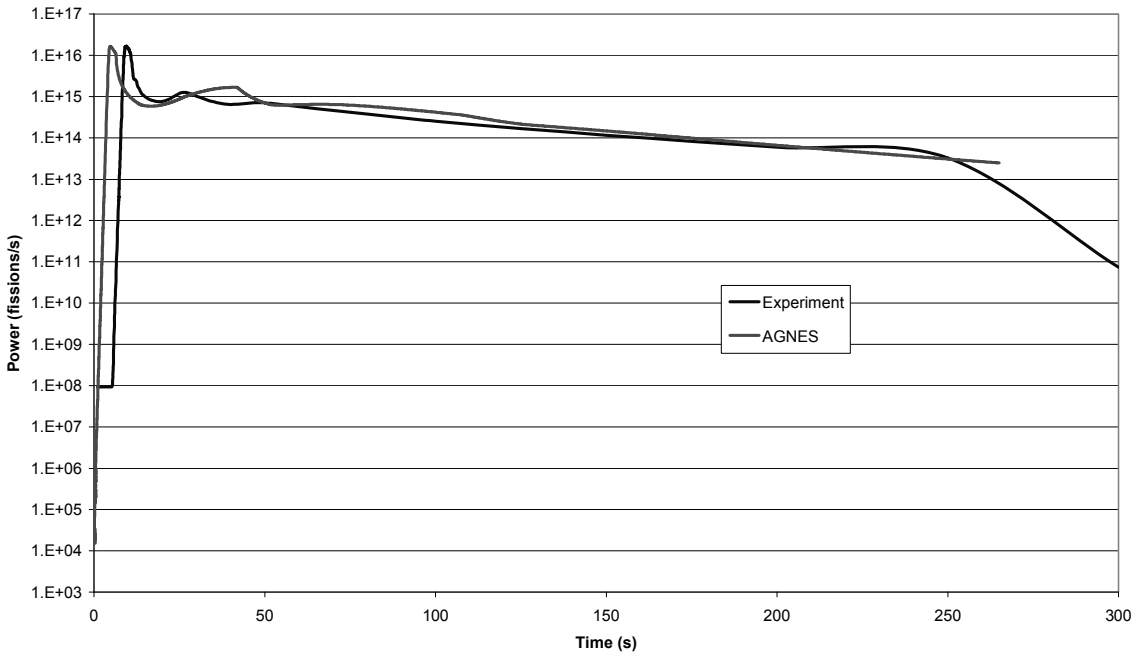

Figure 10.1.6: AGNES – S2-300 energy history – whole profile

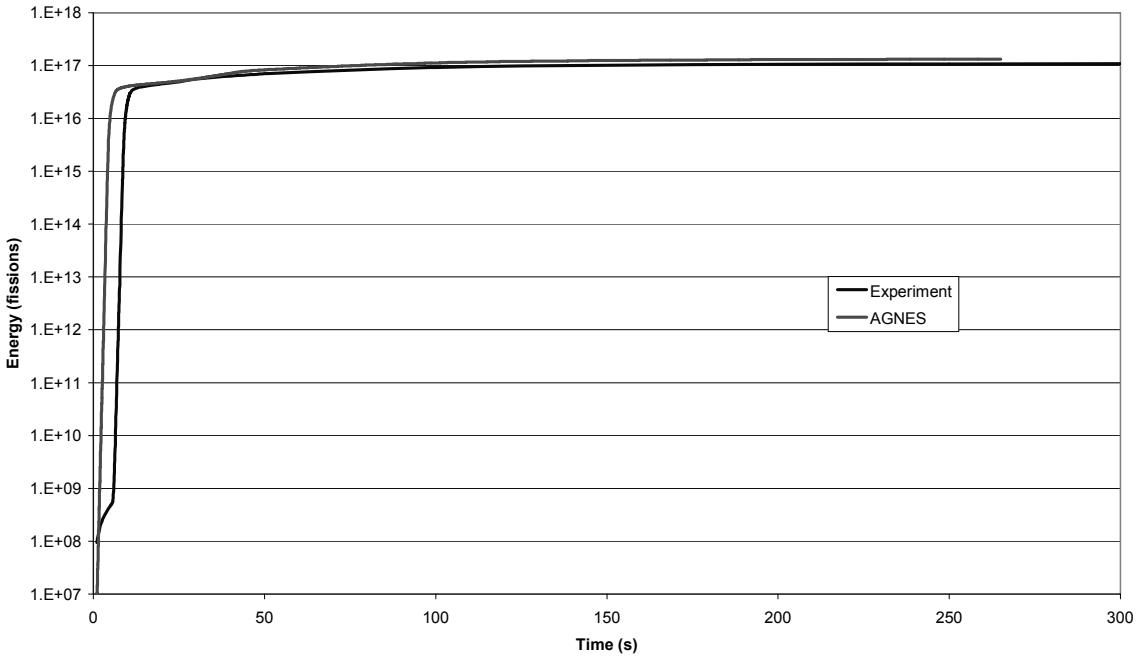

Figure 10.1.7: AGNES – S3-300 power history – first 5 s

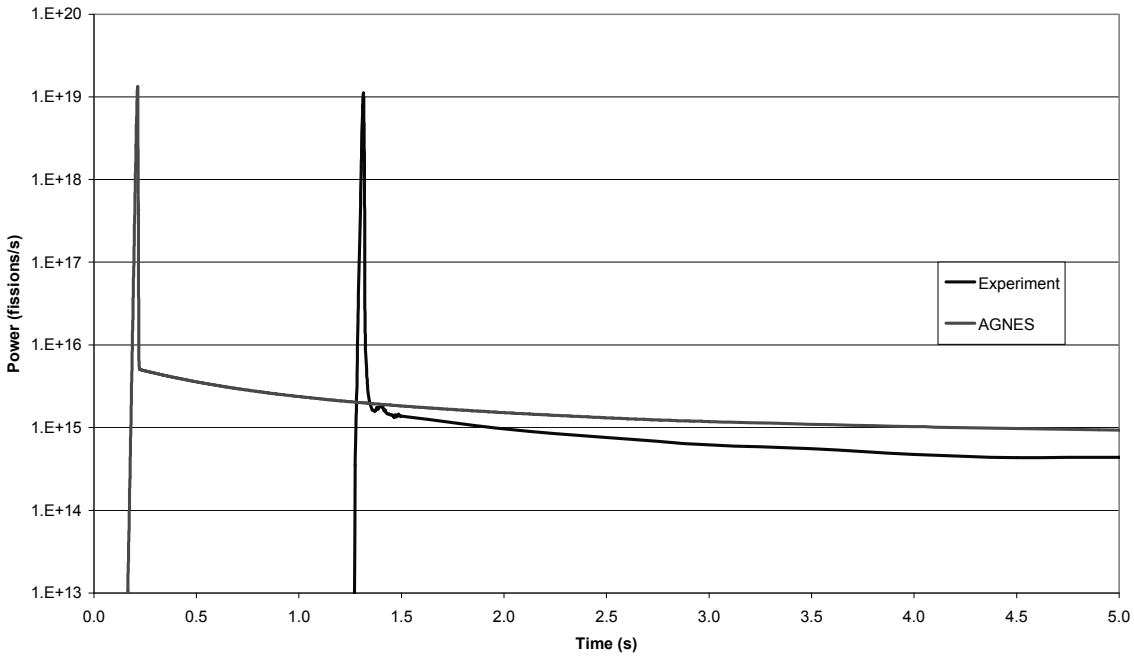

Figure 10.1.8: AGNES – S3-300 power history – whole profile

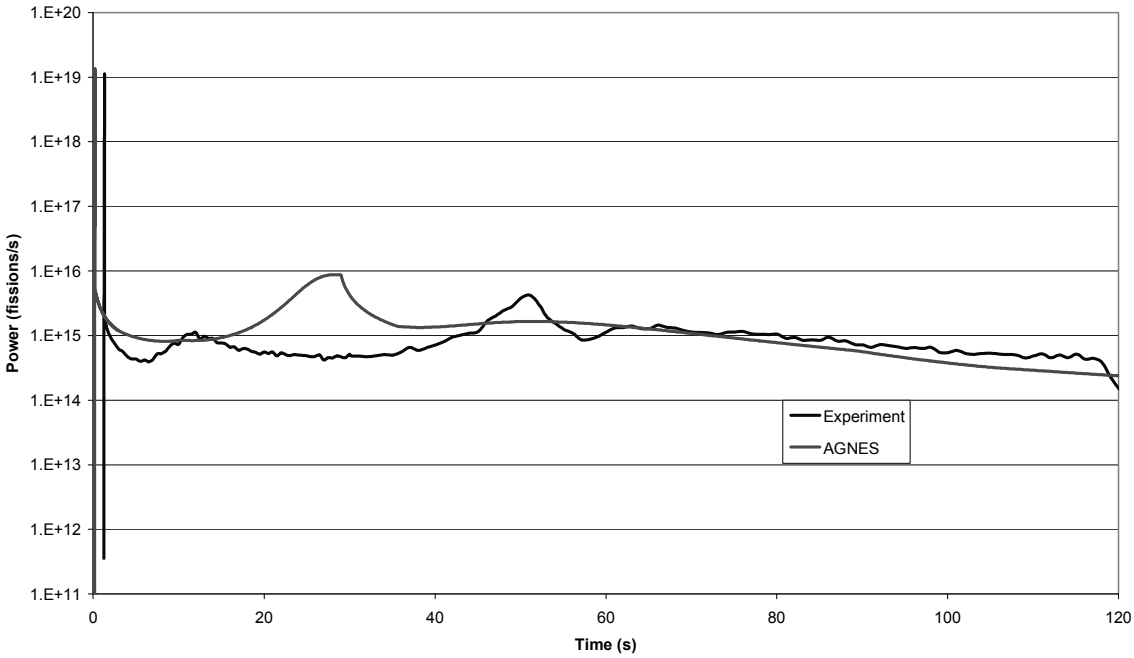

Figure 10.1.9: AGNES – S3-300 energy history – whole profile

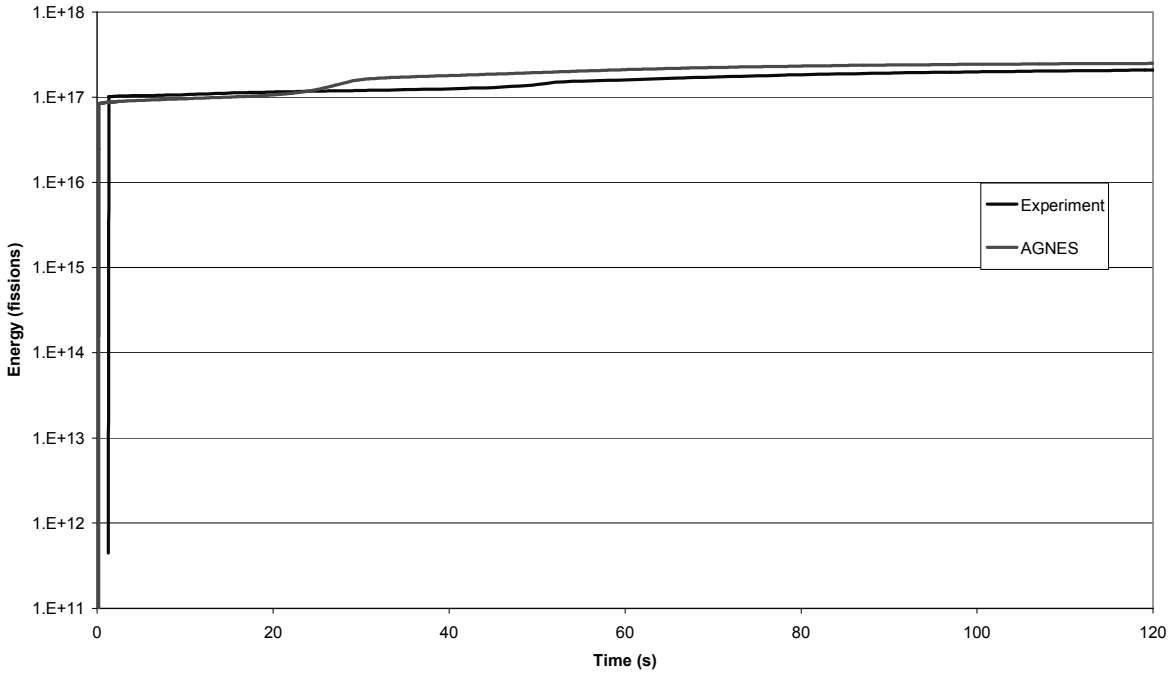

10.1.3 Further calculations with adjusted reactivity insertions

A further set of calculations were performed with the reactivity insertion adjusted by a small amount: a 1.2% increase for S1-300, a 0.62% decrease for S2-300 and a 4.8% decrease for S3-300. The results are displayed in Tables 10.1.4 to 10.1.6 and Figures 10.1.10 to 10.1.18. The results show that small adjustments to the reactivity insertion can produce overall improvements in the predicted behaviour to the first power peak (*i.e.* to the inverse period, peak power and energy released to the first peak), while having little effect on the total energy. This is consistent with Eqs. (3.2) and (6.2), which show that the peak power and inverse period are sensitive to the reactivity insertion for prompt-critical transients.

10.1.4 Conclusions

The AGNES calculations generally agree well with the experimental observations. The shape of the power curve is predicted well in all cases, including the main oscillatory behaviour. The calculation rises later than observed to the peak power in the test with an external neutron source, but rises earlier to the peak in the tests with no external neutron source. This could result from inaccuracies in the initial conditions for the calculations. The code also predicts the release of radiolytic gas shortly after the power peak in the delayed-critical transients and coincident with the peak power in the prompt-critical test, in agreement with experiment. The calculations exhibit a larger second power peak than observed in the experiments, resulting in overestimation of the total energy by about 20%. Small adjustments to the reactivity insertion can produce overall improvement in the predicted behaviour to the first power peak (*i.e.* to the inverse period, peak power and energy released to the first peak), while having little effect on the total energy.

Table 10.1.4: Results of trial calculation (S1-300)

	Calculation	Experiment	C/E
Inserted reactivity ($)	0.516	0.51	–
Inverse period (s^{-1})	0.19	0.18	1.06
First peak power (fissions s^{-1})	1.27×10^{15}	1.27×10^{15}	1.00
Fissions to first peak	1.81×10^{16}	2.20×10^{16}	0.82
Time to first peak	141.2	113.6	–
Final temperature (°C)	40.1	35.7	–
Total fissions	8.29×10^{16}	6.51×10^{16}	1.27
Time of gas release	151.8	132.5	–

Table 10.1.5: Results of trial calculation (S2-300)

	Calculation	Experiment	C/E
Inserted reactivity ($)	0.964	0.97	–
Inverse period (s^{-1})	5.58	5.33	1.05
First peak power (fissions s^{-1})	1.77×10^{16}	1.68×10^{16}	0.93
Fissions to first peak	1.01×10^{16}	$1 \times .3110^{16}$	0.77
Time to first peak	5.2	9.5	–
Final temperature (°C)	50.0	43.7	–
Total fissions	1.32×10^{17}	1.08×10^{17}	1.22
Time of gas release	6.9	10.5	–

Table 10.1.6: Results of trial calculation (S3-300)

	Calculation	Experiment	C/E
Inserted reactivity ($)	2.2	2.31	–
Inverse period (s^{-1})	286.1	285.0	1.00
First peak power (fissions s^{-1})	1.16×10^{19}	1.1×10^{19}	1.04
Fissions to first peak	7.01×10^{16}	6.61×10^{16}	1.06
Time to first peak	0.23	1.31	–
Final temperature (°C)	71.0	61.6	–
Total fissions	2.42×10^{17}	2.08×10^{17}	1.16
Time of gas release	0.23	1.32	–

Figure 10.1.10: Power history (initial 200 s with 0.516$ insertion)

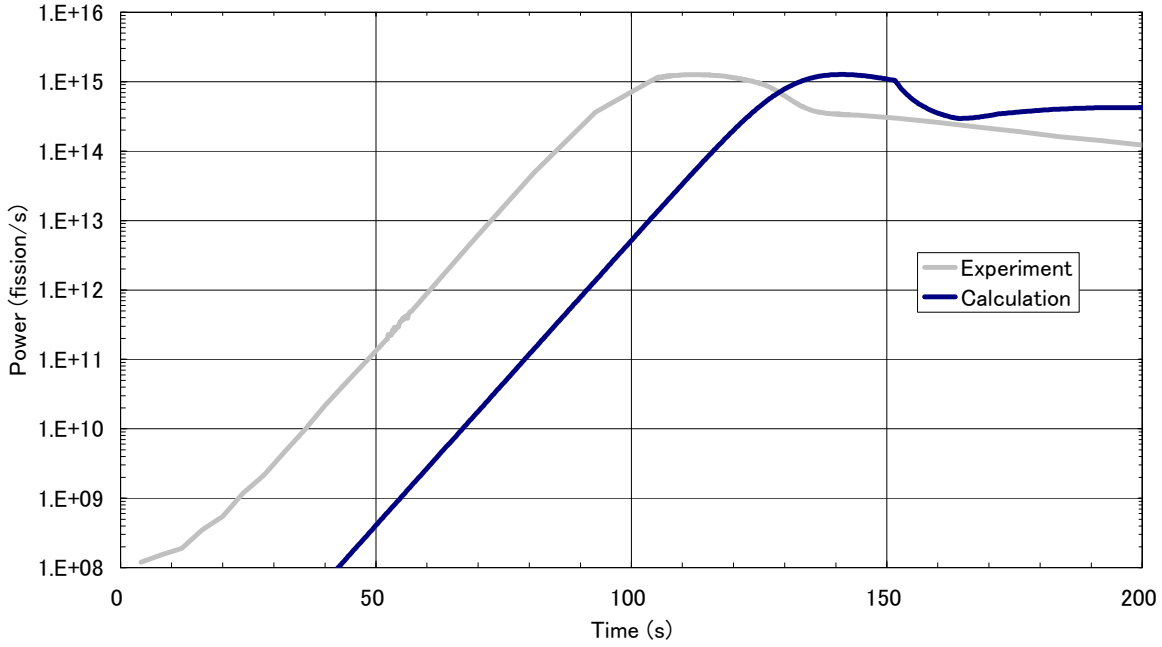

Figure 10.1.11: Power whole profile S1-300 (initial 200 s with 0.516$ insertion)

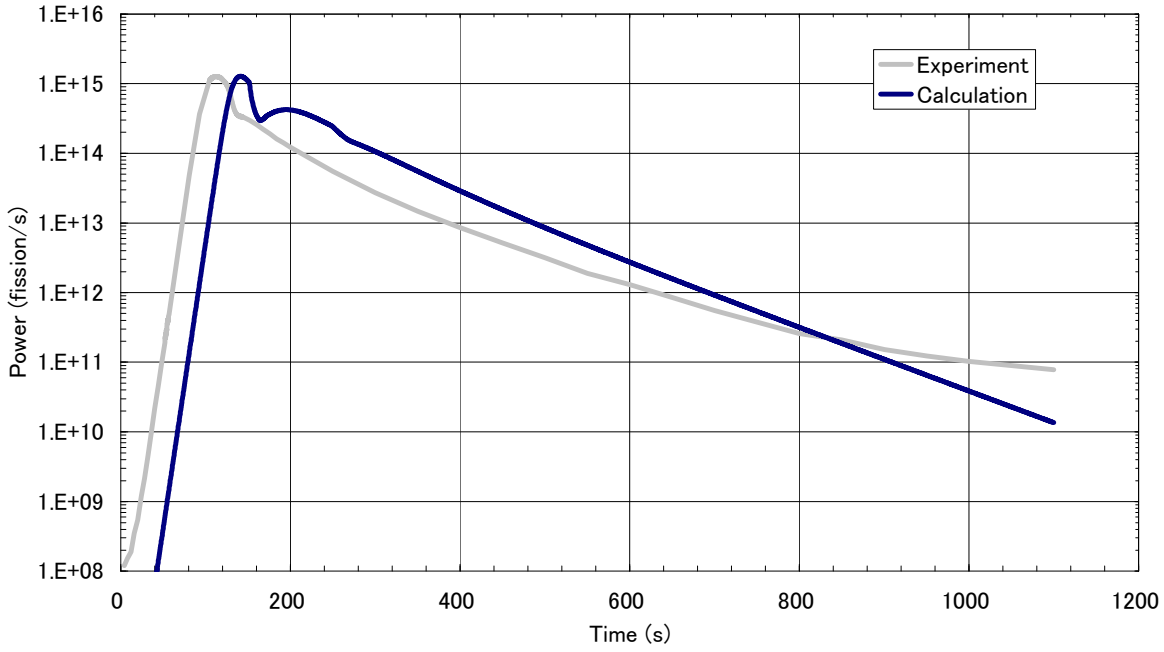

Figure 10.1.12: Energy whole profile S1-300 (initial 200 s with 0.516$ insertion)

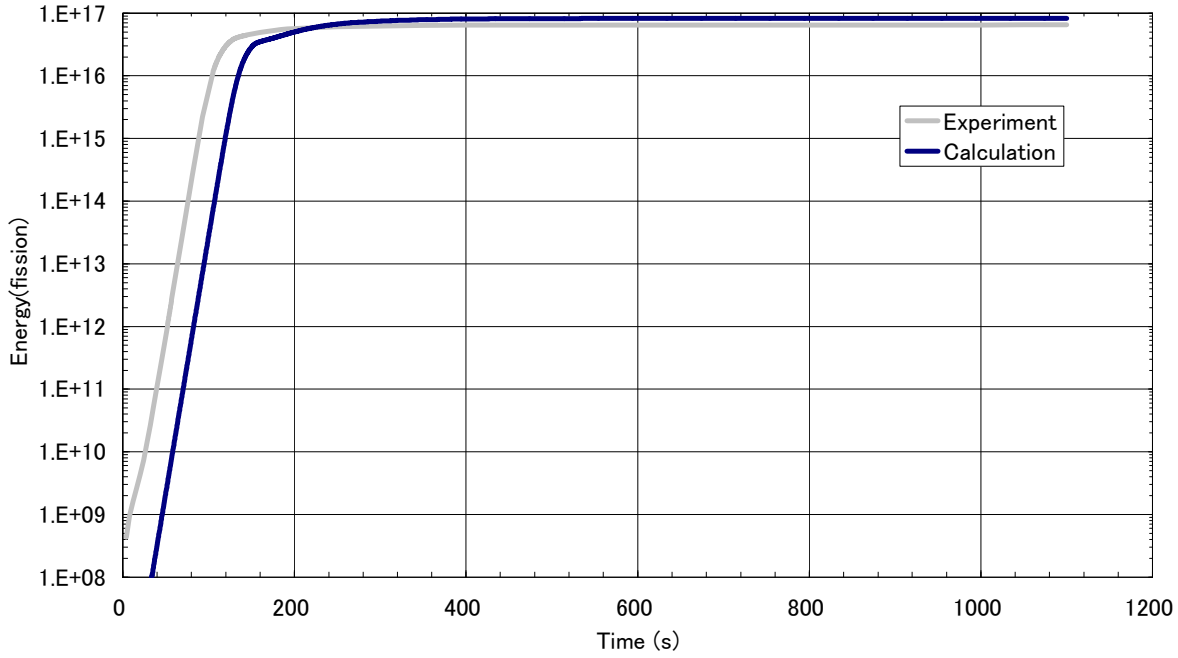

Figure 10.1.13: Power history S2-300 (initial 15 s with 0.964$ insertion)

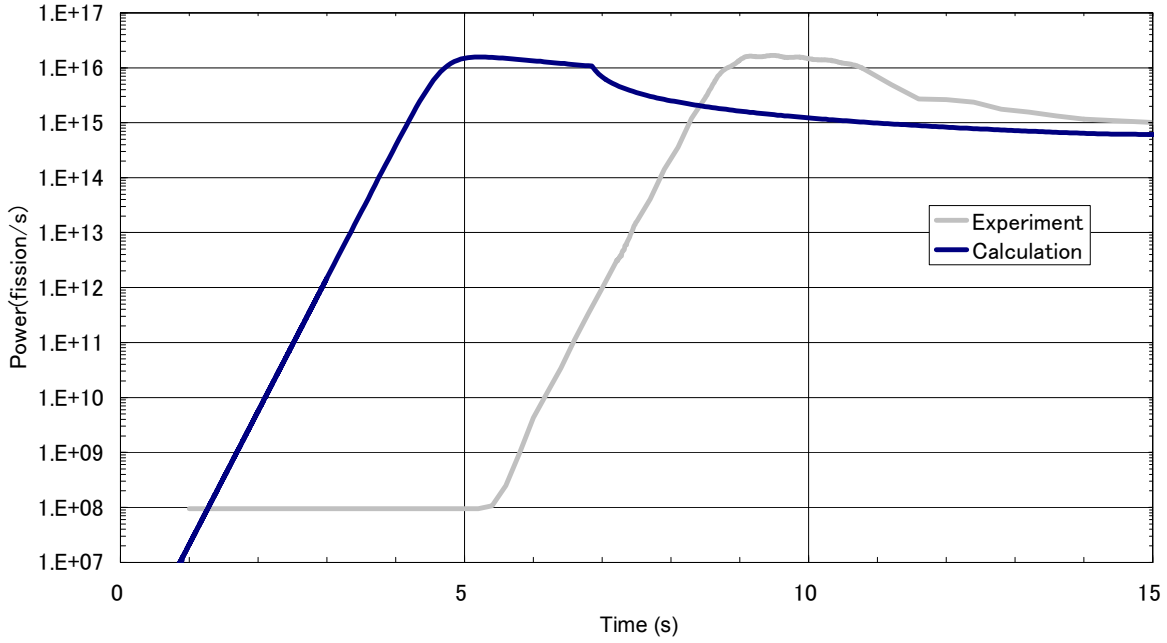

Figure 10.1.14: Power whole profile S2-300 (with 0.964$ insertion)

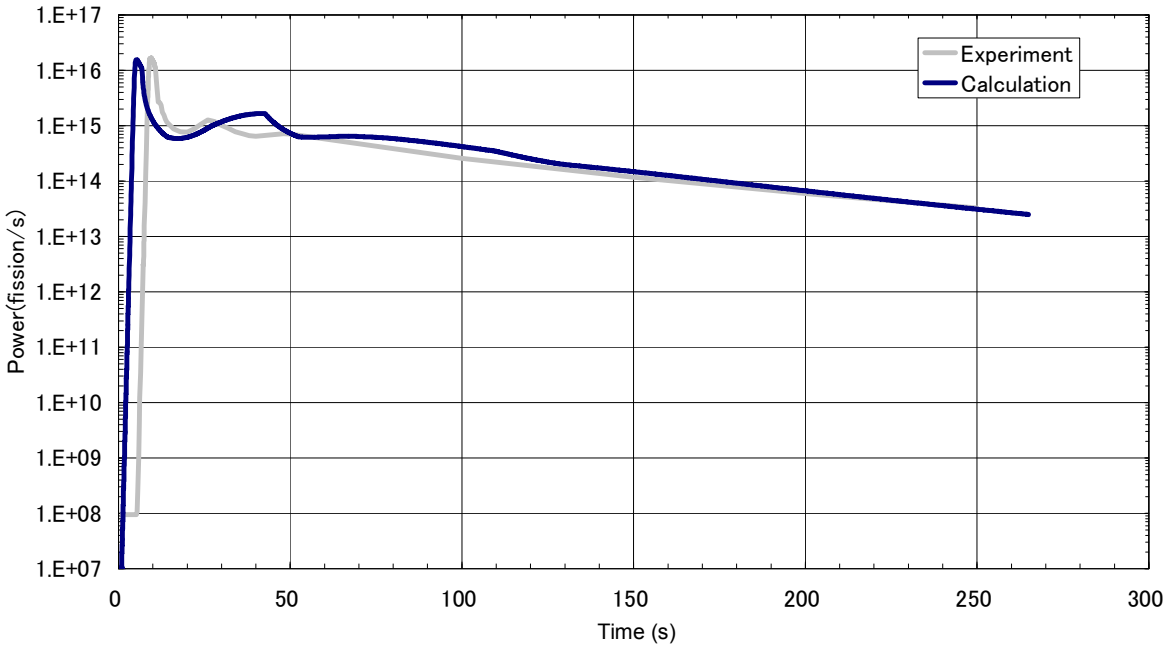

Figure 10.1.15: Energy whole profile S2-300 (with 0.964$ insertion)

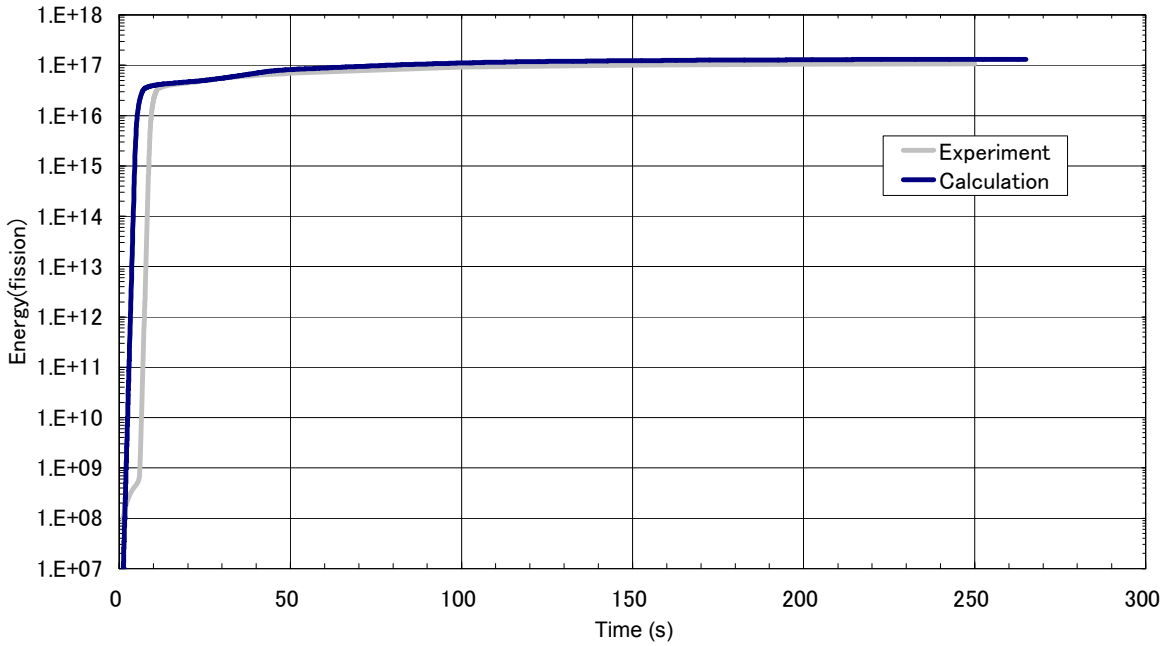

Figure 10.1.16: Power history S3-300 (initial 2 s with 2.2$ insertion)

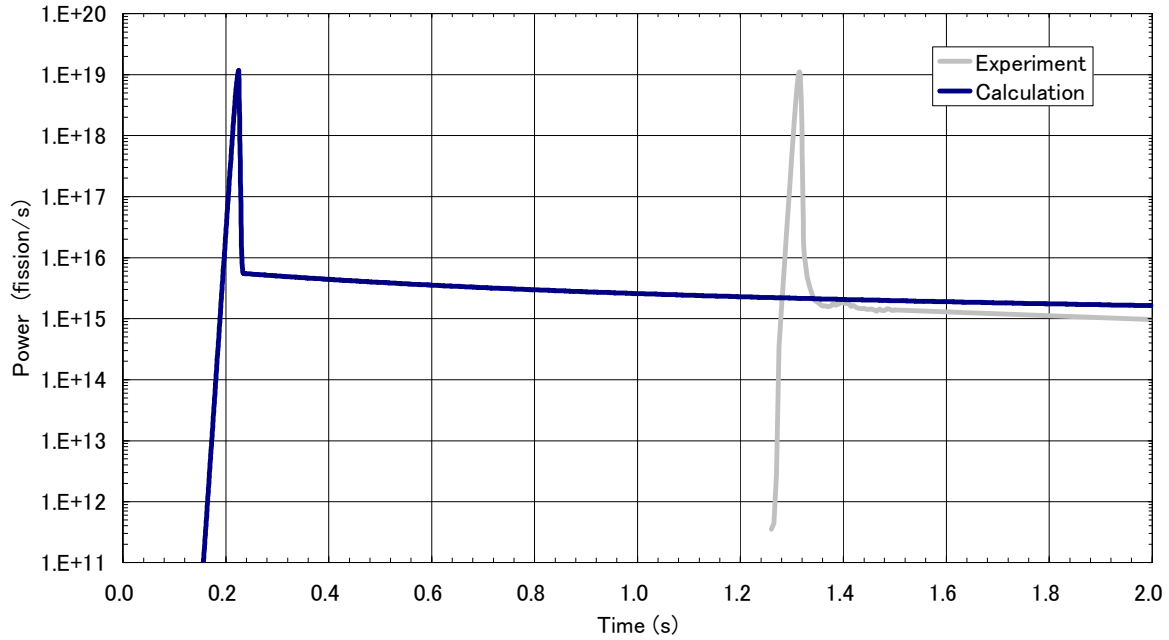

Figure 10.1.17: Power whole profile S3-300 (with 2.2$ insertion)

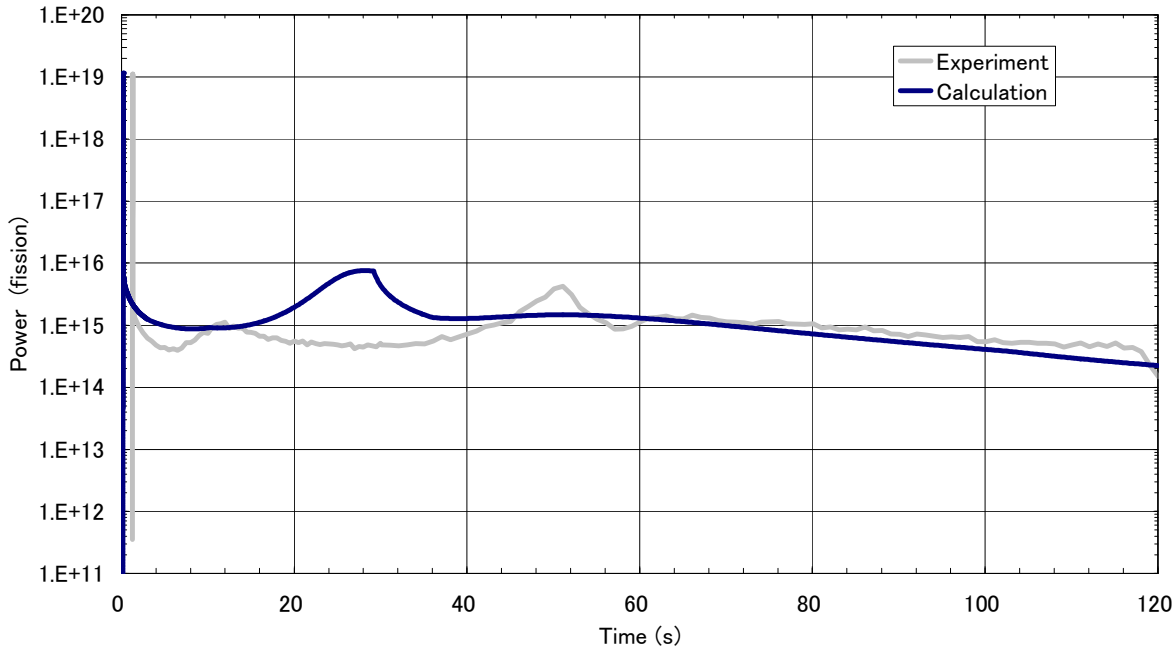

Figure 10.1.18: Energy whole profile S3-300 (with 2.2$ insertion)

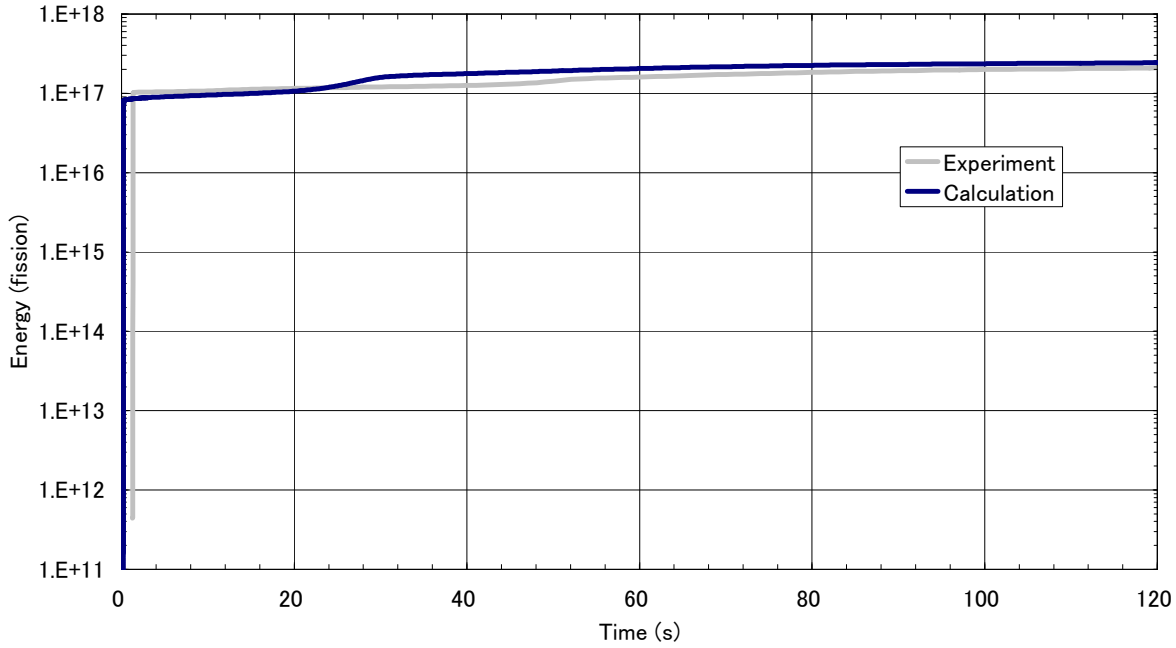

10.2 CRITEX

10.2.1 Input parameters

Grivot (2004) provides the details of the input parameters used.

10.2.2 Results

Grivot (2004) provides a detailed description of the results from the CRITEX calculations.

S1-300

This experiment used an external neutron source. Figures 10.2.1 to 10.2.3 show the results for S1-300 and indicate very good agreement with experiment. The qualitative behaviour is reproduced well and all of the calculated parameters agree with the measured values to within 16%. The calculated time of radiolytic gas release is only 4 s after the power peak, compared with an observed time lag of 22.5 s.

S2-300

Figures 10.2.4 to 10.2.6 show the results for S2-300 and indicate good agreement with experiment. The qualitative behaviour is reproduced well, except that the observed oscillations are not reproduced by the calculation. All of the calculated parameters agree with the measured values to within 13%, with the exception of the time to the first power peak, which is 30% earlier than observed. This results from the the lack of an external neutron source in this experiment, which makes it difficult to define appropriate initial conditions for the calculation and has little effect on the other predicted parameters. The calculated time of radiolytic gas release is 0.87 s after the power peak, 13% less than the observed time lag of 1 s.

S3-300

Figures 10.2.7 to 10.2.9 show the results for S3-300 and indicate good agreement with experiment. The qualitative behaviour is reproduced well, including the the observed oscillation, though the calculation exhibits two additional peaks between the observed second and third power peaks. All of the calculated

parameters agree with the measured values to within 14%, with the exception of the time to the first power peak, which is only one-third of the observed time. This results from the the lack of an external neutron source in this experiment, which makes it difficult to define appropriate initial conditions for the calculation and has little effect on the other predicted parameters. The calculated time of radiolytic gas release is coinicident with the first power peak, in agreement with the experiment.

It is worth noting that Grivot (2004) describes a pulse-type experiment (S2-34) in SILENE, with 71 gU/l and a reactivity insertion of 2 000 pcm in 0.32 s. These conditions are similar to those of S3-300. In S2-34 there was a delay of 1.3 s before the critical excursion was triggered. Figure 10.2.7 shows that there was a similar delay in S3-300. For experiment S3-300, the average chain reaction triggering time on reaching a prompt-critical state is 0.73 s. According to Hansen's theory, if a trigger lag of 0.73 s applies then the time to the first pressure peak is delayed by 0.73 s. Applying such a time lag to the CRITEX calculation for S3-300 leads to an estimated time to the first power peak of 0.73 + 0.47 = 1.2 s. This is only 8% less than the observed time to the first peak.

10.2.3 Conclusions

The agreement between the CRITEX calculations and the experimental results is good, with the calculated parameters agreeing with the measured values to within 16%. The only exception is that the estimated time to the first power peak is much shorter than observed in tests S2-300 and S3-300. This is due to the lack of an external neutron source for these experiments, which makes it difficult to determine appropriate initial conditions for the calculations. However, the errors in the initial conditions (neutron concentration and delayed neutron precursor concentrations) have little effect on the calculated values of the other parameters, such as the maximum inverse period, time to the first power peak, peak power, energy to the first peak. The CRITEX calculations fail to reproduce the observed oscillatory behaviour in S2-300, but do a reasonable job of predicting the kind of oscillatory behaviour observed in S3-300.

Figure 10.2.1: CRITEX – S1-300 power history – first 250 s

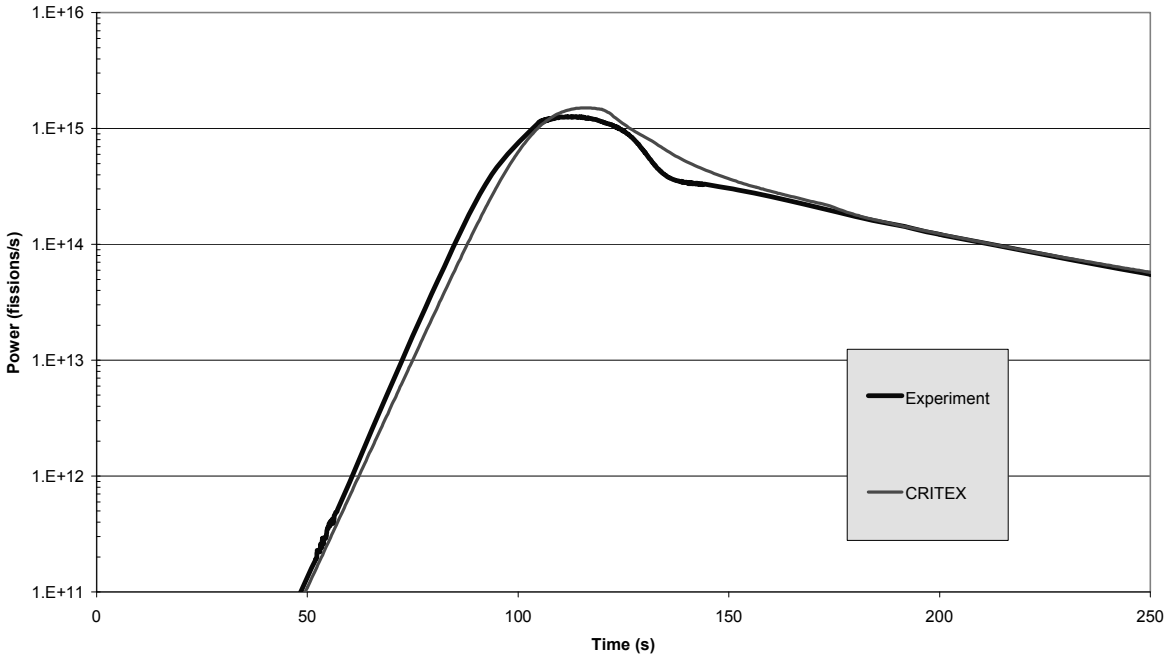

Figure 10.2.2: CRITEX – S1-300 power history – whole profile

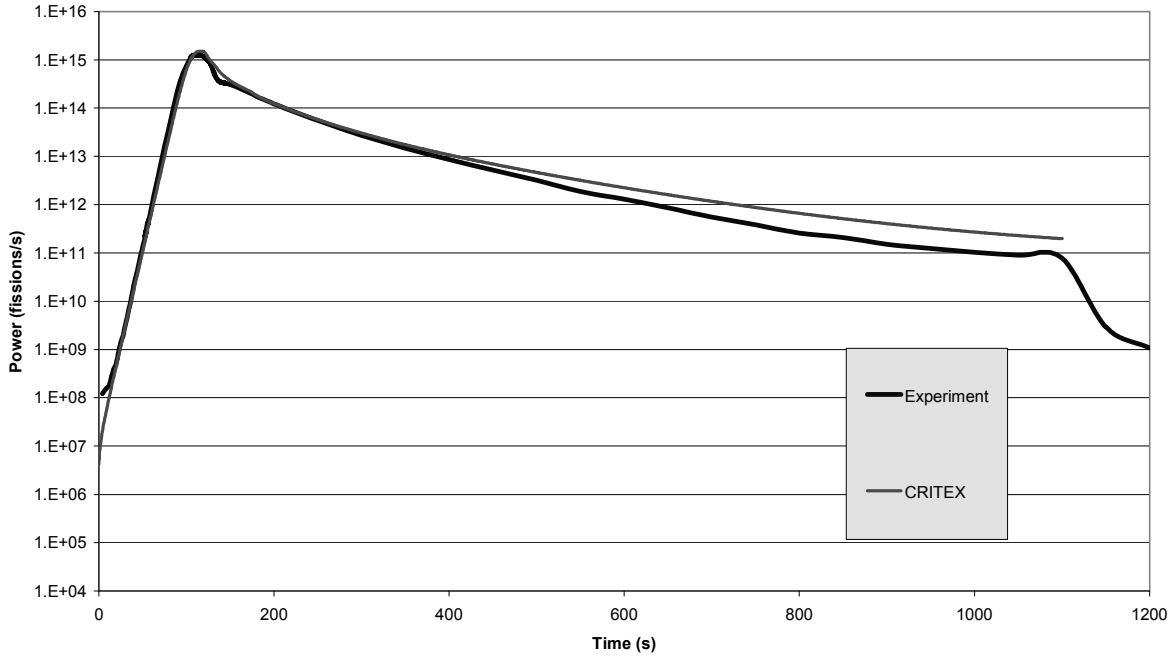

Figure 10.2.3: CRITEX – S1-300 energy history – whole profile

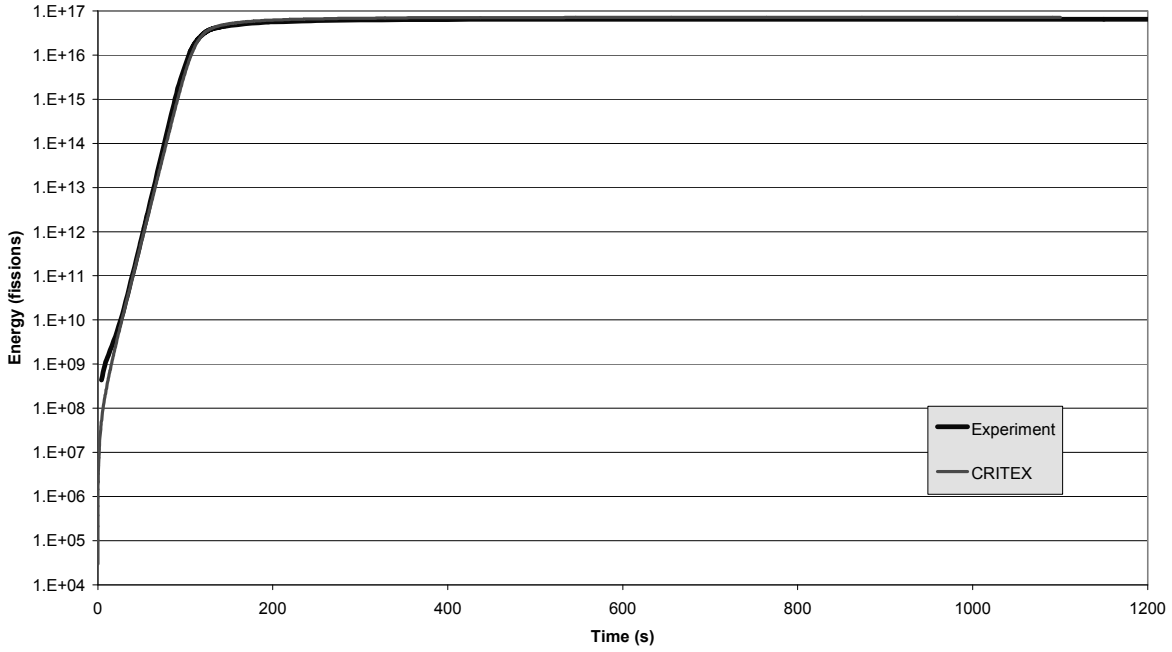

Figure 10.2.4: CRITEX – S2-300 power history – first 30 s

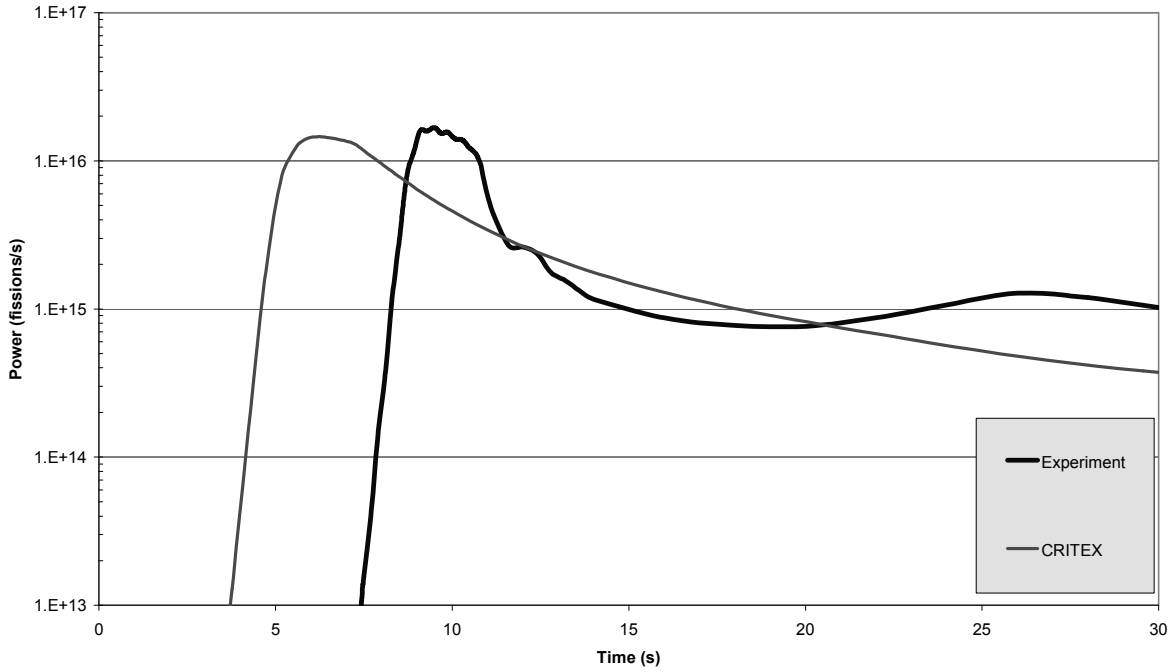

Figure 10.2.5: CRITEX – S2-300 power history – whole profile

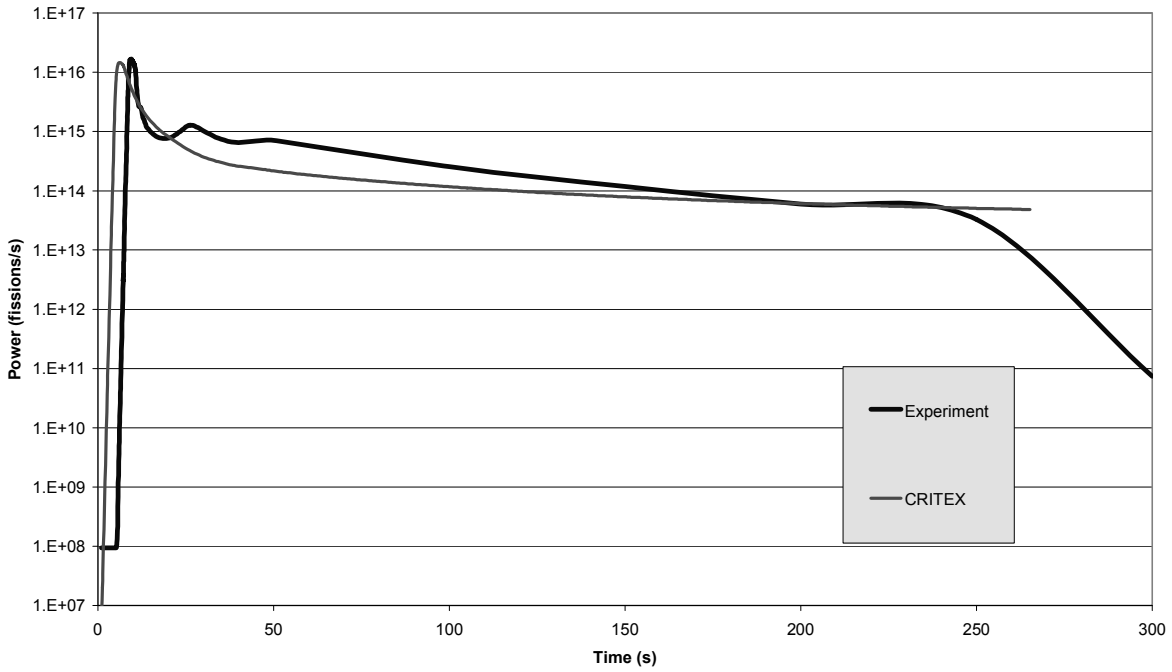

Figure 10.2.6: CRITEX – S2-300 energy history – whole profile

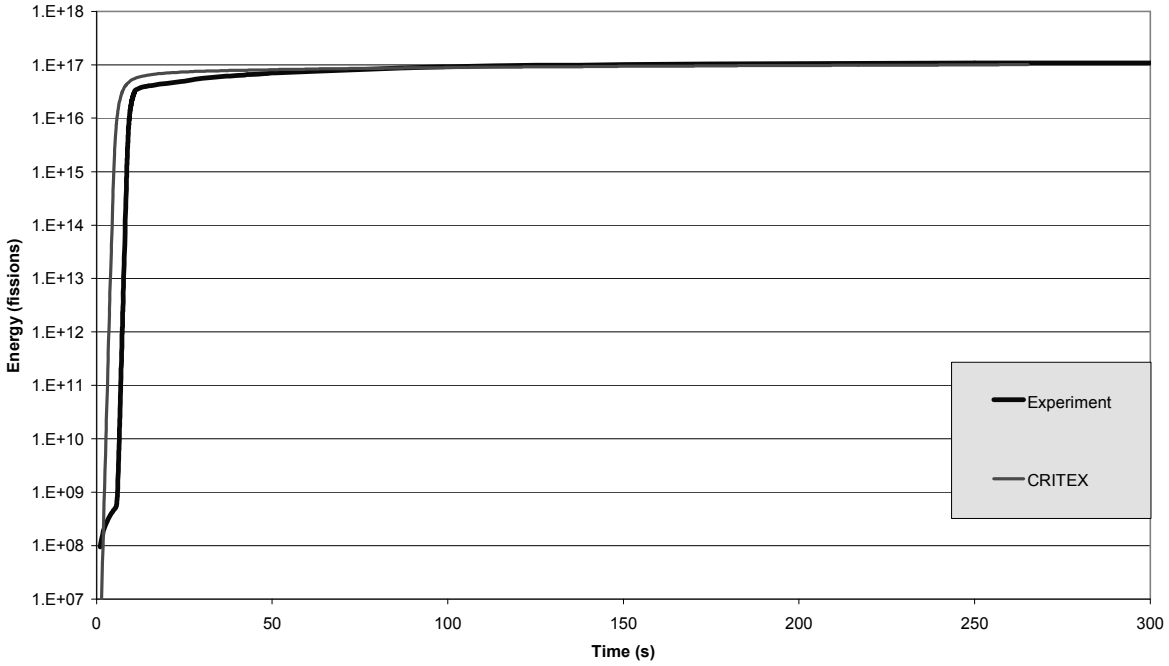

Figure 10.2.7: CRITEX – S3-300 power history – first 5 s

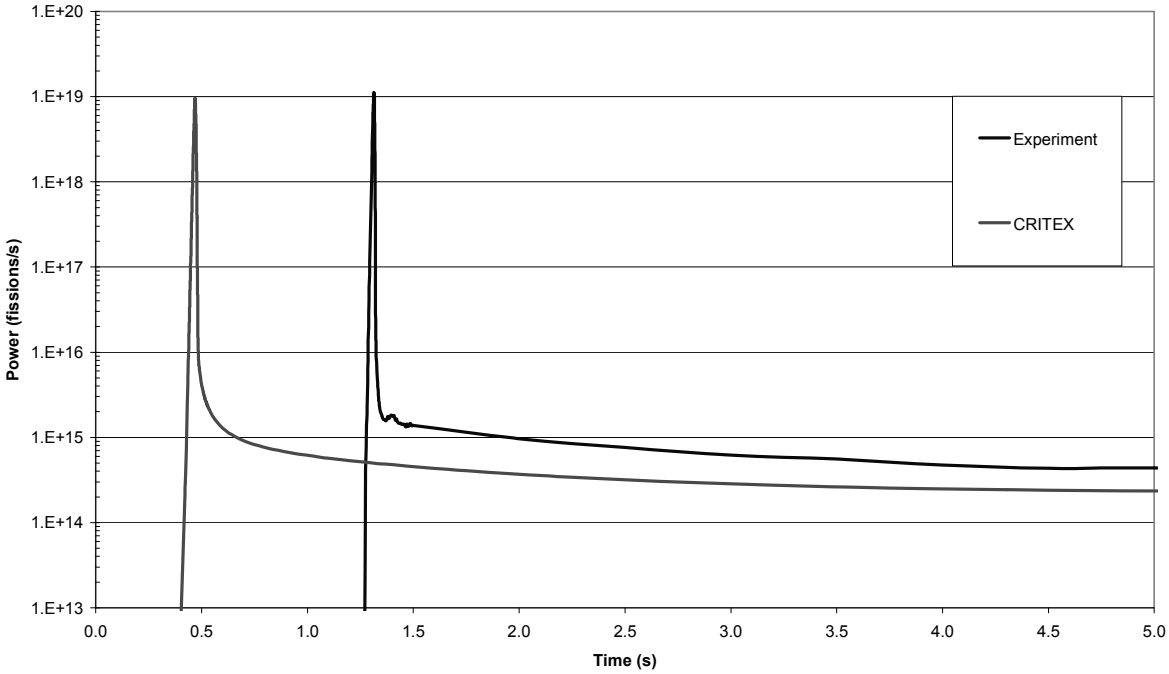

Figure 10.2.8: CRITEX – S3-300 power history – whole profile

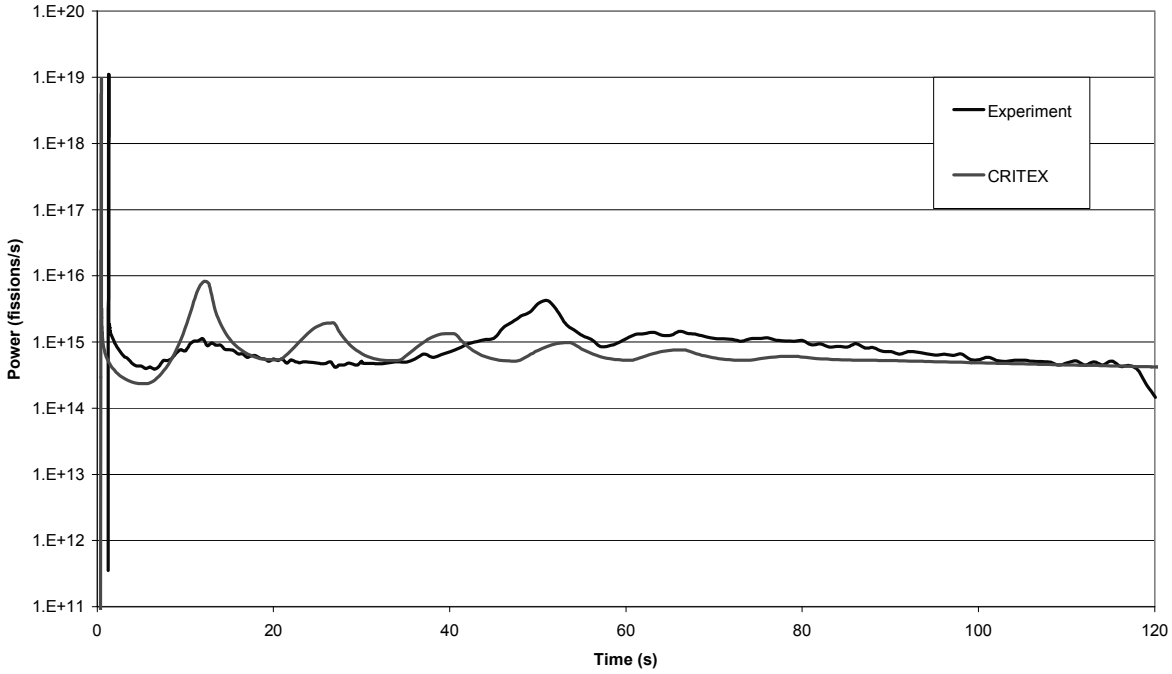

Figure 10.2.9: CRITEX – S3-300 energy history – whole profile

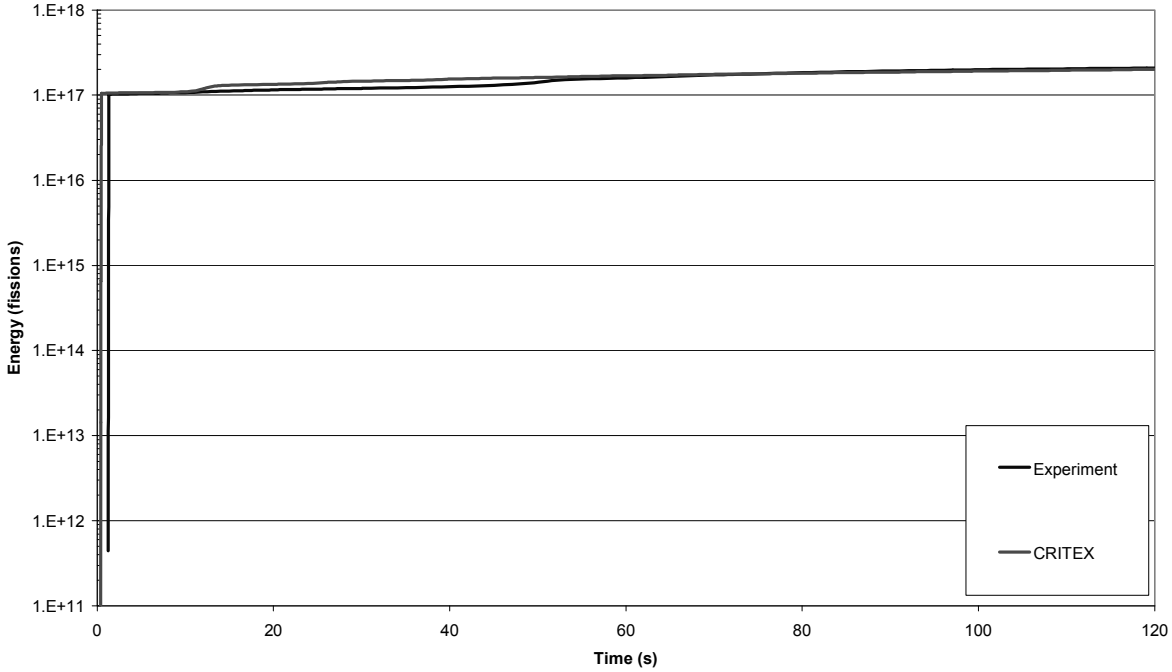

10.3 INCTAC

10.3.1 Input parameters

The composition of the fissile solution used for the INCTAC (Mitake, 2005) code is defined in Section 8.3. During criticality excursions, radiolytic gas production and thermal expansion reduce the density of the fissile solution. Therefore, atomic compositions are estimated for a range of fissile solution densities, in order to evaluate the effect of expansion on reactivity. Using the SST formula, developed in JAERI for evaluating the density of uranyl nitrate solutions, the atomic compositions for the fuel solution with a uranium concentration of 70.78 g/l are as listed in Table 10.3.1.

Table 10.3.1: Atomic number density of fuel solution

Isotopes	Solution density				
	1.16602 g/cm^3	1.10772 g/cm^3	1.04942 g/cm^3	0.99112 g/cm^3	0.93282 g/cm^3
H	6.2848E-02	5.9706E-02	5.6563E-02	5.3421E-02	5.0279E-02
N	1.5668E-03	1.4885E-03	1.4101E-03	1.3318E-03	1.2534E-03
O	3.5885E-02	3.4091E-02	3.2296E-02	3.0502E-02	2.8708E-02
^{234}U	1.0381E-06	9.8620E-07	9.3430E-07	8.8239E-07	8.3048E-07
^{235}U	1.6818E-04	1.5977E-04	1.5136E-04	1.4295E-04	1.3454E-04
^{236}U	4.5144E-07	4.2887E-07	4.0630E-07	3.8373E-07	3.6115E-07
^{238}U	1.1531E-05	1.0955E-05	1.0378E-05	9.8015E-06	9.2250E-06

Units: atoms/barn-cm.

Void (assumed vacuum) fractions up to 20% and temperatures from 20°C to 100°C are considered.

The estimated nuclear kinetics parameters for the fuel solution of the SILENE experiments (fractions β_i and β_{eff}, decay constants (λ_i) and spectra for the first three groups of the nine-group energy structure) are as listed in Table 10.3.2.

Table 10.3.2: Kinetic parameters

Delayed neutron fraction		Decay constant [1/s]	Delayed neutron spectra		
			First group	Second group	Third group
β_1	2.752E-04	1.270E-02	0.00584	0.99416	0.
β_2	1.750E-03	3.170E-02	0.12207	0.87793	0.
β_3	1.581E-03	1.150E-01	0.07061	0.92563	0.00376
β_4	3.170E-03	3.170E-01	0.12405	0.8671	0.00885
β_5	9.276E-04	1.400E+00	0.10188	0.89761	0.00051
β_6	3.378E-04	3.870E+00	0.08901	0.91099	0.
β_{eff} (total)	8.041E-03	–	–		

The following values are used for the radiolytic gas formation parameters:

G: energy to generate radiolysis gas [mol/J]	1.23E-07
C_0: radiolysis gas saturation concentration [mol/m^3]	5.0

10.3.2 Results

S1-300

This experiment has an external neutron source. Figures 10.3.1 to 10.3.3 display the comparison of the calculated and measured power transients for S1-300 and indicate good agreement with experiment. The qualitative behaviour is reproduced well and most of the calculated parameters agree with the measured values to within 14%. The 19% discrepancy in the calculated and measured times to the peak power is due to the use of an inappropriate value for the initial critical power level in the

calculation. In the calculation radiolytic gas production begins 2 s before the power peak is reached in contrast to the experiment where the gas release is observed to occur 22.5 s after the peak power has been reached.

S2-300

Figures 10.3.4 to 10.3.6 display the comparison of the calculated and measured power transients for S2-300 and indicate good agreement with experiment. The qualitative behaviour is reproduced well, with the exception that the observed oscillatory behaviour is not reproduced by the calculation. In this case most of the calculated parameters agree with the measured values to within 32%. The large discrepancy in the calculated and measured times to the peak power is due to the difficulty in choosing an appropriate value for the initial critical power level for an experiment without an external neutron source. However, this discrepancy has little effect on the calculated values of subsequent parameters. In the calculation radiolytic gas production begins 0.64 s after the power peak is reached, which is 36% earlier than observed.

S3-300

Figures 10.3.7 to 10.3.9 display the comparison of the calculated and measured power transients for S3-300 and indicate generally good agreement with experiment. The qualitative behaviour is reproduced reasonably well, with the exception that the observed oscillatory behaviour is not well reproduced, though the calculation does predict a second power peak. In this case most calculated parameters agree with the measured values to within 18%. The exception is the discrepancy in the calculated and measured times to the first peak power, which is due to the difficulty in choosing an appropriate value for the initial critical power level in the calculation, for an experiment without an external neutron source. However, this discrepancy has little effect on the calculated values of subsequent parameters. In the calculation radiolytic gas release is coincident with the first power peak, in agreement with observation.

10.3.3 Conclusions

The agreement between the INCTAC calculations and the experimental results is generally good, with most of the calculated parameters agreeing with the measured values to within 32%. The main exception is that the estimated time to the first power peak is much shorter than observed in tests S2-300 and S3-300. This is due to the lack of an external neutron source for these experiments, which makes it difficult to determine appropriate initial conditions for the calculations. However, the errors in the initial conditions (neutron concentration and delayed neutron precursor concentrations) have little effect on the calculated values of the other parameters, such as the maximum inverse period, time to the first power peak, peak power and energy to the first peak. In test S2-003 radiolytic gas release is predicted to occur before the first power peak is reached, which is contrary to the observation of gas release after the power peak. The INCTAC calculation fails to reproduce the observed oscillatory behaviour in S2-300, and does not match the oscillatory behaviour observed in S3-300 very well.

Figure 10.3.1: INCTAC – S1-300 power history – first 250 s

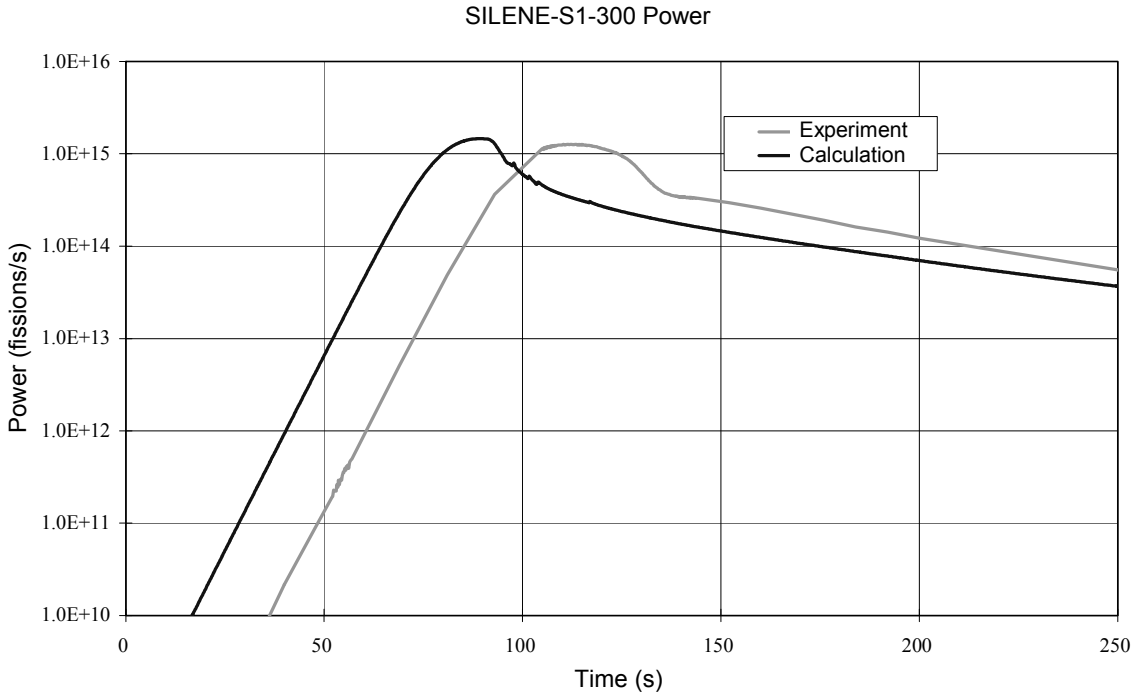

Figure 10.3.2: INCTAC – S1-300 power history – whole profile

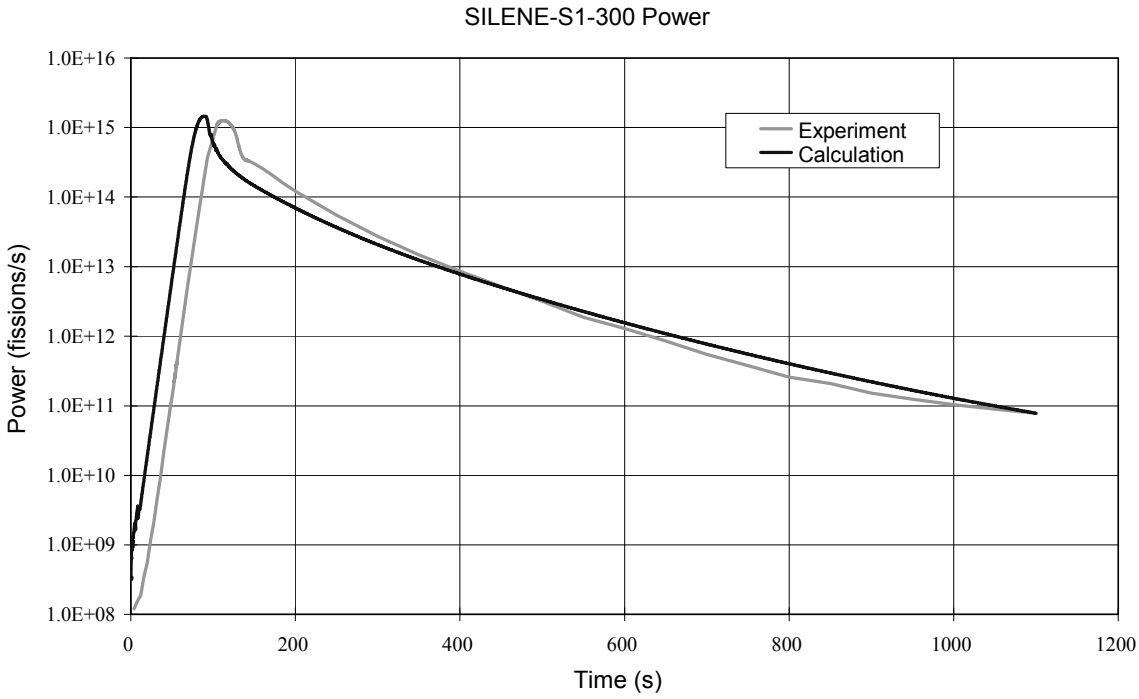

Figure 10.3.3: INCTAC – S1-300 energy history – whole profile

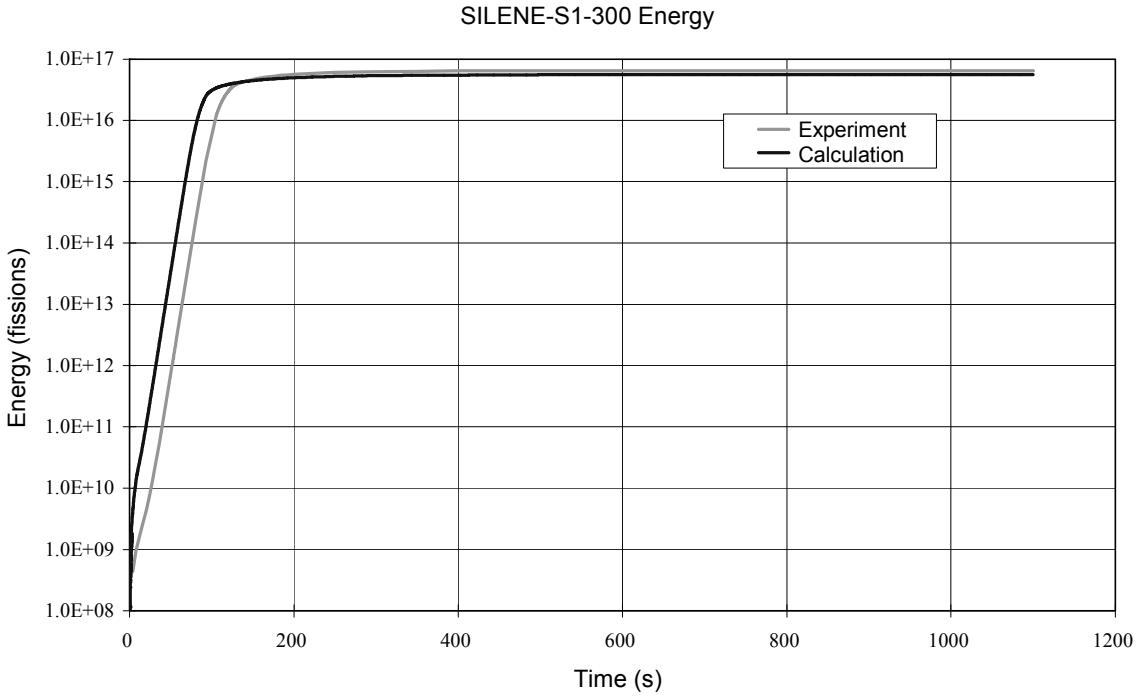

Figure 10.3.4: INCTAC – S2-300 power history – first 30 s

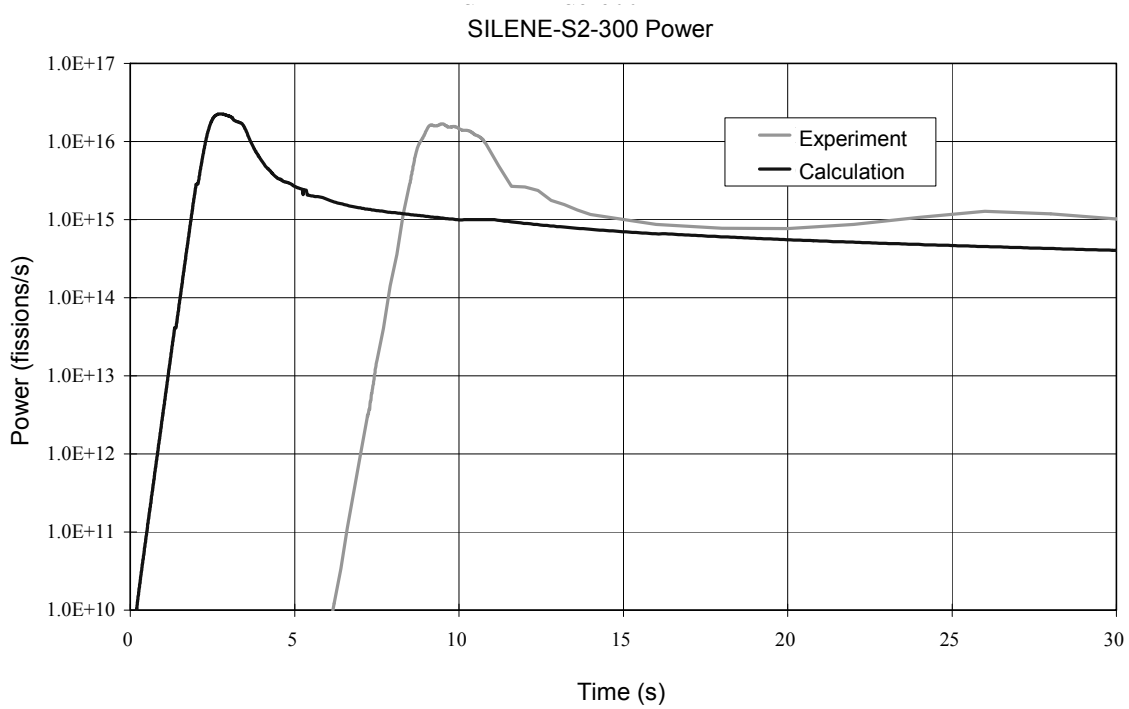

Figure 10.3.5: INCTAC – S2-300 power history – whole profile

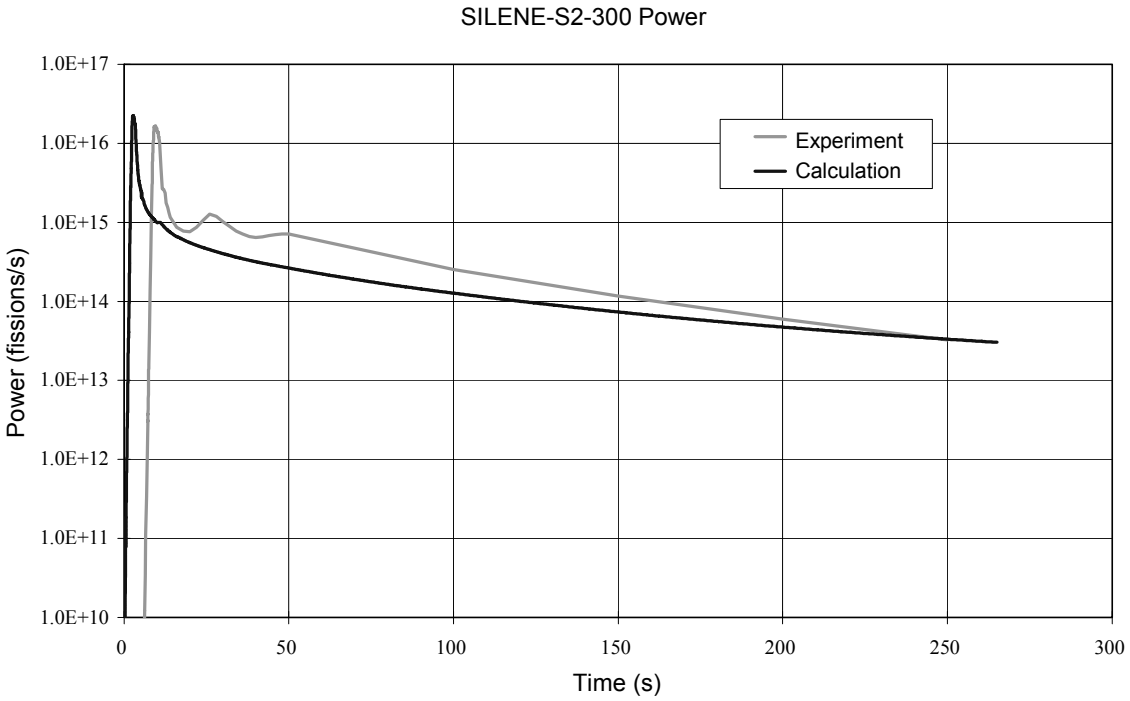

Figure 10.3.6: INCTAC – energy history – whole profile

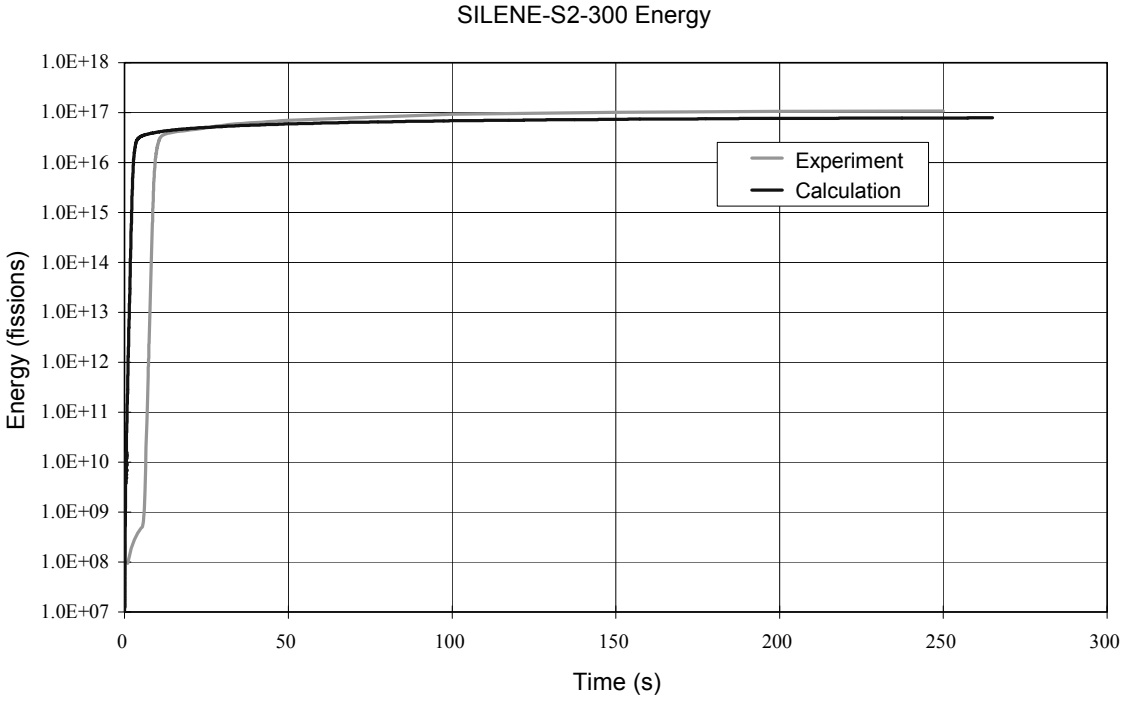

Figure 10.3.7: INCTAC – S3-300 power history – first 5 s

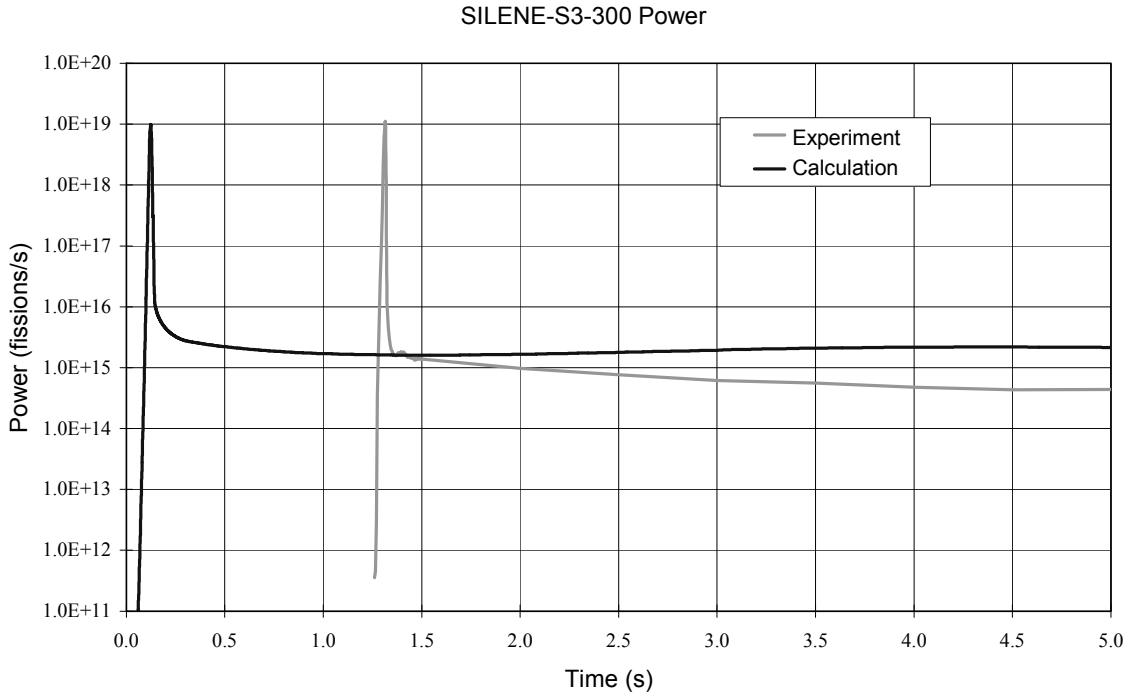

Figure 10.3.8: INCTAC – S3-300 power history – whole profile

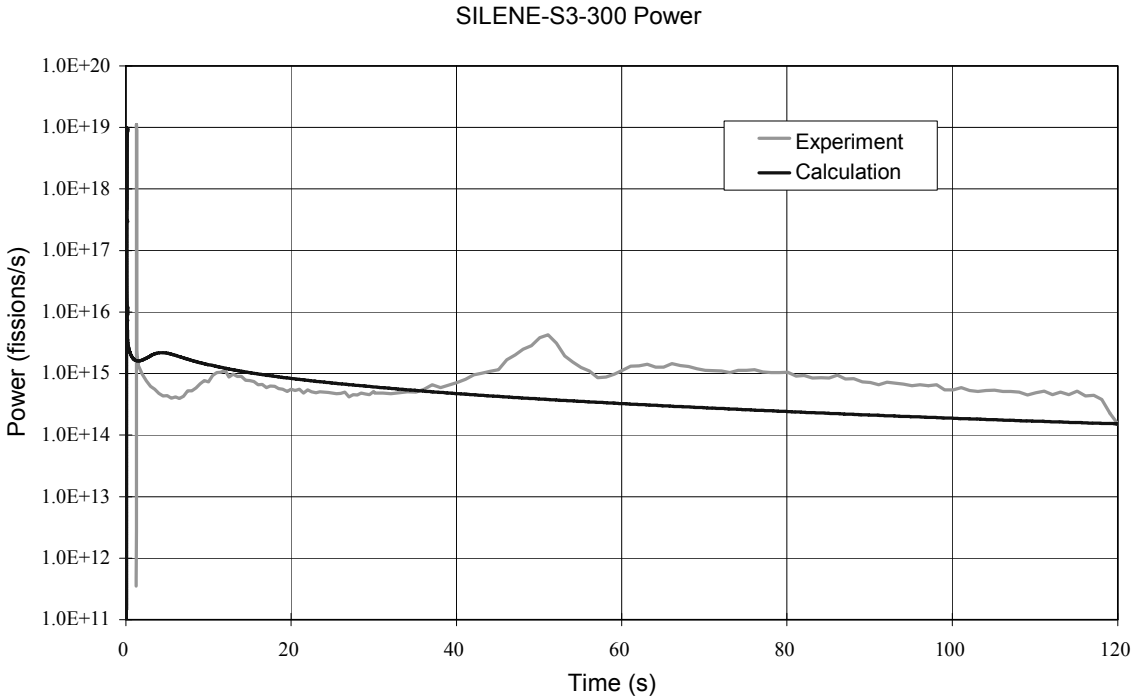

Figure 10.3.9: INCTAC – S3-300 energy history – whole profile

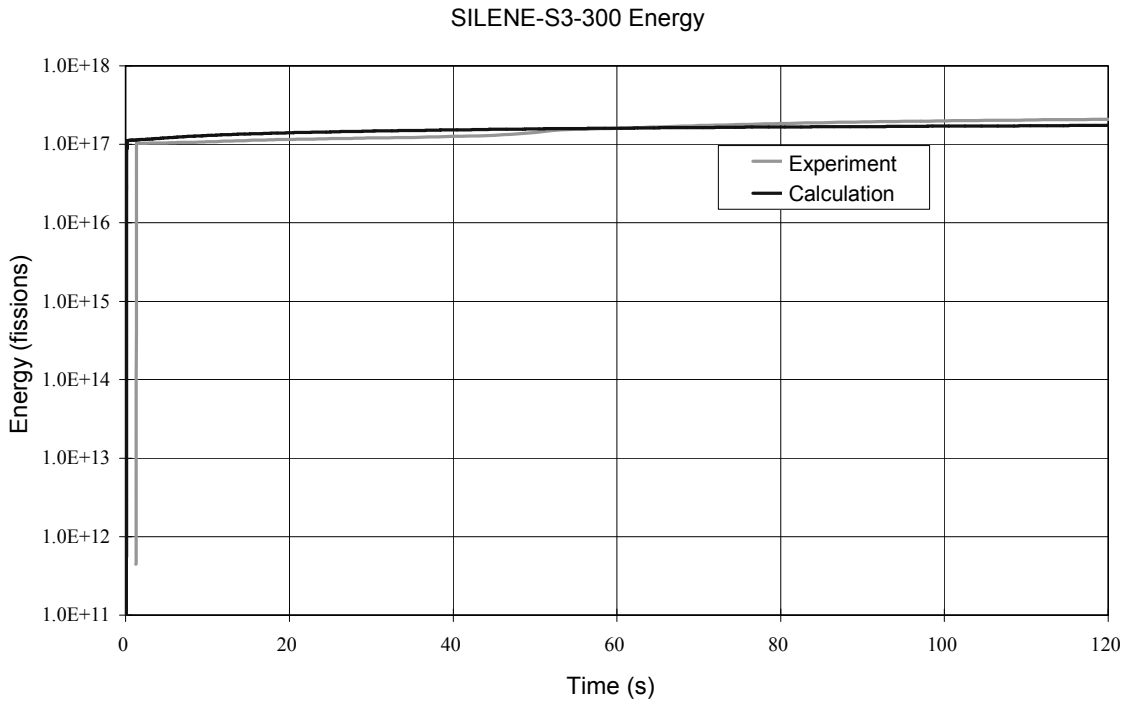

10.4 TRACE

10.4.1 Input parameters

The basic modelling parameters chosen used in the TRACE (Hong, 2005) code for the SILENE benchmark calculations are displayed in Table 10.4.1. The kinetics parameters and reactivity feedback coefficients are presented in Tables 10.4.2 and 10.4.3, respectively.

It should be emphasised that the TRACE calculations were performed without prior knowledge of the benchmark experimental results, and no adjustments or re-calculations were performed (*i.e.* all calculations are blind). Apart from the kinetics parameters and reactivity coefficients, the same parameters and options were used for both TRACY and SILENE benchmarks. This may not be appropriate as the compositions of the fissile solutions of the two benchmarks are quite different.

10.4.2 Results

S1-300

The calculated and measured power transients for S1-300 are displayed in Figures 10.4.1 to 10.4.3 and show reasonable agreement with experiment. The qualitative behaviour is reproduced reasonably well, but there are disagreements of more than a factor of two between some of the calculated and measured parameters. In particular the peak power and energy to the peak are both underestimated by a factor of more than two. The total energy is underestimated by almost 40% and yet the temperature rise is overestimated by a factor of over two. This suggests that the heat capacity of the fissile solution has been underestimated by a factor of about 3.5. This test had an external neutron source, but Figure 10.4.2 suggests that the calculation was initialised with a power that is several orders of magnitude lower than the experiment. This results in a time lag compared to the experiment, but is not expected to have a significant effect on the other parameters. The calculated radiolytic gas release occurs before the calculated power peak in contrast to the observed radiolytic gas release, which occurred after the observed power peak.

Table 10.4.1: TRACE modelling parameters for SILENE benchmark calculations

	Model/parameter	Adopted value
Geometry	2-D cylindrical geometry	Axial: 8 meshes Radial: 5 meshes
Neutronics	Delayed neutron precursors group	6
	Constant power distribution	Axial: cosine Radial: Bessel J_0
Reactivity feedback	Weighting function for temperature and void reactivity feedback calculation	Power
Radiolytic gas formation	G value	1×10^{-7} mol/J
	Volume of void produced per energy added per number of moles of radiolytic gas	0.5×10^{-7} m^3/J.mol
	Critical value for radiolytic gas concentration	20 mol/m^3
Gas bubble velocity	New model (continuous velocity) $\nu = \nu_o + sign(\omega)\nu_g \ln(1 + \lvert\omega\rvert)$ ω = reactor period (s)	ν_o = 0.01 m/s ν_g = 0.07 m/s
Thermal-hydraulics	Fuel solution region: 2-D cylindrical conduction Mixing parameter	1.0 s^{-1}
	Vessel/tank region: Natural circulation at the inner side and bottom walls (lumped parameters)	Heat transfer coefficients are internally calculated in the code
	Surrounding air region: Natural circulation at the outer side and bottom walls	Heat transfer coefficients are internally calculated in the code
Motion	Axial direction motion equation (lumped parameter) Momentum dissipation coefficient	2 600 m/s^2

Table 10.4.2: Kinetic parameters for SILENE benchmark calculations

Parameter	SILENE experiments
Delayed neutron fractions	2.6827E-04
	1.6910E-03
	1.5374E-03
	3.0730E-03
	9.0075E-04
	3.2855E-04
Precursor decay constant (1/s)	1.2700E-02
	3.1700E-02
	1.1500E-01
	3.1100E-01
	1.4000E+00
	3.8700E+00
Generation time (s)	3.4642E-05
Prompt neutron lifetime (s)	3.3428E-05

Table 10.4.3: Temperature and void reactivity feedbacks for SILENE benchmark calculations

Reactivity feedback ($)	SILENE experiments
Temperature variation (ΔT, Kelvin)	$\Delta\rho(\Delta T) = 1.0 \times 10^{-4}\ \Delta T^2 - 0.034\Delta T$
Void (V, % volume)	$\Delta\rho(V) = -0.0034V^2 - 0.6757V$

S2-300

The calculated and measured power transients for S2-300 are displayed in Figures 10.4.4 to 10.4.6 and show reasonable agreement with experiment. The qualitative behaviour is reproduced reasonably well, but there are disagreements of more than a factor of four between some of the calculated and measured parameters. In particular the first peak power is underestimated by a factor of almost three and energy to the first peak is underestimated by a factor of almost four. The total energy is underestimated by one-third and yet the temperature rise is overestimated by a factor of nearly 2.5. This suggests that the heat capacity of the fissile solution has been underestimated by a factor of about 3.7. In this case radiolytic gas release is predicted to occur after the first power peak, but sooner than observed. The calculation does not reproduce the observed oscillatory behaviour.

S3-300

The calculated and measured power transients for S3-300 are displayed in Figures 10.4.7 to 10.4.9 and show reasonable agreement with experiment. The qualitative behaviour is reproduced reasonably well, but there are disagreements of more than a factor of 2.5 between some of the calculated and measured parameters. The time to the first peak is actually underestimated by a factor of seven, but this is due to the difficulty in choosing appropriate initial conditions (neutron density/power and delayed neutron precursor concentrations) for a test without an external neutron source and is not expected to have a significant effect on the other predicted parameters. The first power peak is underestimated by a factor of 2.5 and the energy to the first peak is underestimated by a factor of 2. The total energy is underestimated by nearly one-fifth and yet the temperature rise is overestimated by a factor of over 2.5. This suggests that the heat capacity of the fissile solution has been underestimated by a factor of about 3.3. In this case radiolytic gas release is predicted to occur almost coincidently with the first power peak, in agreement with the observed behaviour. The calculation does not reproduce the observed oscillatory behaviour.

10.4.3 Conclusions

The TRACE calculations are in reasonable qualitative agreement with the observed experimental behaviour, with the exception of not reproducing the oscillatory behaviour observed in tests S2-300 and S3-300. However, the calculations significantly underestimate the peak power by a factor of between two and three and the total energy generated by between 19% and 38%. Despite this, the temperature rise is overestimated by a factor of between 2.15 and 2.66. This suggests that the heat capacity of the fissile solution is too low by a factor of about 3.5 in the TRACE calculations. This will enhance the feedback effect of temperature on the reactivity, as a given energy release will raise the temperature 3.5 times more in the calculation than it does in the experiment. This will result in a greater reduction in reactivity in the calculation than in the experiment and thus underestimates in the predicted powers and energies.

Figure 10.4.1: TRACE – S1-300 power history – first 250 s

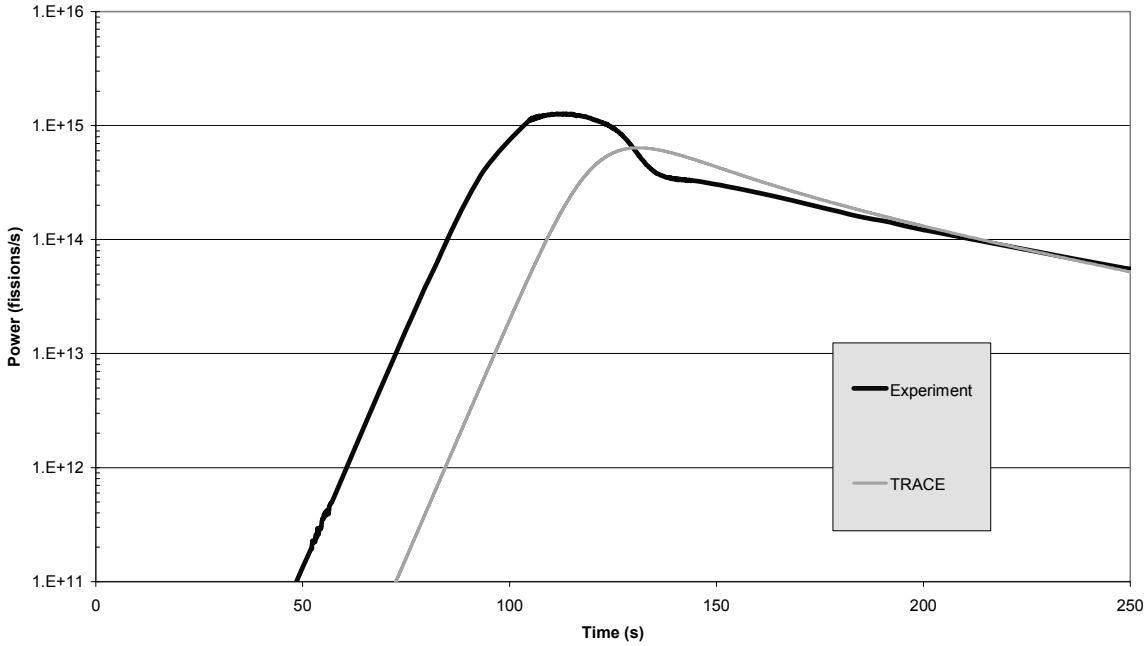

Figure 10.4.2: TRACE – S1-300 power history – whole profile

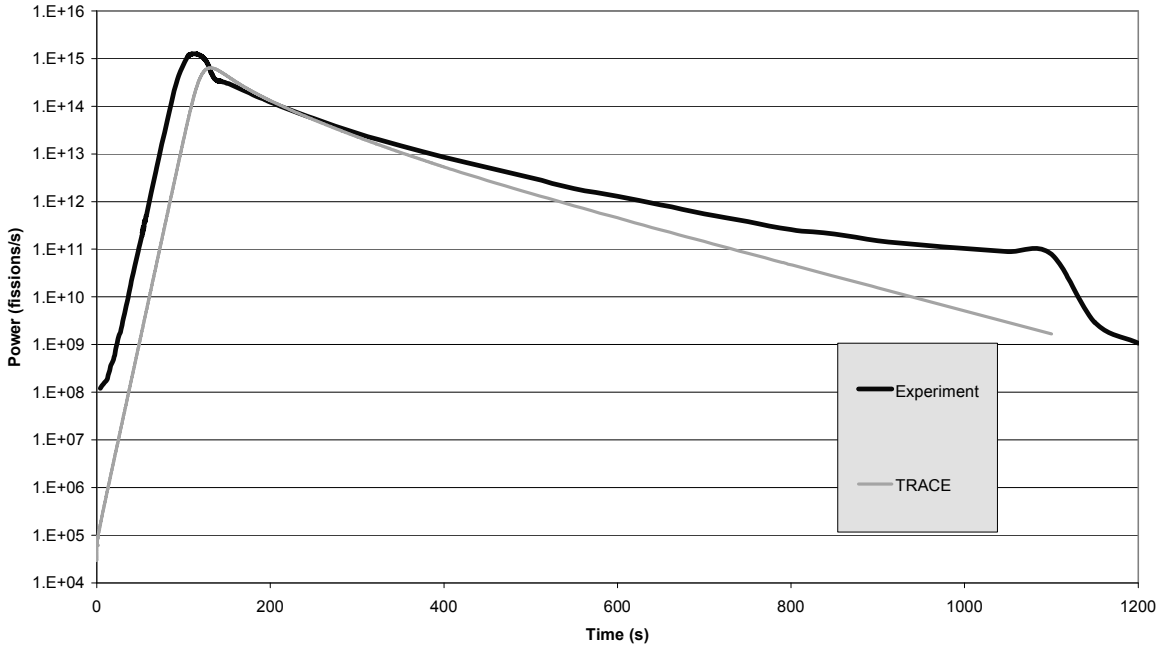

Figure 10.4.3: TRACE – S1-300 energy history – whole profile

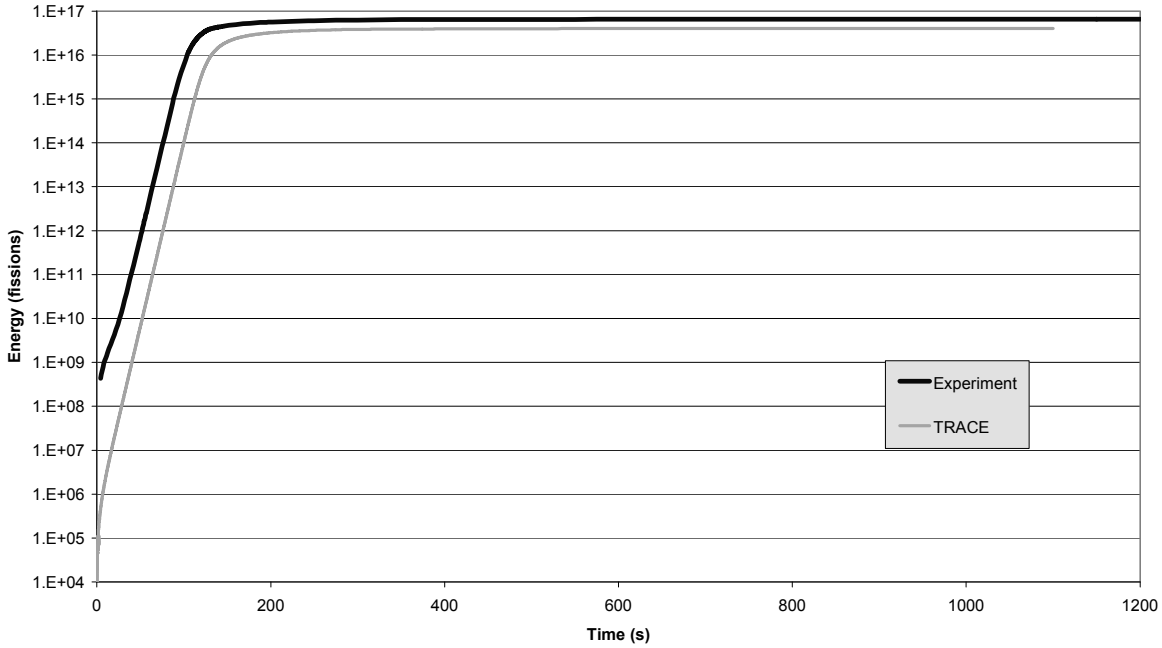

Figure 10.4.4: TRACE – S2-300 power history – first 30 s

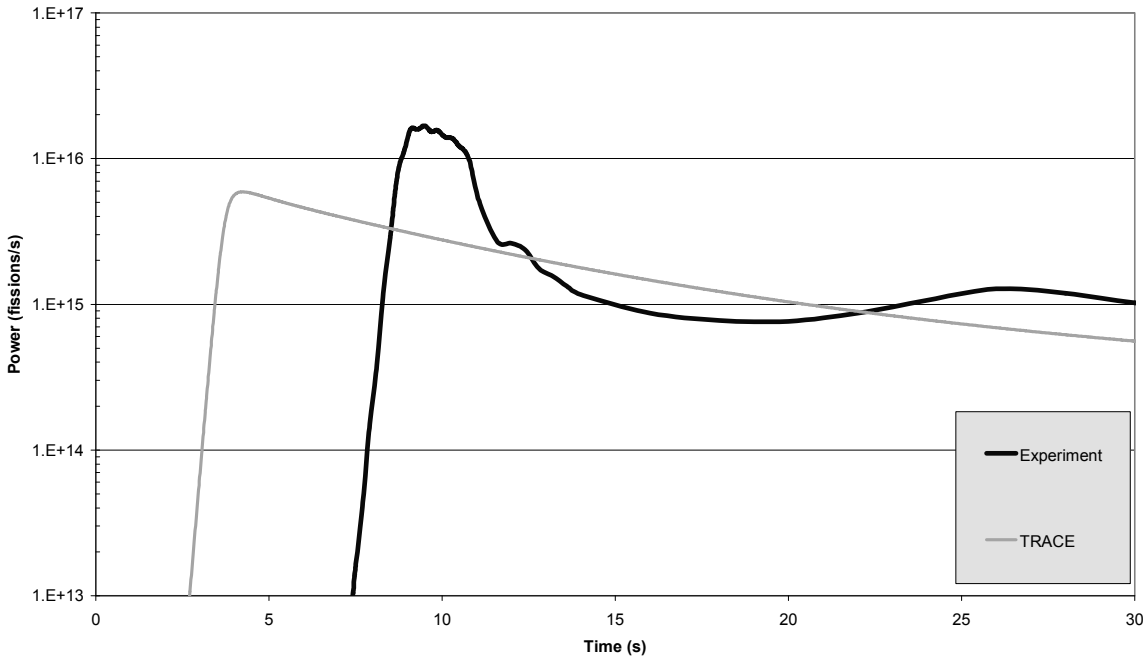

Figure 10.4.5: TRACE – S2-300 power history – whole profile

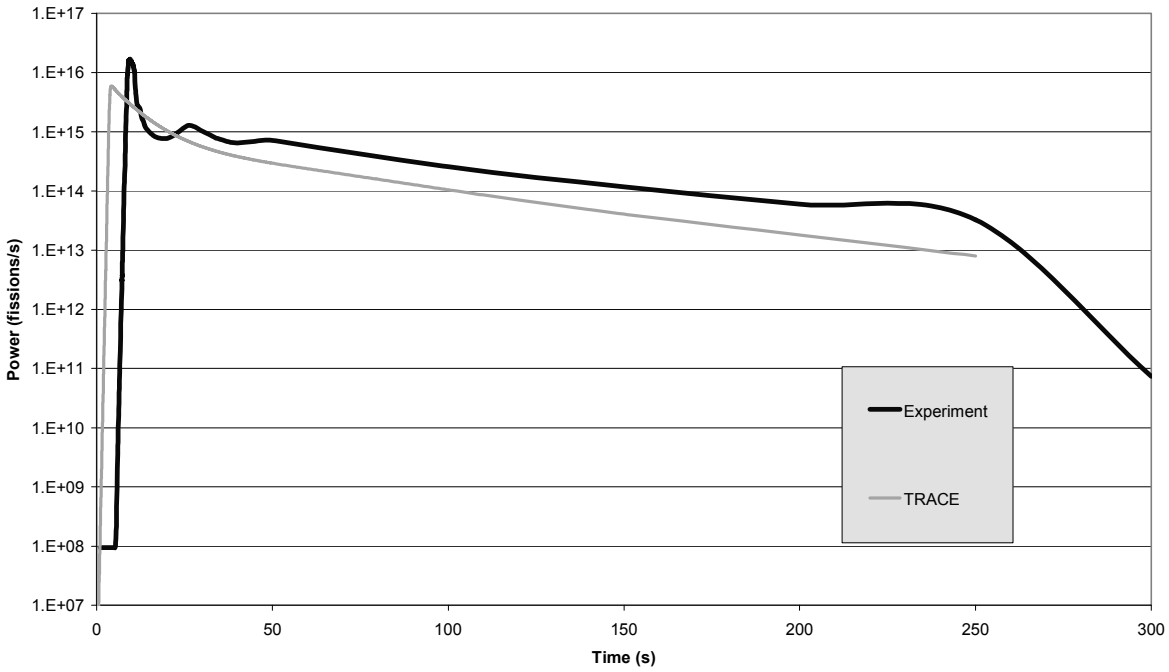

Figure 10.4.6: TRACE – S2-300 energy history – whole profile

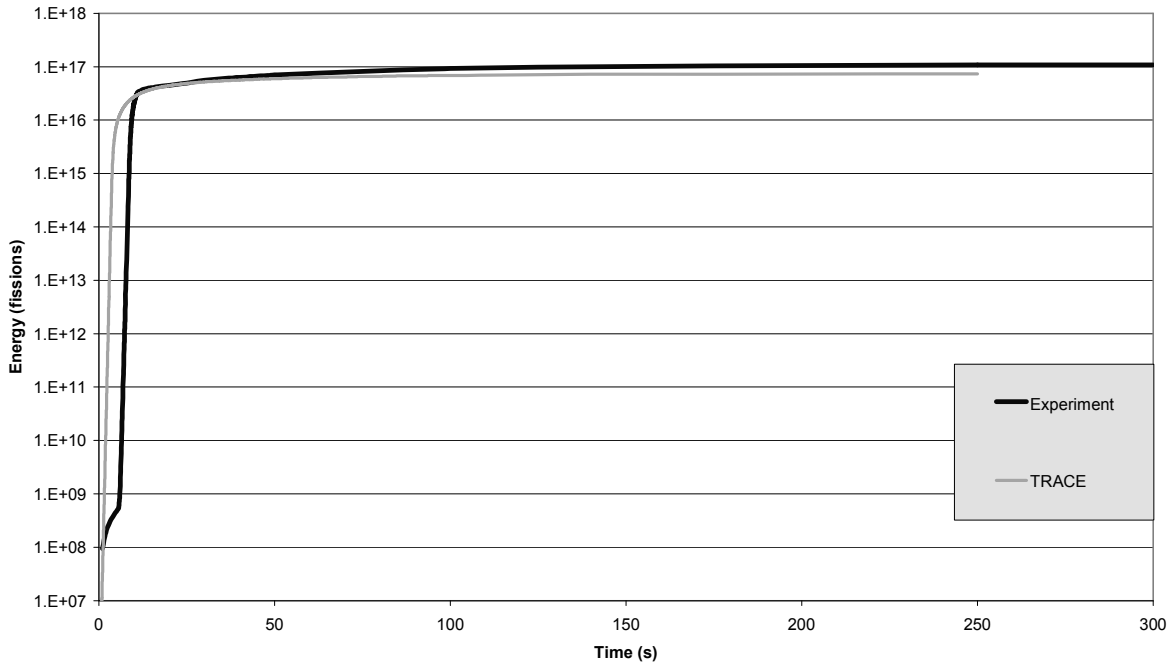

Figure 10.4.7: TRACE – S3-300 power history – first 5 s

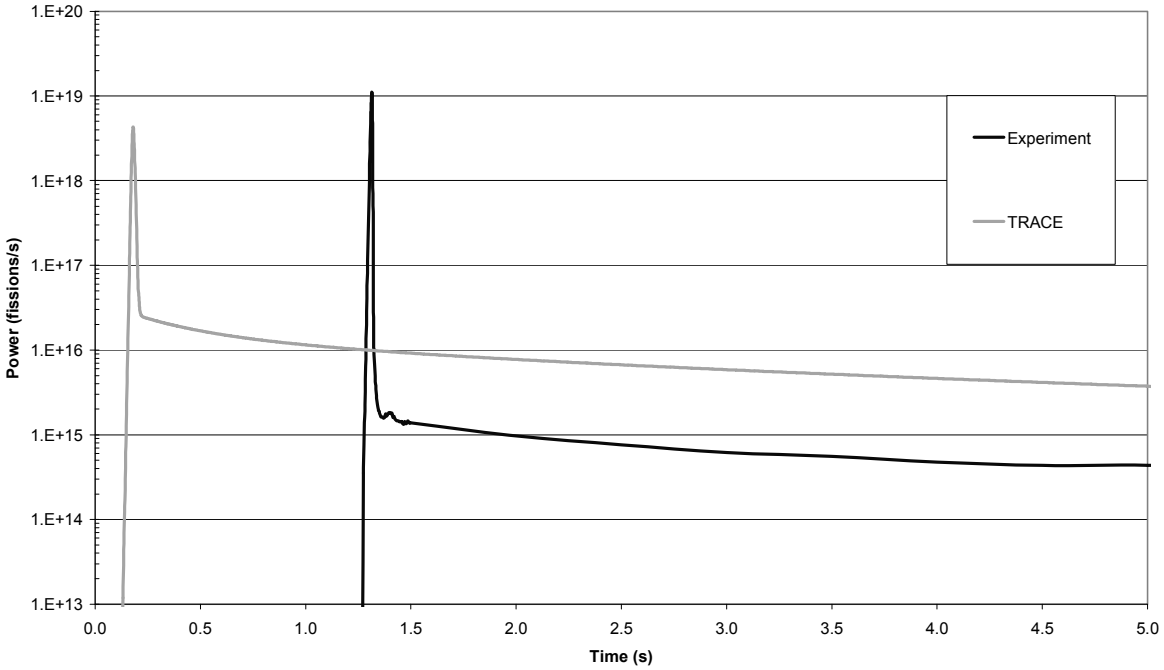

Figure 10.4.8: TRACE – S3-300 energy history – whole profile

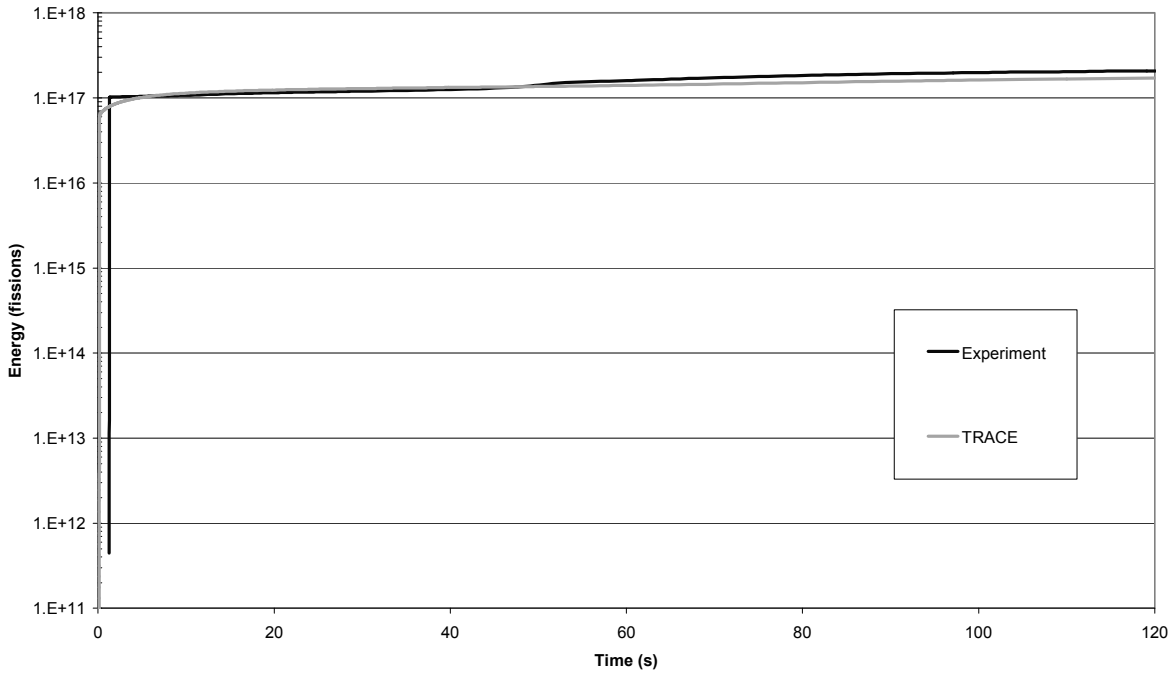

Figure 10.4.9: TRACE – S3-300 power history – whole profile

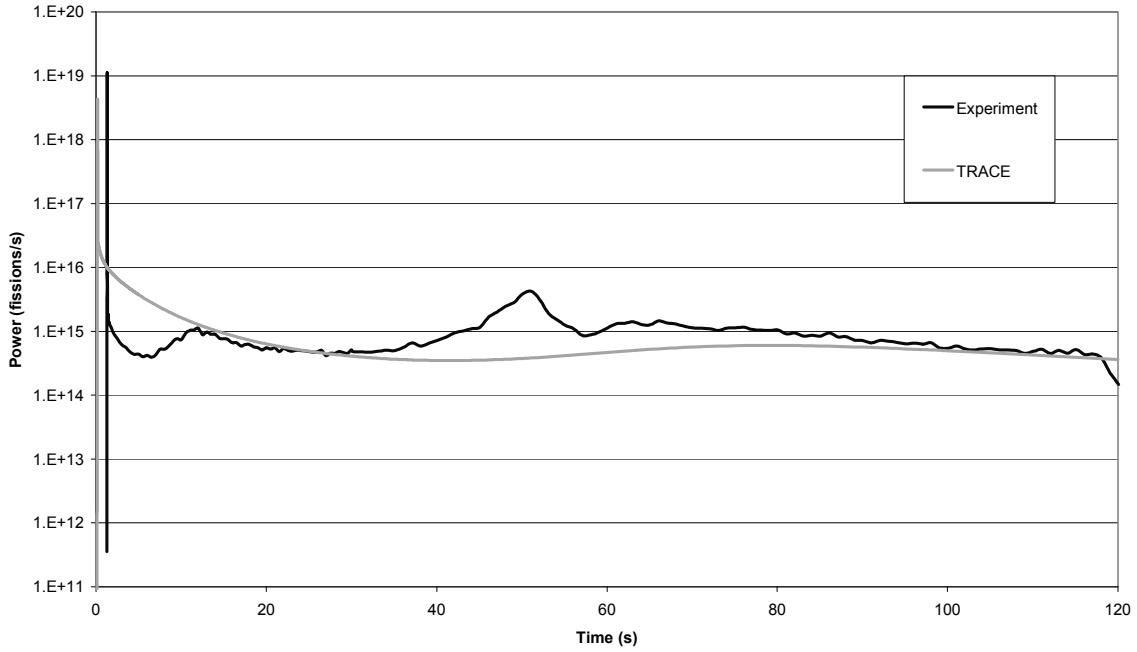

10.5 Summary

The comparison of the code benchmark calculations with the experimental measurements is summarised in Tables 10.5.1 to 10.5.3 and Figures 10.5.1 to 10.5.6.

S1-300

Table 10.5.1 summarises the results for S1-300. Each code reproduces the whole power profile quite well. The calculated maximum inverse periods mostly agree with the experimental value to within 1 to 6%. The estimated time to the power peak is accurate to within 32% in all cases (note that errors in this parameter are not expected to have a significant effect on the other calculated parameters). The calculated peak power and energy to the peak agree with the measured values to within 19% and the total energy and the temperature rise agree within 30% for all codes except TRACE. The TRACE calculation underestimates the power and energies by a factor of roughly two and overestimates the temperature rise by a factor of over two. This is believed to be due to an error in the value of the heat capacity of the fissile solution used in the TRACE calculation. All of the codes predict radiolytic gas release to occur slightly after the peak power is reached, in agreement with observation, except the TRACE calculation which predicts that it occurs slightly before the power peak.

S2-300

Table 10.5.2 summarises the results for S2-300. All of the calculations agree with the measured maximum inverse period, maximum power, energy to the first peak, total energy and temperature rise to within 32%, except the TRACE calculation. There are much bigger differences between the TRACE calculation and the measured values of these parameters. This is believed to be due to an error in the value of the heat capacity of the fissile solution used in the TRACE calculation. There are discrepancies of up to a factor of three in the predicted time of the first power peak. This is due to the difficulty in deriving appropriate initial conditions for the calculations for an experiment without an external neutron source. This discrepancy is not expected to have a significant effect on the other calculated parameters. All of the codes predict that radiolytic gas release occurs shortly after the first power peak, in agreement with observation.

Only the AGNES calculation exhibited oscillatory behaviour in this test, in line with the observed behaviour.

S3-300

Table 10.5.3 summarises the results for S3-300. All of the calculations agree with the measured maximum inverse period, peak power, energy to the first peak, total energy and temperature rise to within 26%, except the TRACE calculation. There are much bigger differences between the TRACE calculation and the measured values of these parameters. This is believed to be due to an error in the value of the heat capacity of the fissile solution used in the TRACE calculation. There are discrepancies of up to a factor of seven in the predicted time of the first power peak. This is due to the difficulty in deriving appropriate initial conditions for the calculations for an experiment without an external neutron source. This discrepancy is not expected to have a significant effect on the other calculated parameters. All of the codes predict that radiolytic gas release is coincident with the first power peak, in agreement with observation.

The AGNES, CRITEX and INCTAC calculations all exhibit some form of oscillatory behaviour in this test, in line with the observed behaviour.

10.5.1 General observations

Graphical comparison of the ratio between calculation and experimental results, C/E, for the maximum inverse period, time to the first power peak, first peak power, fission to the first power peak, total fission and final temperature are shown in Figures 10.5.1 to 10.5.6, respectively.

The maximum inverse time periods are compared in Figure 10.5.1. The calculated values for this parameter are generally in good agreement with experiment, *i.e.* accurate to within roughly 20%. The only significant exceptions are:

- TRACE underestimates the time by an order of magnitude for S1-300. This is thought to be due to an error in reporting the result.
- INCTAC overestimates the time by more than 30% for S2-300.

The first peak powers are compared in Figure 10.5.2. Again the calculated values generally agree with experiment to within roughly 20%. The significant exceptions are:

- TRACE underestimates the first peak power by roughly 60% in all three tests. This is believed to be due to an error in the value of the heat capacity of the fissile solution used in the TRACE calculation.
- INCTAC overestimates the power by over 30% in S2-300.

The times to the first peak powers are compared in Figure 10.5.3. For the S1-300 experiment, which had an external neutron source, calculated values agree with experiment to within about 30%. For tests S2-300 and S3-300, which did not have an external neutron source, the agreement is not so good; the time to the first peak is underestimated by between roughly 40% and 90%. This is due to the difficulty in deriving appropriate initial conditions for the calculations for an experiment without an external neutron source. This discrepancy is not expected to have a significant effect on the other calculated parameters.

The fissions to the first peak are compared in Figure 10.5.4. The calculated values generally agree with experiment to within roughly 20%. The significant exceptions are:

- TRACE underestimates the fissions to the first power peak by roughly 60% in all three tests. This is believed to be due to an error in the value of the heat capacity of the fissile solution used in the TRACE calculation.
- AGNES underestimates the fissions to the first power peak by 30% for S2-300.

The total fissions are compared in Figure 10.5.5. The calculated values generally agree with experiment to within 25%. The only exceptions are the TRACE calculations for S1-300 and S2-300, which underestimate the total fissions by roughly 35%. This is believed to be due to an error in the value of the heat capacity of the fissile solution used in the TRACE calculation.

The final temperatures are compared in Figure 10.5.6. The calculated values generally agree with experiment to within -8% to +17%. The only exceptions are the TRACE calculations which overestimate the temperature rise by a factor of roughly 2.5. This is believed to be due to an error in the value of the heat capacity of the fissile solution used in the TRACE calculation.

10.5.2 Conclusions

The codes generally simulate the major features of the TRACY criticality transients well. The calculated values mostly agree with the measured parameters to within about 20%. There are two significant exceptions to this quantitative behaviour:

- The TRACE calculations exhibit much larger discrepancies. This is believed to be due to an error in the value of the heat capacity of the fissile solution used in the TRACE calculation.
- For tests S2-300 and S3-300, which did not have an external neutron source, the time to the first peak is underestimated by between roughly 40% and 90%. This is due to the difficulty in deriving appropriate initial conditions for the calculations for an experiment without an external neutron source. This discrepancy is not expected to have a significant effect on the other calculated parameters.

A feature that is inconsistently reproduced by the calculations is the oscillatory behaviour that is observed in S1-300 and S2-300. Only one calculation predicts oscillations in S2-300 and three of the four calculations predict oscillations in S3-300. The magnitude, period and number of the oscillations often differ significantly from the observed values. The small-scale, short-period oscillations superimposed on the large-scale oscillations in S3-300 are are not reproduced in any of the calculations.

Table 10.5.1: S1-300 summary

	Units	Experimental data	AGNES	Calc./Exp.	CRITEX	Calc./Exp.	INCTAC	Calc./Exp.	TRACE	Calc./Exp.
Max. inverse period	(s-1)	0.182	0.18	0.99	0.181	0.99	0.193	1.06	2.20E-02	0.12
First peak power	(fissions/s)	1.30E+15	1.23E+15	0.95	1.51E+15	1.16	1.46E+15	1.12	6.41E+14	0.49
	(W)	4.17E+04	3.94E+04		4.84E+04		4.68E+04		2.05E+04	
Energy to the first peak	(fissions)	2.20E+16	1.79E+16	0.81	2.30E+16	1.05	1.97E+16	0.90	9.53E+15	0.43
	(J)	7.05E+05	5.74E+05		7.37E+05		6.32E+05		3.05E+05	
First peak time	(s)	110	145.7	1.32	115.9	1.05	89.27	0.81	131.1	1.19
Total energy	(fissions)	6.50E+16	8.21E+16	1.26	7.18E+16	1.10	5.58E+16	0.86	4.00E+16	0.62
	(J)	2.08E+06	2.63E+06		2.30E+06		1.79E+06		1.28E+06	
Final temperature	(°C)	35.9	40	1.11	34	0.95	36.07	1.00	51.7	1.44
Gas release time	(s)	132.5	156.8	1.18	119.9	0.90	91.27	0.69	121.3	0.92

Table 10.5.2: S2-300 summary

	Units	Experimental data	AGNES	Calc./Exp.	CRITEX	Calc./Exp.	INCTAC	Calc./Exp.	TRACE	Calc./Exp.
Max. inverse period	(s-1)	5.3	6.06	1.14	5.39	1.02	7.00	1.32	6.5	1.23
First peak power	(fissions/s)	1.70E+16	1.65E+16	0.97	1.48E+16	0.87	2.24E+16	1.32	5.91E+15	0.35
	(W)	5.45E+05	5.29E+05		4.74E+05		7.19E+05		1.89E+05	
Energy to the first peak	(fissions)	1.30E+16	9.09E+15	0.70	1.61E+16	1.24	1.01E+16	0.78	3.50E+15	0.27
	(J)	4.17E+05	2.91E+05		5.16E+05		3.24E+05		1.12E+05	
First peak time	(s)	9.5	4.8	0.51	6.25	0.66	2.73	0.29	4.2	0.44
Total energy	(fissions)	1.10E+17	1.32E+17	1.20	1.01E+17	0.92	8.24E+16	0.75	7.41E+16	0.67
	(J)	3.53E+06	4.23E+06		3.24E+06		2.64E+06		2.37E+06	
Final temperature	(°C)	43.8	50.1	1.14	40.4	0.92	42.33	0.97	75.6	1.73
Gas release time	(s)	10.5	6.4	0.61	7.12	0.68	3.37	0.32	4.3	0.41

Table 10.5.3: S3-300 summary

	Units	Experimental data	AGNES	Calc./Exp.	CRITEX	Calc./Exp.	INCTAC	Calc./Exp.	TRACE	Calc./Exp.
Max. inverse period	(s-1)	285	312.23	1.10	245	0.86	287.6	1.01	293.3	1.03
First peak power	(fissions/s)	1.10E+19	1.34E+19	1.22	9.60E+18	0.87	9.87E+18	0.90	4.28E+18	0.39
	(W)	3.53E+08	4.29E+08		3.08E+08		3.16E+08		1.37E+08	
Energy to the first peak	(fissions)	6.60E+16	7.21E+16	1.09	6.41E+16	0.97	6.20E+16	0.94	3.16E+16	0.48
	(J)	2.12E+06	2.31E+06		2.05E+06		1.99E+06		1.01E+06	
First peak time	(s)	1.31	0.21	0.16	0.47	0.36	0.124	0.09	0.18	0.14
Total energy	(fissions)	2.10E+17	2.49E+17	1.19	2.01E+17	0.96	1.73E+17	0.82	1.71E+17	0.81
	(J)	6.73E+06	7.98E+06		6.44E+06		5.55E+06		5.47E+06	
Final temperature	(°C)	62.2	72.6	1.17	57	0.92	62.16	1.00	128.3	2.06
Gas release time	(s)	1.31	0.21	0.16	0.47	0.36	0.12	0.09	0.17	0.13

Figure 10.5.1: Maximum inverse period – calculation/experiment ratio

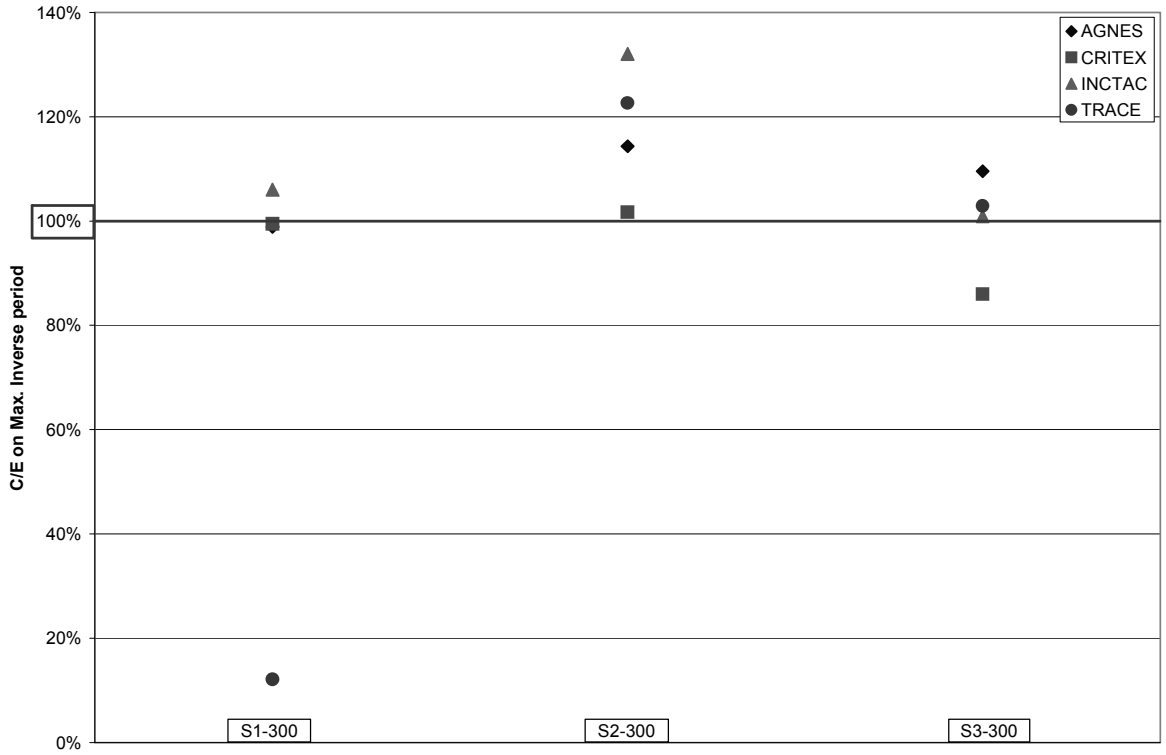

Figure 10.5.2: First peak power – calculation/experiment ratio

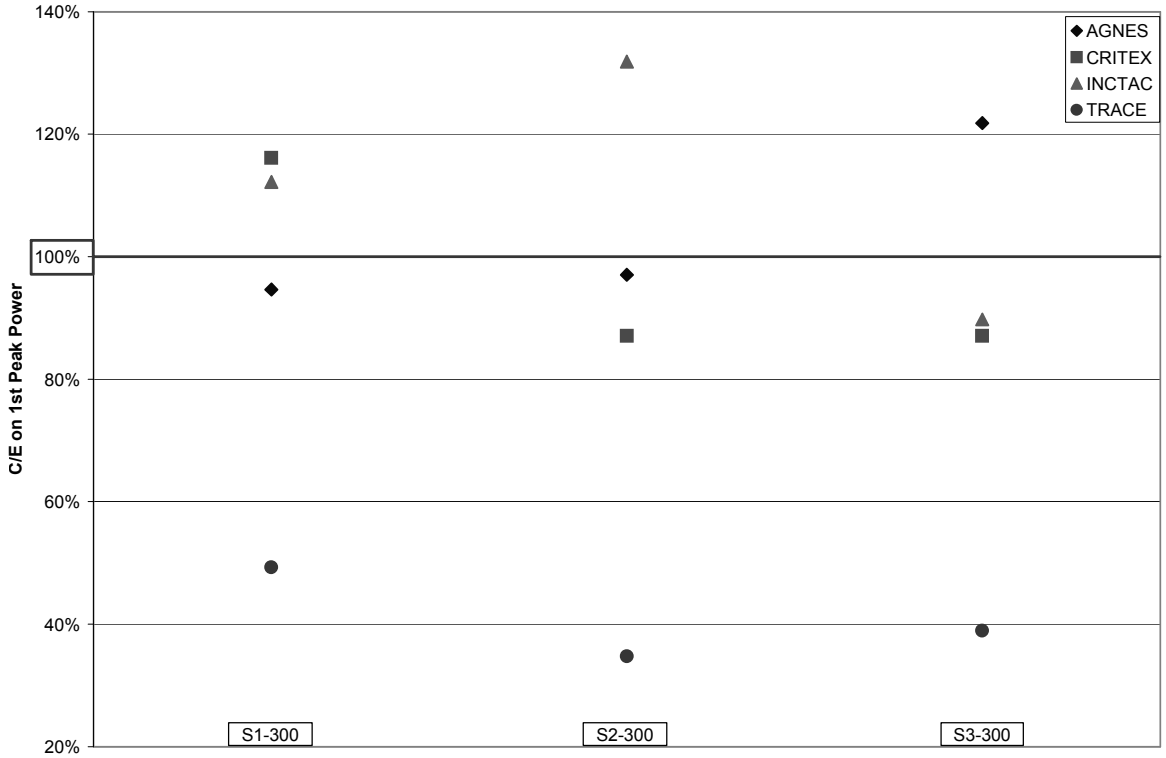

Figure 10.5.3: First peak time – calculation/experiment ratio

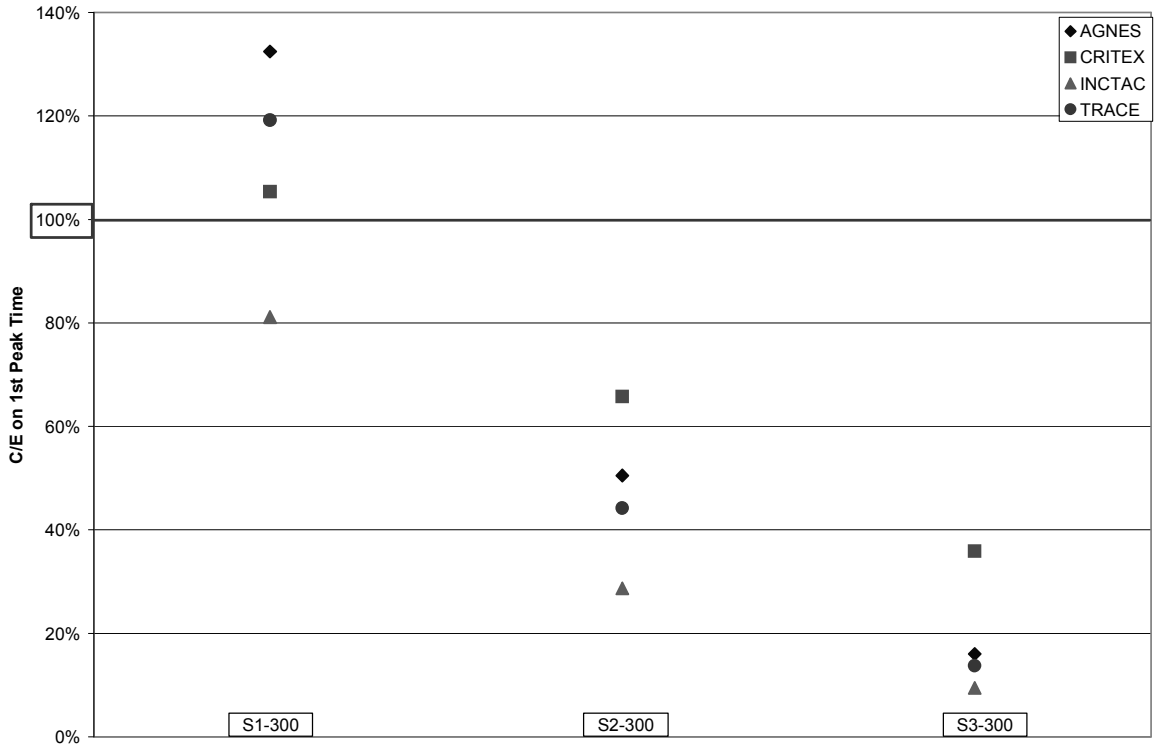

Figure 10.5.4: Energy at first peak – calculation/experiment ratio

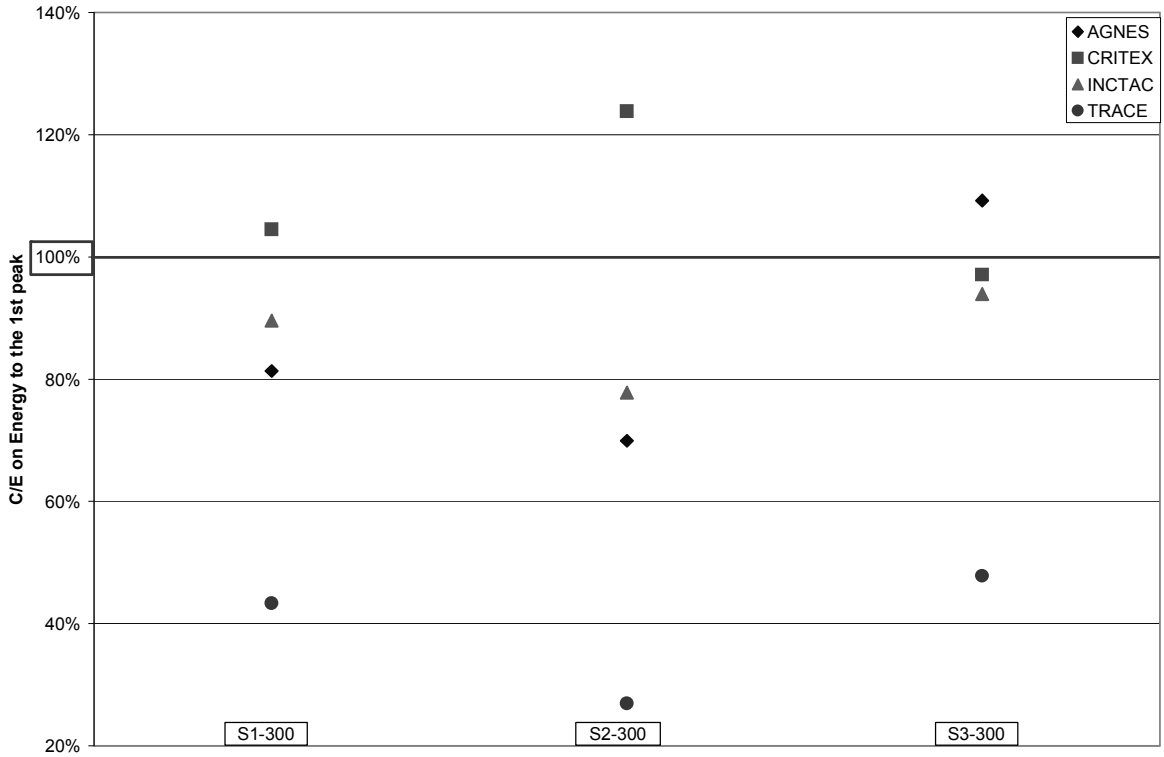

Figure 10.5.5: Total fission yield – calculation/experiment ratio

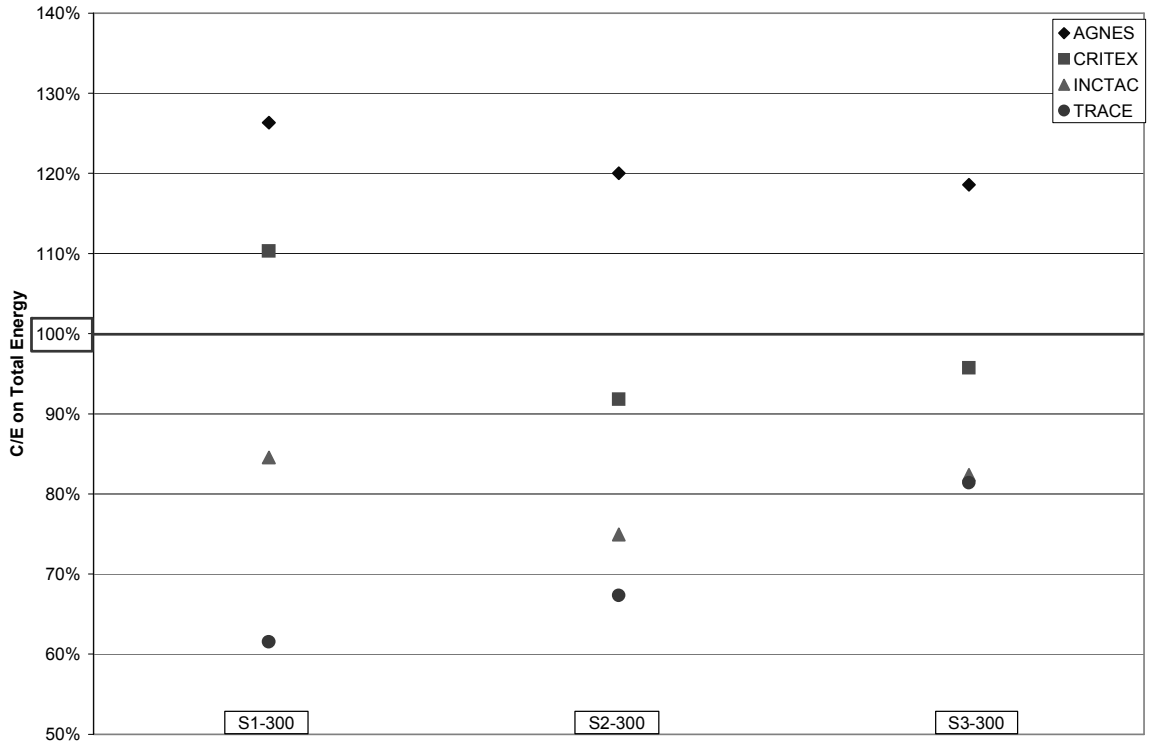

Figure 10.5.6: Final temperature – calculation/experiment ratio

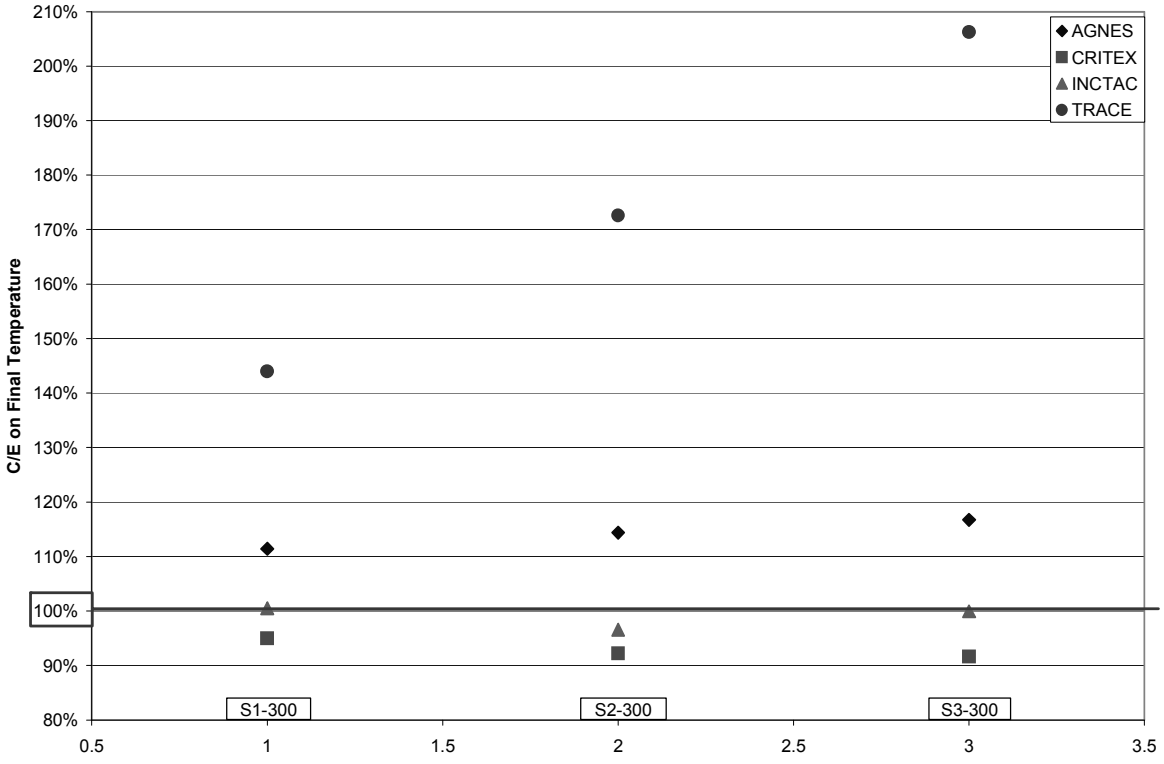

Chapter 11: Conclusions

The TRACY and SILENE experiments are a valuable source of information on criticality transients in fissile solutions, both for understanding the progression of such transients and for validating models of transient criticality. This report provides data on a total of eight tests in the TRACY and SILENE facilities, in a form which is useful for model validation. The five tests reported in the TRACY facility contain low-enriched uranium and the three in SILENE used high-enriched uranium. In all cases the transient is initiated by a sudden insertion of reactivity produced by the rapid withdrawal of the control rod from the centre of the fissile solution, the so-called pulse mode of operation. After operating for the desired period the tests are terminated by the reinsertion of the control rod. The series reported contain a mixture of four delayed-critical tests and four prompt-critical tests. The data provided for the tests include: maximum inverse time period; time to the first power peak; the (first) peak power; energy released or number of fissions before the first peak is reached; total energy released or total number of fissions; temperature rise at the end of the test; maximum pressure or time of gas release.

In all cases the reactivity insertion results in a power rise in the reactor to an initial peak, after which it reduces, tending to a lower, long-term value. In some cases power oscillations are observed, *i.e.* additional smaller peaks in the power after the large initial peak. The generation of energy raises the temperature of the fissile solution, which has a negative feedback effect on the reactivity. The radiation field also generates radiolytic gas in solution in the fissile liquid. If the concentration of dissolved gas exceeds the saturation concentration by a sufficient margin, it nucleates to form bubbles in the solution. The resulting expansion of the solution also has a negative feedback effect on the reactivity. The onset of bubble nucleation is referred to as gas release and raises the pressure of the fissile solution. In the long term the reactor tends to a configuration in which the negative feedbacks from the temperature rise and radiolytic gas release (if present) negate the excess reactivity inserted by the withdrawal of the control rod.

Benchmark calculations from four transient criticality codes (AGNES, CRITEX, INCTAC and TRACE) are compared with the experimental results. The codes generally simulate the major features of the criticality transients well, *i.e.* the power rise to an initial peak after which it falls towards a long-term lower value; the rise in temperature associated with the power generation; the time of gas release or the maximum pressure associated with the gas release. The calculated values mostly agree with the measured parameters to within roughly 20%. Significantly larger discrepancies occur in some cases; many of these are understood and result from a poor choice of value for one or more input parameters. In particular, for tests that were initialised in a subcritical condition (*i.e.* with no specified initial power) and had no external neutron source, some of the calculations significantly underestimate the time of the first power peak. This is due to the difficulty in specifying appropriate initial conditions (power and delayed neutron precursor concentrations) for calculations of initially subcritical experiments without an external neutron source. The resulting inaccuracies in the estimated time to the first peak are not thought to have a significant impact on the other calculated parameters associated with the first peak (maximum inverse period, peak power or energy to the first peak). In addition one set of code calculations exhibits significant discrepancies with many of the measurements for the SILENE experiments. This is believed to be due to an error in the value of the heat capacity of the fissile solution used in these calculations. It has been shown that small adjustments to the reactivity insertion can produce overall improvements in the predicted behaviour to the first power peak (*i.e.* to the inverse period, peak power and energy released to the first peak), while having little effect on the total energy.

A feature that is inconsistently reproduced by the calculations is the oscillatory behaviour that is observed in six of the eight experiments analysed. However, each of the participating codes predicts oscillatory behaviour in at least one of the experiments, though the predicted magnitude, period and

number of the oscillations often differ significantly from the observed values. When the calculations fail to predict the observed oscillations they still tend to reproduce the underlying average behaviour quite well.

The experiments analysed in this study provide important validation and benchmarking of the participating codes for short duration criticality transients in fissile LEU and HEU solutions with step reactivity insertions. However, criticality accidents can be initiated by the addition of fissile material to the system, for example the JCO accident at Toki-Mura; therefore it is important to validate the transient criticality codes for this mode of reactivity insertion. For longer duration transients, heat loss to the surroundings becomes a controlling process, which requires additional validation. Therefore, for future exercises, consideration should be given to benchmarking codes against TRACY and SILENE experiments using the ramp-feed mode of reactivity insertion (*i.e.* by feeding additional fissile solution into the reactor) and tests of longer duration.

References

Alcouffe, R., *et al.* (1995), *DANTSYS: A Diffusion Accelerated Neutral Particle Transport Code System*, Los Alamos National Laboratory, LA-12969-M.

Barbry, F. and J.P. Rozain (1989), *Objectives and Summary of Experiments on the Formation of Radiolysis Gas Carried Out Using the SILENE Reactor*, Technical Report, SRSC 89-08.

Basoglu, B., *et al.* (1998), *Development of a New Simulation Code for Evaluation of Criticality Transients Involving Fissile Solution Boiling*, JAERI-Data/Code 98-011.

CEA/DAM (2002), *Sélection d'Expériences SILENE de Référence pour la Qualification des Codes d'Accidents de Criticité*, Technical Report, SRNC 02-06.

CEA/DAM (2006), *SILENE Pulsed Experiments*, *SILENE-HEU-SOL-STEP S1-300/S2-300/S3-300*, available at: www.nea.fr/html/science/wpncs/excursions/benchmarks/silene_step_specifications.pdf since August.

Dunenfeld, M. and R. Stitt (1963), *Summary Review of the Kinetic Experiments on Water Boilers*, NAA-SR-7087.

Grivot, L. and L. Reverdy (2004), *Criticality Accident in a Fissile Solution Pulse-type Benchmarks. Selected Pulse Experiments Performed in SILENE and TRACY. CRITEX Code Qualification*, Technical Report, SRNC 04-12.

Hong, P. (2005), "TRACY and SILENE Benchmark Calculations by TRACE Code", TRACE Summary (Phase 1) rev1 in Microsoft Excel File and "Power, Energy and Temperature of SILENE S1-300, S2-300 & S3-300 Benchmarks Calculated by TRACE", LIEM (NAIS), February.

Lécorché, P., *et al.* (1973), *A Review of the Experiments Performed to Determine the Radiological Consequences of a Criticality Accident*, Y-CDC-12.

Mather, D.J., *et al.* (1984), *CRITEX – A Computer Program to Calculate Criticality Excursions in Fissile Liquid Systems*, SRD R 380.

Mitake, S., *et al.* (2003), "Development of INCTAC Code for Analyzing Criticality Accident Phenomena", *Proc. 7th International Conference on Nuclear Criticality Safety (ICNC2003)*, JAERI-Conf 2003-019.

Mitake, S. (2005), *Criticality Excursion Analysis Benchmarks – Results with INCTAC Code*, JNES.

Nakagawa, T., *et al.* (1995), "Japanese Evaluated Nuclear Data Library Version 3 Revision-2: JENDL-3.2", *J. Nucl. Sci. Technol.*, 32, 1259.

Nakajima, K., *et al.* (2002a), *A Kinetics Code for Criticality Accident Analysis of Fissile Solution Systems: AGNES2*, JAERI-Data/Code 2002-004.

Nakajima, K., *et al.* (2002b), *TRACY Transient Experiment Databook: 1) Pulse Withdrawal Experiment*, JAERI-Data/Code 2002-005.

Nakajima, K., *et al.* (2002c), *TRACY Transient Experiment Databook: 2) Ramp Withdrawal Experiment*, JAERI-Data/Code 2002-006.

Nakajima, K., *et al.* (2002d), *TRACY Transient Experiment Databook: 3) Ramp Feed Experiment*, JAERI-Data/Code 2002-007.

Okamura, K., *et al.* (1996), *SRAC95; General Purpose Neutronics Code System*, JAERI-Data/Code 96-015.

Sakurai, S. and S. Tachimori (1996), "Density Equation of Aqueous Solution Containing Plutonium (IV), Uranium (VI) and Nitric Acid", *J. Nucl. Sci. Technol.*, 33, 187.

Wilson, W.B., *et al.* (2002), SOURCES 4C: A Code for Calculating (a,n), Spontaneous Fission, and Delayed Neutron Source and Spectra, Los Alamos National Laboratory, LA-UR-02-1617.

Yamane, Y., *et al.* (2003), "Transient Characteristics Observed in TRACY Supercritical Experiments", *Proc. 7th International Conference on Nuclear Criticality Safety (ICNC2003)*, JAERI-Conf 2003-019 (2003).

Yamane, Y. (2005), *The Result of the Analysis of SILENE Benchmark 1 by Using AGNES Code*, JAERI, August.

Appendix A: Description of transient progression

A.1 The initial state

The reactor begins with the absorber rod fully inserted and therefore in a subcritical condition. In some cases the rod is partially withdrawn and the reactor operated at a specified power for a period prior to the commencement of the test.

If the reactor is left to stand for sufficient time with the absorber rod inserted, or partially inserted, the delayed neutron precursors will reach their equilibrium concentrations. Typical decay constants and the equivalent half-lives for a six delayed neutron group scheme are displayed in Table A.1. The half-life of the longest-lived group is almost a minute. Therefore, if the system is left at constant power for an order of ten minutes the delayed neutron precursors will have time to reach their equilibrium concentrations.

Table A.1: Decay constants and half-lives of delayed neutrons

Group	Decay constant (s-1)	Half-life (s)
1	0.0127	54.6
2	0.0317	21.9
3	0.115	6.03
4	0.312	2.22
5	1.40	0.495
6	3.87	0.179

The point kinetics equations relate the neutron concentration, n, (m^{-3}) reactivity, ρ, and the concentrations of the delayed neutron precursor groups, C_i (m^{-3}):

$$\frac{dn}{dt} = \frac{\rho - \beta}{\Lambda} n + \sum_{i=1}^{6} \lambda_i C_i + S$$
$$\frac{dC_i}{dt} = \frac{\beta_i}{\Lambda} n - \lambda_i C_i \qquad \text{(A.1)}$$

where: β = delayed neutron fraction = $\sum_i \beta_i$

β_i = delayed neutron fraction of the i^{th} group

λ_i = decay constant of the i^{th} group (s^{-1})

Λ = neutron generation time (s)

When the system is left to reach a steady state, the time derivatives in the equations approach zero and thus the initial equilibrium concentrations of the delayed neutron precursors, C_{0i}, are related to the initial neutron concentration, n_0, by:

$$C_{0i} = \frac{\beta_i n_0}{\lambda_i \Lambda} \qquad \text{(A.2)}$$

The initial neutron concentration is, in turn, determined by the source and the reactivity before the absorber rod is withdrawn, ρ_0 for a subcritical system, or by the initial power, P_0, for a critical system:

$$\begin{aligned} n_0 &= \frac{\Lambda S}{-\rho_0}: && \textit{initially subcritical} \\ n_0 &= \frac{P_0}{\upsilon_{av}\Sigma_f}: && \textit{specific initial power} \end{aligned} \tag{A.3}$$

Here υ_{av} is the average neutron speed and Σ_f is the macroscopic fission cross-section. Note the ρ_0 is negative when the system is subcritical with the absorber rod inserted. Hence Eq. (A.3) provides a positive value for the initial neutron concentration, as required. If an external neutron source is used in the experiment, it will determine the initial the source required for Eq. (A.3). If no external neutron source is provided, the initial source is provided by spontaneous fission of uranium isotopes.

Note that the time scale for the reactivity insertion is the time taken to withdraw the absorber rod, which is approximately 0.15 s. This is comparable with the half-life of precursor group 6 and fast compared to the half-lives for the other groups. Therefore the delayed neutron precursors will not be at their equilibrium concentrations at the end of the reactivity insertion.

A.2 The transient

The insertion of reactivity into the system will result in an increase in the neutron population, as represented approximately by Eq. (A.1). To see this consider a one-group delayed neutron equation:

$$\begin{aligned} \frac{dn}{dt} &= \frac{\rho-\beta}{\Lambda}n + \lambda C + S \\ \frac{dC}{dt} &= \frac{\beta}{\Lambda}n - \lambda C \end{aligned} \tag{A.4}$$

where: β = delayed neutron fraction

λ = decay constant of the delayed neutron group (s^{-1})

For constant reactivity, ρ, the solution to these equations is:

$$\begin{aligned} n &= Ae^{q_+ t} + Be^{q_- t} - \Lambda S I\rho \\ C &= \frac{\beta}{\Lambda}\left[\frac{A}{(\lambda+q_+)}e^{q_+ t} + \frac{B}{(\lambda+q_-)}e^{q_- t} - \frac{\Lambda S}{\lambda\rho}\right] \end{aligned} \tag{A.5}$$

where: $q_\pm = \frac{1}{2}\left[\frac{\rho-\beta}{\Lambda}-\lambda\right] \pm \sqrt{\frac{1}{4}\left[\frac{\rho-\beta}{\Lambda}-\lambda\right]^2 + \frac{\lambda\rho}{\Lambda}}$.

The constants A and B are chosen to satisfy the initial conditions. Clearly, if $\rho > 0$, then q_+ is positive and q_- is negative. The positive solution will grow exponentially, if the reactivity remains constant. As the neutron flux is equal to the neutron density multiplied by the neutron speed, this implies that the flux and therefore the power will grow without limit.

However, the increase in power will increase the temperature of the fissile solution. The change in temperature of the uranyl nitrate solution will, in turn, change the reactivity of the system. The effect of temperature on reactivity has been estimated by the code participants, using sophisticated neutronics codes. The analysis shows that increasing the temperature reduces the reactivity of the system. It is important to determine if the reactivity feedback will limit the power transient. The extreme case of a prompt-critical transient with negative temperature feedback on the reactivity has been studied by Nordheim and Fuchs and by Fuchs and Hansen. This case is of particular relevance to the current exercise, as half of the experiments studied are prompt-critical excursions.

For a prompt-critical system (ρ – β) is positive and hence from Eq.(A.1) or Eq. (A.4) it is clear that the neutron density will grow exponentially and will soon come to dominate over the delayed neutron precursors. Therefore Eq. (A.1) can be approximated by:

$$\frac{dn}{dt} = \frac{\rho - \beta}{\Lambda} n \tag{A.6}$$

Multiplying both sides by the $v_{av}\Sigma_f E_f$ where E_f is the energy of fission, converts the neutron density into the power. Thus Eq. (A.6) can be written in terms of the power, P:

$$\frac{dP}{dt} = \frac{\rho - \beta}{\Lambda} P \tag{A.7}$$

Expressing the reactivity as a linear function of the temperature rise, ΔT, and the reactivity temperature feedback coefficient, α_T, yields:

$$\frac{dP}{dt} = \frac{\rho_0 + \alpha_T \Delta T - \beta}{\Lambda} P \tag{A.8}$$

where: $\rho_0 = \rho(t = 0)$ = initial reactivity.

Fuchs, *et al.* supplemented this with an adiabatic energy equation (little heat will be lost from the fissile solution in the early stages of the transient), in terms of the mass, M, and specific heat capacity of the fuel (fissile solution in this case):

$$P = MC_p \frac{d\Delta T}{dt} \tag{A.9}$$

They then solved Eqs. (A.8) and (A.9) to get the power, $P(t)$ and fission energy produced, $E(t)$, as a function of the initial power, P_0:

$$\begin{aligned} P &= \frac{2c^2 A e^{-ct}}{b\left(Ae^{-ct} + 1\right)^2} \\ E &= \frac{c + \alpha_0}{b}\left[\frac{1 - e^{-ct}}{Ae^{-ct} + 1}\right] \end{aligned} \tag{A.10}$$

where: $\alpha_0 = (\rho_0 - \beta)/\Lambda$

$b = \alpha_T / (MC_p \Lambda)$

$c = \sqrt{\alpha_0^2 + 2bP_0}$

$A = \dfrac{c + \alpha_0}{c - \alpha_0}$

They also note that the maximum power in the pulse is:

$$P_{max} = -\frac{MC_p(\rho_0 - \beta)^2}{2\Lambda\alpha_T} \tag{A.11}$$

Note the minus sign, as α_T is negative.

The power transient for parameter values relevant to TRACY test 005 are displayed in Figure A.1.

Figure A.1: Nordheim-Fuchs-Hansen pressure pulse

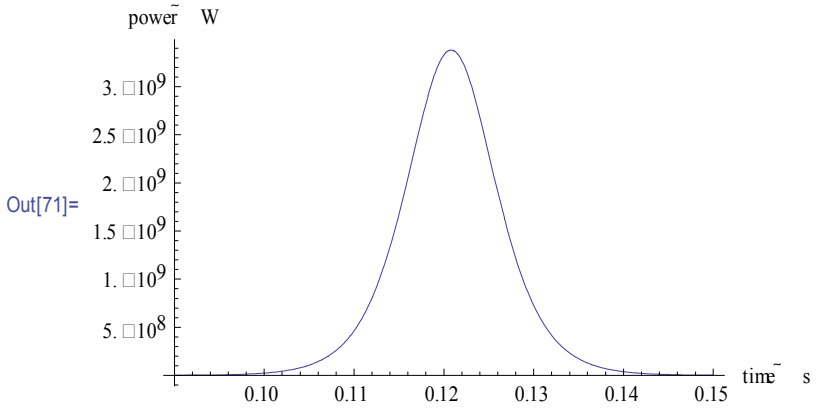

The power is seen to rise initially, but as the temperature rises it reduces the reactivity and eventually drives the power back to zero. In the actual experiments the power is not be expected to return to zero, as heat loss from the reactor becomes important at later times. In reality the power will tend to the value required to offset the heat loss from the reactor vessel when the temperature of the fissile solution is at the value required to reduce the reactivity to zero. This value is determined by the initial reactivity and the temperature feedback on the reactivity.

Temperature is not the only parameter to have an effect on the reactivity. If the radiation field becomes sufficiently intense radiolytic gas is produced and if the fissile solution becomes hot enough boiling will occur. Both of these phenomena reduce the density and consequently increase the volume of the fissile solution. In the first approximation it is assumed that the void is homogeneously introduced throughout the solution. In this case the effective density of the fissile solution decreases and the height of the solution increases correspondingly. The effect that this is likely to have on the reactivity can be deduced by considering the standard buckling equation for a cylinder. In the diffusion approximation k_{eff} is related to k_∞ by:

$$k_{eff} = -\frac{k_\infty}{1 + M^2B^2} \tag{A.12}$$

where: M^2 = migration area (m^2)

B^2 = buckling (m^{-2})

The reactivity is defined by:

$$\rho = \frac{k_{eff} - 1}{k_{eff}} = \frac{k_\infty - 1}{k_\infty} - \frac{M^2B^2}{k_\infty} \tag{A.13}$$

The buckling for a cylinder of radius R and height H is:

$$B^2 = \left(\frac{2.405}{R + \lambda_R}\right)^2 + \left(\frac{\pi}{H + 2\lambda_H}\right)^2 \tag{A.14}$$

where: λ_R = radial extrapolation length (m)

λ_H = axial extrapolation length (m)

If a homogeneous void fraction, v_f, is introduced into the fissile solution then the volume of solution increases from V to $V(1 + v_f)$ and the height increases from H to $H(1 + v_f)$. As the migration area is one-sixth of the mean square distance from the birth of a neutron in a fission to its thermal absorption it increases from M to $M(1 + v_f)^{2/3}$, which is approximately $M(1 + 2v_f/3)$ for small void fractions. Therefore, to first order in v_f the change in reactivity due to the introduction of a small void fraction is:

$$\delta\rho = -2.405^2 M^2 (R+\lambda_R)^2 \left\{ \frac{2}{3} \left\{ 1 + \left[\frac{\pi(R+\lambda_R)}{2.405(H+2\lambda_H)} \right]^2 \right\} - \frac{2H}{(H+2\lambda_H)} \left[\frac{\pi(R+\lambda_R)}{2.405(H+2\lambda_H)} \right]^2 \right\} \upsilon_f \qquad \text{(A.15)}$$

The TRACY experiments considered R = 0.26 m, 0.537 < H < 0.624 m and fits to experimental data indicate that 2λ = 0.102 m. With these values Eq. (A.15) indicates that the introduction of a small void fraction reduces the reactivity. Similarly for the SILENE experiments with R = 0.18 m, 0.3816 < H < 0.4096 m and an extrapolation length up to 0.102 m the introduction of a small void fraction is predicted to decrease the reactivity.

The negative void feedback on reactivity means that the onset of radiolytic gas production and/or boiling reduces the reactivity and consequently results in lower temperatures being attained. It also provides a mechanism for producing oscillations in the experiments. The onset of gas production decreases the reactivity of the system, possibly causing it to go subcritical and terminating gas production. When the gas bubbles rise to the surface due to buoyancy, the void fraction will fall thereby increasing the reactivity and causing the system to go critical again.

Other phenomena may also induce oscillatory behaviour in such a system. For instance, if gas production is inhomogeneous it could result in a non-uniform height for the fissile solution. This would increase the surface area for leakage, thus reducing the reactivity and possibly making it go subcritical. Such sloshing of the liquid therefore has the potential to induce oscillatory behaviour.

The estimates of the total number of fissions that occurred indicate that burn-up was not a significant process in these experiments.

Appendix B: TRACY results using approximate input parameters

Table B.1: Fuel conditions and kinetic parameters at 25.5°C

^{235}U enrichment (%)	9.98
Uranium concentration (gU/L)	390
Acid morality (mol/L)	0.77
Solution height (cm)	50.88
Neutron multiplication factor	1.0111
Effective delayed neutron fraction	7.5×10^{-3}
Prompt neutron lifetime (sec)	4.6×10^{-5}

Table B.2: Atomic number densities of the fissile solution with 390 gU/L at 25.5°C

Nucleus	Number density (atoms/barn.cm)
H	5.7292×10^{-2}
N	2.4394×10^{-3}
O	3.7708×10^{-2}
^{235}U	9.9622×10^{-5}
^{238}U	8.8823×10^{-4}

As a reference for those who use the parameters in Tables B.1 and B.2, a trial calculation using the AGNES code was performed and its results are presented in Tables B.1 to B.5. The difference with experiment is less than 20% for most cases except the first peak power of R72.

Table B.3: Results for sample kinetic parameters for R100

Items	B.MARK	Sample	C/E
Power at first peak (w)	3.16E+04	2.97E+04	-6.05%
Fissions to first peak	4.58E+16	3.91E+16	-14.71%
Total fissions	1.31E+17	1.18E+17	-9.59%

Table B.4: Results for sample kinetic parameters for R143

Items	B.MARK	Sample	C/E
Power at first peak (w)	3.72E+05	3.41E+05	-6.99%
Fissions to first peak	5.55E+16	5.58E+16	1.35%
Total fissions	1.50E+17	1.55E+17	-3.54%

Table B.5: Results for sample kinetic parameters for R72

Items	B.MARK	Sample	C/E
Power at first peak (w)	1.44E+07	8.96E+06	-37.78%
Fissions to first peak	3.43E+16	3.56E+16	3.86%
Total fissions	3.22E+17	3.56E+17	10.64%

Table B.6: Results for sample kinetic parameters for R196

Items	B.MARK	Sample	C/E
Power at first peak (w)	5.66E+08	5.15E+08	-9.01%
Fissions to first peak	1.90E+17	2.11E+17	10.86%
Total fissions	3.48E+17	3.81E+17	9.55%

Table B.7: Results for sample kinetic parameters for R203

Items	B.MARK	Sample	C/E
Power at first peak (w)	2.08E+09	1.68E+09	-19.23%
Fissions to first peak	3.20E+17	2.68E+17	-16.31%
Total fissions	6.32E+17	5.16E+17	-18.41%

Appendix C: Sample inputs for TRACY calculations

C.1 Sample input for AGNES code

```
0000
VER3  TRACY R100 RF 0.3 $
C==== CONTROL DATA
C3 ---KRFILE------KRGEOM------KRTHRM------KEDCRM
C3 ---------KRCNTL------KRNUCL------KRVOID------KRBOIL
           0     0     0     0     0     0     0     0
C4 ---- NMAX ------ NPRT ------ NPLT ------ HMAX ------ TMAX ----- TTIME
   100000000          50         500      1.0E-3       554.8      0.0500
C==== GEOMETRY DATA
C5 ------ IG ---- RAD(1) ----- THIC2 ---- VOL(3) ---- HEIGHT ----- WRATE
           1      0.2471      0.0100       0.010      0.5085        0.00
C6 ----- IZM -------- I1 -------- I2 ------- IZP -------- IV
           5           5           1           0           1
C==== NUCLEAR DATA
C8 ------- M ---- NSTART ------ IRHO ------- ITM
           6           1          -3           1
C9 --- ALIFE  ---- AN(1)  ---- ERROR  ---- GAMMA
  4.8640E-05    1.03E+01    1.00E-04         1.0
C10 --- B(1) ------ B(2) ------ B(3) ------ B(4) ------ B(5) ------ B(6)
 2.54901E-04 1.65210E-03 1.49401E-03 3.00525E-03 8.90835E-04 3.24200E-04
C11 -- AL(1) ----- AL(2) ----- AL(3) ----- AL(4) ----- AL(5) ----- AL(6)
 1.27029E-02 3.17037E-02 1.15247E-01 3.11609E-01 1.40029E+00 3.87396E+00
C13-1 --- R1 -------- R2 -------- R3 ----- RHOSW
         0.0         0.0
        0.10       31.50
     10000.0       31.50
C14 - RTC(1) ---- RTC(2) ---- RTC(3) ------ EXTS
         0.0         0.0         0.0         0.0
C15 --- TIMP
         0.0
C16 - PR(IT) --------- 2 --------- 3 --------- 4 --------- 5
    1.000E+0    1.000E+0    1.000E+0    1.000E+0    1.000E+0
C17  PZ(IZM) --------- 2 --------- 3 --------- 4 --------- 5
    1.000E+0    1.000E+0    1.000E+0    1.000E+0    1.000E+0
C==== THERMAL DATA
C18 --- NTEQ ----- IWEIT ----- IWEIV ------- NWT
           1          -2          -2           0
C18-1-1 -TCA ------- TCB --------TCT
  1.6000E+00  1.0000E+00       500.0
C18-2-1 -VCA ------- VCB --------VCT
  1.6000E+00  1.0000E+00         5.0
C19 --- RHO1 ------- CP1 ----- ALMD1 ------ HTC1 ----- AREA1
  1.5498E+03  2.6675E+03   1.000E+04   1.000E-02   1.043E+00
C20 --- RHO2 ------- CP2 ----- ALMD2 ------ HTC2 ----- AREA2
   8.000E+03   5.043E+02   1.624E+01   1.000E-02   1.043E+00
C21 --- RHO3 ------- CP3 ----- OMEGA ----- TZERO
   1.184E+00   1.006E+03   4.000E-02      298.85
C22 - RC1(1) ---- RC2(1) ---- RC3(1) ---- RCD(1)
 -3.7578E+00 -5.4377E-02       0.000       0.000
```

```
C23 - RC1(2) ---- RC2(2) ---- RC3(2) ---- RCD(2)
       0.000       0.000       0.000       0.000
C24 - RC1(3) ---- RC2(3) ---- RC3(3) ---- RCD(3)
       0.000       0.000       0.000       0.000
C27 ----- PT  (IT+1,IZM) ---  6E12.5 --------- 4 --------- 5 --------- 6
      298.85      298.85      298.85      298.85      298.85      298.85
      298.85
      298.85      298.85      298.85      298.85      298.85      298.85
      298.85
      298.85      298.85      298.85      298.85      298.85      298.85
      298.85
      298.85      298.85      298.85      298.85      298.85      298.85
      298.85
      298.85      298.85      298.85      298.85      298.85      298.85
      298.85
C==== VOID DATA
C28 --- IVEL ------- IST ---- IWEIVD ----- IWEI2 ----- IVEL2
           7           3           0           0           1
C29 ---- VC1 ------- VC2 ------ VALC ------- EPS ----- ICALD
 -4.3700E+1  -9.4600E-1   0.000E+00         1.0           0
C30 ----- CD -------- CG ------ CATV ---- CONSTN ---- CONST1 ---- CONST2
        15.0     6.0E-07   0.000E+00   1.000E-07       0.000       0.000
C31-1  RHO25 ----- PRESG -------- RG ------- CDB ------ CDB1 ------ CDB2
  1.5893E+03   1.000E+00   5.000E-08   8.000E-03   8.000E-03       0.000
C==== SCRAM DATA
C31 - ISCRAM ---- VSCRAM ---- TIMDEL ---- RSCRAM
           4      1000.0         0.0         0.0
C==== BOILING DATA
C32 -- TBOIL ----- DENSI ----- HBOIL ------ VLIQ ----- VVAPE
      377.77      1543.7    2.260E+6    1.670E+0         1.0
C==== PRESSURE DATA
C33 ----- PC -------- PG ------- GH2 -------- T1 ----- AECPX
   6.900E+04   2.900E-05   1.100E+00   2.000E-03   4.170E+07
 9999
```

C.2 Sample input for CRITEX code

```
CRITEX VERSION 6.1 2004

THE JOB NAME IS  TRACY SALVE R100
THE INITIAL STEP REACTIVITY IS  3.00000E-01 $
THE SOLUTION HEIGHT AT DELAYED CRITICALITY IS 4.99760E+01 CM.
THE AXIAL EXTRAPOLATION LENGTH IS  2.19800E+00 CM
THE RADIAL EXTRAPOLATION LENGTH IS  8.86000E-01 CM
THE DIAMETER OF THE VESSEL CONTAINER IS  5.00000E+01 CM
THE INITIAL HEIGHT OF THE SOLUTION IS  5.08520E+01 CM
THERE IS NO CENTRAL ASSEMBLY PRESENT
SOLUTION : NITRATE URANIUM (U235:10% TRACY)
THE CONCENTRATION OF URANIUM TOTAL IS  3.92900E+02 GM/L
THE HYDROGEN ION MOLARITY IS  6.60000E-01 M
THE INITIAL CENTRAL SPECIFIC POWER IS  2.06500E+05 FISSIONS/(GM.SEC)
THE RUN WILL END BY  5.54750E+02 SEC
THE INITIAL SOLUTION TEMPERATURE IS  2.57000E+01 DEGREES C.
THE AMBIENT TEMPERATURE OUTSIDE THE CONTAINER IS  2.57000E+01 DEGREES C.
```

C.3 Sample input for INCTAC code

```
[ INCTAC CODE INPUT DATA FOR TRACY RUN100 ]


[ NUCLEAR DATA ]

 TRACY: CRITICAL ACCEDENT CALCULATION
  RUN NO. 100  0.30$
    900000 1500000 0                              /TWDANT MEMORY BANK
      9  5   8  13  18  19  -1   8    9   8       /Control Card
    7*0.495   0.35   7*2.65  2.635   2*0.5        /R_MESH
    1.0 2*4.0  7*5.0 0.9 4.1 5.0 5.852 1.0
    5.0   5.0    5.0  5.0                        /Z_MESH

     3 3 3 3 3 3 3 3 3 3 3 3 3 3 3 3 3
     3 3 3 3 3 3 3 2 2 2 2 2 2 2 2 2 2
     3 3 3 3 3 3 3 2 2 2 2 2 2 2 2 2 2

     3 3 3 3 3 3 3 2 1 1 1 1 1 1 1 2 2
     3 3 3 3 3 3 3 2 1 1 1 1 1 1 1 2 2
     3 3 3 3 3 3 3 2 1 1 1 1 1 1 1 2 2
     3 3 3 3 3 3 3 2 1 1 1 1 1 1 1 2 2
     3 3 3 3 3 3 3 2 1 1 1 1 1 1 1 2 2
     3 3 3 3 3 3 3 2 1 1 1 1 1 1 1 2 2
     3 3 3 3 3 3 3 2 1 1 1 1 1 1 1 2 2
     3 3 3 3 3 3 3 2 1 1 1 1 1 1 1 2 2
     4 4 4 4 4 4 4 2 1 1 1 1 1 1 1 2 2
     4 4 4 4 4 4 4 2 1 1 1 1 1 1 1 2 2
     4 4 4 4 4 4 4 2 1 1 1 1 1 1 1 2 2
     4 4 4 4 4 4 4 2 1 1 1 1 1 1 1 2 2
     4 4 4 4 4 4 4 2 1 1 1 1 1 1 1 2 2
     4 4 4 4 4 4 4 2 1 1 1 1 1 1 1 2 2

     4 4 4 4 4 4 4 2 1 1 1 1 1 1 1 2 2
     4 4 4 4 4 4 4 2 1 1 1 1 1 1 1 2 2              / Zone Map

     2
     8*-1 1 2 3 4 5 6 7 8 -1 -1
    -1 -1 -1 1 2 3 4 5 6 7 8 9 10 11 12 13 14 15 16   /Channel assign

  200.0  1 3 18 7 3   1.0 44.90  9.0                  /VROD Initial Rod Position

      0.10000E+08 0.82085E+06 0.67380E+05 0.12341E+04 0.17604E+02
      0.18554E+01 0.68256E+00 0.38926E+00 0.97080E-01 1.00000E-05   /Energy Str.

      7.58018E-01 2.34985E-01 6.98150E-03 1.48252E-05 0.00000E+00
      0.00000E+00 0.00000E+00 0.00000E+00 0.00000E+00               /Fission Spec.

      1.9421E+09  7.1588E+08  1.1855E+08  1.4338E+07  3.1668E+06
      1.4547E+06  9.8886E+05  5.4130E+05  2.4293E+05               /Neutron
Velocity

     0.00031936 0.00087734 0.00296057 0.00146973 0.00162848 0.00025084  /beta
     3.87402439 1.40029144 0.31161866 0.11525064 0.03170384 0.01270299  /alpha

     4     1
 0.00584   0.99416 7*0.0
 0.12211   0.87789 7*0.0
 0.07067   0.92555 7*0.0
 0.12405   0.86712 7*0.0
 0.10154   0.89796 7*0.0
```

```
 0.08902   0.91098 7*0.0                                 /REG1 Delayed Neutron Spec.
    9*0.0
    9*0.0
    9*0.0
    9*0.0
    9*0.0
    9*0.0                                               /REG2
    9*0.0
    9*0.0
    9*0.0
    9*0.0
    9*0.0
    9*0.0                                               /REG3
    9*0.0
    9*0.0
    9*0.0
    9*0.0
    9*0.0
    9*0.0                                               /REG4
     9    13     0     1                                      P0 COMPONENT
 3.20000E-11  .00000E+00 2.93150E+02 1.54461E+00 2.93150E+02
 7.58018E-01 4.73055E-04 1.20748E-03 1.31108E-03 2.64826E-01  .00000E+00
  .00000E+00 1.63537E-01  .00000E+00  .00000E+00  .00000E+00  .00000E+00
  .00000E+00

      -
      -       [ The following data is omitted. ]
      -
      -
      -
      -



[ THERMAL-HYDRAULIC DATA ]

free format
*
*
*************
* main data *
*************
*
*
*       numtcr          ieos         inopt          nmat
           -1             0             1             0
IDNO      20040318
*
*****************
* namelist data *
*****************
*
 &inopts
  igas=2,noair=0,isolcn=1,nifsh=1,ccif=1.0e+4,
  nhtstr=1,nrslv=1,
 &end
*
*       cntlmn         cnmin        cntlmx         cnmax
    3.0300e+02    1.0000e+02    3.7300e+02    1.0000e+02
*        cgas0          ggas          niu0          niu2          pgam
    5.0000e+00    8.8200e-08    0.0000e+00    0.0000e+00    1.0000e+00
*        dstep         timet
```

```
             0    0.0000e+00
*       stdyst         transi          ncomp           njun           ipak
             0              1              6              4              1
*         epso           epss
    5.0000e-03    1.0000e-04
*       oitmax         sitmax         isolut         ncontr
         10000             10              1              0
*         ntsv           ntcb           ntcf           ntrp           ntcp
             8              0              0              0              0
*
************************
* component-number data *
************************
*
* iorder*              1            10            11            20            21
* iorder*            999e
*
*
************************
* signal variable       *
************************
*
*     idsv     isvn   ilcn    icn1    icn2
         1       20      1    2014    2001  * reactor liquid level
         2       20      1    3014    3001  * reactor liquid level
         3       20      1    4014    4001  * reactor liquid level
         4       20      1    5014    5001  * reactor liquid level
         5       20      1    6014    6001  * reactor liquid level
         6       20      1    7014    7001  * reactor liquid level
         7       20      1    8014    8001  * reactor liquid level
         8       20      1    9014    9001  * reactor liquid level
*
******************
* component data *
******************
*
*******   type           num            id        ctitle
vessel           1       1 $1$ reactor vessel
*         nasx          nrsx          ntsx          ncsr        ivssbf
            16             9             1             2             0
*         idcu          idcl          idcr          icru          icrl
             9             2             0            16             1
*         icrr         ilcsp         iucsp         iuhp          iconc
             0             0             0             0             1
*        igeom         nvent         nvvtb        nsgrid
             0             0             0             0
*        shelv          epsw
    0.0000e+00    0.0000e+00
* z      *     5.0000e-02    1.0000e-01    1.5000e-01    2.0000e-01    2.5000e-01
* z      *     3.0000e-01    3.5000e-01    3.5900e-01    4.0000e-01    4.5000e-01
* z      *     5.0852e-01    5.1852e-01    5.6852e-01    6.1852e-01    6.6852e-01
* z      *     1.9370e+00e
* rad    *     3.8150e-02    6.4650e-02    9.1150e-02    1.1765e-01    1.4415e-01
* rad    *     1.7065e-01    1.9715e-01    2.2365e-01    2.5000e-01e
* th     *     6.2832e+00e
*        lisrl         lisrc         lisrf         ljuns
            16             9             3            11
             1             9             3            21
*
* level   1
*
* cfzl-t* f   1.0000e+04e
```

```
* cfzl-z* f   1.0000e+04e
* cfzl-r* f   1.0000e+04e
* cfzv-t* f   0.0000e+00e
* cfzv-z* f   0.0000e+00e
* cfzv-r* f   0.0000e+00e
* vol   * f   1.0000e+00e
* fa-t  * f   1.0000e+00e
* fa-z  * f   1.0000e+00e
* fa-r  * r01 0.0000e+00 r07 1.0000e+00r01 0.0000e+00e
* hd-t  * f   1.0000e+00e
* hd-z  * f   1.0000e+00e
* hd-r  * f   1.0000e+00e
* alpn  * r01 0.0000e+00 r08 0.0000e+00e
* vvn-t * f   0.0000e+00e
* vvn-z * f   0.0000e+00e
* vvn-r * f   0.0000e+00e
* vln-t * f   0.0000e+00e
* vln-z * f   0.0000e+00e
* vln-r * f   0.0000e+00e
* tvn   * f   2.9935e+02e
* tln   * f   2.9935e+02e
* pn    * f   1.0000e+05e
* pan   * f   1.0000e+05e
* conc  * r01 0.0000e+00 r08 2.5180e-01e
* solid * f   1.5604e+03e
*

      -
      -       [ The following data is omitted. ]
      -
      -
      -
      -
```

C.4 Sample input for TRACE code

```
TRACY RUN-100: 0.3$/0.1 SECS (ALMOST STEP REACTIVITY INS)

 $general    title="TRACY100",amat="uni",amcn="sst"
             $end

 $lsode
             itol=1,
             rtol= 1.d-5, atol= 1.d-10,
             itask=1, istate=1, iopt=1, lrw=30100, liw=300, mf=10
             $end

 $timing     tend=554.8,tfast=200.,tslow=300.,tvslow=400.,
             tinc=1.d-4,tincf=1.d-4,tincs=1.d-4,tincvs=1.d-4
             $end

 $geometric  nnradf=5,nnaxif=8   $end

 $neutronic  irflg=3,ifflg=2,ieflg=2,
             beta=2.51397E-04, 1.61992E-03, 1.46888E-03,
                  2.95048E-03, 8.75153E-04, 3.18918E-04,
             amda=1.27029E-02, 3.17037E-02, 1.15241E-01,
                  3.11595E-01  1.40028E+00  3.87388E+00,
             gen=4.85851E-05,zlife=4.76242E-05,sour=0.d0,
             bcoef=0.0,zext=0.0,pd0=15.0d0,srp=0.0,
```

```
            rhotmp1=-0.0335,rhotmp2=6d-5,
            rhovoi1=-406.29,rhovoi2=-1131.8,
            rhocon1=0.0,rhocon2=0.0,
            rhoext0=0.0,rhoext1=3d0 $end

$radgas     ivgflg=3,icflg=1,vel1=1.0d-2,vdgsk=0.07,
            veldw=0.d0,velup=4.0d-2,gvalue=1.0d-7,satc=20.d0,
            a0=0.5d-7,a1=0.d0,a2=0.d0,b0=5.d-2,b1=0.d0,
            b2=3.d1,b4=0.d0,hmol=1.d1,rgbura=5.d-6,
            ioflg=0  $end

$thermal    imflg=0,idflg=2,hitc=1.0d0,xy=299.35,
            tinf=299.35,ivar=6,ithermo=0,jthermo=0,
            amout="air"
            $end

$boiling    iyflg=1 ,ikflg=2,ilflg=1,isflg=0,ivsflg=3,
            radeq=2.5d-6,cbc1=2.0d-7,cbc2=1.0d0,
            cbc3=1.0d0,cbc4=1.0d0,afreq=0.25d0,stbura=0.7d-6,
            svel1=1.2d-2,svdgsk=0.07d0,evcoef=5.d-3,
            ftbura=0.7d-6  $end

$motion
            izflg=0,discof=2.6d3
            $end

$plot       pdata="pow",ipflg=0,xmin=1.d10,xmax=1.d20,
            reamax=10.,reamin=-10.,voimax=3.d-3,
            voimin=0.d0,tdelta=4.,tdelst=20.,
            iouti=1000, ioutif=5000, ioutis=10000, ioutivs=10000
            $end

$counter
            icrtra=1, icrit=70, corfac=1.0d0
            $end

$pressure
            itflg=1,
            zcons= 2.9d-5, pbias= 6.9d4, prp=2.0d-3, gh2= 1.2d0,
            prcons= 2.0d-8
            $end

$aero       inflg=1,ihflg=1,iaflg=5,xperc=5.d1,fde=0.25,
            fcth=1.0d-8,hdist1=1.d-2   $end

$sonic      cor=0.d0,0.d0,0.d0,0.d0,7.35d-2,1.8d2,
            3.4525d-1,0.d0,0.d0,0.6905,1.47d-1,4.5d1,
            delt1=0.d0,delt2=0.d0
            $end

$source
            ibflg=2
            $end
```

Appendix D: Sample inputs for SILENE calculations

D.1 Sample input for AGNES code

```
1                                          INPUT DATA
*0---------1---------2---------3---------4---------5---------6---------7---------8*
1* 0000                                                                           *
2*VER3 SLINE S3-300 2.31$                                                         *
3*C                                                                               *
 4*C GENERAL CONTROL FLAGS                                                         *
5*C                                                                               *
6*C---KRFILE-KRCNTL-KRGEOM-KRNUCL-KRTHRM-KRVOID-KEDCRM-KRBOIL-KREVAP-KRVOLT *
7*          0     0     0     0     0     0     1     0     0     0              *
8*C ----- NMAX  ----- NPRT -----  NPLT  ----- HMAX ------ TMAX ----- TTIME       *
9*  1000000000          50         500      1.0E-3      120.00         0.1       *
10*C---- TSHIFT  ---- TDETS ----- TDETE  ----NPRTWD ---- NPLTWD ---- HMAXWD       *
11*         0.0          0.        120.        1000        1000      1.0E-5       *
12*C                                                                              *
13*C GEOMETRY DATA                                                                *
14*C                                                                              *
15*C --SOL-- I1 -------- I2 -------  IV ------ IFIN                               *
16*           6           1           1          -1                               *
17*C ----RAD(1) ---WIDTH(2) ---- VOL(3) ----- WRATE ----- TRATE                   *
18*       0.1759       0.004      1.0E+5     0.00E+0      299.05                   *
19*C --TOP-  J1 ---SOL-- J2 ---BOT-  J3                                           *
20*           3           6           8                                          *
21*C --WITDH(4) ---- HEIGHT -- WIDTH(6)                                          *
22*        0.01      0.4096        0.08                                         *
23*C                                                                              *
24*C KINETIC DATA                                                                *
25*C                                                                              *
26*C -------- M ---- NSTART ------ IRHO ------- ITM ---                         *
27*           6           1           0           1                              *
28*C ---- ALIFE ----- AN(1) ----- ERROR ----- GAMMA                              *
29*   3.2848E-5   1.0000E-5    1.000E-4         1.0                              *
30*C-----------------        BETA (1)-(6)      ----------------                  *
31*  2.62600E-4  1.71610E-3  1.55640E-3  3.05750E-3  9.00150E-4  3.28410E-4       *
32*C-----------------       AL    (1)-(6)      ----------------                  *
33*  1.24400E-2  3.05400E-2  1.11400E-1  3.01400E-1  1.13590E+0  3.01399E+0       *
34*C                                                                              *
35*C-------- R1 -------- R2 -------- R3 ----- rhosw ----- for IRHO=0              *
36*         0.0    2310.000         0.0                                         *
37*C                                                                              *
38*C --- RTC(1) ---- RTC(2) ---- RTC(3) ------ EXTS                              *
39*         0.0         0.0         0.0         0.0                             *
40*C                                                                              *
41*C TIME DEP. POWER DISTRIBUTION DATA                                           *
42*C                                                                              *
43*C TIMP(1:ITM)                                                                 *
44*         0.0                                                                  *
45*C -------------------RADIAL  PR(1:I1) -----------------------                 *
46*    1.000E+0    1.000E+0    1.000E+0    1.000E+0    1.000E+0    1.000E+0       *
47*C -------------------AXIAL   PZ(1:J2) -----------------------                 *
48*    1.000E+0    1.000E+0    1.000E+0    1.000E+0    1.000E+0    1.000E+0       *
49*C                                                                              *
*0---------1---------2---------3---------4---------5---------6---------7---------8*
```

```
                                CONTINUE
*0---------1---------2---------3---------4---------5---------6---------7---------8*
50*C THERMAL FEEDBACK AND THERMAL EFFECT DATA                                      *
51*C                                                                               *
52*C ----- NTEO ----- IWEIT ----- IWEID ------- NWT ----- ICOOL                    *
53*           1          -2          -2           0           1                    *
54*C                                                                               *
55*C THERMAL AND VOID REACTIVITY COEFF MULTIPLICATION FACTORS AND THEIR DECAY CONST*
56*C                                                                               *
57*C--TCA(start)--TCB(end)----TCT time(s)                                          *
58*  1.5000E+00  1.0000E+00  5.0000E-01                              FOR TEMPERATUR*
59*  1.5000E+00  1.0000E+00  5.0000E-01                              FIR VOID COEFF*
60*C                                                                               *
61*C THERMAL PROPERTIES PER REGION                                                 *
62*C                                                                               *
63*C--RHO(kg/m3)-CP(J/kg/K)--COND(W/m/K)-HTC(W/m2/K)--AREA(m2)                     *
64*  1.1588E+03  3.4413E+03  1.0000E+04    1.00E-02     0.46325      region 1      *
65*  8.0000E+03  5.0425E+02  1.0000E+04     1.00000    1.197726      region 2 (LUMP*
66*C--- TZERO(3)                                                                  *
67*  2.9815E+02                                                     region 3 (LUMP*
68*C --- DISTX --- TZERO(9)                                                       *
69*         1.0  2.9500E+02                                         region 8 & 9  *
70*C                                                                               *
71*C NATURAL CONVECTION DATA (IF HTC OF REG 2, 4, 6 IS NEGATIVE)                  *
72*C                                                                               *
73*C---  PRANDL   --- CONDC  ---  VISCO  --- HEIGHT                               *
74*C       0.717     0.02614   0.1583E-4      0.4096                             *
75*C                                                                               *
76*C TEMPERATURE REACTIVITY COEFFICIENTS FOR REG. 1, 2, 3                          *
77*C                                                                               *
78*C--(CENT/K)---(CENT/K**2)-------RC3---------RCD---                              *
79*  -2.1214E+0  -1.6434E-1        0.00        0.00                  REGION 1      *
80*        0.00        0.00        0.00        0.00                  REGION 2      *
81*        0.00        0.00        0.00        0.00                  REGION 3      *
82*C                                                                               *
83*C INITIAL TEMPERATURE (K) PER REGION                                            *
84*C                                                                               *
85*C --------------------- TEMP(1:9) ---------------------                         *
86*      295.45      295.45      295.00                                           *
87*C                                                                               *
88*C VOID CALCULATION CONTROL                                                      *
89*C (IWEI2 AND IVEL2 ARE NOT USED ANYMORE)                                        *
90*C                                                                               *
91*C ----- IVEL ------- IST ---- IWEIVD ----- IWEI2 ----- IVEL2 --                 *
92*           7           3           0           0           0                   *
93*C                                                                               *
94*C VOID REACTIVITY COEFFICIENTS FOR REG. 1                                       *
95*C                                                                               *
96*C --- CENT/% - CENT/%**2 -----  VALC ------- EPS ---- ICALCD                   *
97* -6.8091E+01 -1.6137E+00    0.000E+0    5.000E-1           0                   *
98*C                                                                               *
99*C RADIOLYTIC GAS CALCULATION PARAMETERS                                         *
*0---------1---------2---------3---------4---------5---------6---------7---------8*
                                CONTINUE
*0---------1---------2---------3---------4---------5---------6---------7---------8*
100*C                                                                              *
101*C ------- CD --------- G ------- TAU ------- NUY -------- A1 -------- A2       *
102*        15.0    5.616E-7    0.000E+0    1.000E-7        0.00        0.00       *
103*C ---- ROU25 ------- PT1 --------- R -------- B0 -------- B2 -------- B4       *
104*   1.5890E+3    1.000E+0    5.000E-8    2.000E-3        4.00        4.00       *
105*C                                                                              *
106*C EXTERNAL SCRAM REACTIVITY CONTROL                                           *
107*C                                                                              *
108*C --- ISCRAM ---- VSCRAM ---- TIMDEL --- TSCREND --- RSCRAM0 --- RSCRAM1       *
109*           4     10000.0         0.0       100.0         0.0         0.0       *
110*C -- RSCRAM2                                                                  *
```

```
111*         0.0                                                                *
112*C                                                                            *
113*C PRESSURE MODEL CALCULATION PARAMETERS                                     *
114*C                                                                            *
115*C ------- PC -------- PG ------- GH2 -------- TI ----- AECPX                 *
116*    6.900E+4    2.900E-5    1.100E+0    2.000E-3    4.170E+7                *
117*C                                                                            *
118*C CONTINUATION CARD (9999=STOP)                                             *
119*C                                                                            *
120* 9999                                                                       *
    *0---------1---------2---------3---------4---------5---------6---------7---------8*
                                  END INPUT DATA
```

D.2 Sample input for CRITEX code

```
CRITEX VERSION 6.1 2004

THE JOB NAME IS  SILENE S2-300
THE INITIAL STEP REACTIVITY IS  9.70000E-01 $
THE SOLUTION HEIGHT AT DELAYED CRITICALITY IS 3.73600E+01 CM.
THE AXIAL EXTRAPOLATION LENGTH IS  1.77500E+00 CM
THE RADIAL EXTRAPOLATION LENGTH IS  5.97000E-01 CM
THE DIAMETER OF THE VESSEL CONTAINER IS  3.60000E+01 CM
THE INITIAL HEIGHT OF THE SOLUTION IS  3.89100E+01 CM
THERE IS NO CENTRAL ASSEMBLY PRESENT
THE SOLUTION IS URANYL NITRATE
THE CONCENTRATION OF URANIUM TOTAL IS  7.07800E+01 GM/L
THE HYDROGEN ION MOLARITY IS  2.00000E+00 M
THE URANIUM ENRICHMENT IS  9.300E+01   %
THE INITIAL CENTRAL SPECIFIC POWER IS  4.59000E-02 FISSIONS/(GM.SEC)
THE RUN WILL END BY  2.65000E+02 SEC
THE INITIAL SOLUTION TEMPERATURE IS  2.21000E+01 DEGREES C.
THE AMBIENT TEMPERATURE OUTSIDE THE CONTAINER IS  2.21000E+01 DEGREES C.
```

D.3 Sample input for INCTAC code

```
 [ INCTAC CODE INPUT DATA FOR SILENE S1-300 ]

[ NUCLEAR DATA ]

 20030402
  SILENE S1-300 reactivity  769pcm initial hight 38.16 cm
    900000 1500000  0                              /TWODANT MEMORRY BANK
      9  5   8  13  12  24  -1   8   9   8
    1.75   1.75  0.3 1.0 6*2.0 1.2 0.4             /R_MESH
    5.0 5.0 5.0 5.0 5.0  5.0  5.00 3.45 8*1.0
    1.71  1.0  5.84   5*8.4                        /Z_MESH

     3 3 3 3 3 3 3 3 3 3 3
     3 3 2 2 2 2 2 2 2 2 2
     3 3 2 1 1 1 1 1 1 1 2
     3 3 2 1 1 1 1 1 1 1 2
     3 3 2 1 1 1 1 1 1 1 2
     3 3 2 1 1 1 1 1 1 1 2
     3 3 2 1 1 1 1 1 1 1 2
     3 3 2 1 1 1 1 1 1 1 2
     4 4 2 1 1 1 1 1 1 1 2
     4 4 2 1 1 1 1 1 1 1 2
     4 4 2 1 1 1 1 1 1 1 2
     4 4 2 1 1 1 1 1 1 1 2
     4 4 2 1 1 1 1 1 1 1 2
     4 4 2 1 1 1 1 1 1 1 2
```

```
    4 4 2 1 1 1 1 1 1 1 2
    4 4 2 1 1 1 1 1 1 1 2
    4 4 2 1 1 1 1 1 1 1 2
    4 4 2 1 1 1 1 1 1 1 2
    4 4 2 1 1 1 1 1 1 1 2
    4 4 2 1 1 1 1 1 1 1 2
    4 4 2 1 1 1 1 1 1 1 2
    4 4 2 1 1 1 1 1 1 1 2
    4 4 2 1 1 1 1 1 1 1 2
    4 4 2 3 3 3 3 3 3 2 2                          /ZONE MAP

    2
   -1 -1 -1 1 2 3 4 5 6 7 8 -1
   -1 -1  1 2 3 4 5 6 7 8 9 10 11 12 13 14 15 16 17 18 19 20 21 22 /Channel assign

  200.0  1 2 18 2 3 0.01 38.45 10.0   /VROD , Initial Rod Position

     1.00000E+07 8.20850E+05 6.73800E+04 1.23410E+03 1.76040E+01
     1.85540E+00 6.82560E-01 3.89260E-01 9.70800E-02 1.00000E-05 /Energy Str.

     7.58005E-01 2.34998E-01 6.98197E-03 1.48263E-05 0.00000E-00
     0.00000E-00 0.00000E-00 0.00000E-00 0.00000E-00             /Fission Spec.

     1.94240E+09 7.17980E+08 1.18920E+08 1.42740E+07 3.16460E+06
     1.45530E+06 9.89020E+05 5.49380E+05 2.46280E+05             /Neutron Velocity
  0.00033780 0.00092760 0.00317000 0.00158100 0.00175000 0.00027520 /Beta
    3.87000000 1.40000000 0.31700000 0.11500000 0.03170000 0.01270000 /Alpha

    4     1
    0.00584   0.99416   0.00000 0.0 0.0 0.0 0.0 0.0 0.0
    0.12207   0.87793   0.00000 0.0 0.0 0.0 0.0 0.0 0.0
    0.07061   0.92563   0.00376 0.0 0.0 0.0 0.0 0.0 0.0
    0.12405   0.86710   0.00885 0.0 0.0 0.0 0.0 0.0 0.0
    0.10188   0.89761   0.00051 0.0 0.0 0.0 0.0 0.0 0.0
    0.08901   0.91099   0.00000 0.0 0.0 0.0 0.0 0.0 0.0   /REG1
    0.00584   0.99416   0.00000 0.0 0.0 0.0 0.0 0.0 0.0
    0.12207   0.87793   0.00000 0.0 0.0 0.0 0.0 0.0 0.0
    0.07061   0.92563   0.00376 0.0 0.0 0.0 0.0 0.0 0.0
    0.12405   0.86710   0.00885 0.0 0.0 0.0 0.0 0.0 0.0
    0.10188   0.89761   0.00051 0.0 0.0 0.0 0.0 0.0 0.0
    0.08901   0.91099   0.00000 0.0 0.0 0.0 0.0 0.0 0.0   /REG2
    0.00584   0.99416   0.00000 0.0 0.0 0.0 0.0 0.0 0.0
    0.12207   0.87793   0.00000 0.0 0.0 0.0 0.0 0.0 0.0
    0.07061   0.92563   0.00376 0.0 0.0 0.0 0.0 0.0 0.0
    0.12405   0.86710   0.00885 0.0 0.0 0.0 0.0 0.0 0.0
    0.10188   0.89761   0.00051 0.0 0.0 0.0 0.0 0.0 0.0
    0.08901   0.91099   0.00000 0.0 0.0 0.0 0.0 0.0 0.0   /REG3
    0.00584   0.99416   0.00000 0.0 0.0 0.0 0.0 0.0 0.0
    0.12207   0.87793   0.00000 0.0 0.0 0.0 0.0 0.0 0.0
    0.07061   0.92563   0.00376 0.0 0.0 0.0 0.0 0.0 0.0
    0.12405   0.86710   0.00885 0.0 0.0 0.0 0.0 0.0 0.0
    0.10188   0.89761   0.00051 0.0 0.0 0.0 0.0 0.0 0.0
    0.08901   0.91099   0.00000 0.0 0.0 0.0 0.0 0.0 0.0   /REG4
    9    13     0     1                                   P0 COMPONENT
 3.20000E-11  .00000E+00 2.93150E+02 1.16602E+00 2.93150E+02
 7.58005E-01 2.14206E-04 7.84687E-04 5.84366E-04 2.67881E-01  .00000E+00
  .00000E+00 1.61345E-01  .00000E+00  .00000E+00  .00000E+00  .00000E+00
  .00000E+00
  -
  -  [The following data is omitted. ]
  -
```

```
 [ THERMAL-HYDRAULIC DATA ]

free format
*
*
*************
* main data *
*************
*
*
*       numtcr          ieos         inopt          nmat
           -1             0             1             0
IDNO      20040312
*
*****************
* namelist data *
*****************
*
 &inopts
  igas=2,noair=0,isolcn=1,nifsh=1,ccif=1.0e+5,
  nhtstr=1,nrslv=1,
 &end
*
*       cntlmn         cnmin        cntlmx         cnmax
    3.0300e+02    1.0000e+02    3.7300e+02    1.0000e+02
*        cgas0          ggas          niu0          niu2          pgam
    5.0000e+00    1.2300e-07    0.0000e+00    0.0000e+00    1.0000e+00
*        dstep         timet
             0    0.0000e+00
*       stdyst        transi         ncomp          njun          ipak
*            0             1             5             4             1
             0             1             6             4             1
*         epso          epss
    5.0000e-03    1.0000e-04
*       oitmax        sitmax        isolut        ncontr
         10000            10             1             0
*         ntsv          ntcb          ntcf          ntrp          ntcp
             7             0             0             0             0
*
*************************
* component-number data *
*************************
*
* iorder*              1            10            11            20            21
* iorder*            999e
*
*
*************************
* signal variable       *
*************************
*
*     idsv     isvn   ilcn    icn1    icn2
         1       20      1    2021    2001  * reactor liquid level r=2
         2       20      1    3021    3001  * reactor liquid level r=3
         3       20      1    4021    4001  * reactor liquid level r=4
         4       20      1    5021    5001  * reactor liquid level r=5
         5       20      1    6021    6001  * reactor liquid level r=6
         6       20      1    7021    7001  * reactor liquid level r=7
         7       20      1    8021    8001  * reactor liquid level r=8
*
```

```
******************
* component data *
******************
*
*******   type           num            id        ctitle
vessel           1       1 $1$ reactor vessel
*         nasx          nrsx          ntsx          ncsr        ivssbf
             22             9             1             2             0
*         idcu          idcl          idcr          icru          icrl
              9             2             0            22             1
*         icrr         ilcsp         iucsp          iuhp         iconc
              0             0             0             0             1
*        igeom         nvent         nvvtb        nsgrid
              0             0             0             0
*        shelv          epsw
    0.0000e+00    0.0000e+00
* z     *     5.0000e-02    1.0000e-01    1.5000e-01    2.0000e-01    2.5000e-01
* z     *     2.8450e-01    2.9450e-01    3.0450e-01    3.1450e-01    3.2450e-01
* z     *     3.3450e-01    3.4450e-01    3.5450e-01    3.6450e-01    3.8160e-01
* z     *     3.9160e-01    4.5000e-01    5.3400e-01    6.1800e-01    7.0200e-01
* z     *     7.8600e-01    8.7000e-01e
* rad   *     3.8000e-02    4.8000e-02    6.8000e-02    8.8000e-02    1.0800e-01
* rad   *     1.2800e-01    1.4800e-01    1.6800e-01    1.8000e-01e
* th    *     6.2832e+00
*        lisrl         lisrc         lisrf         ljuns
            22             9             3            11
             1             9             3            21
*
* level   1
*
* cfzl-t* f   1.0000e+04e
* cfzl-z* f   1.0000e+04e
* cfzl-r* f   1.0000e+04e
* cfzv-t* f   0.0000e+00e
* cfzv-z* f   0.0000e+00e
* cfzv-r* f   0.0000e+00e
* vol   * f   1.0000e+00e
* fa-t  * f   1.0000e+00e
* fa-z  * f   1.0000e+00e
* fa-r  * r01 0.0000e+00 r07 1.0000e+00r01 0.0000e+00e
* hd-t  * f   1.0000e+00e
* hd-z  * f   1.0000e+00e
* hd-r  * f   1.0000e+00e
* alpn  * r01 0.0000e+00 r08 0.0000e+00e
* vvn-t * f   0.0000e+00e
* vvn-z * f   0.0000e+00e
* vvn-r * f   0.0000e+00e
* vln-t * f   0.0000e+00e
* vln-z * f   0.0000e+00e
* vln-r * f   0.0000e+00e
* tvn   * f   2.9535e+02e
* tln   * f   2.9535e+02e
* pn    * f   1.0000e+05e
* pan   * f   1.0000e+05e
* conc  * r01 0.0000e+00 r08 6.0714e-02e
* solid * f   1.16579e+03e
*

 -
 -  [ The following data is omitted. ]
 -
 -
```

D.4 Sample input for TRACE code

```
SILENE S1-300: 0.51$/0.1 SECS (ALMOST STEP REACTIVITY INS)

 $general    title="S1-300",amat="uni",amcn="sst"
             $end

 $lsode
             itol=1,
             rtol= 1.d-5, atol= 1.d-10,
             itask=1, istate=1, iopt=1, lrw=30100, liw=300, mf=10
             $end

 $timing     tend=1100.,tfast=200.,tslow=400.,tvslow=800.,
             tinc=1.d-5,tincf=1.d-4,tincs=1.d-3,tincvs=1.d-2
             $end

 $geometric  nnradf=5,nnaxif=8   $end

 $neutronic  irflg=3,ifflg=2,ieflg=2,
             beta=2.68273E-04, 1.69102E-03, 1.53736E-03,
                  3.07300E-03, 9.00748E-04, 3.28548E-04,
             amda=1.27000E-02, 3.17000E-02, 1.14999E-01,
                  3.10997E-01, 1.40000E+00, 3.86999E+00,
             gen=3.46424E-05,zlife=3.34277E-05,sour=0.d0,
             bcoef=0.0,zext=0.0,pd0=1.d-4,srp=0.0,
             rhotmp1=-0.034,rhotmp2=1d-4,
             rhovoi1=-1859.7,rhovoi2=-25922.0,
             rhocon1=0.0,rhocon2=0.0,
             rhoext0=0.0,rhoext1=5.1d0 $end

 $radgas     ivgflg=3,icflg=1,vel1=1.0d-2,vdgsk=0.07,
             veldw=1.d-3,velup=4.0d-2,gvalue=1.0d-7,satc=20.d0,
             a0=0.5d-7,a1=0.d0,a2=0.d0,b0=5.d-2,b1=0.d0,
             b2=3.d1,b4=0.d0,hmol=1.d1,rgbura=5.d-6,
             ioflg=0  $end

 $thermal    imflg=0,idflg=2,hitc=1.0d0,xy=295.35,
             tinf=295.35,ivar=6,ithermo=0,jthermo=0,
             amout="air"
             $end

 $boiling    iyflg=1 ,ikflg=0,ilflg=0,isflg=0,ivsflg=3,
             radeq=2.5d-6,cbc1=2.0d-7,cbc2=1.0d0,
             cbc3=1.0d0,cbc4=1.0d0,afreq=0.25d0,stbura=0.7d-6,
             svel1=1.2d-2,svdgsk=0.07d0,evcoef=5.d-3,
             ftbura=0.7d-6  $end

 $motion
             izflg=0,discof=2.6d3
             $end

 $plot       pdata="pow",ipflg=0,xmin=1.d10,xmax=1.d20,
             reamax=10.,reamin=-10.,voimax=3.d-3,
             voimin=0.d0,tdelta=4.,tdelst=20.,
             iouti=1000, ioutif=5000, ioutis=10000, ioutivs=10000
             $end

 $counter
             icrtra=1, icrit=70, corfac=1.0d0
             $end
```

```
$pressure
            itflg=1,
            zcons= 2.9d-5, pbias= 6.9d4, prp=2.0d-3, gh2= 1.2d0,
            prcons= 2.0d-8
            $end

$aero       inflg=1,ihflg=1,iaflg=5,xperc=5.d1,fde=0.25,
            fcth=1.0d-8,hdist1=1.d-2   $end

$sonic      cor=0.d0,0.d0,0.d0,0.d0,7.35d-2,1.8d2,
            3.4525d-1,0.d0,0.d0,0.6905,1.47d-1,4.5d1,
            delt1=0.d0,delt2=0.d0
            $end

$source
            ibflg=2
            $end
```